Treatment of Organic Wastewaters Using Microbial Fuel Cell Technology

A Thesis submitted to the College of

Graduate and Postdoctoral Studies

In Partial Fulfillment of the Requirements for the

Degree of Doctor of Philosophy (Ph.D.)

In the Department of Chemical and Biological Engineering

University of Saskatchewan

Saskatoon

By

Lyman Moreno

PERMISSION TO USE

In presenting this thesis in partial fulfilment of the requirements for a Postgraduate degree from the University of Saskatchewan, I agree that the Libraries of this University may make it freely available for inspection. I further agree that permission for copying of this thesis in any manner, in whole or in part, for scholarly purposes may be granted by the professor or professors who supervised my thesis work or, in their absence, by the Head of the Department or the Dean of the College in which my thesis work was done. It is understood that any copying or publication or use of this thesis or parts thereof for financial gain shall not be allowed without my written permission. It is also understood that due recognition shall be given to me and to the University of Saskatchewan in any scholarly use which may be made of any material in my thesis. Requests for permission to copy or to make other use of material in this thesis in whole or part should be addressed to:

Head of the Department of Chemical and Biological Engineering
57 Campus Drive
University of Saskatchewan
Saskatoon, Saskatchewan S7N 5A9
Canada

OR

Dean
College of Graduate and Postdoctoral Studies
University of Saskatchewan
Room 116 Thorvaldson Building, 110 Science Place
Saskatoon, Saskatchewan S7N 5C9
Canada

ABSTRACT

The ability of microbial fuel cells (MFCs) to convert chemical or biochemical energy directly into electricity makes them well suited for treatment of wastewaters. Expanding the understanding of the processes and mechanisms that transpire in an MFC was the overall goal of this project with focus placed on the biological aspects of such systems. Biodegradation of model organic compounds of different structures commonly found in wastewaters, specifically lactate, acetate and phenol, and subsequently a representative wastewater was evaluated in H-type MFCs.

Biodegradation of evaluated compounds was achieved with concomitant generation of electricity. In MFCs with rod electrodes and suspended microbial cells, substrate biodegradation was accompanied by microbial growth and rise in open circuit potential (OCP). Preferential use of model compounds and effectiveness of biodegradation was observed with lactate being the most favourable substrate followed by acetate and phenol. To promote cell immobilization, granular electrodes were employed which resulted in higher biodegradation rates and electrochemical outputs than those with rod electrodes.

Biodegradation performance and associated power and current were improved in continuously operated MFCs. Higher biodegradation rates or removal efficiencies led to higher OCP, power and current indicating a correlation between biodegradation performance and electrochemical output. This correlation was evident in the biodegradation of organics in an internal process stream wastewater whereby the highest electrochemical output was attained when COD removal and coulombic efficiencies were at maximum.

Application of neutral red (NR) enhanced the biodegradation of phenol and eliminated inhibition effects in batch MFCs but showed no improvement during continuous operation. Phenol biodegradation was not enhanced when combined with lactate, while the presence of phenol at high concentrations ($\geq$500 mg L^{-1}) negatively impacted the biodegradation of lactate. Co-biodegradation of lactate was more effective than phenol, especially in the continuous systems, and as a result higher power and current output were obtained with lactate.

The developed biokinetic model was able to predict microbial growth and biodegradation kinetics in the MFC with high accuracy. The magnitude of biokinetics in MFCs were lower than those reported for conventional bioreactors indicating the need for development of suitable culture along with design of more sophisticated MFC bioreactors.

ACKNOWLEDGEMENTS

I would like to thank my supervisors Dr. Mehdi Nemati and Dr. Bernardo Predicala, for providing me an outstanding research environment throughout this project. Their invaluable guidance and immense patience is greatly appreciated. I would also like to thank the members of my graduate advisory committee, Drs. Richard Evitts, Catherine Niu, Gordon Putz and Jafar Soltan, for their valuable critique and suggestions.

I would also express my gratitude to the Saskatchewan Ministry of Agriculture (Agriculture Development Fund) and the Natural Sciences and Engineering Research Council of Canada (NSERC) for their financial support.

TABLE OF CONTENTS

LIST OF TABLES

LIST OF FIGURES

ABBREVIATIONS

ATP	Adenosine triphosphate
BET	Brunauer-Emmett-Teller analysis
BOD	Biochemical oxygen demand
BR	Biodegradation rate
CE	Coulombic efficiency
COD	Chemical oxygen demand
CSTR	Continuously stirred tank reactor
EPS	Extracellular polymeric substances
FADH	Flavin adenine dinucleotide
HRT	Hydraulic retention time
LSV	Linear sweep voltammetry
MFC	Microbial fuel cell
NADH	Nicotinamide adenine dinucleotide
NADPH	Nicotinamide adenine dinucleotide phosphate
NR	Neutral red
NSSD	normalized sum of squared differences
OCP	Open circuit potential
OD	Optical density
PEM	Proton exchange membrane
SEM	Scanning electron microscope
SSD	Sum of squared differences

NOMENCLATURE

D	dilution rate (h^{-1})
F	proportion of reactions involved in lactate degradation (complete vs. incomplete oxidations)
k	rate constant (h L (mg cell)$^{-1}$)
$K_{s\text{-}Ace}$	saturation constant for acetate degradation (mg acetate L^{-1})
$K_{s\text{-}Lac}$	saturation constant for lactate degradation (mg lactate L^{-1})
$K_{s\text{-}Phe}$	saturation constant for phenol degradation (mg phenol L^{-1})
$K_{d\text{-}Lac}$	endogenous decay coefficient for lactate degradation (h^{-1})
$K_{d\text{-}Ace}$	endogenous decay coefficient for acetate degradation (h^{-1})
$K_{d\text{-}Phe}$	endogenous decay coefficient for phenol degradation (h^{-1})
Q	volumetric flow rate of influent and effluent (mL h^{-1})
R	ratio of residual to initial lactate concentrations
r_s	substrate utilization rate (mg phenol L^{-1} h^{-1})
r_x	biomass growth rate (mg cell L^{-1} h^{-1})
S_{Ace}	acetate residual concentration (mg acetate L^{-1})
S_{Lac}	lactate residual concentration (mg lactate L^{-1})
$S_{0\text{-}Phe}$	phenol initial concentration in batch MFC; influent phenol concentration in continuous MFC (mg phenol L^{-1})
S_{Phe}	phenol residual concentration in batch MFC; effluent phenol concentration in continuous MFC (mg phenol L^{-1})
t	time (h)
V	working volume of MFC anodic chamber (mL)
X_0	biomass initial concentration in batch MFC; influent biomass concentration in continuous MFC (mg cell dry weight L^{-1})

X biomass concentration in batch MFC; effluent biomass concentration in continuous MFC (mg cell dry weight L^{-1})

$Y_{x\text{-}Lac}$ yield constant for lactate degradation (mg cell-dry weight (mg lactate)$^{-1}$)

$Y_{x\text{-}Ace}$ yield constant for acetate degradation (mg cell-dry weight (mg acetate)$^{-1}$)

$Y_{x\text{-}Phe}$ yield constant for phenol degradation (mg cell-dry weight (mg phenol)$^{-1}$)

Greek Letters

μ specific growth rate (h^{-1})

$\mu_{max\text{-}Ace}$ maximum specific growth rate, acetate degradation (h^{-1})

$\mu_{max\text{-}Lac}$ maximum specific growth rate, lactate degradation (h^{-1})

$\mu_{max\text{-}Phe}$ maximum specific growth rate, phenol degradation (h^{-1})

Chapter 1

Introduction

1.1 Background and overview

Large volumes of wastewaters are produced as a result of domestic, agricultural and industrial activities. Some specific waste streams such as those produced in livestock operations or those generated during the processing of oil sands are simply stored in varied types of confined structures such as manure lagoons and oil sand tailing ponds. Agriculture production has shifted towards larger centralized operations and as a result large volumes of high strength wastewaters containing organic and nitrogenous compounds are produced such as those from food processing plants and livestock operations. The development of new and emerging technologies aimed at increasing productivity, has not only increased the amount of generated wastewater but more importantly the strength, most notably biochemical oxygen demand (BOD) and chemical oxygen demand (COD) contents, of these wastewaters (Carawan and Waynick, 1996; Corcoran et al., 2010).

Different types of organic compounds are present in wastewaters including proteins, carbohydrates, fatty acids and aromatics (Tchobanoglous et al., 2003). The anaerobic degradation of complex organics from wastewater (i.e. anaerobic digestion of sludge) results in streams that are rich in fatty acids with potential to inhibit the degradation process especially at high levels of these compounds (Sorensen et al., 1990 and Hao, 2003, Oh et al., 2010). Acetate and lactate are

typical short chain fatty acids which are present in wastewaters and in the effluent of anaerobic digesters. Aromatics, such as phenol, are organic compounds that are more difficult to degrade than linear-structured compounds such as fatty acids. Phenols, sometimes referred to as "tar acids", are found in a variety of industrial wastes such as those from gas liquor, coal tar, plastic, rubber-proofing, varnish, textile and petroleum refining industries (Mancy and Weber, 1971; Kumar et al., 2005; Christen et al., 2012). Many phenolic compounds are considered priority pollutants by Environment and Climate Change Canada (ECCC, 2016) and the United States Environmental Protection Agency (EPA, 2016) and have been shown to be toxic to fish, humans and plants even at low concentrations (Hill and Robinson, 1975; Babich and Davis 1981; Seker et al., 1997; Kumar et., al, 2005; Wang et al. 2011; Pradeep et al., 2014).

With the advent of climate change and global warming, the world has never been more environmentally conscious. Stricter environmental regulations are being set and enforced affecting a wide range of processes and required treatments for wastewaters, especially those from the agriculture and industrial sectors. Among the various methods employed in treatment of wastewaters, including those relying on physical, chemical and biological processes, biological treatment methods have gained significant attention due to their low operational costs, being environmentally friendly, high public acceptance and more importantly, their ability to completely mineralize many pollutants including those that are considered hazardous such as phenol (Cookson, 1995; Vidali, 2001; Agarry et al., 2008; Al-Khalid and El-Naas, 2012; Christen et al., 2012).

An innovative biological treatment technology that could effectively treat waters contaminated by fatty acids and aromatic compounds and to treat municipal wastewaters, in general, can be developed based on microbial fuel cell technology (MFCs). An MFC is a device that operates as a bioreactor by utilizing microorganisms as biocatalysts to oxidize organic and even inorganic compounds and in the process generate electrical energy (Allen and Bennetto, 1993; Logan, 2008; Wang et al., 2015). Hence, MFC systems hold great promise with their ability to generate electricity while degrading organic and even inorganic contaminants. This ability of the MFC makes it well suited for treatment of wastewaters.

It is known that wastewaters, especially those from industrial and agricultural operations, contain large amounts of organic matter that can be exploited by MFC technology. Not only that wastewaters contain high levels of easily degradable organic material, which results in net positive energy even when heating is required, they also carry a high water content which averts the necessity to add water, making them ideal substrates for bioprocessing (Angenent et al., 2004). Furthermore, the potentially significant amounts of energy in wastewaters if recovered could provide considerable amounts of energy to various applications including the wastewater treatment process itself making it self-sufficient (Logan, 2008). To be more specific, energy spent to remove organic and inorganic contaminants in wastewaters could be offset by the energy produced through the use of MFCs.

Within the past decade, there has been a rise in the development of various technologies geared towards the production of renewable and sustainable energies. Technologies such as those utilizing biofuels, biomass, geothermal, solar and wind energies have gained favorable attention for being

considered environmentally friendly. One emerging technology in this class is the MFC, having shown its potential as a green energy technology (Rabaey et al., 2004). Among current technologies designed for deriving energy from organic matter, MFC systems possess operational and functional advantages. The most relevant is the ability of MFCs to convert substrate energy directly into electricity without an intermediary step such as the need to incorporate a turbine or generator. Moreover, unlike most bio-energy processes, MFCs operate efficiently at ambient, and even at lower temperatures and under atmospheric pressure. (Rabaey and Verstraete, 2005; Lovley, 2006a).

As MFC technology is evolving, more and more substrates of different structures are being evaluated and adapted for utilization in these systems but the greatest promise so far is the use of wastewater. The treatment of wastewaters offer the most potential for practical application of MFC technology in terms of its technical and economic viability (Logan, 2008). Significant advances in MFC design and operation have been achieved, however, further improvement is required to enhance efficiency, both in terms of electricity generation and removal of contaminants, and to maintain consistency of performance to establish its potential as a viable technology (Logan, 2010; Fan et al., 2012; Janicek et al., 2014). Moreover, capital cost especially with regard to structure of the cathodic component is still very high to make the technology economically-feasible for large scale operations (Fan et al., 2012).

Innovation in the design of new MFC-type bioreactors has been driven by the desire to increase power output and decrease capital costs (Oh et al., 2010), with emphasis placed on maximum power densities rather than the extent of contaminants removal (Zhang et al., 2015). As expected,

most studies have prioritized the enhancement in magnitude and efficiency of electricity generation in MFCs. Unfortunately, this has led to a large number of these studies to seemingly overlook, if not completely disregard, the outcomes and more importantly the importance of the biodegradation process. Even if the main focus of MFC research is on the optimization of energy generation, a better understanding of the microbial metabolism and biodegradation kinetics under conditions prevailing in the MFC, as well as the interaction with its microenvironment is essential, as power generated in an MFC is dependent on both biological and electrochemical processes (Rabaey and Verstraete 2005).

As a bioreactor, the underlying biological processes in the MFC play a vital role not only in the generation of energy but also in the effective degradation of contaminants. For the MFC to be a reliable technology for treatment of wastewaters, at the very least, its effectiveness to degrade organic and inorganic contaminants has to be established and the influence of the biodegradation process to the overall performance of MFC should be investigated. Hence, an in-depth knowledge of these bioprocesses and the associated biokinetics is essential for successful operation, control and most importantly for the design and scale-up of MFCs, more so if the intended application is directed towards degradation of organic and inorganic contaminants, rather than generation of energy alone.

With the lack of understanding of the biological processes that contribute to the operation of a MFC, its potential as an effective and reliable means of treating wastewaters, given the ample availability of these, along with its associated energy generation capability might not be fully realized. To further understand the working principles of the MFC as a bioreactor, the overall goal

of this Ph.D. research was to advance the understanding of the bioprocesses that occur in the MFC and raise awareness of their importance as vital as the electrochemical aspects of the technology. Furthermore, experiments in MFCs were formulated to gain insight into the interconnecting relationship between the bioprocesses, indicated mainly by microbial growth and substrate degradation, and the resulting electrochemical outputs.

Knowing the complex nature of wastewaters, specifically its diverse composition, experiments were carried out utilizing model organic compounds of different molecular structures, namely lactate, acetate and phenol, or their combination as substrates. The use of known organic compounds enabled biokinetic evaluation and modeling of the degradation process similar to those conducted in conventional bioreactors. Access to detailed kinetic information is critical in the design, operation and control of large scale treatment systems utilizing MFC technology. Moreover, utilization of model organic compounds enabled operation and monitoring of experiments with repeatability and consistency. Investigation of biodegradation performance resulted in determination of intrinsic biokinetic parameters and other important information such as biodegradation rate and removal efficiency, among others, which were correlated to corresponding electrochemical performance as indicated by power and current output and coulombic efficiency. With information obtained from studies on biodegradation of model organic compounds, a preliminary investigation of the treatment of an internal process stream wastewater in the MFC system was also carried out.

1.2 Layout of thesis

This PhD thesis has been prepared based on the guidelines set by the University of Saskatchewan for a manuscript-style thesis. It is comprised of eight chapters mainly detailing the research work formulated and carried out throughout this PhD project with an overall goal of furthering the understanding of the processes and mechanisms that transpire in a MFC, with focus on the biological component of the technology. Overall structure of the thesis shows the progression of the entire study as each research objective was achieved. In Chapter 2, relevant review of literature is presented providing a state of the art overview of the MFC technology and its applications, especially in the field of wastewater treatment. Literature specific to topics investigated in this work has been elaborated in more details in the relevant chapters. Chapters 3, 4, 5, and 6 present the bulk of research work carried out in dual-chamber MFCs utilizing different model organic compounds as substrate with corresponding MFC performance assessed in terms of biodegradation kinetics and electrochemical output. In Chapter 3, fatty acids, specifically lactate and acetate, were utilized to investigate the effects of type and concentration of organic compounds on MFC performance. Moreover, biokinetic evaluation and modeling of microbial growth and utilization of lactate and acetate are also presented. To enhance MFC performance, the biodegradation of lactate and acetate were carried out by equipping MFCs with granular graphite instead of rods (i.e. different electrode structures) with the rationale being that the granular electrode would promote immobilization of microbial cells and improve electron transfer through increased surface area. Results of these experiments are presented and comparison of the two electrode structures are discussed in Chapter 4. Following successful biodegradation of fatty acids, a more complex and known recalcitrant compound, specifically phenol, was utilized as substrate in MFCs equipped with both rod and granular electrodes. To aid phenol biodegradation, addition of neutral red as

electron mediator was also investigated. Results of experiments with phenol as sole substrate are presented in Chapter 5. Additionally, development and evaluation of biokinetic model of phenol degradation and associated microbial growth in the MFC was carried out and results are included in Chapter 5. Co-biodegradation of lactate and phenol in both rod and granular electrode MFCs with or without the presence of neutral red are reported in Chapter 6. Findings on whether the presence of the more amenable compound (i.e. lactate) could promote faster biodegradation of phenol and conversely, if the potential inhibitory effects of phenol could affect the biodegradation of lactate are discussed in the chapter. In order to assess the potential of the MFC for practical applications, a preliminary investigation on treatment of an actual wastewater was conducted, details of which are described in Chapter 7. Lastly, Chapter 8 presents a summary of findings achieved throughout the study, as well as conclusions and recommendations drawn from this research work. References used in all chapters are listed at the end of the thesis. Additional information such as calibration curves and list of contributions by the author are provided in appendices. It is important to note that chapters 3 and 5 have been published and Chapter 4 is under internal review for submission to a peer-reviewed journal. The chapters on the published work are more extensive than the journal manuscripts as any relevant information that was not included in the manuscripts has been added in the thesis.

Chapter 2

Literature review, Knowledge gaps and Objectives

2.1 Background and working principle of MFC

The first observed account of electricity generation accompanying the decomposition of organic compounds by microorganisms was reported over 100 years ago by Potter (1911). However, it was only in the mid-1980's when development of modern day MFC systems were started with the utilization of different microorganisms, electron mediators and new device configurations (Roller et al., 1984; Bennetto et al., 1985; Thurston et al., 1985; Bennetto, 1990a, 1990b; Allen and Bennetto, 1993). Since then, the interest in MFCs has grown exponentially, in fact, the bulk of articles and reviews covering microbial fuel cells has been published in the last 15 years and growing yearly (Figure 2.1).

The structure of a typical MFC consists of two compartments, the anodic and cathodic chambers, that are separated by a semi-permeable membrane, commonly a proton exchange membrane (PEM). In the anodic chamber, microorganisms grow through degradation (oxidation) of electron donors, typically organic substrates. Through the process of oxidation, electrons are liberated and then transported via reduced co-enzymes (nicotinamide adenine dinucleotide - NADH, flavin adenine dinucleotide - FADH, nicotinamide adenine dinucleotide phosphate - NADPH) to a respiratory chain creating a proton gradient. When the protons move back into the cell, 1 ATP molecule is created from 1 ADP for every 3-4 protons (Caccavo et al., 2003; Rabaey and

Verstraete, 2005; Lovley, 2006a). In nature or in a conventional system, the electrons are released to a terminal electron acceptor such as oxygen, nitrate or sulphate or other oxidizing compounds. However, in the MFC, the anodic chamber is kept anoxic thereby creating an environment which forces microorganisms to switch from their natural electron acceptor to an insoluble acceptor such as an electrode. Oxygen, being the conventional natural electron acceptor, reduces or inhibits electricity generation and hence it has to be absent (anaerobic) or at an extremely low level (anoxic) in the anodic chamber (Caccavo et al., 2003; Rabaey and Verstraete, 2005; Logan and Regan, 2006; Lovley, 2006b; Logan, 2008).

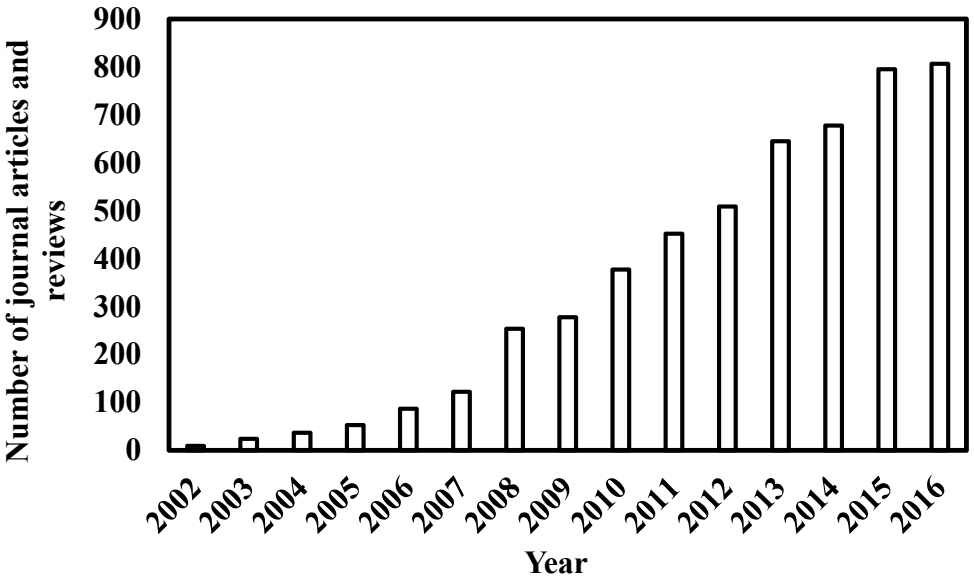

Figure 2.1 Number of published journal articles and reviews that contain the phrase "microbial fuel cell" in the article title, abstract or keywords. Source: Scopus on 02/25/2017; document type: article or review.

MFC chambers are equipped with electrodes that are connected through an external circuit, similar to those in conventional fuel cell systems. There are several mechanisms that describe how microorganisms transfer electrons to an electrode and are categorized as either direct or mediated

electron transfer (Schroder, 2007). For direct electron transfer, physical contact of the bacterial cell membrane or a membrane organelle to the electrode surface is required with no diffusional redox species involved. Certain types of bacteria, specifically *Geobacter* and *Shewanella* species, have been shown to produce membrane bound cytochromes that attach directly to the electrode surface, or possess conductive appendages or nanowires that allow the transfer of electrons to a more distant surface (Reguera et al., 2005; Gorby et al., 2006, Reguera et al., 2006; Schroder, 2007).

Mediated electron transfer, on the other hand, requires the presence of electron-shuttling mediator that travels in and out of the microbial cell to accept and transfer electrons to the electrode surface (Lovley, 2006b; Schroder, 2007). Electron mediators can either be exogenous or artificial such as neutral red and methylene blue (Park and Zeikus, 2000) or produced endogenously by the microorganisms themselves such as pyocyanin that is produced by *Pseudomonas aeruginosa* (Rabaey et al., 2004; Rabaey et al., 2005a). Once electrons are transferred to the electrode, they flow through an external circuit into the cathode. The flow of electrons along with the potential difference between the cathode and anode create the electrical power. For every electron that is produced, a proton must be transported to the cathode through the electrolyte and PEM to maintain the current flow (Logan and Regan, 2006). The electron acceptor in the cathode reacts with the electrons and protons and is reduced. In the case of oxygen as the terminal electron acceptor, it is reduced to water. Chemical catholytes, such as ferricyanide and manganese oxide, and even nitrate can be used as alternatives to oxygen (Logan et al., 2006).

Potter (1911) stated the electrical effects in an MFC is an expression of microbial activity and is influenced by several factors including the concentration of organic nutrient and number of organisms present. As summarized by Mohan et al. (2008), the function and efficiency of MFC with respect to power generation is generally dependent on factors such as nature of carbon source, dimensions, volume and configuration of the fuel cell (bioreactor), nature and type of electrodes, mediators and electrolytes used, operating temperature, nature of inoculum (i.e. microbial culture) used in the anodic and in case of biocathodes cathodic chambers, and nature of the PEM. The overall performance of the MFC is dependent on both biological and electrochemical processes that are characterized by different factors including substrate degradation rate, anode and cathode overpotentials, PEM performance and internal resistance of the MFC (Rabaey and Verstraete, 2005).

2.2 MFC configurations

Several MFC configurations have been used to date and improved designs are expected to be developed as the technology advances. A widely used and inexpensive design is dual chamber MFC fabricated as an "H" shape bioreactor. It is the simplest MFC design consisting of two chambers connected by a flange tube wherein a PEM separates the two chambers (Logan et al, 2006). H-type systems are commonly used in MFC studies because they allow relative ease in monitoring different environmental parameters. These systems, on the other hand, typically produce low power densities due to their high internal resistance (~1300 Ω) caused by the large electrode spacing (Logan, 2008) and resistances of the PEM and electrolyte between the electrodes (Rabaey and Verstraete, 2005).

Another simple and useful design of MFC is the air-cathode MFC. The common air-cathode MFC has a cubic structure. A single chamber air-cathode cubic system has the anode and cathode placed on either side of a block of tubes, with the anode sealed against a flat plate and the cathode exposed to air on one side and substrate on the other (Liu and Logan, 2004). Air-cathode MFCs can be configured to test different electrode materials and architecture. These systems can have one (Liu and Logan, 2004) and two chambers (Kim et al., 2007) and can contain a brush anode and tubular cathode (Zuo et al., 2007). The bioreactor can also have removable sections that enable the anode to be placed at different distances from the cathode (Cheng et al., 2006). Typically, air-cathode MFCs have higher power densities compared to H-type systems because of their lower internal resistance.

The above configurations are the basic MFC designs and several variations have emerged in an effort to increase the power density or provide continuous flow of substrate through the anode (Logan 2008). A flat plate MFC was designed by Min and Logan (2004) based on a hydrogen fuel cell architecture aimed to produce more power. Tubular type MFCs, with design resembling that of upflow packed-bed bioreactors, have been tested mainly to investigate continuous feeding of substrate to the anode. An MFC resembling an upflow fixed-bed biofilm reactor with anode and cathode separated by an inclined membrane was used by He et al. (2005) which was later modified to contain an interior cathode compartment formed with a U-shape (He et al., 2006). A tubular MFC with its tube made of cation exchange membrane and surrounded with cathode made of woven graphite mat allowing catholyte to overflow outside of the column was configured by Rabaey et al. (2005b). A multi-compartment, two-chamber batch type MFC similar to a cube air-cathode system, except enclosing the cathode chamber to hold an aqueous catholyte, was used by

Rabaey et al. (2005a). Current MFC designs still produce considerably low voltages but by stacking several MFCs in series one can increase the system overall voltage (Aelterman et al., 2006).

2.3 Microorganisms in MFCs

Different types of microorganisms have been evaluated for application in MFCs including bacteria, fungi and consortia of different cultures like those from activated sludge (Angenent et al., 2004). The most widely used microbes in MFCs are bacteria. Bacteria that transfer electrons outside the cell are referred to as exoelectrogens or electricigens and can generate electricity in the absence of exogenous mediators or by producing endogenous mediators (Lovley, 2006a; Logan, 2009). The first group of exoelectrogens include *Gammaproteobacteria* (e.g. *Escherichia coli*), *Shewanella* spp., *Deltaproteobacteria* (e.g. sulphur- and sulphate reducing bacteria), and members of the *Geobacteracae* family, *Betaproteobacteria* such as *Rhodoferax ferrireducens*, and *Firmicutes* and *Clostridia*. Only a few of the known exoelectrogens have been discovered to produce endogenous mediators and only a few studies on electricity generation by these bacteria have been conducted. The known exoelectrogen species that produces endogenous mediators are *Pseudomonas aeruginosa* and *Geothrix fermentans* (Logan, 2008).

Although not as widely used as *Pseudomonas aeruginosa*, *Pseudomonas putida* has been utilized as biocatalyst in a few MFC studies achieving modest results. The use of *P. putida* in MFCs has shown its capability to effectively degrade complex structured substrates such as in removing 78% of toluene (Friman et al., 2012a) and at least 85% COD in a synthetic wastewater (Juang et al.,

2011). *P. putida* was also evaluated in treating oil refinery wastewater in an air-cathode MFC but only achieved a COD removal efficiency of 30% (Majumder et al., 2014).

To date, power densities produced by pure cultures are in general lower compared to those generated using mixed cultures in the same MFC (Logan, 2008 and Zuo et al., 2008). Despite its advantage in terms of energy generation, the use of mixed culture biocatalysts could create obstacle in repeatability and reproducibility of the results (Madiraju, 2013).

2.4 MFCs for wastewater treatment

The MFC is an attractive technology especially for wastewater treatment as it not only treats the wastewater but also generates energy at the same time. There is more than ample supply of wastewaters from varied sources that can be utilized in MFCs. For instance, to enhance productivity, agriculture production has shifted towards larger centralized operations and as a result large volumes of high strength wastewaters containing organic and nitrogenous compounds are produced, with the typical examples including those generated in livestock operations and food processing plants. In terms of energy potential, wastewaters contain significant amounts of recoverable energy which is estimated to be 9.3 times the amount of energy needed to treat the wastewater itself in conventional treatment plants (Shizas and Bagley, 2004).

To take advantage of the capabilities of MFC and the energy contained in wastewater, numerous studies have been conducted to investigate the effectiveness of MFCs in treating wastewater and generating practical amounts of electrical energy. Especially in the past 15 years, significant advances in MFC research on wastewater treatment have been achieved. The first significant

breakthrough in wastewater treatment using MFCs was achieved by Liu et al. (2004) when their single chamber MFC removed up to 80% of the COD of domestic wastewater and produced a maximum electrical power output of 26 mW m^{-2}. Ahn and Logan (2009) were able to achieve considerably higher power density of 422 mW m^{-2} in treating domestic wastewater under continuous flow and mesophilic conditions in a single chamber air-cathode MFC. The effectiveness of MFCs in treating wastewater is not limited to domestic wastewaters and these systems have been used for the treatment of industrial wastewaters as well. Lu et al. (2009) were able to successfully treat wastewater from starch processing by reducing COD by as much as 98%, while generating a maximum power density of 239.4 mW m^{-2}. A continuous flow MFC used to treat brewery wastewater produced a maximum power density of 660 mW m^{-2} although the COD removal efficiency was quite low at 20.7% (Wen et al., 2009). Although producing a low power output of 50 mW m^{-2} and COD removal of 30%, an air-cathode MFC was able to utilize oil refinery wastewater as substrate that contained relatively high COD concentration of over 2000 mg L^{-1} (Majumder et al., 2014).

Wastewaters generated from agricultural operations have also been utilized as substrates in MFCs. Using wastewater from a livestock operation, Min et al. (2005a) were able to generate a maximum power density of 261 mW m^{-2}, while reducing the soluble COD by as much as 92% in a single chamber air-cathode MFC. Treatment of real field dairy wastewater using a single chamber open-air cathode MFC was investigated by Mohan et al. (2010). Their system was able to reduce not only the COD of the wastewater by 95.5% but also the amount of proteins, carbohydrates and turbidity by 78.1, 92.0 and 99.0%, respectively, while generating a maximum volumetric power production of 1100 mW m^{-3}.

Numerous studies have reported a wide range of actual wastewaters that have been tested as substrates in MFCs ranging from those with low strength (<300 mg BOD L^{-1}), such as domestic wastewater to high strength wastewaters (>2000 mg BOD L^{-1}) such as those from brewery and livestock operations. The review by Gude (2016) alone enumerated about 50 separate studies of actual wastewaters treatment in MFC systems.

2.4.1 Utilization of synthetic wastewaters and/or model organic compounds

The versatility of MFCs is notably manifested in their capability to effectively utilize different types of biodegradable substrates for generation of renewable energy. A review by Pant et al. (2010) revealed that more than 50 different types of substrates from a wide variety of sources have been investigated in MFCs. More recent reviews have further shown a wider scope of different substrates that have been tested in MFCs (Wang and Ren, 2013; Janicek et al., 2014; Gude, 2016; Mathuriya and Yakhmi, 2016). These varied substrates are typically organic compounds such as carbohydrates, fatty acids and aromatics. Lesser known substrates that have been evaluated in MFC systems include inorganic compounds such as ammonia and sulphide (Rabaey et al., 2006; Puig et al., 2010), as well as plant-based substrates such as cellulose and starch (Niessen et al., 2004; Rezaei et al., 2009; Greenman et al., 2009; Behera et al., 2010).

Since actual wastewaters possess a relatively complex composition, MFC studies, especially those dealing with more fundamental investigations, utilize model organic compounds solely or in mixtures, along with microbial growth media, to create synthetic wastewater (Jang et al., 2004; Mohan et al., 2008; Aldrovandi et al., 2009; Jadhav and Ghangrekar, 2009; Janicek et al., 2014; Gude, 2016). Of the numerous organic compounds that have been evaluated in MFCs, glucose and

acetate are most common (Pant et al., 2010; Wang and Ren, 2013; Gude, 2016). Having a simple chemical structure, these compounds are more degradable than actual wastewaters and have been observed to generate higher electrical energy output. For years, glucose has been one of the most common organic compounds used in microbial growth experiments and hence its selection as one of the earliest substrates utilized in MFCs was expected (Delaney et al., 1984; Roller et al., 1984). The highest power output from the utilization of glucose is 4.3 W m^{-2} (calculated power density in terms of volume: 253 W m^{-3}) which was achieved with an average loading rate of 1 g glucose L^{-1} d^{-1} and electron transfer efficiency of 81% (Rabaey et al., 2004). This output was attained in a two-chamber Plexiglas MFC with a cathode enriched with potassium hexacyanoferrate for optimized electrode-oxygen charge transfer and using a mixed bacterial culture that underwent an enrichment procedure.

Acetate, along with lactate, is a typical short chain fatty acid commonly present in wastewaters and in the effluent of digesters as a result from the anaerobic degradation of complex organic compounds (Sorensen et al., 1990 and Hao, 2003). During the early years of modern day MFC research, most studies have utilized acetate as the substrate of choice in various MFC trials designed with the main purpose of enhancing electricity generation (Pant et al., 2010; Gude, 2016). Studies involving the use of acetate as substrate in MFCs cover a wide range including investigations on reactor designs (Min and Logan, 2004; He et al., 2005; Liu et al., 2005a; Aelterman et al., 2006; Clauwaert et al., 2009; Dekker et al., 2009; Fan et al., 2012;), scaling-up (Dekker et al., 2009; Cheng and Logan, 2011; Heijne, et al., 2011), type and efficiency of electrode (Liu et al., 2005b; Rabaey et al., 2005b; Aelterman et al., 2006; Logan et al., 2007; Ishii et al.,

2008), PEM performance (Kim et al., 2007), biocatalyst characterization (Jung and Regan, 2007), effect of temperature (Liu et al., 2005b; Min et al., 2008), among others.

Having a similar structure with acetate, lactate has also been utilized as substrate in MFCs, although it has not been as popular. Along with glucose, lactate and acetate were compared as substrates for characterization of biocatalysts in two-chamber MFCs (Jung and Regan, 2007), whereby peak voltage and power and current densities were found higher with lactate than acetate and glucose although coulombic efficiency was highest with acetate. Most of the works involving lactate as electron donor have engaged in more fundamental investigations such as electron flow in mediator-less MFC (Kim et al., 2002) and characterization and evaluation of biocatalysts, most notably *Shewanella* spp. (Bretschger et al., 2009; Call and Logan, 2011). As in conventional bioreactors, biodegradation of lactate in MFCs has revealed production of intermediates such as acetate and pyruvate (Bretschger et al., 2009; Call and Logan, 2011).

Another rarely utilized substrate in MFCs is phenol. Being an aromatic compound, it has a more complex structure than lactate and acetate making it a harder compound to degrade. Given the less favorable conditions for biodegradation of compounds in MFCs compared to conventional bioreactors, in addition to its source being found only in specific waste streams, studies of phenol degradation in MFCs have been rare. Compared to other substrates, utilization of phenol in MFCs is relatively new with the first results on phenol biodegradation in an air-cathode MFC reported only in 2009 by Luo et al. In this study, 90% of phenol was removed. Using mixed consortia of microorganisms, about 66% phenol removal was achieved in a single-chamber MFC (Buitron and Moreno-Andrade, 2014), while up to 93% of phenol was removed from a coconut husk retting

wastewater in a dual-chamber MFC (Jayashree et al., 2014). With a pure culture of *Cupriavidus basilensis*, 86% of initial phenol concentration was removed in a mediator-less dual-chamber MFC (Friman et al., 2012b). When compared to complete biodegradation of lactate and acetate in MFCs which have been reported in different studies, the lower biodegradation efficiencies reported for phenol show its recalcitrant nature especially in the more challenging environment of the MFC.

Despite the numerous studies conducted in MFCs, power output has increased from only a few milliwatts per square meter of electrode to 6.9 W m^{-2} (Fan et al., 2008; Logan, 2010). In fact, the highest power output generated so far by an MFC, which is 2.87 kW m^{-3}, was achieved using acetate (100 mM) as substrate (Fan et al., 2012). The race to achieve commercially viable and reliable energy output from MFCs is still ongoing. In the pursuit of this goal, the understanding of the bioprocesses involved in MFCs such as microbial growth and substrate biodegradation kinetics, while certainly critical on the extent of electrochemical outputs, have been overlooked by researchers. Other than reporting the percent of substrate removal, most MFC studies did not focus on biokinetics nor provided detailed information such as those available for conventional bioreactors, while many focused solely on electrochemical aspects. Of the few that attempted to understand the kinetics of the bioprocesses that occur in the MFC, the developed models have focused on predicting the energy output (Picioreanu et al., 2007; Hamelers et al., 2011; Madiraju, 2013; Song et al., 2014).

2.5 Knowledge gap and objectives

Majority of the studies conducted in MFCs have focused mainly on enhancing the generation of electrical energy with limited information on the associated bioprocesses that occur in the system

and are critical in generation of energy. Development of the MFC as a source of renewable energy is indeed promising but the greatest potential of this technology for adoption into practical use is for it to be employed as a means to degrade organic and inorganic contaminants with electricity generation as an added benefit. It is, therefore, very crucial to understand the interconnecting relationship between the biological and electrochemical aspects that exists in the MFC systems. Moreover, development of detailed biokinetic information is essential and necessary in the scale-up and design, operation and control of MFC systems for practical and large scale applications.

Recognizing the importance of the biological processes occurring in an MFC and their impact on the overall performance and a thorough understanding of the biokinetics under environmental conditions that prevail in an MFC are essential for the advancement of MFC technology and realization of its potential for practical applications. With this necessity in mind, this Ph.D. research was formulated to evaluate the factors that influence ability and efficiency of an MFC system to sustain microbial growth, degrade organic compounds of different chemical structure, and simultaneously generate electricity. Specifically this study aimed to evaluate the involved bioprocesses and to generate detailed biokinetic data in an MFC environment and to compare these with similar data generated in conventional bioreactors.

The specific objectives of this research were as follows:

1. To utilize two different groups of model organic compounds, specifically two fatty acids of different carbon numbers (lactate and acetate), and an aromatic compound (phenol) as substrate in the MFC and investigate the effects of type (in terms of chemical structure) and concentration of the organics on the performance of MFC in terms of biodegradation

kinetics and electrochemical outputs. Biodegradation kinetics was assessed in terms of biomass growth and substrate utilization, while electrochemical performance was evaluated in terms of open circuit potential, power and current densities and coulombic efficiency.

2. To investigate the effect of different electrode structures on the biodegradation and electrochemical performance of MFC. Two types of electrode structures, specifically rod which allowed suspension of bacterial cells in the anodic chamber, and granular which enabled immobilization of cells and increased surface area for enhanced electron transfer were employed and compared.

3. To develop and evaluate a biokinetic model of microbial growth and substrate degradation that occurs in the MFC and to determine relevant biodegradation coefficients, and finally comparing the results to those from conventional bioreactors.

4. To assess the performance of MFC under different modes of operation, i.e. batch vs. continuous modes of operation, using different substrate and electrode structures. To determine the effect of substrate loading rate on performance of continuously operated MFC.

5. To investigate the effect of neutral red, as electron mediator, on the biodegradation of a recalcitrant substrate (i.e. phenol) and generation of energy.

6. To investigate the co-biodegradation of phenol and lactate with the aims to i) determine whether the presence of lactate, a compound more amenable to biodegradation, could facilitate and enhance biodegradation of phenol; and ii) investigate the potential inhibitory effects of phenol on the biodegradation of lactate.

7. To conduct a preliminary investigation on the treatment of an internal process stream wastewater collected from the fermenter of the Saskatoon wastewater treatment plant, using the evaluated MFC and assess its performance in terms of effectiveness of biodegradation and electrical energy generation.

Chapter 3

Biodegradation of Fatty Acids (Lactate and Acetate) and its Associated Biokinetics in MFCs with Single Rod Electrodes

A similar version of this chapter has been published in the Bioprocess and Biosystems Engineering journal:

Moreno, L., Predicala, B. and Nemati (2015). Biokinetic evaluation of fatty acids degradation in microbial fuel cell type bioreactors. Bioprocess and Biosystems Engineering 38:25-38.

The written text of the submitted manuscript was prepared by Lyman Moreno, while Dr. Mehdi Nemati and Dr. Bernardo Predicala provided editorial input.

3.1 Introduction

The development of various technologies geared towards the production of renewable and sustainable energies has been widely promoted. A potential green energy technology that has gained considerable interest is the use of biological fuel cells (Rabaey et al., 2004). Moreover, MFCs have been shown to have the capability to utilize a variety of organic compounds including carbohydrates and fatty acids as well as inorganic compounds such as ammonia and sulphide as substrates (energy source and electron donor). The anaerobic degradation of complex organics from wastewater (i.e. anaerobic digestion of sludge) results in streams which are rich in short chain fatty acids (Sorensen et al., 1990 and Hao, 2003). Acetate and lactate are typical short chain fatty acids which are present in some wastewaters and in the effluent of anaerobic digesters. A number

of earlier studies have explored the use of lactate and acetate as model organic compounds in microbial fuel cells (Kim et al., 2002; Bond and Lovley, 2003; Min and Logan, 2004; Liu et al., 2005; Min et al., 2005b; Bretschger et al., 2009; Manohar and Mansfeld, 2009). However, majority of these studies have focused mainly on the configuration and electrochemical aspects of the MFC and the involved biological processes have been considerably overlooked.

As a bioreactor, the underlying biological processes in the MFC play a vital role in the effective biodegradation of organic compounds, as well as in the generation of energy. Therefore, an in-depth knowledge of these bioprocesses and the associated biokinetics is essential for the proper operation, control and most importantly for the design and scale-up of MFCs. In the design and scale-up of a bioreactor, knowledge of microbial growth kinetics and substrate utilization is vital wherein parameters such as maximum specific growth rate, saturation constant and growth yield are required. The determination of these parameters involves establishing a growth kinetic model that accurately represents the operation of the system.

Of the numerous works conducted in MFCs, only a few have attempted to mathematically model MFC performance and interestingly these works have mainly focused on the electrochemical parameters affecting the MFC. In these works, the generated models and corresponding evaluation have relied primarily on power and current output data and very limited, if any, biokinetic data were utilized in the process (Marcus et al., 2007; Picioraneau et al., 2007; Zeng et al., 2010; Hamelers et al., 2011; Madiraju, 2013). The success of MFC technology entails the process of identifying, understanding and predicting the various interrelating phenomena that determines its performance, hence continued modeling efforts are crucial (Torres, 2014). The development of a

suitable biokinetic model that describes the removal of contaminants from wastewater is considerably complicated due to the complex nature of wastewaters and presence of multiple contaminants. Taking into account the electrochemical processes that occurs in an MFC further complicates the modeling process. Hence the use of model organic compounds representative of a wastewater mixture is a feasible and practical approach to develop the required knowledge.

In this part of the research, biodegradation of two model short chain fatty acids, namely lactate and acetate, were investigated in batch and continuously operated MFCs equipped with single rod electrodes which allowed free suspension of microbial cells in the bioreactor and enabled us to determine the detailed biokinetics and associated parameters. Performance of MFC in terms of biodegradation and electrochemical performance was evaluated. Given that earlier biodegradation studies by others had concentrated mainly on the electrochemical aspects of MFC performance, the focus in this work was mainly on the kinetics of biodegradation process in the MFC, specifically the kinetics of microbial growth and substrate utilization. Using the generated data, suitable kinetic models for microbial activity and biodegradation of model organic compounds under environmental conditions prevailing in an MFC were developed.

3.2 Materials and methods

3.2.1 Microbial culture, medium and concentrated cell suspension

A pure strain of *Pseudomonas putida* (ATCC 23973) was utilized in all experiments. This allowed the comparison of biodegradation kinetics observed in the MFC with those reported in literature for the same bacterial strain in conventional bioreactors. Moreover, *Pseudomonas* species are commonly used for biodegradation of organic contaminants and have been identified as one of the

main species of activated sludge microbial community that are commonly used for the treatment of wastewaters. Modified McKinney's medium, a common medium used for microbial growth, especially in biodegradation studies, was used for growth and culture maintenance. The composition of McKinney's medium is presented in Table 3.1. Pure cultures were maintained in 250 mL Erlenmeyer flasks containing 100 mL McKinney's medium with 1000 mg L^{-1} of either lactate or acetate as the substrate. Flasks containing the growth medium were sterilized in an autoclave for 30 minutes at 121°C. After cooling to room temperature, each flask was inoculated with 10 mL of a two-week old *P. putida* culture (10% v/v). Cultures were maintained on a rotary shaker at 150 rpm (Figure 3.1) and room temperature (24±2 °C). Sub-culturing was done on a bi-weekly basis.

Table 3.1 Composition of modified McKinney's medium (Paslawski et al., 2009).

Component	**Chemical formula**	**Concentration (mg L^{-1})**
Potassium dihydrogen phosphate	KH_2PO_4	840
Potassium hydrogen phosphate	K_2HPO_4	750
Ammonium phosphate dibasic	$(NH_4)_2HPO_4$	474
Sodium chloride	NaCl	60
Calcium chloride	$CaCl_2$	60
Magnesium sulphate	$MgSO_4.7H_2O$	60
Ferrous ammonium sulphate	$Fe(NH_4)_2SO_4.6H_2O$	20
Trace mineral solution*	-	1 mL/L

*Trace mineral solution: H_3BO_3 (600 mg L^{-1}); $CoCl_3$ (400 mg L^{-1}); $ZnSO_4.7H_2O$ (200 mg/L); $MnCl_2$ (60 mg/L); $NaMoO_4.7H_2O$ (60 mg/L); $NiCl_2$ (40 mg/L); $CuCl_2$ (20 mg/L)

To carry out experiments in MFCs, concentrated *P. putida* cell suspensions were prepared by centrifugation of approximately 60 mL of a freshly grown *P. putida* culture at 10,000 rpm (11000

×g) for 30 minutes, using an Allegra X-12R centrifuge (Beckman Coulter, Fullerton, USA). The collected cell pellets were then re-suspended in 1.5 mL of the supernatant liquid. Concentrated cell suspensions were used for inoculation of the anodic chamber of MFCs, where biodegradation of lactate or acetate was studied.

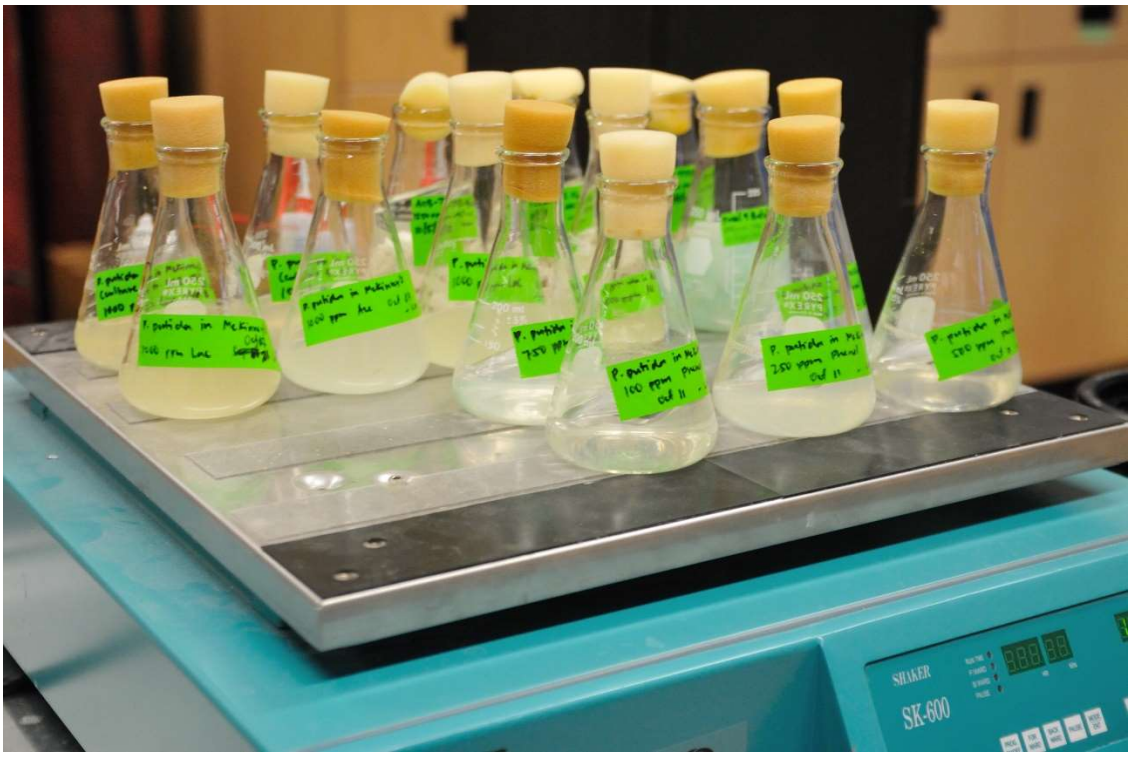

Figure 3.1 Cultures of *P. putida* maintained in flasks stirred continuously on a rotary shaker.

3.2.2. Experimental set-up and operation

Identical H-type dual-chamber MFC type bioreactors were used in all experiments. The different components of each MFC bioreactor before assembly are shown in Figure 3.2. Each MFC consisted of two identical glass cylindrical chambers (anodic and cathodic chambers) equipped with inlet and outlet ports, and a flanged glass extension in the lower part which allowed the attachment of the chambers by an adjustable clamp. Each of the specially fabricated glass

chambers had a working volume of 245-285 mL. Once assembled, the anodic and cathodic chambers were separated by a 0.09 mm thick Nafion high exchange capacity proton exchange membrane (HEPEM, NE-1035 Alfa Aesar, Ward Hill, MA, USA). A rubber O ring was placed between the flanged extensions to prevent leakage. The top of each chamber was capped with a rubber stopper. Each chamber was also equipped with a sampling port in the middle that was capped with a rubber septum. A single graphite rod (L= 102 mm, D= 6.15 mm) was used as an electrode in each chamber. The graphite rod was fixed into the rubber stopper with one end connected to a chrome wire. An alligator clip was attached to the other end of the chrome wire and used to connect the electrodes to the terminals of a multimeter. Prior to assembly of the MFC, graphite rod electrodes were cleaned with reverse osmosis (RO) water using a sonifier which was operated for 10 minutes, and then air dried. A Keithley 2700 multimeter, equipped with a 7700 datalogger (Keithley Instruments Inc., Cleveland, USA) and linked to a computer, was used and operated through its associated software (ExceLINX) for real time monitoring of circuit potential. The experimental setup of one of the MFCs with real time monitoring of circuit potential is shown in Figure 3.3.

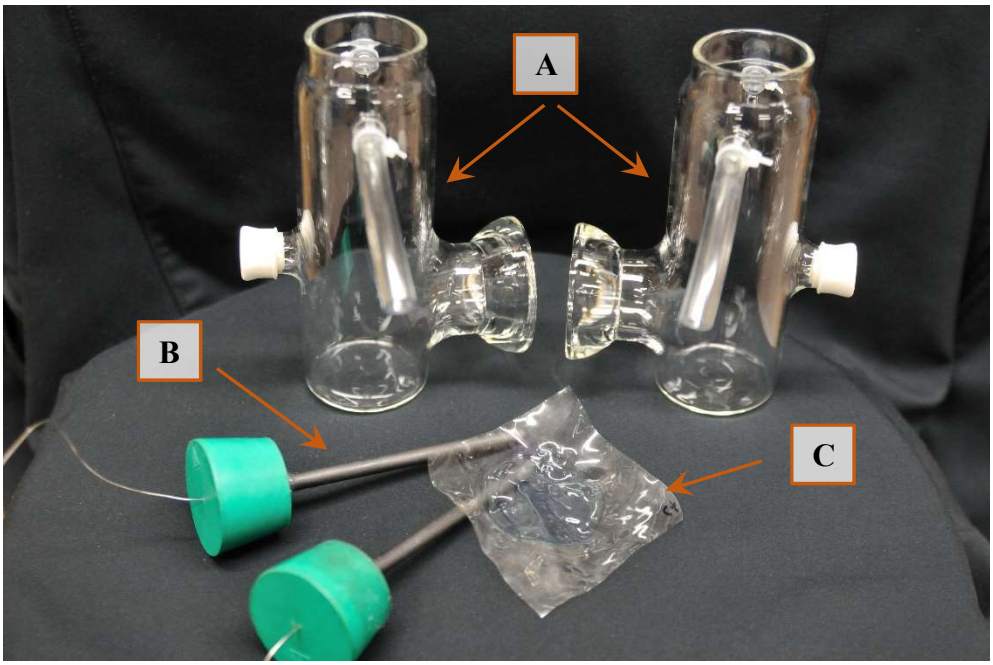

Figure 3.2 Different components of H-type MFC assembly including anodic and cathodic chambers with extended flange and sampling port covered with rubber septum (A), graphite rod electrodes (B) fixed onto rubber stoppers and attached to chrome wires and a PEM (C).

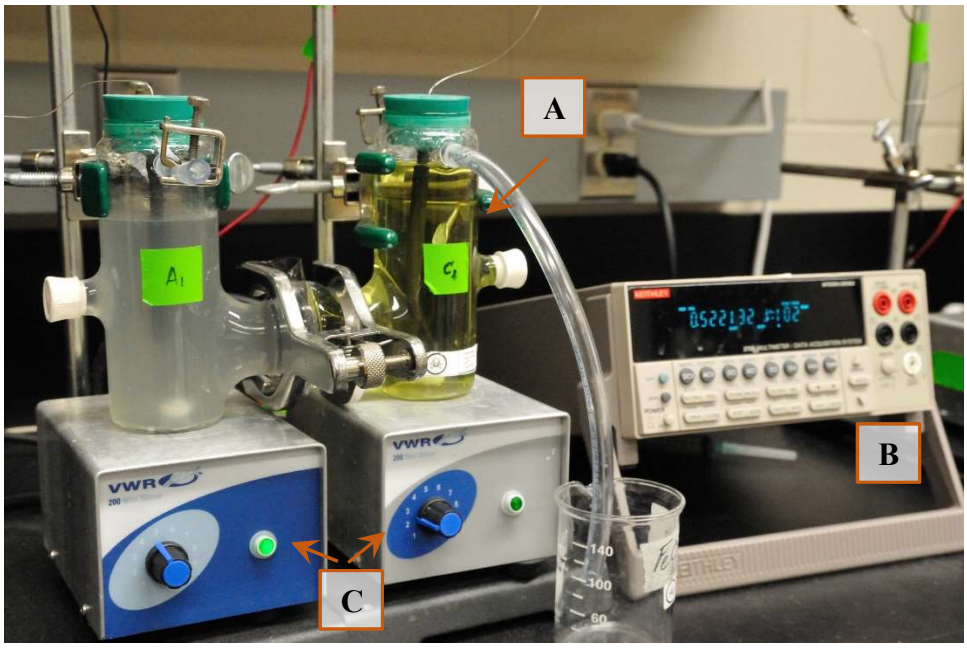

Figure 3.3 Photograph of an assembled experimental system. H-type MFC (A) is connected to multimeter (B) equipped with a datalogger for continuous recording of circuit potential readings. Magnetic stirrers (C) were utilized to mix the contents of each chamber of the MFC.

Before each experimental run, the liquid content of the anodic chamber (modified McKinney's medium) was purged with nitrogen gas (industrial grade) for about 10 minutes to ensure oxygen was removed and anoxic conditions were achieved. In the cathodic chamber, a chemical electron acceptor, specifically potassium ferricyanide, was used. The potassium ferricyanide solution was prepared by adding potassium ferricyanide (98% purity) and potassium phosphate (as buffering agent) to reverse osmosis (RO) water to final concentrations of 50 mM for potassium ferricyanide and 100 mM for potassium phosphate. Potassium ferricyanide solution in the cathodic chamber was replenished with fresh solution as soon as the cathodic potential decreased below 250 mV, which represented approximately 25% decrease in the potential compared to the initial potential of a fresh potassium ferricyanide solution. This replenishment was done to maintain a relatively constant potential in the cathodic chamber thereby ensuring that only environmental conditions in the anodic chamber, where biodegradation of substrate took place, affected the resulting potential. Each experiment was initiated by adding the necessary substrate, either lactate or acetate, and inoculum into the anodic chamber. Prior to this, the open circuit potential (OCP) of the MFC was monitored for about 5 hours. This allowed the potential to stabilize and establish the baseline value. Throughout the experiment, the contents of the anodic and cathodic chambers were mixed using two small magnetic stirrers. All experiments were conducted at room temperature (24±2 °C).

3.2.3 Biodegradation of Na-lactate and Na-acetate

Batch mode of operation: Biodegradation of sodium lactate and sodium acetate, referred to as lactate and acetate for the rest of this thesis, as model organic substrates were studied separately in the MFC bioreactors. In batch operated MFCs, different concentrations of each model organic compound, specifically 1000, 2500 and 5000 mg L^{-1} of lactate or acetate ions, were evaluated.

Effects of substrate concentration on biodegradation kinetics and electrochemical outputs were investigated. Following the purging of anodic liquid with nitrogen gas and stabilization of circuit potential, lactate or acetate at the desired concentration was added to the anodic solution through the sampling port using a sterilized syringe. This was done by drawing a small quantity of the anodic liquid (approximately 5 mL) and dissolving specific amount of lactate or acetate to give the designated concentration after injecting back this concentrated solution into the anodic chamber. This was immediately followed by inoculation of the anodic chamber through addition of 1 mL of freshly prepared concentrated suspension of *P. putida* cells. The anodic chamber was sampled regularly to monitor the concentrations of biomass, lactate and acetate. At least one sample was collected daily, with higher frequency of sampling done in experiments with lower substrate concentrations in anticipation of shorter biodegradation times.

After depletion of substrate, the experiment was repeated by adding similar amount of substrate to the anodic chamber. This was conducted to investigate the effect of sequential addition of substrate on the MFC performance. However, when higher concentrations of acetate (2500 and 5000 mg L^{-1}) were tested, significantly longer biodegradation period (>768 h) was needed to completely remove the substrate. Due to time constraints, sequential addition of acetate at these concentrations was not carried out.

Continuous mode of operation: Following the completion of batch experiments, biodegradation of lactate and acetate in continuous MFC bioreactors was investigated. The MFC set-up used in these experiments was similar to those employed in batch experiments but included a peristaltic pump which allowed continuous flow of the feed into the anodic chamber at various flow rates.

Feed was prepared by adding specific amounts of lactate or acetate to modified McKinney's medium to achieve final concentrations of 5000 and 1000 mg L^{-1}, respectively. Based on the results from batch experiments that showed acetate biodegradation was considerably more challenging than lactate and the duration for complete removal was significantly longer, a lower acetate concentration of 1000 mg L^{-1} was used. This was not the case for lactate and thus a high concentration of 5000 mg L^{-1} was applied. Every batch of feed (0.25-10 L, depending on flow rate) was autoclaved at 121 °C for 30 minutes, cooled down to room temperature and then purged with nitrogen gas for about 10 minutes immediately before being used in the experiment.

The effect of lactate or acetate loading rate on biodegradation kinetics and electrochemical performance of the MFC was investigated. The MFC was run batchwise initially similar to previous batch experiments described above. Anodic chamber was monitored for the progress of substrate biodegradation. Once complete biodegradation of substrate was achieved, the system was switched to continuous mode and feed was provided to the anodic chamber using a peristaltic pump. The pump was pre-calibrated to determine the approximate flowrate at each pump setting. With lactate, feed was pumped at an initial flow rate of 2.5 mL h^{-1}. Flow rate of the feed was then increased incrementally up to a maximum value of 250 mL h^{-1}.

The anodic chamber was sampled regularly to determine biomass, lactate and biologically produced acetate (as intermediate) concentrations. At each flow rate, sufficient time was given for the system to reach steady state conditions. Steady state conditions were assumed to have been achieved when there was less than 10-15% variation in the residual concentrations of lactate and accumulated acetate. Following the establishment of steady-state conditions, MFC was operated

at the same flow rate for at least three additional residence times before switching to a higher flow rate. The average value of data and associated standard deviation obtained during this part of operation were used to present the data.

With acetate in the feed, initial flow rate was set at 1.8 mL h^{-1} and biodegradation progress was monitored until acetate biodegradation was found to have deteriorated (i.e. application of higher flow rates was not possible). Figure 3.4 shows the MFC equipped with rod electrodes operated continuously, in this case, with acetate as feed. The setup includes an intermediary glass device installed along the feed line to prevent potential contamination of feed through transfer of bacterial cells from the anodic chamber and tubings into the feed container. To ensure the desired concentration of feed, samples from the feed line at close proximity of the inlet port of the anodic chamber were collected and analyzed regularly. As indicated earlier the data obtained at steady state conditions were used to calculate the average values and associated standard deviations. Moreover, circuit potential was monitored and recorded at 20 minute intervals. Current and power were determined by applying external resistors as biodegradation occurred. Circuit potential and current measurement are described in more detail in Section 3.2.4.

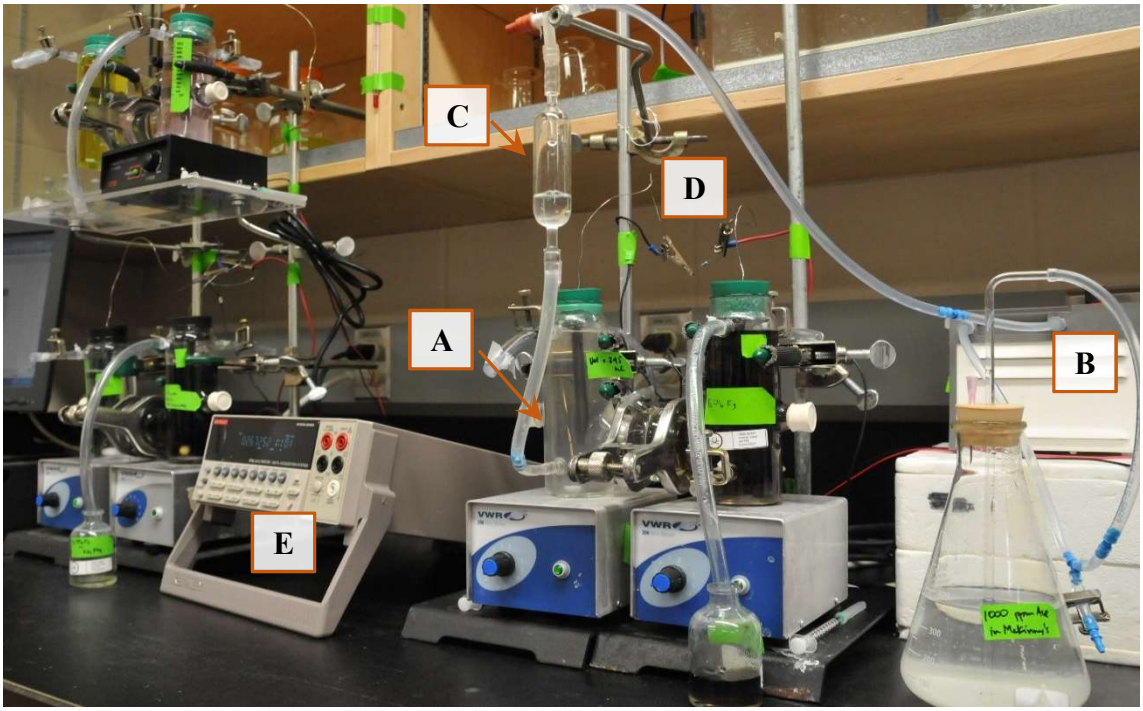

Figure 3.4 Experimental system used in continuous biodegradation of acetate in an MFC with single rod electrodes and freely suspended bacterial cells. Feed is drawn into the anodic chamber (A) using a peristaltic pump (B) passing through the intermediary glass device (C) used to prevent contamination of feed. An external resistor (D) is attached to the anode and cathode terminals which are also connected to a multimeter (E) equipped with a datalogger.

3.2.4 Analyses

Monitoring of the biodegradation process in the MFC entailed determination of biomass, lactate and acetate concentrations. Biomass concentration was determined by measuring the optical density (OD) at 620 nm using a spectrophotometer (Shimadzu Uvmini 1240). A calibration curve was developed and used to convert OD reading to biomass concentration (mg cell-dry weight L^{-1}). The OD to biomass concentration calibration curve is shown in the Appendix (Figure A.1). Immediately after measurement of OD, samples were centrifuged for 5 min at 10000 rpm (9180 ×g) using a microfuge (Microfuge 18 Centrifuge, Beckman Coulter, Fullerton, USA). The resulting supernatant liquid was collected for measurement of lactate and acetate concentrations

using a High Performance Liquid Chromatography (HPLC) instrument. The HPLC (Agilent Technologies 1200) instrument was equipped with a Di-Array detector (DAD) and a BIO-RAD Aminex Ion Exclusion column (300 mm x 7.8 mm dia.). Blank and standard solutions of lactate and acetate with concentrations in the range of 5-100 mg L^{-1} were used to develop the required calibration curves, as shown in Appendix Figures B.1-B.2, respectively. When necessary, samples were diluted with deionized water to attain the resultant chromatograph peaks within the established range of calibration.

For determination of electrochemical outputs, circuit potential of MFCs were continuously monitored and recorded using Keithley 2700 multimeters which were equipped with 7700 dataloggers (Keithley Instruments Inc., Cleveland, USA). Each set of monitoring equipment was connected to a computer and operated using its associated software (ExceLINX). In the cathodic chamber, potential was periodically measured against a Calomel reference electrode using a Fluke 189 True RMS handheld multimeter (Fluke, Everett, WA, USA) with its positive terminal connected to the cathode and negative terminal to a calomel reference electrode (Cole-Parmer, Vernon Hills, IL, USA). To determine current and power generated from the MFC, external resistors (1000-6000 ohms; You et al., 2006) were applied during the biodegradation of substrate. Resistance was applied only after potential was found stable. Immediately after the application of resistance, the potential rapidly dropped and reached a stable level typically after several hours. At this point, external resistor was removed which resulted in sudden rise of potential. Once potential was stable again, another resistance was applied. The measured closed circuit potential was then used to determine current and power, using Ohm's law (i.e. I=V/R and P=VI, where I is the current in mA, V is the measured potential in mV, R is the applied resistance in ohm and P is power in

mW). Current and power densities were calculated using the effective surface area of the electrode (submerged portion). Equivalent current and power densities in terms of anodic working volume were also calculated. Efficiency of electron recovery from the oxidation of substrate in the MFC was also determined by calculating the Coulombic efficiency (CE) as described in detail in Appendix H.

3.2.5 Biodegradation modelling

Substrate biodegradation in the MFC occurs under anaerobic or anoxic conditions. To develop an appropriate biokinetic model, lactate and acetate consumption was assessed based on the reactions that take place under anaerobic conditions. In an anaerobic environment, lactate biodegradation could occur through two pathways: 1) incomplete oxidation via reaction 3.1, leading to formation of acetate and CO_2; 2) complete oxidation, as described by reaction 3.2, leading to formation of CO_2 as the end product (Lovley et al., 1989; Call and Logan, 2011). On the other hand, anaerobic oxidation of acetate results in the formation of CO_2 as the final product (reaction 3.3). Reaction 3.3 applies to utilization of acetate either as the original substrate or as biologically produced intermediate from reaction 3.1.

$$CH_3CHOHCOO^- + 2H_2O \rightarrow CH_3COO^- + HCO_3^- + 4H^+ + 4e^- \quad (3.1)$$

$$CH_3CHOHCOO^- + 6H_2O \rightarrow 3HCO_3^- + 14\ H^+ + 12e^- \quad (3.2)$$

$$CH_3COO^- + 4H_2O \rightarrow 2HCO_3^- + 9\ H^+ + 8e^- \quad (3.3)$$

In developing a model for microbial growth and lactate biodegradation kinetics in the MFC, it was assumed that reactions 3.1, 3.2 and 3.3 were all involved as part of lactate biodegradation and

subsequent utilization of the biologically produced acetate as an intermediate. The experimental results obtained from batch experiments (described in Section 3.3.1) confirmed the validity of this assumption where no other intermediate other than acetate or any other by-product was found throughout the biodegradation process. Furthermore, it was assumed that microbial growth was coupled with lactate and acetate utilizations and followed Monod kinetics. The mass balances for biomass, lactate and acetate (as intermediate) in a MFC operated batchwise are given by equations 3.4, 3.5 and 3.6, respectively.

$$\frac{dX}{dt} = \left(\frac{\mu_{max-Lac}\, S_{Lac}}{K_{S-Lac}+ S_{Lac}} - K_{d-Lac}\right) X + \left(\frac{\mu_{max-Ace}\, S_{Ace}}{K_{S-Ace}+ S_{Ace}} - K_{d-Ace}\right) X \tag{3.4}$$

$$\frac{dS_{Lac}}{dt} = -\frac{1}{Y_{X-Lac}}\left(\frac{\mu_{max-Lac}\, S_{Lac}}{K_{S-Lac}+S_{Lac}} - K_{d-Lac}\right) X \tag{3.5}$$

$$\frac{dS_{Ace}}{dt} = \frac{1}{Y_{X-Lac}}\left(\frac{\mu_{max-Lac}\, S_{Lac}}{K_{S-Lac}+S_{Lac}} - K_{d-L}\right) X - \frac{1}{Y_{X-Ace}}\left(\frac{\mu_{max-Ace}\, S_{Ace}}{K_{S-Ace}+S_{Ace}} - K_{d-Ace}\right) X \tag{3.6}$$

All involved equations were solved simultaneously using 4th order Runge-Kutta method and Excel software. The experimental data generated from the batch tests were fitted into the model. Using least square minimization, the value of various biokinetic coefficients were determined through utilization of Solver function in Microsoft Excel (An et al., 2011; An et al., 2012). The objective function used for the least square minimization is given by equation 3.7.

$$f = \sum_i^n (S_{i-Lac-meas} - S_{i-Lac-predicted})^2 + \left(S_{i-Ace-measured} - S_{i-Ace-predic}\right)^2 + \left(S_{i-X-measured} - S_{i-X-predicted}\right)^2 \tag{3.7}$$

A similar model was also developed for the kinetics of microbial growth and biodegradation of acetate as original substrate in batch operated MFCs. The mass balances for biomass and acetate used in the biodegradation kinetic modeling are given by equations 3.8 and 3.9, respectively. Similar to modeling of lactate biodegradation, the experimental data generated from batch operated MFCs with acetate as substrate were fitted into the model and least square minimization was utilized to determine the biokinetic coefficients. Through the Solver tool in Excel, the objective function given by equation 3.10 was employed for the least square minimization.

$$\frac{dX}{dt} = \left(\frac{\mu_{max-Ace}\, S_{Ace}}{K_{S-Ace}+S_{Ace}} - K_{d-Ac}\right) X \tag{3.8}$$

$$\frac{dS_{Ace}}{dt} = -\frac{1}{Y_{X-Ace}}\left(\frac{\mu_{max-Ace}\, S_{Ace}}{K_{S-Ace}+S_{Ace}} - K_{d-Ace}\right) X \tag{3.9}$$

$$f = \sum_i^n \left(S_{i-Ace-measur} - S_{i-Ace-predic}\right)^2 + \left(S_{i-X-measured} - S_{i-X-predicte}\right)^2 \tag{3.10}$$

To assess the extent by which the predictions of the developed model was influenced by the calculated biokinetic coefficients, sensitivity analysis was conducted. This was carried out by varying a particular coefficient at 10% intervals within a range up to 50% above and below the best fit value, while maintaining other coefficients constant (An et al., 2011; An et al., 2012). Following least square minimization, the sum of squared differences (SSD) based on the measured and predicted values of biomass, lactate, and acetate concentrations (equation 3.7) was calculated for each varied parameter. The ratio of SSD calculated with the varied parameter over the SSD calculated with the best fit parameter was then determined as the normalized sum of squared differences (NSSD). The NSSD represents the degree by which the variation of a particular

coefficient affects the predicted results. The sensitivity of the model to each coefficient was then assessed by evaluating the effect of coefficient variation on the NSSD value. Similar procedures were employed to assess sensitivity of biokinetic model for biodegradation of acetate as original substrate with SSD calculations using the objective function given by equation 3.10.

3.3 Results and discussion

3.3.1 Batch mode of operation

Biodegradation of lactate at various concentrations from 1000 to 5000 mg L^{-1} were carried out in MFCs equipped with single rod electrode and operated batchwise with freely suspended cells. The profiles of biomass, lactate and acetate concentrations as well as open circuit potential during the biodegradation of 1000 mg L^{-1} lactate is shown in Figure 3.5.

Results showed that after inoculation with *P. putida*, gradual increase in biomass concentration was observed coupled with a continual decrease in lactate concentration. This pattern was accompanied by a sudden rise in MFC open circuit potential (OCP). During this initial stage, only changes in lactate and biomass concentrations and OCP were observed (i.e. no acetate was detected), despite the expected production of an intermediary product as has been commonly observed in biological systems including those in the present work during sub-culturing of *P.* putida in shake flasks. As discussed previously in Section 3.2.5, acetate could be biologically produced as an intermediary product of lactate biodegradation (shown in reaction 1). Formation of acetate was indeed observed but only after a lag period. Acetate was detected at around 125 h after inoculation and continued to accumulate afterwards.

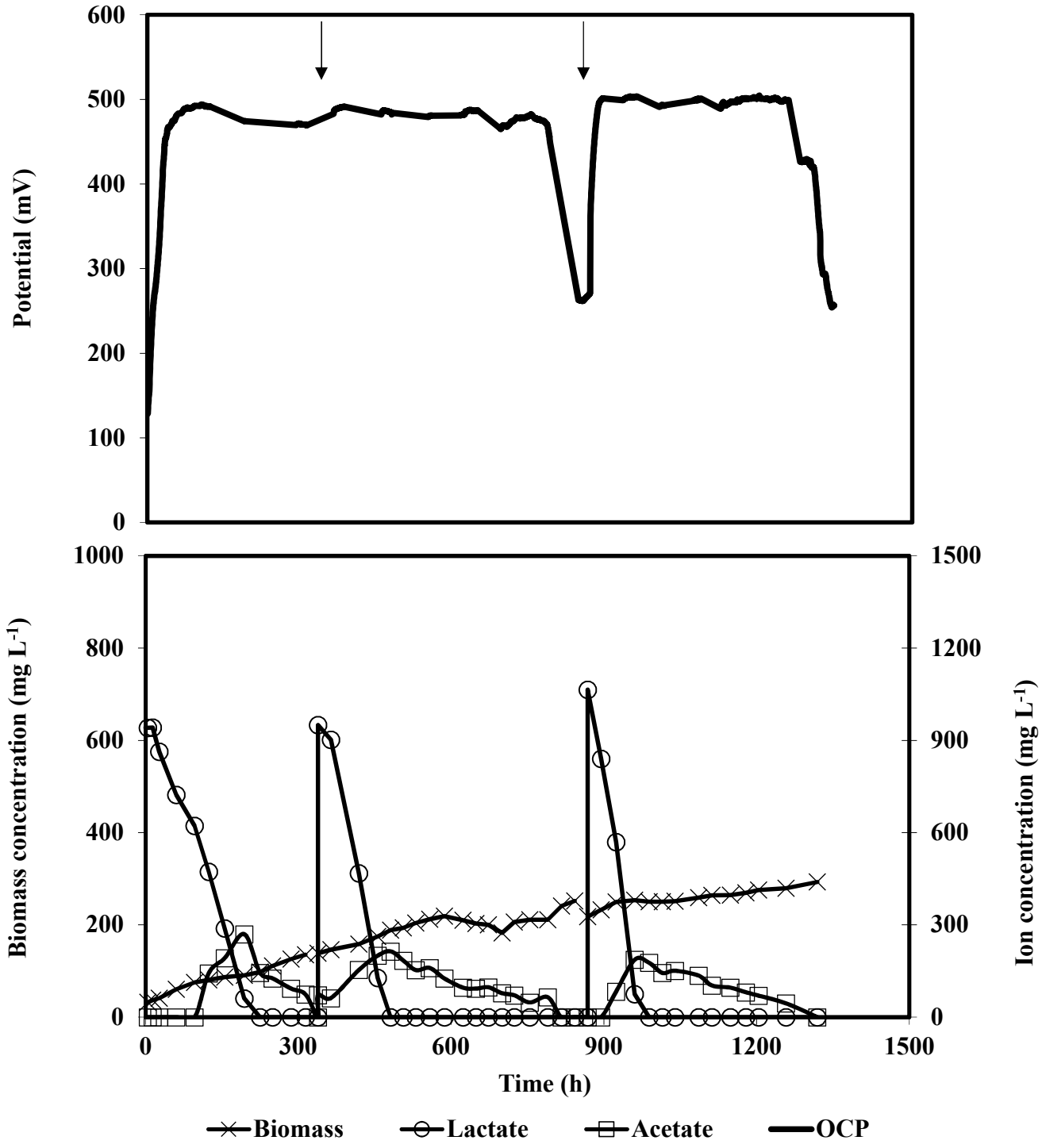

Figure 3.5 Profiles of biomass, lactate, and acetate concentrations and open circuit potential during the biodegradation of a 1,000 mg L^{-1} lactate in batch MFCs. Arrows indicate sequential addition of lactate.

Acetate was the only intermediary product identified throughout the oxidation of lactate even after complete exhaustion of the lactate as the original substrate. One could speculate that intermediates other than acetate, such as pyruvate, could have formed during this period as well. However, examination of the samples taken during the lag period and those collected in the remainder of experiments by HPLC did not show any additional peak, even after running the samples in the HPLC for a prolonged period covering the retention times of all potential intermediates. This could indicate that within the lag period, lactate was completely oxidized into CO_2 thereby biodegradation occurring exclusively through reaction 3.2. The formation of acetate after 125 h persisted and its accumulation continued until complete exhaustion of lactate. It is important to note that the amount of accumulated acetate was less than that expected from the stoichiometry of reaction 3.1. For instance, based on reaction 3.1 incomplete biodegradation of 1,000 mg L^{-1} lactate should lead to accumulation of 708 mg L^{-1} acetate. However, maximum concentration of accumulated acetate in this case was only 270 mg L^{-1}. This finding clearly indicated that after the lag period, reactions 3.1, 3.2 and 3.3 occurred simultaneously. In other words, portion of biologically produced acetate underwent biodegradation at the same time as the lactate.

Immediately after the exhaustion of lactate, a slow but continual decrease in the concentration of accumulated acetate was observed, as shown in Figure 3.5 at 225 h. This was accompanied by further increase in biomass concentration which showed a sustained biodegradation activity indicating minimal or non-existent effect of the transition in the utilization of lactate to biologically produced acetate (i.e. diauxic growth was not evident). Decrease in the concentration of accumulated acetate continued and just before its complete exhaustion another batch of lactate at a final concentration of 1,000 mg L^{-1} was added to the anodic chamber. The freshly added lactate

was utilized by the microbial cells immediately resulting in further increase in biomass concentration and accumulation of acetate. Similar to results of the first batch, detection of biologically produced acetate occurred only after a lag and at concentrations which were lower than those expected from the stoichiometry. Furthermore, concentration of accumulated acetate decreased only after the exhaustion of lactate, indicated by the cessation of acetate production and that only acetate utilization was occurring.

Lactate and accumulated acetate profiles were reproduced when lactate (~1000 mg L^{-1}) was added to the anodic solution for the third time. The addition of another batch of lactate led to further increase in biomass concentration. It is important to note that lactate concentration profiles showed different patterns in these sequential batch runs and lactate biodegradation appeared to proceed faster as further batches were run. To quantify this variation, the biodegradation rate of lactate was calculated using the slope of the linear part of lactate concentration profiles. This confirmed that lactate biodegradation rates were faster in the succeeding batches with calculated biodegradation rates being 4.6, 7.1, and 9.5 mg L^{-1} h^{-1} in the first, second, and third batches, respectively. The increase in biodegradation rate could be attributed to the increase in biomass concentration in the anodic chamber after each sequential batch. In contrast, biodegradation rate of accumulated acetate showed no particular trend throughout the 3 batches and proceeded at a rate which was much slower than that of lactate with rates being 0.6, 0.8 and 0.5 mg L^{-1} h^{-1} for the first, second and third batches, respectively.

Lactate biodegradation at higher initial concentrations of 2500 and 5000 mg L^{-1} was also evaluated and results are shown in Figures 3.6 and 3.7, respectively. In both experiments, profiles of biomass,

lactate and accumulated acetate concentrations, as well as OCP, were observed to behave similarly with corresponding profiles during the biodegradation of 1000 mg L^{-1} lactate. This finding further attests to the consistency of the observed trends. With 2500 and 5000 mg L^{-1} lactate, the formation of biologically produced acetate was also detected only after a lag period, indicating repeatability of the occurring phenomenon. The detection of biologically produced acetate was observed at 250 and 350 h after inoculation in the experiment with 2500 and 5000 mg L^{-1} lactate, respectively. The lag period in all experiments was found to be dependent on the initial lactate concentration. A longer lag period was observed to transpire at higher concentrations of lactate. Furthermore, at these initial lactate concentrations, the level of biologically produced acetate was also significantly below the stoichiometric amount expected from equation 3.1. The incomplete biodegradation of 2,500 and 5,000 mg L^{-1} lactate should have led to accumulation of 1,770 and 3,535 mg L^{-1} acetate but actual maximum concentrations of accumulated acetate were only 676 and 2,110 mg L^{-1}, respectively. These findings again suggest that after the lag period, all three reactions took place simultaneously.

Due to the considerably longer period required for complete biodegradation of lactate and the resulting accumulated acetate at 2,500 and 5,000 mg L^{-1} lactate, a third sequential batch test was not carried out. Similarly, given that the much lower maximum accumulated acetate concentration from the biodegradation of 2,500 mg L^{-1} lactate needed approximately 900 h to be fully degraded, biodegradation of accumulated acetate in the experiment with 5,000 mg L^{-1} lactate was monitored for only 200 h after reaching maximum concentration, and then the experiment was terminated.

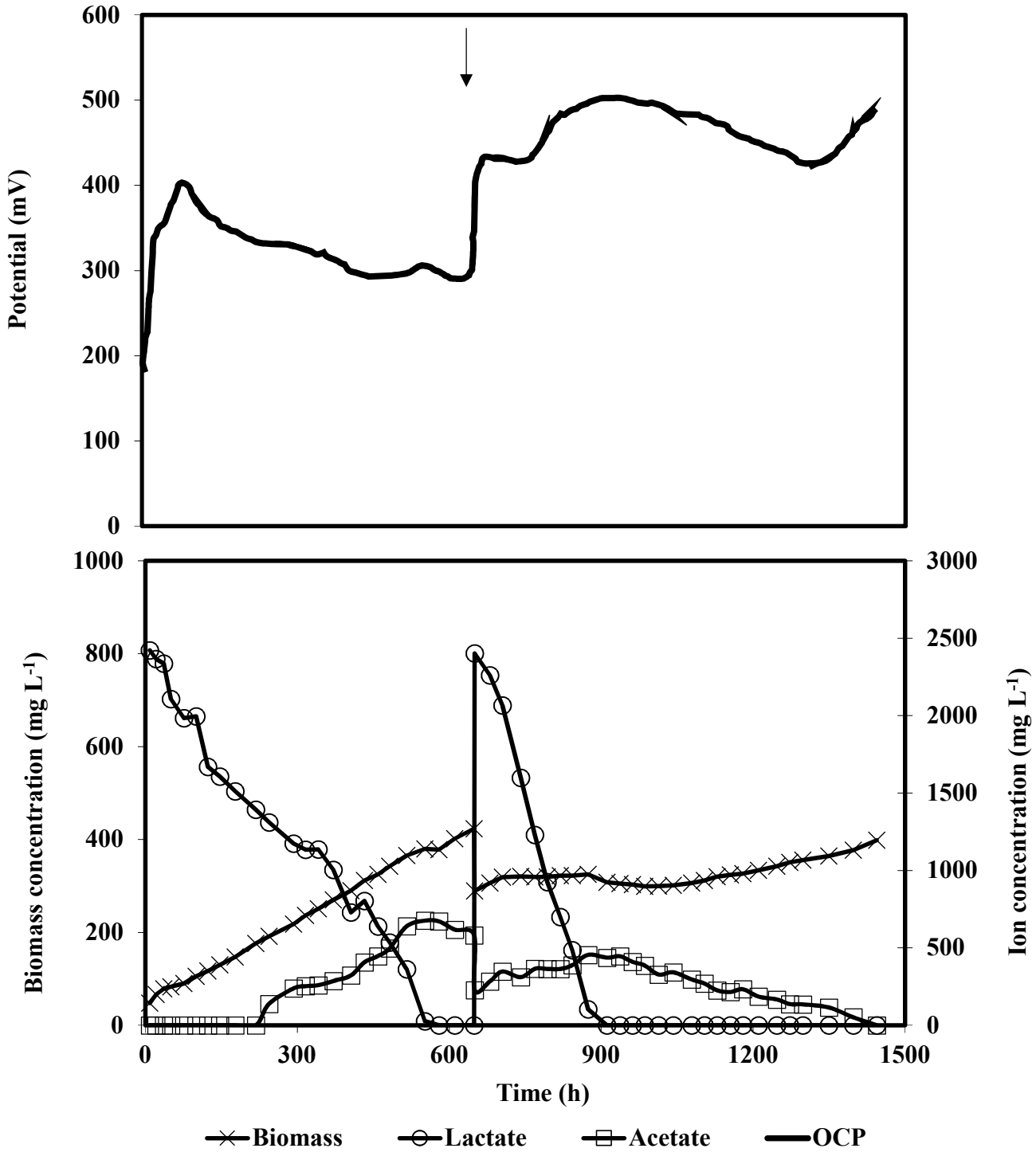

Figure 3.6 Profiles of biomass, lactate, and acetate concentrations and open circuit potential during the biodegradation of 2,500 mg L^{-1} lactate in batch MFCs. Arrows indicate sequential addition of lactate.

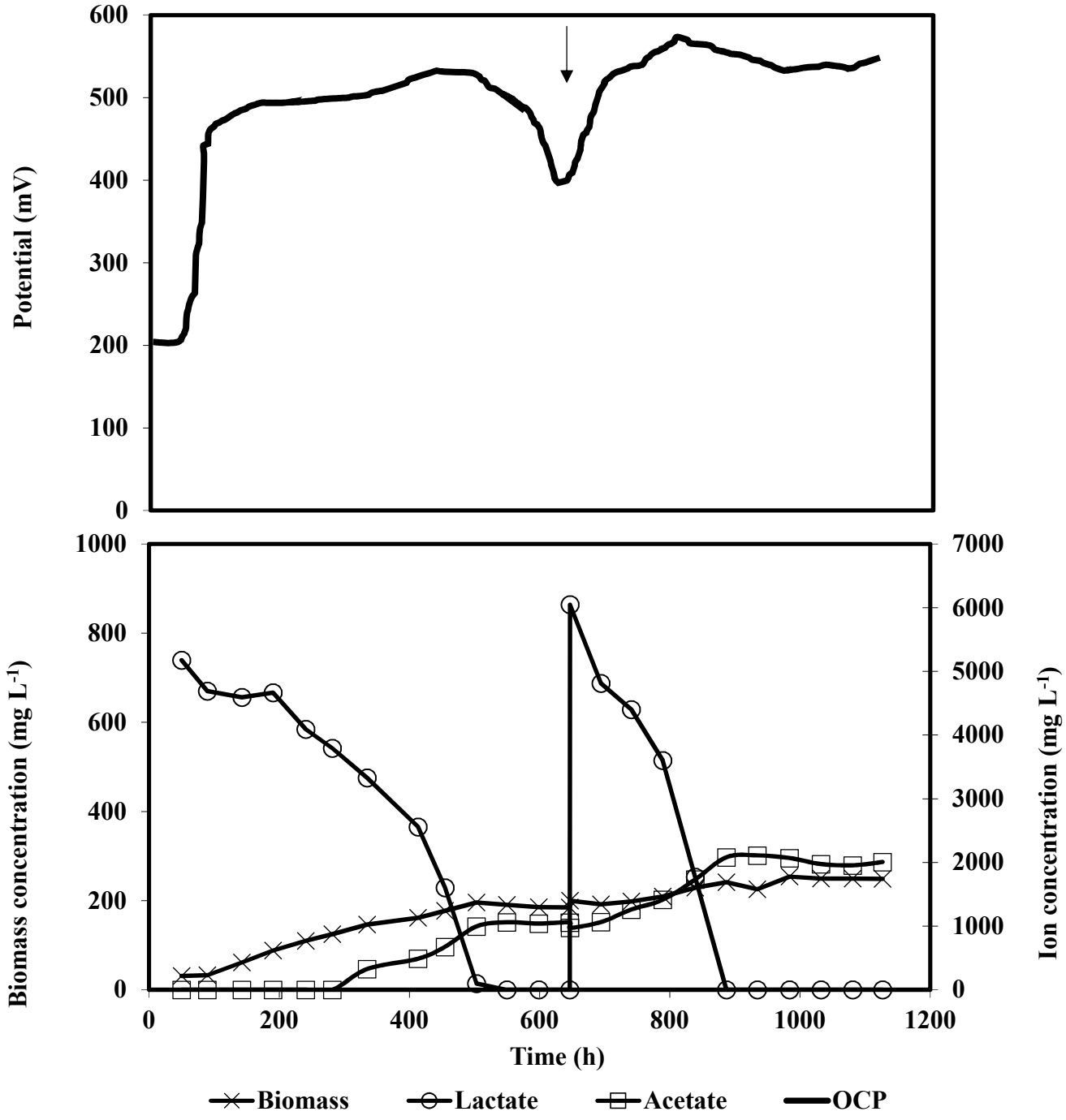

Figure 3.7 Profiles of biomass, lactate, and acetate concentrations and open circuit potential during the biodegradation of 5,000 mg L^{-1} lactate in batch MFCs. Arrows indicate sequential addition of lactate.

As experiments proceeded, there were few instances where volume of liquid in the anodic chamber had to be replenished after multiple withdrawals of sample especially in experiments that required more frequent collection of samples. This was carried out by injecting sterile McKinney's medium into the anodic chamber which resulted in dilution and decrease in concentrations of biomass and remaining accumulated acetate. To minimize this effect, the bulk of replenishment was done after complete exhaustion of lactate and immediately before addition of another batch of fresh lactate such as that shown in Figure 3.6 at approximately 650 h which resulted to an abrupt decrease in biomass and accumulated acetate concentrations after adding 95 mL of McKinney's medium.

Calculating average values of lactate biodegradation rate as function of its initial concentration would not necessarily be representative due to its incremental increases with every sequential batch run which appears more pronounced with higher initial lactate concentration. In fact, calculated standard deviations were highest with 5,000 followed by 2500 and 1000 mg L^{-1} lactate with the values being 7.3, 4.4 and 2.5 mg L^{-1} h^{-1}, respectively. As an alternative approach, a trendline was constructed incorporating all biodegradation rates across all lactate concentrations. As projected by the trendline (Figure 3.8), it can be observed that biodegradation rate increases with initial lactate concentration. Using the linear function representing this line, lactate biodegradation rates at initial concentration of 1,000, 2,500 and 5,000 mg L^{-1} were calculated as 5.73, 10.08 and 17.33 mg lactate L^{-1} h^{-1}, respectively. It is also important to note that the determination of lactate biodegradation rates (i.e. slope of lactate concentrations with respect to time) was considerably accurate with corresponding trendlines registering R^2 values above 0.95.

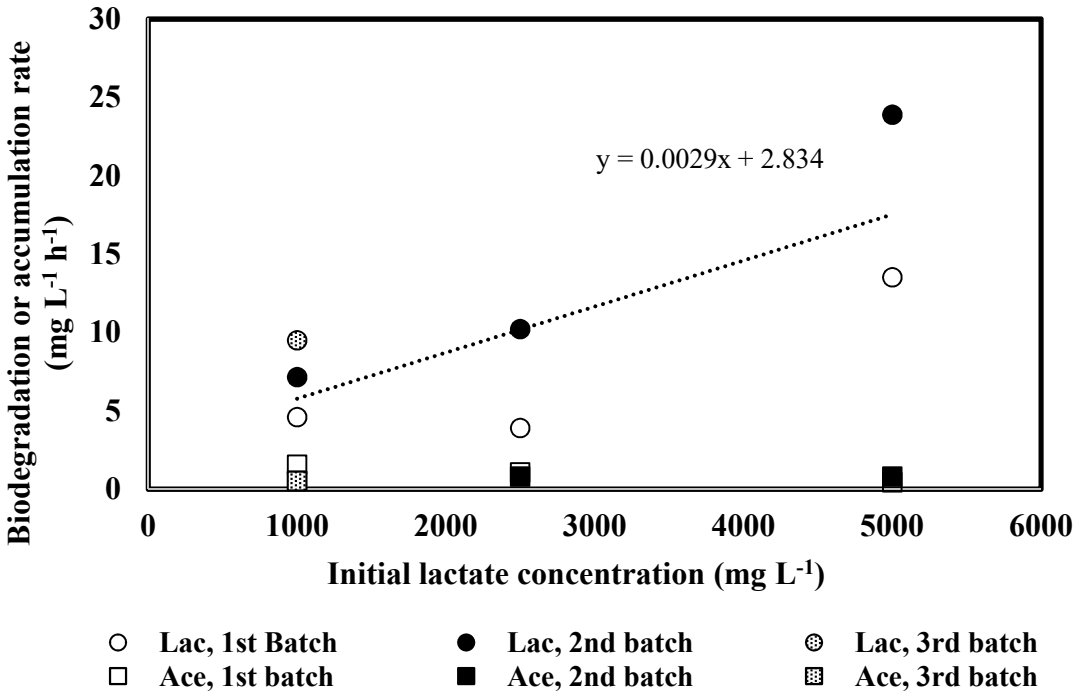

Figure 3.8 Biodegradation rates of lactate and accumulation rate of acetate obtained at different sequential batch tests in MFCs fed with lactate at various initial concentrations. Trendline represents all lactate biodegradation rates.

Results reveal a potentially high capacity of *P. putida* in its ability to utilize lactate in the MFC, given that time spent for the degradation of 2500 and 5000 mg L^{-1} lactate was relatively the same (580 vs 550 h). This indicates that the activity of *P. putida* and the performance MFC system as a whole was not negatively impacted by the exposure to considerably high concentrations of lactate. No known substrate inhibition by lactate has been reported to have occurred in a MFC. Similar results were reported by Call and Logan (2011) and Jung and Regan (2007) where their respective MFC systems were able to effectively degrade approximately 1000 mg L^{-1} lactate. In fact, the complete oxidation of 10 mM lactate by *Geobacter sulfurreducens* within roughly 4 days in the work by Call and Logan (2011) results to a calculated biodegradation rate of 9.4 mg L^{-1} h^{-1} which is within the range of biodegradation rates achieved in this study.

In a similar manner the linear portion of acetate concentration profiles in all tested lactate concentrations were identified and the corresponding slope was determined as the accumulation rate of acetate. In all experiments with different lactate concentrations, the accumulation of biologically produced acetate proceeded at a rate much slower than that of lactate biodegradation rate. For instance, at the initial lactate concentration of 5,000 mg L^{-1}, the acetate accumulation rate was as much as a 31 fold slower than the corresponding lactate biodegradation rate. As shown in Figure 3.8, accumulation rates of acetate were not affected by sequential batch operation with variation within each tested lactate concentration noticeably small. Specifically average rates of acetate accumulation during the experiments with 1,000, 2,500 and 5,000 mg L^{-1}were calculated as 0.85±0.59, 0.92±0.18 and 0.61±0.26 mg L^{-1} h^{-1}, respectively.

The results of biodegradation of 1,000, 2,500 and 5,000 mg L^{-1} acetate in MFCs operated batchwise and with suspended cells of *P. putida* are shown in Figures 3.9-3.11. With acetate as original substrate, microbial activity led to a constant decrease in acetate concentration until complete exhaustion of the substrate. This was accompanied by a sharp increase in OCP. After complete exhaustion of 1,000 mg L^{-1} acetate, which occurred 286 h after inoculation, another batch of 1,000 mg L^{-1} acetate was added to the anodic chamber that was immediately utilized by the microbial population. Complete exhaustion of the second batch of 1,000 mg L^{-1} acetate transpired at the same timeframe as the initial batch taking effect exactly 286 h after the sequential addition.

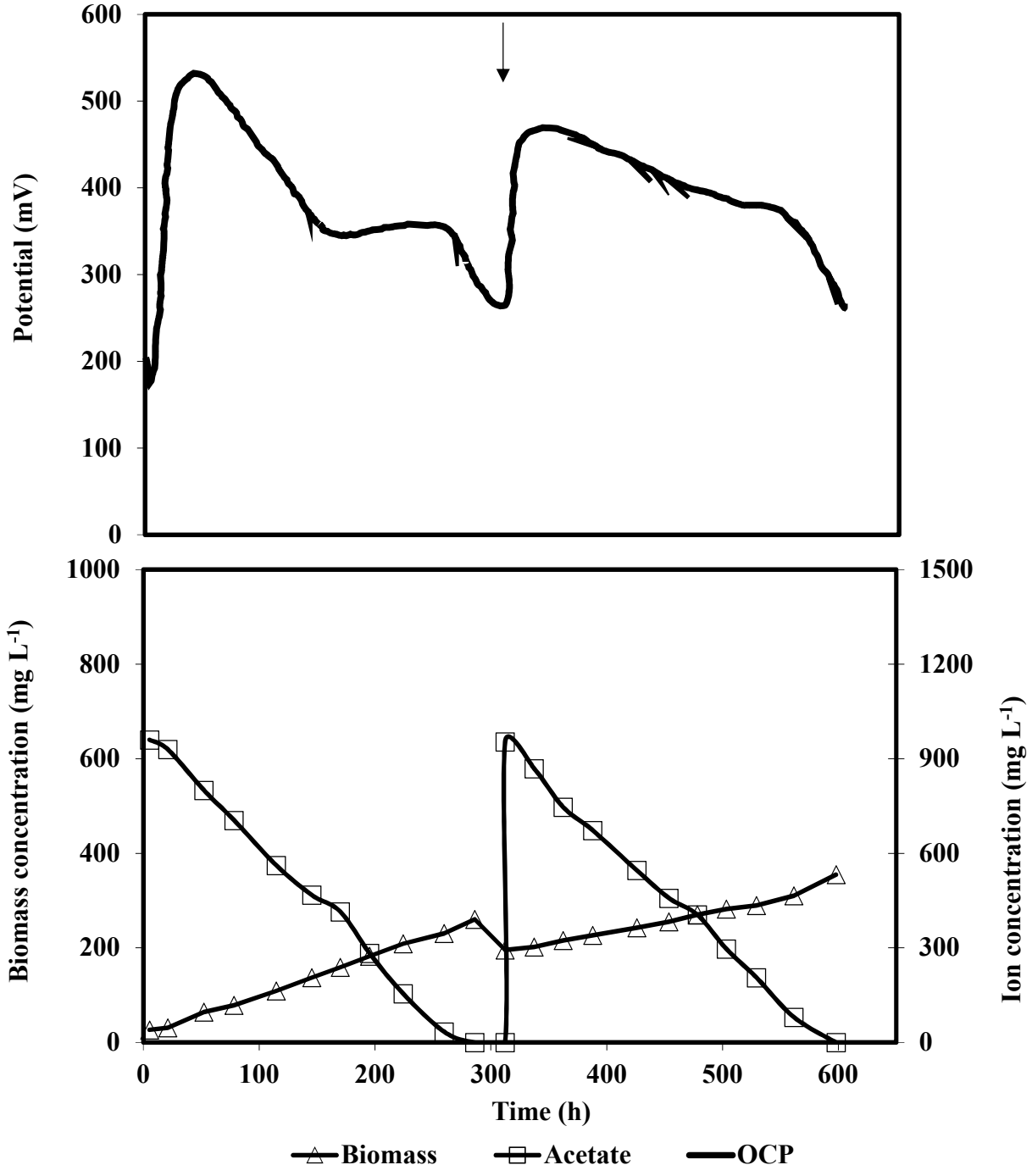

Figure 3.9 Profiles of biomass and acetate concentrations and open circuit potential during the biodegradation of 1,000 mg L^{-1} acetate in batch MFCs. Arrow indicates sequential addition of acetate.

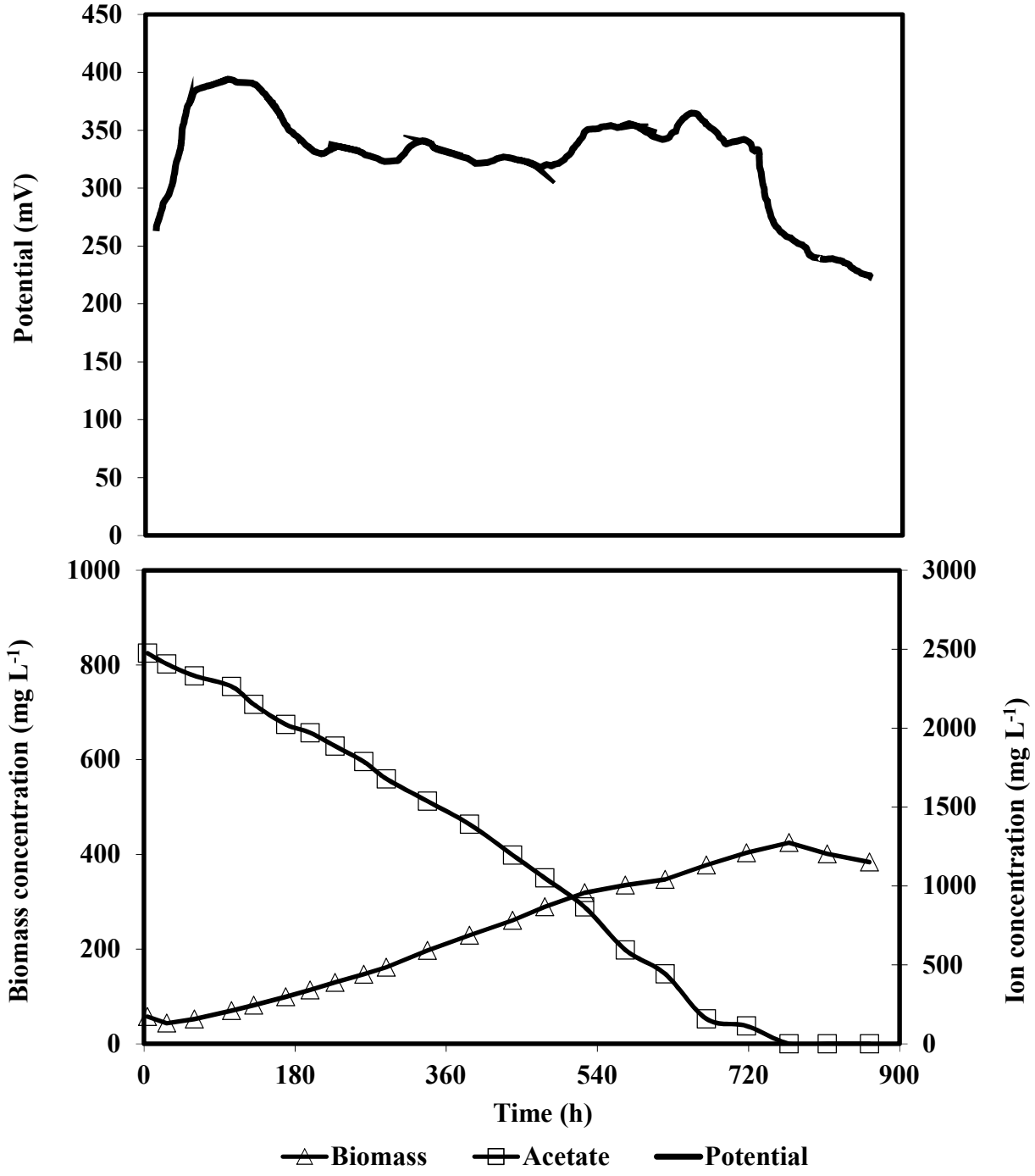

Figure 3.10 Profiles of biomass and acetate concentrations and open circuit potential during the biodegradation of 2,500 mg L^{-1} acetate in batch MFCs.

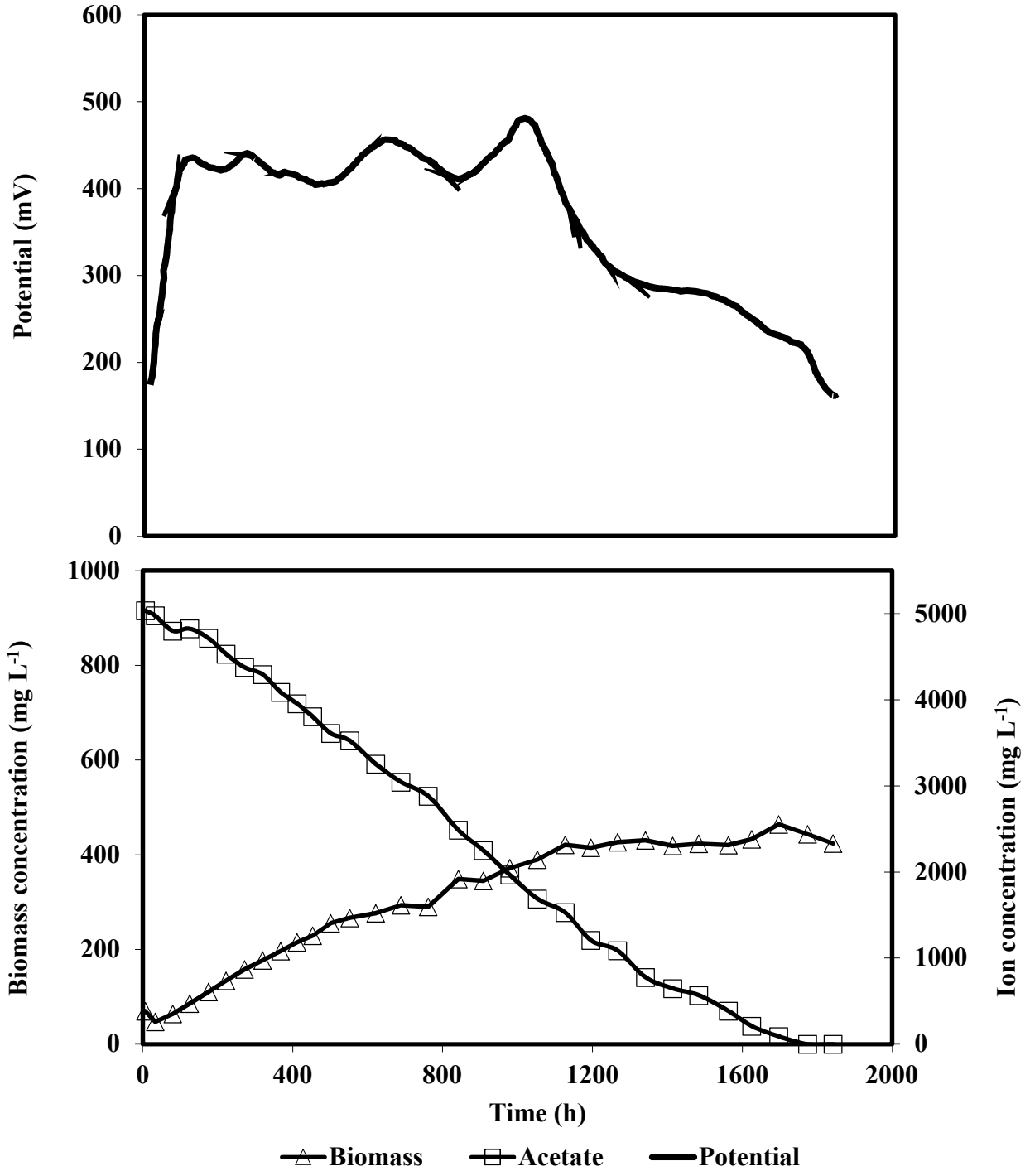

Figure 3.11 Profiles of biomass and acetate concentrations and open circuit potential during the biodegradation of 5,000 mg L^{-1} acetate in batch MFCs.

At higher initial concentrations of 2,500 and 5,000 mg L^{-1} acetate, complete exhaustion of acetate took longer at 768 and 1775 h, respectively. Moreover, with higher concentrations of acetate, a very short period of decline in biomass concentration was detected immediately after inoculation, which was not observed with 1,000 mg L^{-1} acetate. Sudden exposure to higher concentrations of acetate could have required the microbial community to go through a very short adaptation period before resuming its growth. Relative to the total length of time spent for complete exhaustion of acetate, this adjustment period (within 23 and 26 h for 2,500 and 5,000 mg L^{-1} acetate, respectively) was considerably short, specifically 3% and 1.5% of the total degradation time, respectively, and did not affect overall acetate utilization.

As shown in Figure 3.9, biomass concentration further increased with the provision of another batch of 1,000 mg L^{-1} acetate. However, no noticeable improvement in the rate of acetate utilization was observed with biodegradation rates in the first and second batches being 3.6 and 3.4 mg L^{-1} h^{-1}, respectively. Given the significant length of time needed for complete exhaustion of 2,500 and 5,000 mg L^{-1} acetate, sequential batch addition was not carried out at these concentrations.

Contrary to that observed with lactate, with 1,000 mg L^{-1} acetate sequential batches led to biodegradation rates that were close. Another finding that contrasted with lactate was that the acetate biodegradation rate showed no improvement with increase in acetate initial concentration. Biodegradation rates in MFCs operated with 1,000, 2,500 and 5,000 mg L^{-1} acetate were relatively close at 3.6, 3.4 and 3.1 mg L^{-1} h^{-1}, respectively. Determination of acetate biodegradation rates was considerably accurate with resulting R^2 values greater than 0.99.This result suggests that the rate

of acetate biodegradation is not influenced by the initial concentration. Furthermore, the resulting acetate biodegradation rates were as much as 8-fold lower than those obtained from lactate at the same initial concentration, indicating that acetate was considerably more difficult to degrade than lactate and that lactate was the preferred substrate when compared with acetate.

Biodegradation rates of acetate were lower than those when lactate was utilized as substrate. This finding could be attributed to the standard reduction potential (E^0) resulting from the oxidation of either substrate which is also directly related to the change in Gibbs free energy of said reactions. Lactate represents a lower standard potential or a larger negative redox potential value than acetate. This means that lactate is a stronger reducing substrate possessing a higher electron-transfer potential than acetate. As discussed by Logan et al. (2006), the Gibbs free energy is a measure of the maximal work that can be derived from the oxidation of substrate which can then be harnessed by the system including that for microbial activity. Although there is no strict connection between the standard reduction potential or Gibbs free energy changes and microbial activity, it is often observed that the utilization of electron donors which allow higher levels of Gibbs free energy changes leads to higher microbial activity and consequently faster substrate utilization rates (Rabus et al., 2006).

Power, current and OCP: A correlation between microbial activity and open circuit potential (OCP) of the MFC was observed where OCP rose rapidly from a range of 150–200 mV to 400–500 mV as bacteria grew and utilized lactate. During the biodegradation, the rising trend of OCP started to level off and eventually decreased as the substrate was consumed. With acetate as the original substrate microbial activity led to a sharp increase in open circuit potential from initial

values of 130-230 mV to values in the range of 385-530 mV. Moreover, measurements of cathodic and anodic potentials with respect to a reference electrode showed that the overall circuit potential of MFC was dictated by the level of the anodic potential. As microbial activity progressed, the level of anodic potential decreased which consequently resulted in the rise of the MFC circuit potential. On the other hand, the level of cathodic potential showed a gradual decrease due to the reduction of potassium ferricyanide as the experiment progressed.

In terms of power and current output, MFC operated with 1000 mg L^{-1} lactate produced average power and current densities of 0.21 ± 0.20 mW m^{-2} and 5.57 ± 2.18 mA m^{-2}, respectively. At the higher initial concentrations of 2500 and 5000 mg L^{-1} lactate, power and current densities were considerably higher with 2.18 ± 1.07 mW m^{-2} and 39.75 ± 5.18 mA m^{-2} and 1.44 ± 0.49 mW m^{-2} and 29.47 ± 8.44 mA m^{-2}, respectively. In terms of anodic chamber working volume, equivalent power and current densities generated in MFCs operated with 1000, 2500 and 5000 mg L^{-1} lactate were 1.26 ± 1.22, 8.92 ± 5.85, 8.11 ± 2.53 mW m^{-3} and 32.99 ± 13.24, 154.66 ± 19.83, 165.16 ± 37.44 mA m^{-3}, respectively. Taking into account the resulting biodegradation rates which were found to be faster at higher lactate concentrations, these results suggest direct correlations between initial lactate concentration, biodegradation rate and power and current output.

The extent of power and current generated was directly affected by the efficiency of electron recovery as indicated by corresponding coulombic efficiencies. At 0.17%, CE at 1000 mg L^{-1} lactate was the lowest and coupled that with its corresponding low biodegradation rate likely resulted to its substantially low power and current output. Between the improved amounts of power and current at the higher initial concentrations, output at 2500 mg L^{-1} lactate was slightly higher,

despite the lower biodegradation rate (10.1 vs 17.3 mg L^{-1} h^{-1}), most likely due to its greater efficiency in electron recovery which attained a higher CE of 1.71% as compared to that from 5000 mg L^{-1} which was only 0.20%.

With acetate as substrate, biodegradation rates, power and current outputs were not affected by acetate initial concentration. At acetate concentrations of 1000, 2500 and 5000 mg L^{-1}, average power densities achieved were 1.60 ± 0.73, 0.45 ± 0.58 and 0.84 ± 0.44 mW m^{-2} respectively, while current densities were 24.48 ± 13.65, 9.35 ± 2.22 and 17.12 ± 4.10 mA m^{-2} respectively. This trend conforms to that with acetate biodegradation rates which were not also affected by initial concentration. This finding further confirms the correlations between initial concentration, biodegradation rate and power and current output as observed previously with lactate. Furthermore, similar to that observed with lactate, power and current outputs were directly influenced by CE. Corresponding CE at concentrations of 1000, 5000 and 2500 mg L^{-1} acetate, where sequence shows highest to lowest energy output, were 1.14%, 0.90%, 0.51%, respectively. This finding reveals that with relatively similar biodegradation rates, efficiency of electron recovery was the significant factor in the resulting energy output. The equivalent power and current densities in terms of anodic working volume attained at 1000, 2500 and 5000 mg L^{-1} acetate were 9.00 ± 4.33, 2.55 ± 3.33 and 4.34 ± 2.05 mW m^{-3} and 138.87 ± 82.22, 51.96 ± 13.68, 90.96 ± 22.85 mA m^{-3}, respectively.

When comparing the substrates used, power and current output generated using lactate were generally higher than those from acetate. Specifically, maximum power and current densities obtained using lactate were higher with 3.30 mW m^{-2} and 48.19 mA m^{-2}, respectively, than those

from acetate with 2.28 mW m^{-2} and 40.18 mA m^{-2}, respectively. Again, this finding is consistent with the indicated correlation considering that lactate achieved higher biodegradation rates. The higher energy output generated from lactate over acetate was also observed by Jung and Regan (2007) where average maximum power and current values were higher in lactate-fed MFCs than in acetate-fed systems.

The power densities achieved in this study are consistent with those reported from MFCs operated with lactate as sole substrate. Kim et al. (2002) provided 890 mg L^{-1} lactate to a dual-chamber MFC inoculated with *Shewanella putrefaciens* IR-1 and reported a maximum power density of 0.64 mW m^{-2}. In similar dual-chamber MFCs, higher power densities of 14 and 10 mW m^{-2} were achieved when operated with 445 mg L^{-1} lactate and *S. putrefaciens* W3-18-1 (Bretschger et al., 2009) and 1,600 mg L^{-1} lactate and *S. oneidensis* MR-1 (Manohar and Mansfeld, 2009), respectively. With acetate as original substrate, power densities achieved from other studies employing similar MFC operation were generally higher. Min et al. (2005b) and Bond and Lovely (2003) used acetate in dual-chamber MFCs inoculated with *Geobacter Spp*. and reported power densities of 40 and 49 mW m^{-2}, respectively. It should be noted, however, that direct comparison of power output may not necessarily be accurate due to variations in terms of MFC configuration, experimental conditions, and microbial cultures used in different works. More importantly, this work utilized a relatively simple MFC configuration which allowed evaluation of biodegradation kinetics more reliably (main objective of this study) rather than generating high power output.

3.3.2. Kinetic modelling of biodegradation processes

To model the microbial growth and biodegradation kinetics, results from each first batch run at different initial concentrations obtained in the sequentially operated MFCs were used. In experiments where MFC was operated with lactate as substrate, results consistently revealed the occurrence of a delay in the formation of biologically produced acetate, while no other intermediate was detected during this period. A close look at lactate concentration profiles revealed that biologically produced acetate was only detected when the ratio of residual to initial lactate concentration (designated as R) reached a value of approximately 0.65, corresponding to a period where 35% of the initial lactate concentration had been utilized. This remarkable finding was consistent and observed in all experiments, regardless of lactate initial concentration. The value of R specifies that when R≥0.65, no acetate formation was observed and biodegradation of lactate occurred exclusively through reaction 3.2. On the other hand, when the ratio decreases to values below 0.65 (R<0.65) due to further consumption of lactate, accumulation of acetate was observed indicating that from this stage onward reactions 3.1, 3.2 and 3.3 were involved until complete exhaustion of lactate wherein reaction 3.3 became the only occurring reaction. The decrease in concentration of accumulated acetate observed only after complete exhaustion of lactate indicates a preference for lactate over acetate as substrate. To accommodate the delay in acetate accumulation into the proposed model, a modification was done with the inclusion of R in the model as described below:

If $R \geq 0.65$ $\quad \frac{dS_{Ace}}{dt} = 0$ (3.11)

If $R < 0.65$ $\quad \frac{dS_{Ace}}{dt} = F\left[\frac{1}{Y_{X-Lac}}\left(\frac{\mu_{max-Lac}S_{Lac}}{K_{S-Lac}+S_{Lac}} - K_{d-Lac}\right)X\right] - \frac{1}{Y_{X-Ace}}\left(\frac{\mu_{max-Ace}S_{Ace}}{K_{S-Ace}+S_{Ace}} - K_{d-Ace}\right)X$ (3.12)

Since the formation of biologically produced acetate is dependent on the biodegradation of lactate and taking into account the fact that the amount of accumulated acetate was considerably lower than the expected stoichiometric value from reaction 1, an additional coefficient (F) which accounted for the proportion of reactions through which lactate degradation occurred was also introduced into the proposed model as shown in Eq. 3.12. More specifically, F=0 corresponds to complete lactate oxidation via reaction 3.2, F=1 corresponds to incomplete oxidation through reaction 3.1 while 0<F<1 corresponds to a combination of reactions 3.1 and 3.2 with F defining the proportion of these reactions. The closer F is to 0, the lower is the amount of biologically produced acetate. For the biodegradation of acetate as original substrate, no modification to the proposed model was required.

The goodness of fit of model predictions (solid lines) for biomass growth, lactate biodegradation and acetate accumulation with the corresponding experimental data (symbols) in batch operated MFCs with 1000, 2500 and 5000 mg L^{-1} lactate are shown in Figure 3.12, panels A, B, and C, respectively. The various biokinetic coefficients determined from accurate predictions based on the developed model are summarized in Table 3.2. As seen in all cases, the predicted lines show considerable accuracy in predicting the trend of experimental data.

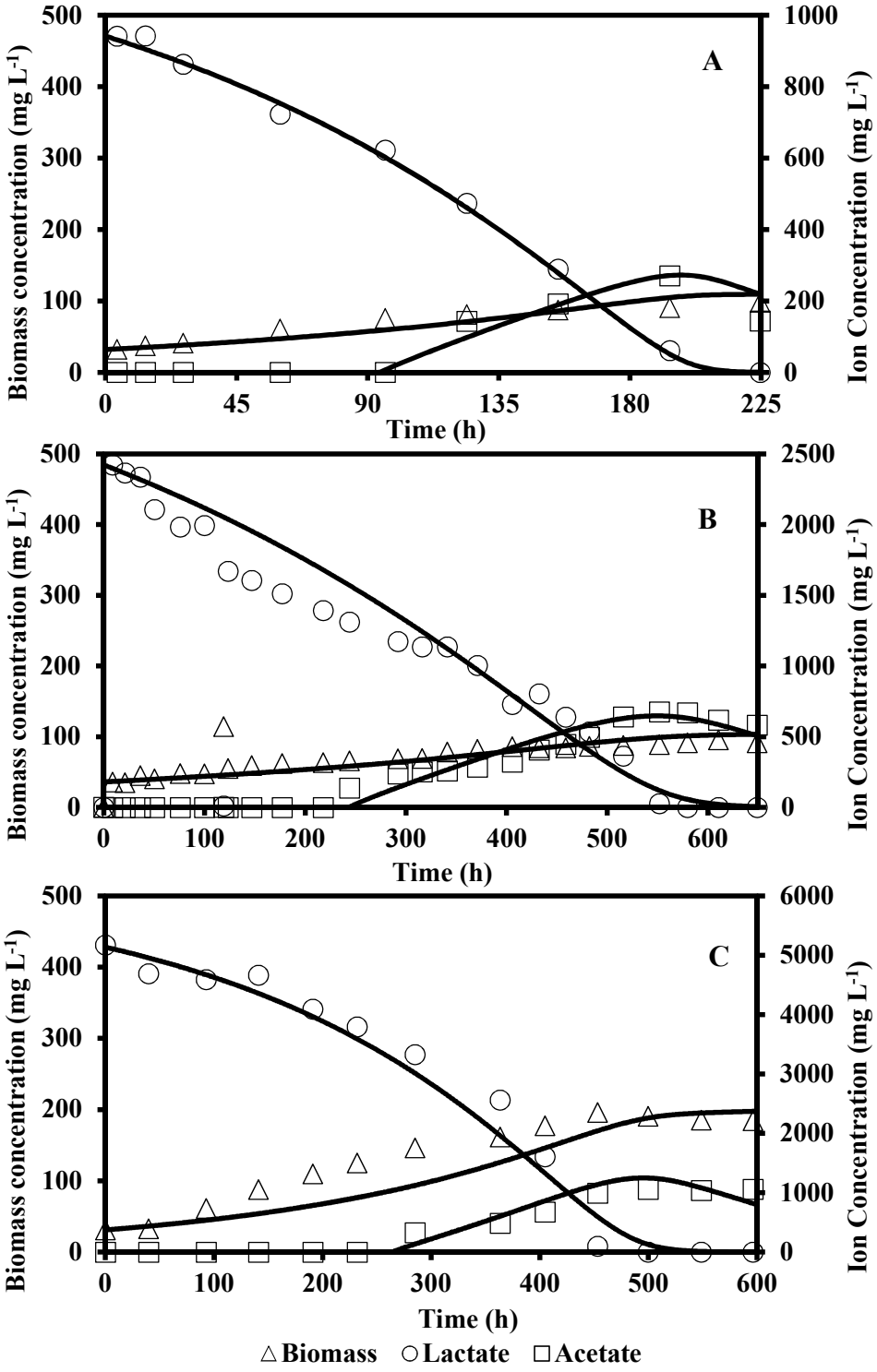

Figure 3.12 The goodness of fit of model predictions (solid lines) and experimental data (symbols) for biomass growth, lactate biodegradation and acetate formation and consumption in batch microbial fuel cells operated with 1,000 mg L^{-1} (A), 2,500 mg L^{-1} (B) and 5,000 mg L^{-1} (C) lactate. This figure is derived in part from an article published in Bioprocessing and Biosystems Engineering Jan 2015 Springer Berlin Heidelberg, available online: https://doi.org/10.1007/s00449-014-1240-3.

Table 3.2 Biokinetic coefficients for biodegradation of lactate and accumulation of biologically produced acetate in batch operated MFCs with suspended cells of *P. putida*.

Coefficient	Lactate concentration (mg L^{-1})		
	1000	**2500**	**5000**
$\mu_{max\text{-}Lac}$ (h^{-1})	0.0068	0.0022	0.0043
$K_{S\text{-}Lac}$ (mg Lac L^{-1})	49.98	228.90	479.80
$Y_{X\text{-}Lac}$ [mg cell-dry weight (mg Lac)$^{-1}$]	0.0808	0.0261	0.0303
F	0.80	0.76	0.69
R	0.6500	0.6500	0.6500
$\mu_{max\text{-}Ace}$ (h^{-1})	0.0002	0.0002	0.0002
$K_{S\text{-}Ace}$ (mg Ace L^{-1})	119.10	120.00	109.90
$Y_{X\text{-}Ace}$ [mg cell-dry weight (mg Ace)$^{-1}$]	0.0041	0.0061	0.0061

As shown in Table 3.2, the highest microbial activity observed during the operation of MFC was during the provision of 1000 mg L^{-1} lactate as reflected in the highest values of maximum specific growth rate ($\mu_{max\text{-}Lac}$) and yield constant ($Y_{X\text{-}Lac}$). At the higher initial concentrations of 2500 and 5000 mg L^{-1} lactate, microbial activity indicators were relatively similar, such as $Y_{X\text{-}Lac}$ showing almost identical values but were significantly lower than the corresponding $Y_{X\text{-}Lac}$ value with 1000 mg L^{-1} lactate. This finding suggests that exposure to lower concentrations of lactate allows the microbial population to adapt faster and function with little difficulty in this environment, resulting to favourable microbial activity. However, this seems not to conform to observed trends of overall biodegradation rates which were found to increase with initial concentration. As described earlier, the calculated biodegradation rates represent the decrease in substrate concentration over time without taking into account changes in biomass concentration. The biokinetic model proposed in this study was formulated to involve all biodegradation data simultaneously, hence corresponding results provide a more comprehensive understanding of biodegradation process and associated kinetics.

To assess the biodegradation of lactate in association with the biomass kinetics, one need to look at the specific utilization rate of lactate. The specific utilization rate (q_{Lac}) was related to microbial growth and specific growth rate (μ) through the yield coefficient ($Y_{x\text{-}Lac}$) as described by Eq. 3.13.

$$q_{Lac} = \mu_{Lac} Y_{x\text{-}Lac}^{-1} \quad (3.13)$$

Calculation of q_{Lac} showed that when the specific growth rate was at maximum ($\mu_{Lac}=\mu_{max\text{-}Lac}$), corresponding q_{Lac} was 0.0842, 0.0843 and 0.1419 h^{-1} for lactate at initial concentration of 1000, 2500 and 5000 mg L^{-1}, respectively. The highest specific utilization rate was achieved at the highest initial lactate concentration, which is the same concentration at which the highest biodegradation rate was determined. This finding indicates that at 5000 mg L^{-1} lactate, the rate of lactate biodegradation had a more imposing effect than the corresponding growth of microorganisms resulting to higher q_{Lac}. In other words, the provision of higher amounts of lactate afforded the microorganisms to utilize more of the substrate per unit mass of biomass.

The saturation constant ($K_{S\text{-}Lac}$) as expected showed an increasing trend with increase in initial lactate concentration. The saturation constant is the concentration of substrate when the associated specific growth rate is half of its maximum value (i.e. when $\mu=0.5\mu_{max}$). The resulting $K_{S\text{-}Lac}$ values were approximately 5-10% of the initial lactate concentration and reached when substrate was nearing complete exhaustion. Figures 3.13-3.15 show the variation of specific growth rate of lactate and biologically produced acetate during the biodegradation of 1000, 2500 and 5000 mg L^{-1} lactate, respectively. Values of respective specific growth rates and concentrations of lactate and

biologically produced acetate predicted from the modeling process were plotted against time. Calculation of specific growth rates followed Monod equation as shown in Equation 3.14.

$$\mu = \frac{\mu_{max} S}{K_S + S} \tag{3.14}$$

Results show that microbial growth and activity were reasonably high almost throughout the entire period of lactate biodegradation with the exception of periods immediately before lactate depletion (Figures 3.13-3.15, Panel A). Moreover, at about the same period $K_{S\text{-}Lac}$ was reached, the specific growth rate with biologically produced acetate ($\mu_{max\text{-}Ace}$) attained its maximum which also coincided with peak formation of biologically produced acetate (Figures 3.13-3.15, Panel B). These results show that microbial community was able to utilize newly converted acetate for its growth. Once all of lactate was exhausted, formation of biologically produced acetate ceased, resulting to decline in concentration as its utilization continued. Consequently, specific growth rate of biologically produced acetate declined as remaining available substrate was depleted.

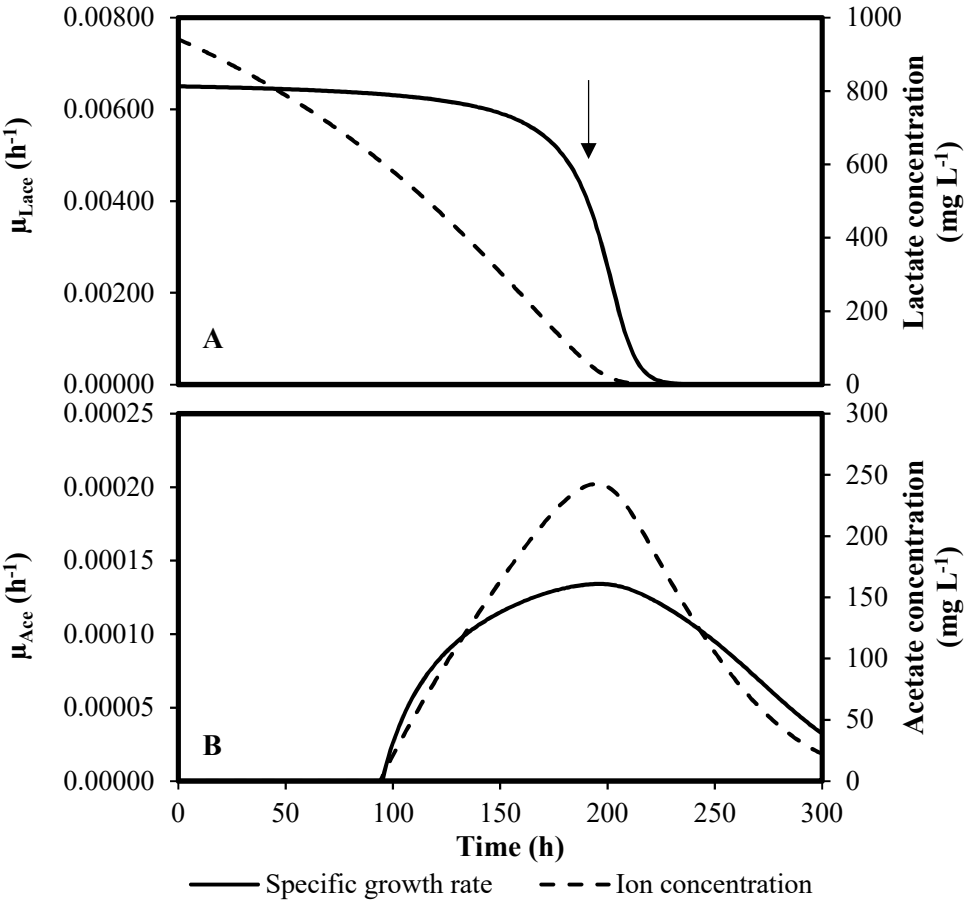

Figure 3.13 Variation of specific growth rate of lactate and biologically produced acetate, calculated from Eq. 3.14 during the biodegradation of 1,000 mg L^{-1} lactate in batch MFC. Arrow indicate the time $K_{s\text{-}Lac}$ was reached.

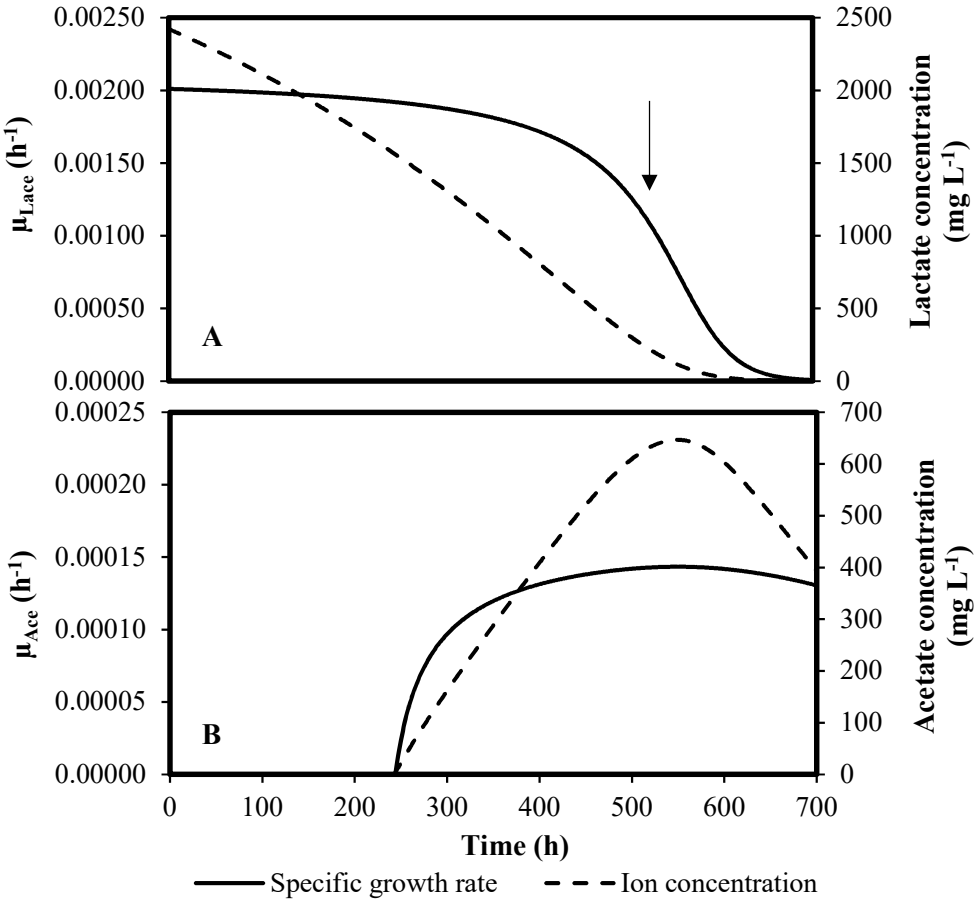

Figure 3.14 Variation of specific growth rate of lactate and biologically produced acetate, calculated from Eq. 3.14 during the biodegradation of 2,500 mg L^{-1} lactate in batch MFC. Arrow indicate the time $K_{s\text{-}Lac}$ was reached.

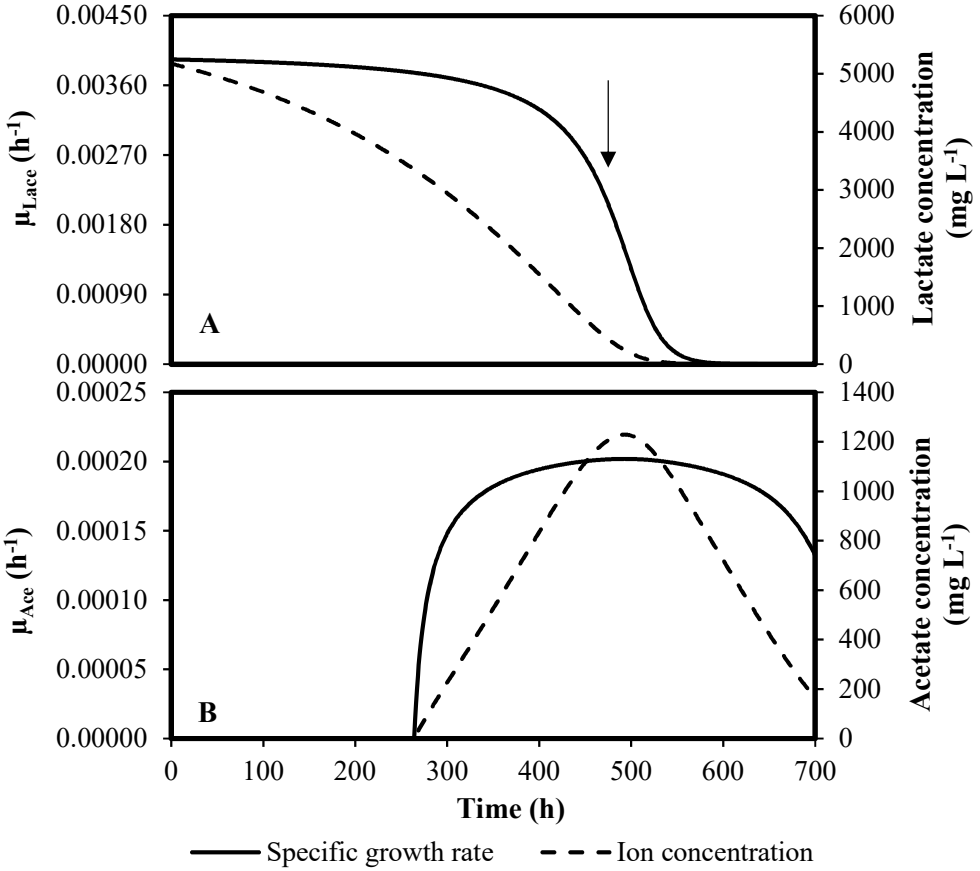

Figure 3.15 Variation of specific growth rate of lactate and biologically produced acetate, calculated from Eq. 3.14 during the biodegradation of 5,000 mg L^{-1} lactate in batch MFC. Arrow indicate the time $K_{s\text{-}Lac}$ was reached.

The biokinetic coefficients associated with degradation of biologically produced acetate, especially maximum specific growth rate ($\mu_{max\text{-}Ace}$) and cell yield ($Y_{X\text{-}Ace}$) were at least one order of magnitude lower than the corresponding values for the lactate. The magnitude of these coefficients strongly indicates the slow nature of degradation of biologically produced acetate in MFCs, especially when compared to lactate, which further attests to the observed preference on lactate over acetate as carbon source in the MFC.

The values of F shown in Table 3.2 indicate that following the delay in formation of biologically produced acetate, around 70-80% of lactate degradation occurred via reaction 3.1 (i.e. incomplete

oxidation of lactate) and the remaining 20-30% occurred via reaction 3.3 (i.e. complete oxidation of lactate). A low F value indicates that a higher degree of complete lactate oxidation transpired. The lower F value with increase in initial lactate concentration could be an indication of faster lactate biodegradation. The corresponding biodegradation rates reported earlier, which were found to be higher with increase in initial concentration, seem to coincide with this trend. It can be speculated that at higher initial lactate concentrations, more complete oxidation occurs which in turn increases the overall speed of lactate utilization and hence the higher biodegradation rates.

The goodness of fit of model predictions (solid lines) for biomass growth and acetate biodegradation for acetate as the original (sole) substrate with the experimental data (symbols) obtained in batch MFCs operated with 1000, 2500 and 5000 mg L^{-1} acetate, are shown in Figure 3.16 (panels A, B, C, respectively). Table 3.3 presents the biokinetic coefficients associated with acetate biodegradation, determined as part of kinetic modelling of microbial growth and acetate biodegradation. As was the case with lactate, the model predictions for acetate match the experimental data reasonably well. The patterns with regard to impact of acetate concentration on microbial growth are somewhat similar to that observed with lactate. The highest level of microbial activity, as reflected in values of maximum specific growth rate ($\mu_{max\text{-}Ace}$) and yield constant ($Y_{X\text{-}Ace}$) are observed with 1000 mg L^{-1} acetate.

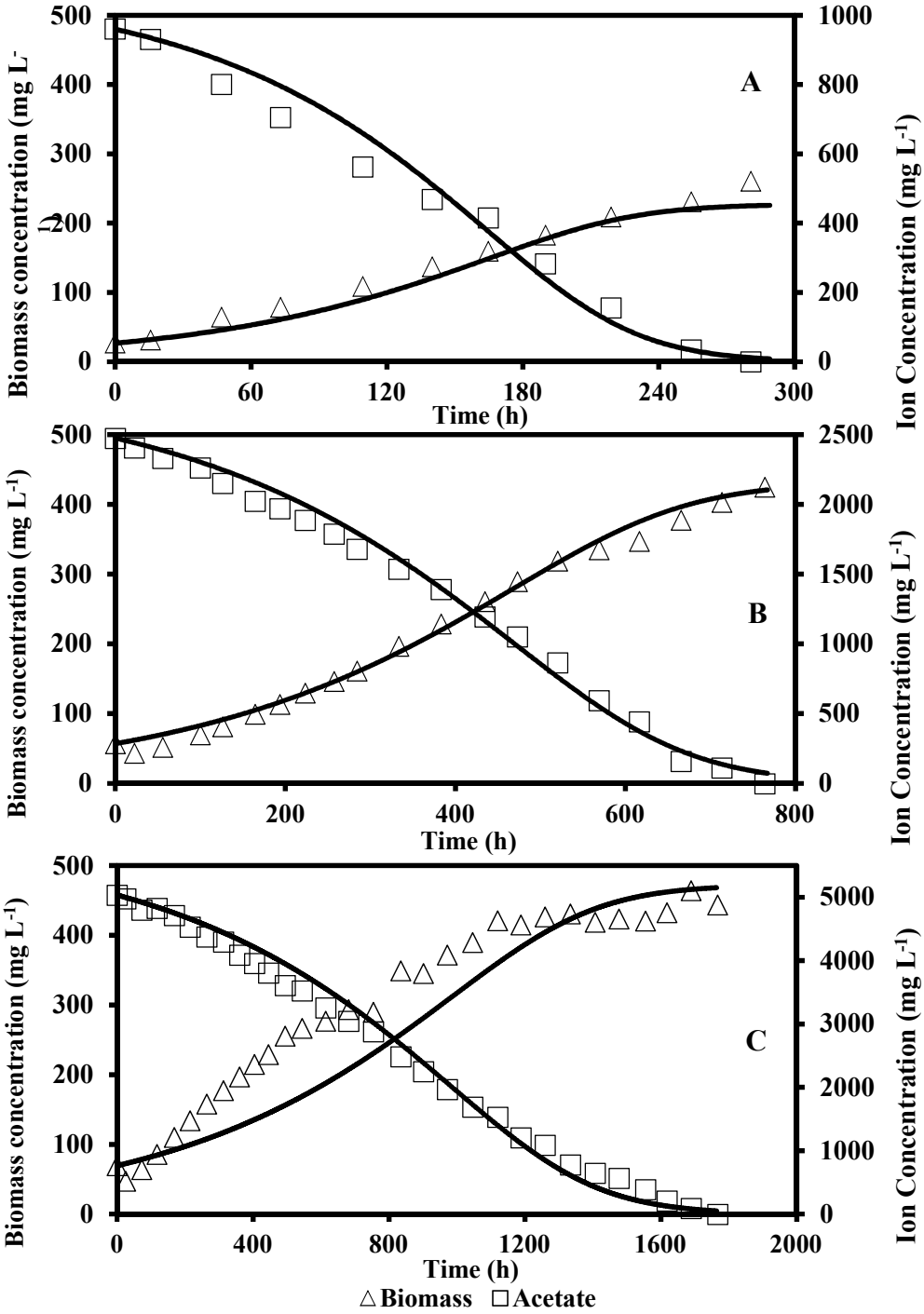

Figure 3.16 The goodness of fit of model predictions (solid lines) and experimental data (symbols) for biomass growth and acetate biodegradation in batch microbial fuel cells operated with 1,000 mg L^{-1} (A), 2,500 mg L^{-1} (B) and 5,000 mg L^{-1} (C) acetate. This figure is derived in part from an article published in Bioprocessing and Biosystems Engineering Jan 2015 Springer Berlin Heidelberg, available online: https://doi.org/10.1007/s00449-014-1240-3.

Table 3.3 Biokinetic coefficients for biodegradation of acetate in batch operated MFCs with suspended cells of *P. putida*.

Coefficient	Acetate concentration (mg L^{-1})		
	1000	**2500**	**5000**
$\mu_{max\text{-}Ace}$ (h^{-1})	0.0168	0.0056	0.0024
$K_{S\text{-}Ace}$ (mg Ace L^{-1})	432.3	1,185.5	2,101.0
$Y_{X\text{-}Ace}$ [mg cell-dry weight (mg Ace)$^{-1}$]	0.2092	0.1514	0.0800

The increasing trend in the value of saturation constant as a result of increase in acetate concentration was also similar to that observed with lactate. It is very important to note that the microbial activity and acetate degradation when acetate was used as original substrate were much higher than that in the presence of biologically produced acetate. This can be clearly seen by a comparison of the values of maximum specific growth rate and yield constant which in case of biologically produced acetate are 1-2 order of magnitudes smaller than their counterparts for biodegradation of acetate as the original substrate.

The results of sensitivity analysis of the biokinetic model for biodegradation of lactate are presented in Figure 3.17 panels A, B, C for 1000, 2500 and 5000 mg L^{-1} lactate, respectively. The maximum specific growth rate ($\mu_{max\text{-}Lac}$) and yield constant ($Y_{X\text{-}Lac}$) were the most influential coefficients affecting the theoretical predictions by the model, with the impact of $\mu_{max\text{-}Lac}$ being greater than $Y_{X\text{-}Lac}$. By contrast, the variation in saturation constant ($K_{S\text{-}Lac}$) did not influence the model predictions significantly. For instance, in the case of 1000 mg L^{-1} lactate (Figure 3.17, panel A), decrease in the values of $\mu_{max\text{-}Lac}$ and $Y_{X\text{-}Lac}$ by 50% increased the corresponding NSSDs by 116 and 62 folds, respectively, while a similar decrease in $K_{S\text{-}Lac}$ increased the NSSD by only 8 folds. Similar patterns were observed with the data obtained from the degradation of 2500 and 5000 mg L^{-1} lactate. The model predictions with regard to accumulation of biologically produced

acetate did not exhibit noticeable sensitivity to the biokinetic coefficients (not included in Figure 3.17 but is shown in Appendix Figure C.1). This is somewhat expected due to the small values of biokinetic coefficients indicating the very slow nature of the degradation process.

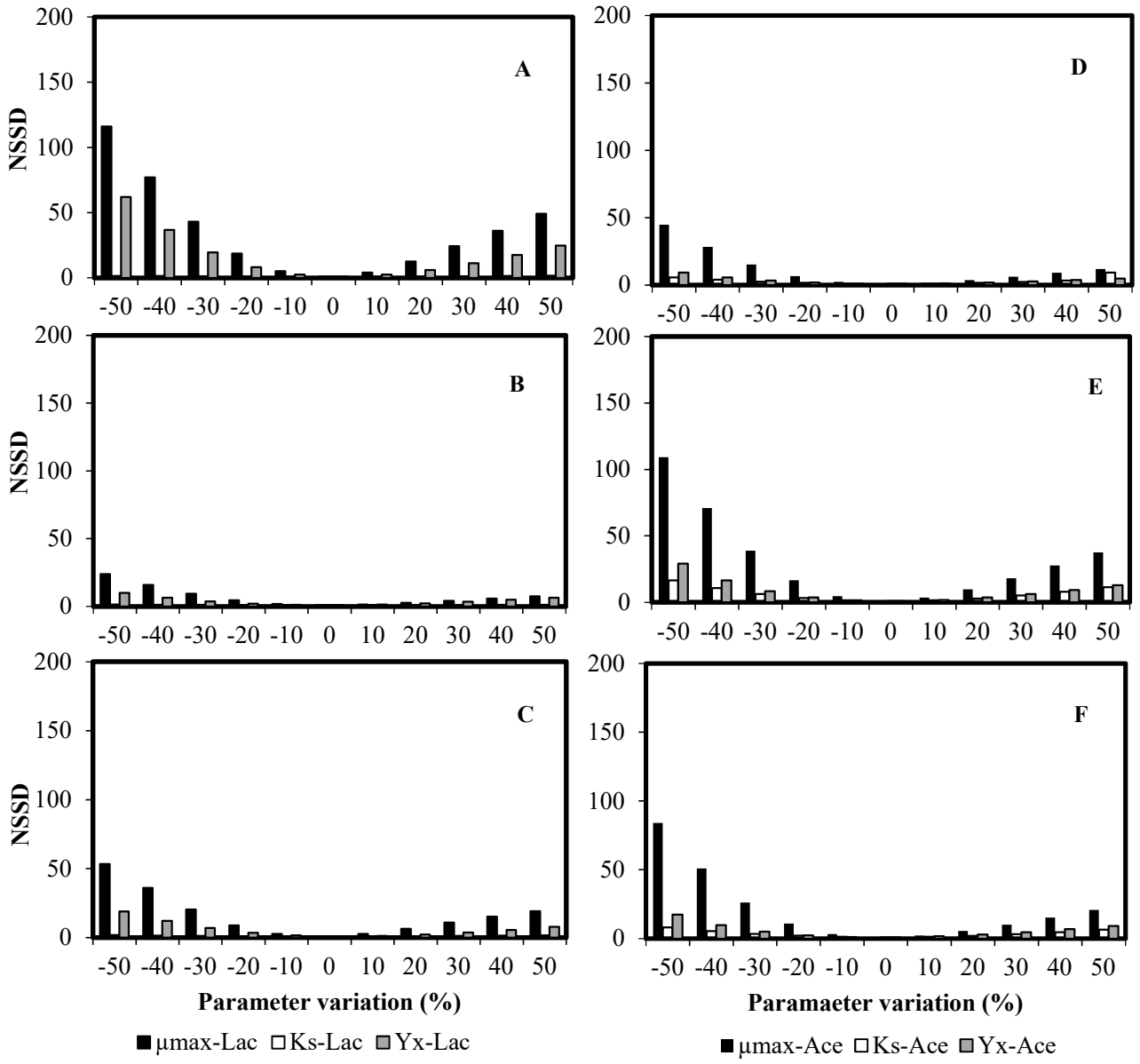

Figure 3.17 Analysis of model sensitivity to various biokinetic coefficients. A) 1,000 mg L^{-1}, B) 2,500 mg L^{-1}, C) and 5,000 mg L^{-1} lactate; D) 1,000 mg L^{-1}, E) 2,500 mg L^{-1} and F) 5,000 mg L^{-1} acetate. This figure is derived in part from an article published in Bioprocessing and Biosystems Engineering Jan 2015 Springer Berlin Heidelberg, available online: https://doi.org/10.1007/s00449-014-1240-3.

Included in Figure 3.17 are the results of sensitivity analysis for biodegradation of 1000, 2500 and 5000 mg L^{-1} acetate as the original substrate (panels D, E, F, respectively). The sensitivity of model predictions to biokinetic coefficients in case of acetate biodegradation was similar to that observed for lactate to some extent. As observed, the maximum specific growth rate ($\mu_{max\text{-}Ace}$) and yield constant ($Y_{X\text{-}Ace}$) were the most influential coefficients with the effect of $\mu_{max\text{-}Ace}$ being greater. Contrary to that observed with lactate, variation in saturation constant ($K_{S\text{-}Ace}$) also affected the model predictions though not at the same magnitude as those of $\mu_{max\text{-}Ace}$ and $Y_{X\text{-}Ace}$. For instance in the biodegradation of 1000 mg L^{-1} acetate, a 50% decrease in values of $\mu_{max\text{-}Ace}$, $Y_{X\text{-}Ace}$ and $K_{S\text{-}Ace}$ led to 44.7, 9.3 and 5.7 fold increases in NSSD, respectively. Similar patterns were also observed when the data associated with 2500 and 5000 mg L^{-1} acetate were examined (panels D, F).

3.3.3 Continuously operated MFCs systems

Lactate as the substrate: With 5000 ppm lactate as feed, the continuous MFC was operated for more than 200 days during which various flow rates ranging from 2 to 235 mL h^{-1} (corresponding lactate loading rates: 50 to 4800 mg L^{-1} h^{-1}) were applied. As indicated earlier the MFC was initially operated batchwise during which biomass growth, lactate biodegradation and acetate accumulation and subsequent biodegradation showed patterns similar to those observed in the earlier batch experiments. Following this confirmation, MFC was switched to continuous mode of operation and biomass growth, lactate biodegradation and OCP were monitored accordingly. As shown in Figure 3.18A, the continuous operation led to a substantial increase in OCP from an initial level of 400 mV, which was observed towards the end of the batch phase to a level of about 700 mV which was maintained for the remainder of the experiment.

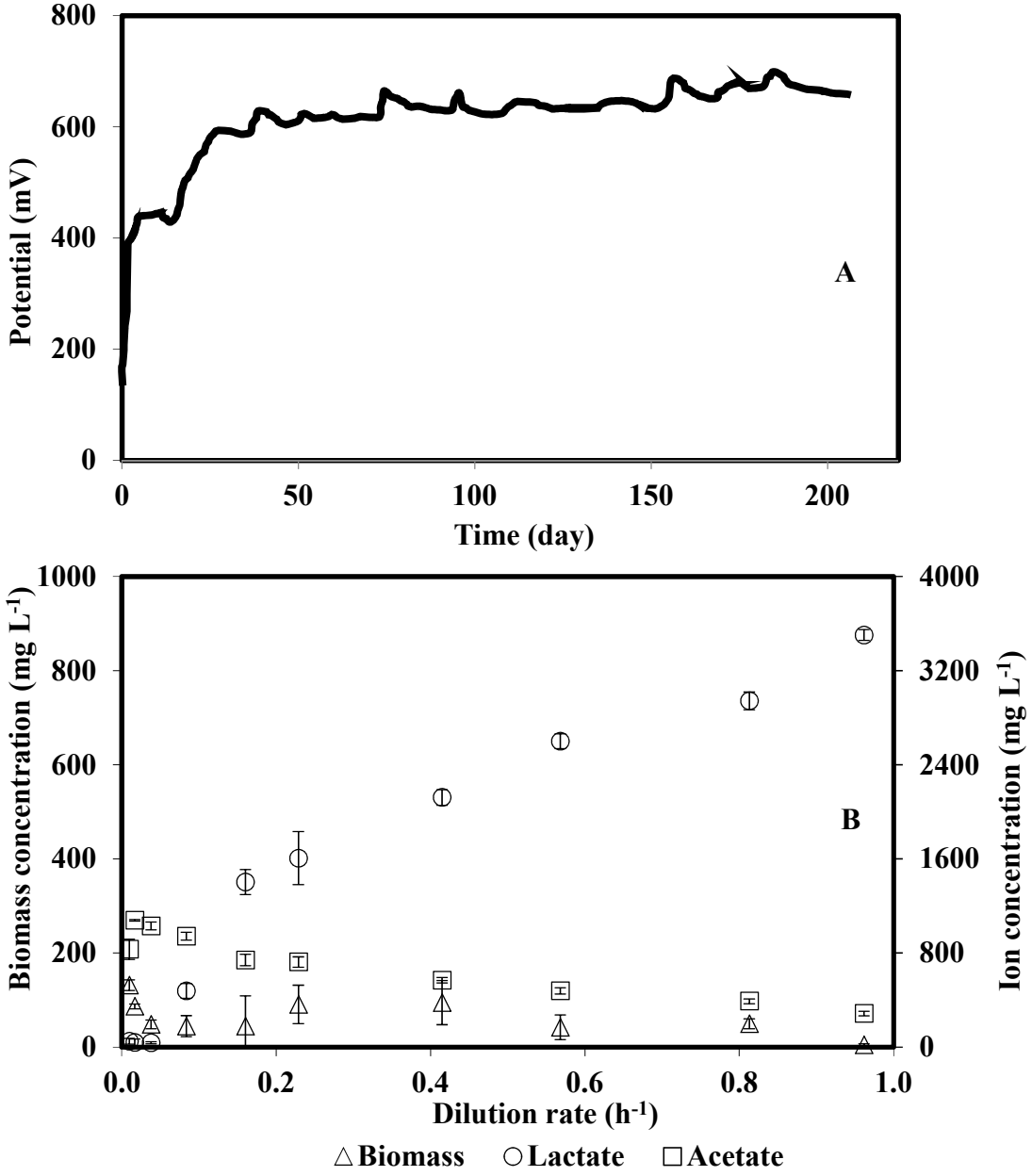

Figure 3.18 Open circuit potential (A), and steady-state concentration profiles of biomass, lactate and accumulated acetate concentrations as a function of dilution rate (B) in an MFC with single rod electrode, fed continuously with 5,000 mg L^{-1} lactate. Error bars represent standard deviation of steady state residual lactate and acetate concentrations. This figure is derived in part from an article published in Bioprocessing and Biosystems Engineering Jan 2015 Springer Berlin Heidelberg, available online: https://doi.org/10.1007/s00449-014-1240-3.

Figure 3.18B shows the steady state concentration profiles of biomass, lactate and accumulated acetate as a function of dilution rate. The dilution rate is the volumetric rate by which feed is introduced to the anodic chamber and is the inverse of the hydraulic retention time (HRT) (Shuler and Kargi, 2001). After switching the mode of operation to continuous flow for dilution rates up to 0.04 h^{-1} (corresponding HRT=26.3 h), low residual lactate concentrations in the range 0-39 mg L^{-1} were observed during which the highest concentration of accumulated acetate in the range of 1030-1080 mg L^{-1} were also measured. As was the case in the batch operated MFCs, the level of accumulated acetate was lower than that expected from the stoichiometry of incomplete lactate oxidation (reaction 3.1), indicating that reactions 3.1 and 3.2 occurred simultaneously.

Further increase in dilution rate led to increase in residual lactate concentration and gradual decrease in concentration of accumulated acetate. It should be pointed out that the increase in residual lactate concentration was considerably abrupt for dilution rates in the range of 0.04-0.16 h^{-1} (residence time: 26.3 to 6.2 h) but continued at a slower pace when dilution rate was increased above 0.16 h^{-1}. Concentration of accumulated acetate decreased gradually as dilution rate was increased from 0.02 h^{-1} up to the highest rate of 0.96 h^{-1}. The decrease in accumulated acetate concentration was consistent with the decrease in lactate removal efficiency considering that acetate was produced as intermediate of lactate biodegradation. The lactate and accumulated acetate concentrations at the highest applied dilution rate of 0.96 h^{-1} (HRT=1.0 h) were approximately 3,500 and 285 mg L^{-1}, respectively.

Figure 3.19 Biomass attached to the surfaces of the anodic chamber wall and single rod electrode as result of lactate biodegradation in the MFC fed continuously with 5,000 mg L^{-1} lactate with loading rates up to 4800 mg L^{-1} h^{-1}.

In terms of microbial growth, the highest suspended biomass concentration (131.6 mg L^{-1}) was observed at the lowest dilution rate of 0.01 h^{-1} and fluctuated in the range 44.4-94.5 mg L^{-1} for dilution rates up to 0.41 h^{-1}. The concentration of suspended biomass decreased when dilution rate was increased further, with the extent of suspended biomass being negligible at the highest applied dilution rate (0.96 h^{-1}). Upon checking the contents of anodic chamber after draining of the liquid contents, substantial biomass in the attached state was found as shown in Figure 3.19 where thick layers of biomass remained on the walls of the anodic chamber and around the rod electrode. It should be noted that the biodegradation patterns and the relatively consistent OCP observed during the continuous operation of MFC not only reflected the microbial activity by suspended biomass

but biofilm formation on the anodic chamber walls and electrode would also have contributed to the observed patterns. For the entire range of applied dilution rates, the pH in the anodic chamber liquid remained in the range of 6.2-7.1. It is also noteworthy that frequent replenishment of the potassium ferricyanide in the cathodic chamber was needed and carried out throughout the experiment.

To determine the effectiveness of the MFC in the continuous biodegradation of lactate, the variation of lactate biodegradation rate and its corresponding removal efficiency (%) with respect to its loading rate were calculated and is shown in Figure 3.20. Included in the figure is also the accumulation rate of acetate as a function of lactate loading rate. At the lower range of lactate loading rates up to 190.3 mg L^{-1} h^{-1} (residence time: 26.3 h), the removal percentage of lactate was more than 99% with the lactate biodegradation rate increasing from an initial level of 49.80 to 188.9 mg L^{-1} h^{-1}. Further increase in loading rate led to a continual decrease in lactate removal percentage, while lactate biodegradation rate continued to increase and passed through a maximum. The highest biodegradation rate of lactate was 1668.2 mg L^{-1} h^{-1} which was obtained at a loading rate of 4054.7 mg L^{-1} h^{-1} and corresponding to a HRT of 1.2 h.

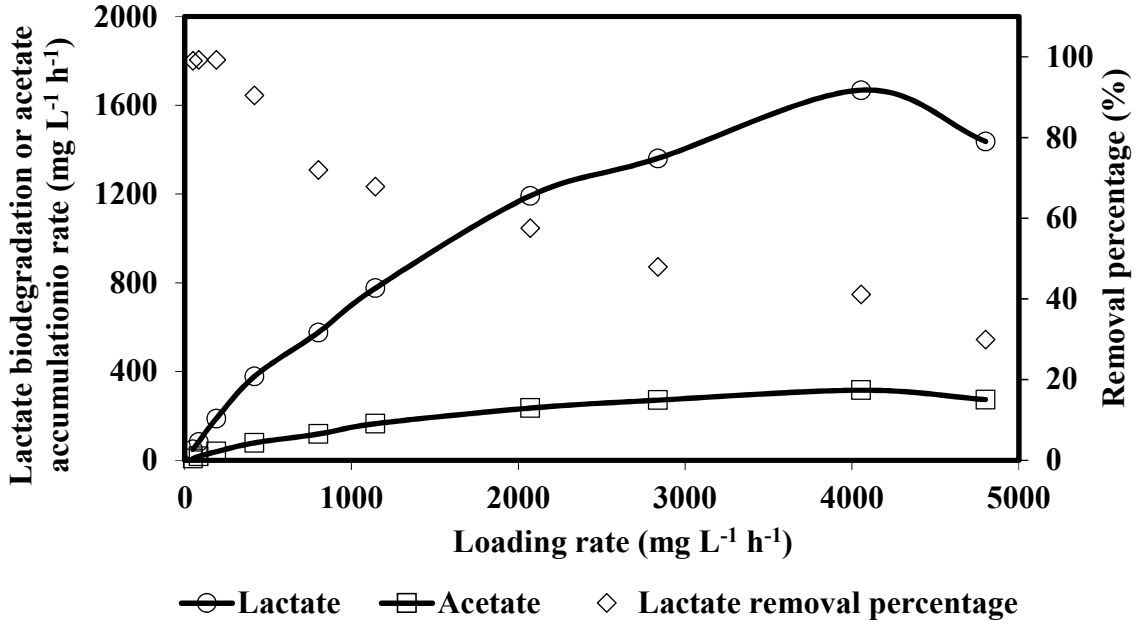

Figure 3.20 Variation of lactate biodegradation rate and removal percentage, and accumulation rate of acetate as a function of lactate loading in an MFC with single rod electrode, fed continuously with 5,000 mg L^{-1} lactate. This figure is derived in part from an article published in Bioprocessing and Biosystems Engineering Jan 2015 Springer Berlin Heidelberg, available online: https://doi.org/10.1007/s00449-014-1240-3.

The maximum lactate biodegradation rate achieved in the continuously operated MFC was around 69-fold faster than that in the MFCs operated batchwise (1,668.2 vs. 23.9 mg L^{-1} h^{-1}). As expected, the accumulation rate of biologically produced acetate was coupled to the biodegradation rate of lactate and displayed an increasing trend with increase in lactate biodegradation rate. Moreover, acetate accumulation rate reached its peak at the same loading rate where the maximum biodegradation rate was achieved and then started to diminish. This finding indicates that the extent of acetate accumulation depended on the biodegradation of lactate, similar to that observed in the batch experiments. It is important to note that the accumulation rate of acetate was much lower than the rate expected from stoichiometry of lactate biodegradation, again confirming that lactate biodegradation occurred via reactions 3.1 and 3.3. The highest accumulation rate of acetate was

316.1 mg L^{-1} h^{-1} which coincided with the maximum lactate biodegradation rate of 1668.2 mg L^{-1} h^{-1}.

Power and current output: As stated in Section 3.2.4, power and current were measured by applying external resistors, ranging from 100-6000 ohms, across the circuit. The resulting power output was found to be dependent on the ohmic value of the resistor. Specifically, at the lower resistance range of 100-500 ohms, considerably low values of power were measured for various loading rates generating an average value of only 0.27 mW m^{-2} as compared to 2.72 mW m^{-2} which was measured at the higher resistance range of 1000-6000 ohms. Hence, to refrain from underestimation of power output and for more accurate representation of results, only those values measured using resistors with high ohmic values were reported and included in this discussion. Figure 3.21 shows the variation of power and current densities generated in the MFC at various applied loading rates.

The lowest power and current output generated from the MFC of 0.20 mW m^{-2} and 6.72 mA m^{-2}, respectively, were measured when the MFC was operated at the lowest loading rate (49.80 mg L^{-1} h^{-1}). At this very early stage, the MFC system was subjected to an adaptation period following the shift of operational mode from batch to continuous and hence the corresponding low power and current output. It can also be recalled that it was during this stage that an abrupt rise in OCP (Figure 3.18A) occurred before it stabilized throughout the rest of the experiment.

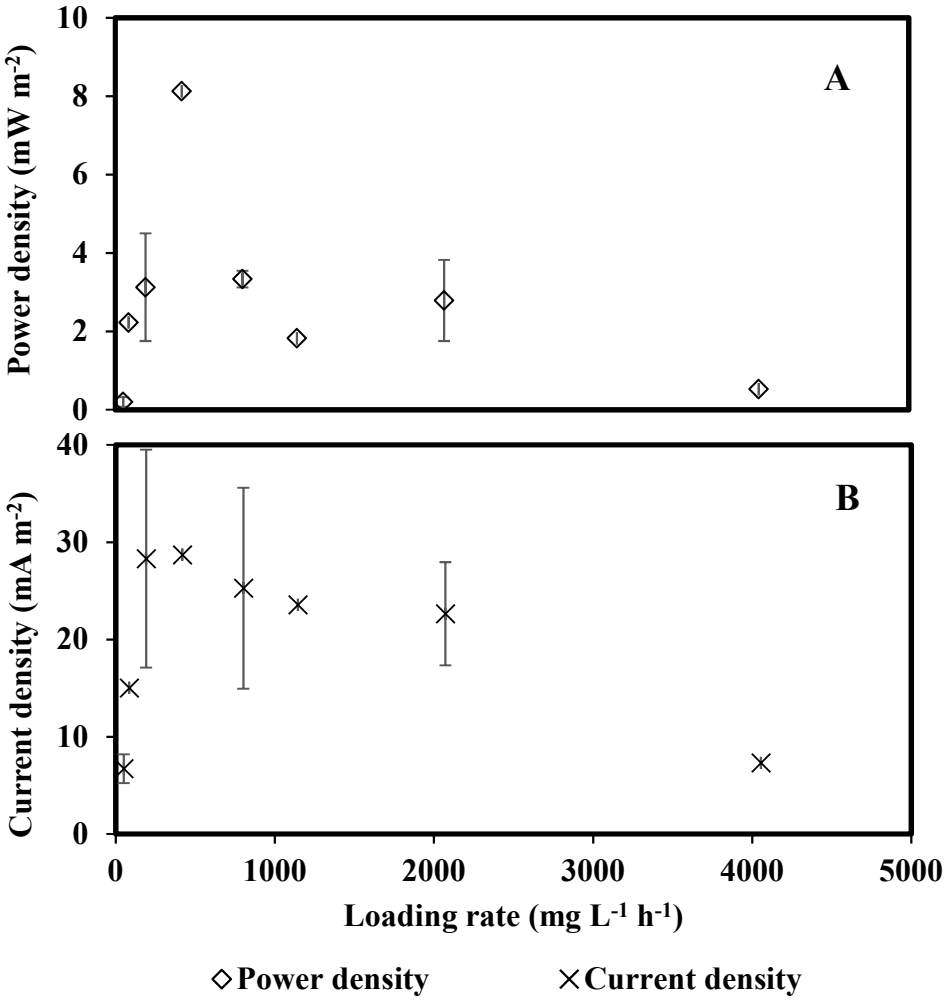

Figure 3.21 Profiles of power (A) and current densities (B) measured at various lactate loading rates in an MFC with single rod electrodes, fed continuously with 5,000 mg L^{-1} lactate. Error bars represent standard deviation of power and current densities at each loading rate.

As loading rate was increased, resulting power and current densities were found to increase as well, reaching their peak when the loading rate was increased to 418.7 mg L^{-1} h^{-1}. At a relatively narrow range of loading rates from 49.8-418.7 mg L^{-1} h^{-1}, the increase in power and current output was rather fast while further increase in loading rate resulted to a more gradual decrease in power and current. Throughout the continuous operation of the MFC, the maximum power and current densities were 8.1 mW m^{-2} and 36.2 mA m^{-2}, respectively, with equivalent output in terms of

working volume of 49.4 mW m^{-3} and 198.1 mA m^{-3}. The peak power and current densities were generated at the lower range of loading rates where corresponding lactate biodegradation rates were still improving with increase in loading rate.

Looking more closely on the profiles of power and current densities revealed a correlation with the respective profile of lactate removal efficiency. As recalled in Figure 3.20, the application of lower range of loading rates (49.8-418.7 mg L^{-1} h^{-1}), where power and current densities were found to increase and reached their peak values, coincided with high removal efficiencies (>90%), while further increase in loading rate proceeded with a gradual decrease in removal percentage regardless of the resulting biodegradation rates. This finding suggests that in a continuous system, removal efficiency influences the resulting power and current output more substantially than the biodegradation rate. In other words for loading rates that result in high removal efficiency the corresponding levels of power and current would be higher than those corresponding to lower removal efficiency regardless of the biodegradation rate. For all evaluated loading rates in the continuous MFC, the CE was significantly lower than those calculated from batch experiments. However, with the vastly superior biodegradation rates, resulting energy output from the continuous system was generally higher.

To summarize, the range of power and current densities generated in the continuous flow MFC with rod electrodes were 0.22-8.13 mW m^{-2} and 7.31-43.00 mA m^{-2}, respectively, with the average values being 2.72 ± 1.85 mW m^{-2} and 20.90 ± 7.85 mA m^{-2}. The equivalent average power and current densities in terms of working volume were 16.54 ± 11.28 mW m^{-3} and 126.95 ± 47.66 mA m^{-3}, respectively. When compared to the MFC operated batchwise, both average and maximum

power densities as well as the OCP achieved during the continuous operation were considerably higher, while current densities were comparable. Relevant comparison of energy output from other MFC systems was impractical due to limited or unavailability of information covering similar work especially for lactate degradation in continuous flow MFCs with suspended biomass. A miniature MFC (1.2 cm^3 volume) inoculated with *Shewanella oneidensis* DSP10 and fed continuously with 4950 mg L^{-1} (55 mM) lactate at relatively fast HRTs ranging from 0.06-2 min was able to achieve a significantly higher maximum power density of 10 mW m^{-2}, while current densities reaching 32 mA m^{-2} were comparable to those in current work (Ringeisen et al., 2006). This superior power output was most likely due to the use of graphite felt as electrodes which certainly allowed effective cell immobilization. As with most MFC studies, no information on effectiveness of lactate biodegradation and associated kinetics were reported.

Acetate as the substrate: Continuous biodegradation experiment with acetate as substrate was also conducted in an identical MFC with rod electrodes. As with previous continuous experiment with lactate, batch degradation of acetate was completed before switching the MFC to continuous mode of operation. Figure 3.22 shows the profiles of biomass and acetate concentrations immediately after completion of batch run and throughout the continuous run.

Biomass build-up from the initial batch run was comparable to those observed in previous batch experiments. As MFC was switched to continuous mode with an initial flow rate of 1.5 mL h^{-1}, biomass concentration decreased, while residual acetate concentration gradually increased (Figure 3.22A). This trend was observed as the experiment progressed eventually reaching residual acetate concentration that was already over 80% of the feed concentration (~800 mg L^{-1}), while only 25%

of the original biomass build-up remained. At this stage which translated to 193 h of operation, no indication of the system performance improvement was observed and hence the MFC was switched back to batch mode of operation to allow the residual acetate to be utilized by microbial community and biomass build-up to occur.

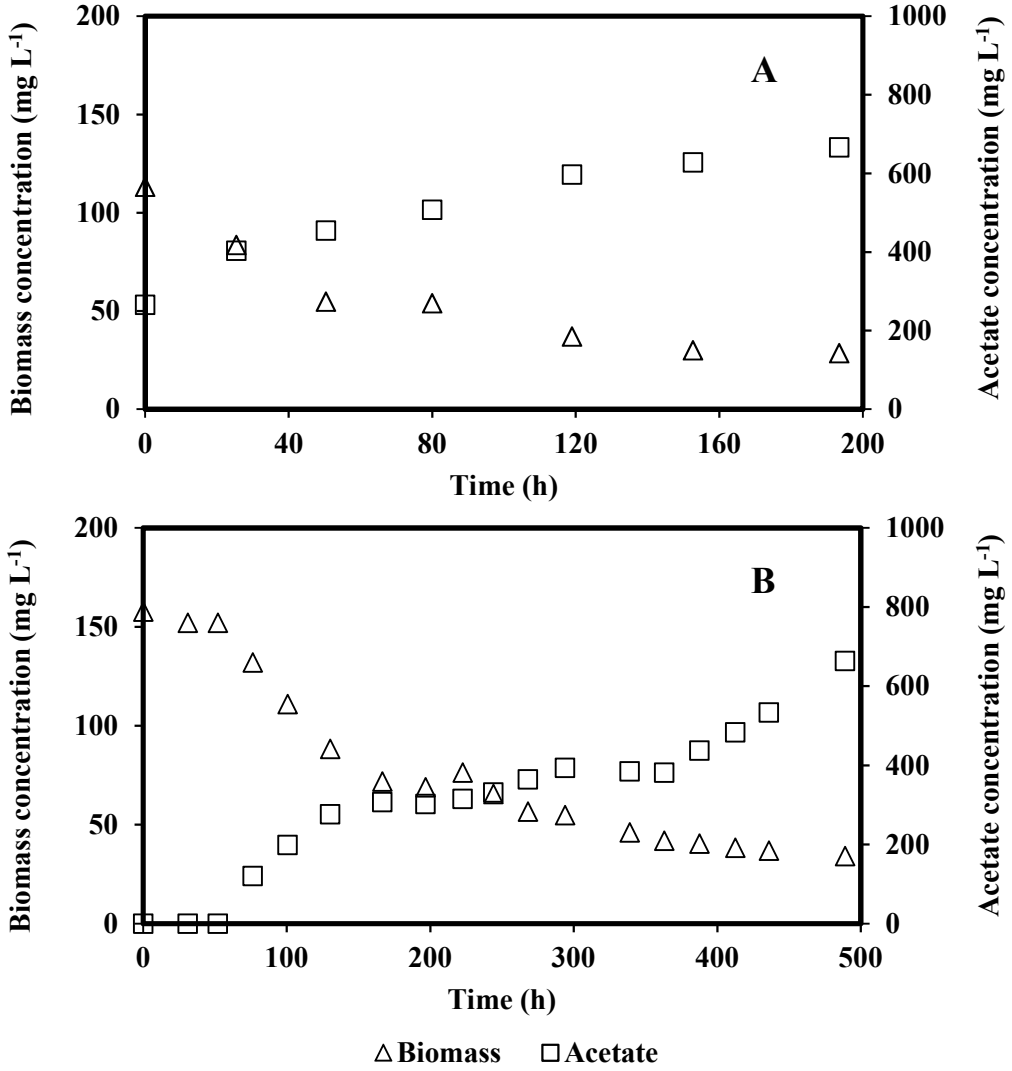

Figure 3.22 Profiles of biomass and acetate concentrations as a function of time during the continuous biodegradation of 1,000 mg L^{-1} acetate in a MFC with single rod electrodes and suspended cells of *P. putida*. Results from the initial continuous run is shown in panel A, while those from the subsequent run is shown in panel B.

After complete degradation of the residual acetate, feed was introduced again at a flow rate of 1.5 mL h^{-1}. Complete degradation of acetate was observed at the early stages (<52 h) of the continuous run (Figure 3.22B). However, this did not translate to improvement in biomass growth. In fact, as the continuous experiment progressed, biomass concentration started to decrease again and conversely residual acetate started to accumulate. Essentially, the trends observed in the initial continuous run was repeated resulting in a residual acetate concentration that was around 85% of the feed concentration.

Despite the inability of operation at higher flow rate, a slight improvement during the subsequent continuous run was observed where deterioration in performance occurred after a longer period (i.e. continuous acetate removal of at least 25% was attained for 489 h, while approximately the same amount of acetate removal in the first run lasted for only 193 h. The slight improvement in continuous acetate degradation after repeated biomass build-up could indicate that a substantially longer adaptation period would be essential for an effective continuous biodegradation of acetate. Inferior performance of MFC fed continuously with acetate further attested to the favourability of lactate as substrate over acetate, as has been revealed previously in the batch experiments.

3.4 Conclusions

The MFC systems with rod electrodes, inoculated with *P. putida* as microbial culture was able to successfully degrade two model short chain fatty acids, namely lactate and acetate, with concomitant generation of electricity. Results of this study revealed that the sequential operation of batch MFCs could lead to higher lactate biodegradation rates but this mode of operation did not

have a marked effect on the biodegradation of acetate, whether as original substrate or as intermediate of the lactate degradation.

The resulting biodegradation rates were found to correlate with the power and current outputs. This correlation was clearly evident in batch MFCs where increase in initial lactate concentration led to higher biodegradation rates and consequently higher power and current densities. With acetate as the original substrate the increase in initial concentration of acetate did not affect the biodegradation rate and hence the extent of corresponding power and current outputs were independent of acetate initial concentration.

The biodegradation of lactate proceeded at rates faster than that of acetate which was consequently reflected in resulting power and current densities where those generated from lactate were considerably higher than those from acetate. The biodegradation of lactate led to formation and accumulation of acetate as an intermediate which was utilized by the microbial community, especially after consumption of lactate but at a rate which was much slower than that of acetate as the original substrate.

The use of MFC with rods as electrodes and effective mixing allowed a detailed biokinetic evaluation of microbial growth and fatty acids biodegradation and collection of data needed to develop a model for microbial growth and biodegradation kinetics. The biokinetic models developed was able to predict microbial growth and biodegradation kinetics of lactate and acetate with high accuracy. Results showed that magnitude of biokinetics and associated coefficients were lower than those reported for conventional bioreactors, pointing to the slow nature of microbial

growth and activity in MFC type bioreactors and the need for development of culture suitable for this purpose and use of more sophisticated MFC type bioreactors.

In the continuous MFC, increase in lactate loading rate led to increase in biodegradation rate which passed through a maximum and then declined with further increase in loading rate. The highest lactate biodegradation rate of 1668.2 mg L^{-1} h^{-1} was obtained at a loading rate of 4054.7 mg L^{-1} h^{-1} and a residence time of 1.2 h. With acetate in the feed, continuous biodegradation in the same MFC was found ineffective which further exhibits the favourability of lactate as substrate over acetate. Lactate biodegradation rates in the continuously fed MFC were around 69-fold higher than those in the batch MFCs. Correspondingly, open circuit potential, power and current densities in the continuous flow MFC were higher than those in the batchwise operated MFC which again attests to the indicated correlation between biodegradation activity and electrochemical output.

Chapter 4

Biodegradation of Fatty Acids (Lactate and Acetate) in MFCs with Granular Electrodes

4.1 Introduction

Different types of compounds contained in wastewaters that require removal can also be used as substrate in microbial fuel cells. A variety of organic compounds including carbohydrates, fatty acids, as well as inorganic compounds such as ammonia and sulphide have been evaluated as potential electron donors in the anodic compartment of MFCs (Angenent et al. 2004; Min et al., 2005b; Liu et al.a, 2005; Rabaey et al., 2006; Du et al., 2007; Pant et al., 2010; Puig et al., 2010). Along with other organic compounds, fatty acids in wastewater and digester effluent need to undergo degradation before wastewater can be considered for discharge. As discussed in the previous chapter, utilization of lactate and acetate as substrate was investigated in batch and continuous flow MFCs with single rod electrodes and freely suspended cells of *P. putida* and in addition to generating detailed kinetic data models that describe the microbial growth and biodegradation kinetics with lactate and acetate as substrate were developed.

Previous works in utilization of MFCs for degradation of organic compounds have reported that the use of graphite granules as electrodes could lead to relatively high power and current output (Rabaey et al., 2005b; You et al., 2007; Feng et al., 2010; Tremouli et al., 2016). The reason for this improved performance is the extended surface area of the granular electrodes that facilitates

the formation of biofilm on the surface of electrode (anode) that consequently improve biodegradation of substrate and also promotes the transfer of electrons thereby increasing the power and current outputs.

As with most MFC studies, the earlier works utilizing electrodes in granular form did not focus nor attempt to look into the biodegradation aspects of the MFC. It is in that context and with the aim of improving the performance of MFC in terms of biodegradation and power output in the next phase of this research biodegradation of lactate and acetate were investigated in batch and continuously operated MFCs with granular graphite electrodes under conditions similar to those applied in MFCs with single rod electrodes and freely suspended cells. Performance of MFC in terms of biodegradation performance and energy generation was assessed and compared to those from identical MFCs with rod electrodes presented previously in Chapter 3.

4.2 Materials and Methods

4.2.1 Experimental set-ups

All experiments were conducted in H-type MFC bioreactors with set-up identical to those described in Section 3.2.2. Graphite granules were placed inside the anodic and cathodic chambers occupying approximately 70% of the volume (i.e. the working volume of each chamber was approximately 85 mL). Granular graphite particles were prepared by crushing graphite blocks typically used as conductor for electric motors followed by sieving to obtain granules with sizes in the range of 2.9 to 4.0 mm (Figure 4.1). The selection of this range was based on literature data whereby the use of granular graphite as electrode in the size range of 1.5 mm to 5 mm have been reported (Aelterman et al., 2006; Logan, 2008). Prior to use, graphite particles were disinfected

with bleach solution and then rinsed thoroughly with reverse osmosis (RO) water. With the use of granular electrode, stirring was not possible. Thus to achieve the mixing, a recirculation loop was devised where liquid content in the anodic chamber was withdrawn from the top and reintroduced into the bottom of the chamber using a peristaltic pump. The recirculation flow rate was approximately 3000 mL h^{-1} which was determined by trial and error as the highest flowrate that did not cause the motion and/or fluidization of granules (i.e. the system resembled a packed-bed configuration). As with previous experiments, *Pseudomonas putida* was used as the microbial culture in all experiments. The procedures for preparation and maintenance of *P. putida* cell suspension were similar to those described in Section 3.2.1.

Figure 4.1 Graphite granules used as electrode in MFC.

A graphite rod, similar to those described in Section 3.2.2, was used to connect the granules to the electrode terminal. Chrome wires were used to connect the electrode terminals in both anodic and

cathodic chambers to a Keithley 2700 multimeter, equipped with a 7700 datalogger (Keithley Instruments Inc., Cleveland, USA) and a personal computer which allowed real time monitoring of MFC circuit potential. The associated software, ExceLINX, facilitated measurement and datalogging of circuit potential. Other details of MFC assembly and preparation procedures were similar to those described for MFCs with rod electrodes in Section 3.2.2.

After setting up of MFC, the anodic chamber was filled with sterilized modified McKinney's medium which was then purged with nitrogen gas (industrial grade) for about 10 minutes to ensure oxygen was removed and anoxic conditions were achieved. Preparation of modified McKinney's medium has been described previously in Section 3.2.1. In the cathodic chamber, potassium ferricyanide solution (50 mM potassium ferricyanide and 100 mM potassium phosphate buffer) was used as a chemical electron acceptor.

Prior to addition of lactate or acetate and inoculation of the anodic chamber with *P. putida*, MFC open circuit potential (OCP) was monitored for about 5 hours for potential to stabilize and establish the baseline OCP value. As with previous experiments in MFCs with rod electrodes (Chapter 3.2.2), replenishment of potassium ferricyanide solution was done when the cathodic potential decreased below 250 mV (approximately 25% reduction from initial potential). This was carried out to maintain a relatively constant potential in the cathodic chamber. All experiments were conducted at room temperature (24±2 °C).

4.2.2 Batch experiments

Effects of lactate and acetate concentrations on the MFC performance in terms of biodegradation and electrochemical outputs were evaluated in batch experiments. Concentrations in the range 500-4500 mg L^{-1} for lactate (actual concentrations: 532, 1013, 1758 and 4400 mg L^{-1}) and 1000-5000 mg L^{-1} for acetate (1367, 2505 and 4970 mg L^{-1}) were evaluated. Effect of sequential addition of each substrate was also investigated. It is important to note that the aim was to investigate the effect of initial concentrations in the range 1000-5000 mg L^{-1}. However, with granular electrodes the adjustment of concentration at the designated value was challenging on occasions.

The experiment was started by adding a small volume of a concentrated lactate solution through the sampling port of the anodic chamber which reached an initial concentration of around 700 mg L^{-1}. Immediately after addition of lactate, inoculation was carried out by injecting 1 mL of a concentrated cell suspension of *P. putida*. Preparation of cell suspension has been described in detail in Section 3.2.1. Concentration of lactate was monitored and after complete degradation of substrate, volume of McKinney's medium in the anodic chamber was made up to the original level and another batch of lactate (1000 mg L^{-1}) was added. These initial runs constituted the start-up stage after which actual experiments with different lactate concentrations, initially at the lowest level of 500 mg L^{-1}, were conducted. Regular sampling of anodic liquid was done, at least once a day, to monitor concentration of lactate in the anodic chamber. Moreover, circuit potential of MFC was constantly monitored and power and current were periodically measured as described in Section 4.2.4.

After completion of all experiments with lactate, similar experiments were conducted with acetate as substrate starting with the lowest concentration (1000 mg L^{-1}). Sampling and analysis were similar to those described for lactate. MFC performance in terms of substrate biodegradation, power and current production was evaluated.

4.2.3 Continuous experiments

Following the completion of batch experiments, MFC with granular electrode was switched to continuous mode of operation. Feed in these experiments was modified McKinney's medium containing either lactate or acetate. Prior to use in the experiment, feed was sterilized and purged with nitrogen gas for about 10 minutes. A calibrated variable flow peristaltic pump was used to pump the feed continuously into the anodic chamber. Feed flowrate was determined during the experiments through collection and measurement of the effluent volume over a specified period of time. The experimental setup of a continuously operated MFC with granular electrodes, in this case fed with lactate, is shown in Figure 4.2. Similar to continuously operated MFC with rod electrodes, an intermediary glass device was installed in the feed line to prevent contamination of the feed through transfer of bacterial cells from the anodic chamber. To monitor the concentration of feed and to ensure contamination did not occur, regular sampling and analysis of feed collected at the proximity of the inlet port of the anodic chamber were done.

Effect of loading rate on MFC performance was evaluated by varying the flowrate and concentration of the substrate in the feed. In the experiment with lactate as substrate, feed concentrations of 1000, 2500 and 5000 mg L^{-1} were examined. On the other hand, a feed

concentration of 1000 mg L^{-1} was utilized when acetate was used as substrate. Given the results obtained with acetate in MFC with rod electrodes only a low acetate concentration was evaluated.

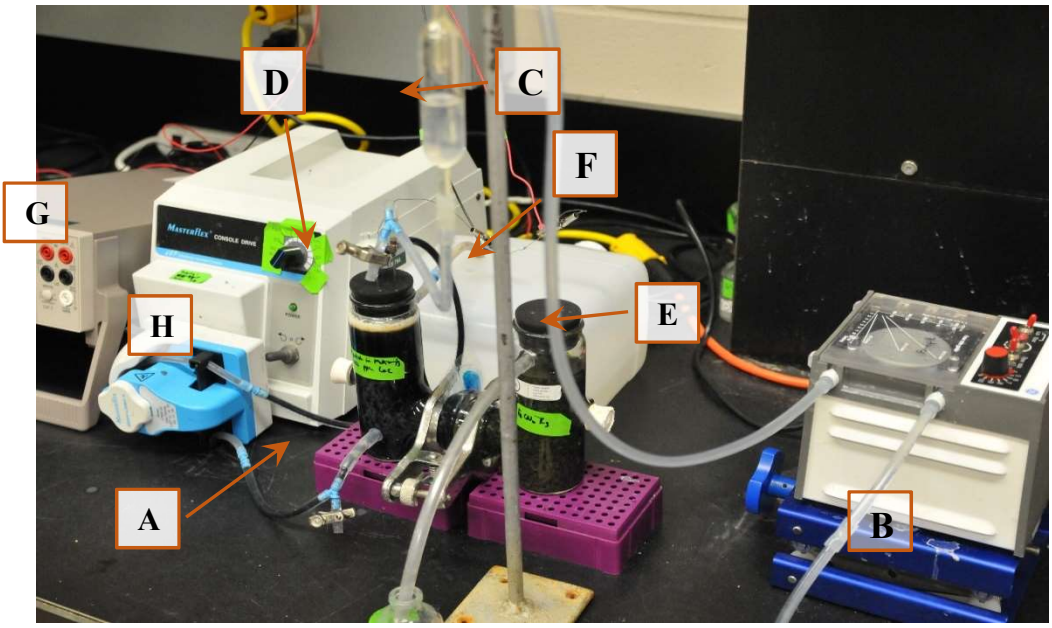

Figure 4.2 Experimental system used in continuous biodegradation of lactate in a MFC with granular electrodes. Feed is drawn into the anodic chamber (A) using a peristaltic pump (B) passing through the intermediary glass device (C) used to prevent contamination of feed. Sampling of feed line was done near the inlet port (D) which is sealed with a clamp and only opened during collection. Effluent left the chamber into the effluent container (E). An external resistor (F) is attached between the anode and cathode terminals which are connected to a multimeter (G) equipped with a datalogger. Second peristaltic pump (H) was used to recirculate the anodic liquid.

Experiments started using a low flowrate of approximately 2 mL h^{-1}. The flowrate was increased incrementally after steady-state conditions was established at each flow rate. Steady-state conditions were assumed when there was less than 10-15% variation in the residual concentration of lactate or acetate in the anodic chamber. Following the establishment of steady-state conditions, MFC was operated at the same flowrate for at least three additional residence times before increasing the flowrate. Incremental increase in flowrate continued until performance of MFC started to deteriorate resulting in a considerable decrease in the biodegradation rate of substrate.

Throughout the experiment, the anodic chamber was sampled regularly to monitor the concentration of lactate and acetate. Sampling was done at least once a day at low flow rates. The sampling frequency was increased as higher flowrate was applied. Average value of data generated after establishment of steady state and associated standard deviation were used in presenting the results.

The MFC fed with 1000 mg L^{-1} lactate was operated to a maximum flowrate of approximately 400 mL h^{-1} before deterioration in performance was observed. Similar procedures were followed in experiments with higher lactate feed concentrations of 2500 and 5000 mg L^{-1}. Upon completion of these set of experiments, lactate was substituted with 1000 mg L^{-1} acetate and performance of MFC was assessed using the same approach used for lactate. With 1000 mg L^{-1} acetate in the feed, the MFC was able to handle a narrower range of flowrates from 2.0 to 28.6 mL h^{-1} or equivalent loading rates of 19.4-331.1 mg L^{-1} h^{-1} before deterioration in its performance was observed. Hence, experiments at higher acetate concentrations, which result in higher loading rates, was considered impractical.

Along with measurement of lactate and acetate concentrations, MFC circuit potential was also constantly monitored and power and current output was periodically measured. For a more accurate determination of power and current output, Linear Sweep Voltammetry (LSV) was conducted and polarization curves were developed for MFC operated under various loading rates of lactate or acetate. Monitoring of circuit potential and measurement of energy output is described in Section 4.2.4. With granular graphite as electrode, determination of biomass concentration was not carried out due to interference of particle turbidity in measurement of optical density.

Moreover, a major portion of biomass was present in the form of attached cells (biofilm). Thus, optical density would not have represented the total biomass hold-up in the system.

4.2.4 Analyses

Sample collection, centrifugation and analysis using an HPLC to determine concentrations of lactate and acetate as well as the monitoring of MFC circuit potential has been described previously in Section 3.2.4. Measurement of cathodic potential was conducted using a handheld multimeter (Fluke 189 True RMS, Everett, WA, USA) and a calomel reference electrode (Cole-Parmer, Vernon Hills, IL, USA). Electrochemical output was determined by generating polarization and power curves. Polarization curves were developed by running Linear Sweep Voltammetry (LSV) analyses using a Gamry R600 potentiostat (Gamry Instruments, Warminster, USA). Each measurement was done for the entire fuel cell with the anode as working electrode and cathode as both the counter and reference electrodes. The range of potential sweep was from -550 mV to 10 mV at a scan rate of 0.1 mV s^{-1}. This range was extracted after trimming a wider range of potential sweep, employed during multiple initial measurements, of its excess portions (generating irrelevant results) in order to reduce run times.

After polarization or voltage-current curve was generated, corresponding power was calculated (i.e. P=VI) and plotted against the current to form the resulting power curve. External resistance was re-applied immediately after measurement. Corresponding current and power densities were calculated based on the working volume of the anodic chamber. During the early part of the study, the potentiostat was not available and hence, current and power densities were reported based on output of applied external resistance and calculations following Ohm's law, as has been described

in Section 3.2.4. Calculation of coulombic efficiency (CE) was done following procedures detailed in Appendix H.

Additional analyses were also carried out to examine the changes in the properties, especially in the surface area, of the granules. Surface area, pore size and pore volume of fresh (unused) and exposed graphite granules were determined through BET analysis using an ASAP 2020 Surface Area and Porosity Analyzer (Micromeritics Instrument Corp., Norcross, GA, USA). Before analysis, granular graphite samples were dried overnight in an oven at 110 °C. Samples were analysed using 30 relative pressure points at the mesopore range. Graphite granules (fresh and after completion of experiments) were also examined by a scanning electron microscope (SEM). Granule samples were prepared by freeze drying over a 24-h period using a Modulyo D freeze drying system (Thermosavant Instruments Inc, Holbrook, NY, USA). Samples were then gold plated, fixed to a stub and visualized using a field emission SEM (SU 6600 Hitachi, Hi-Tech Corp, Japan), operated at 10 KeV and 5 uA probe current and at a working distance of 21 mm.

4.3 Results and discussion

Batch experiments in MFC with granular electrodes were conducted with two model fatty acids as substrates, initially with lactate and subsequently with acetate. The motivation behind the use of the granules was to increase the available surface area for formation of biofilm on the electrode surface, which could in turn enhance substrate degradation, as well as to promote the effective transfer of electrons through a larger surface area and thus to enhance energy output.

4.3.1 Biodegradation of lactate

Batch operated MFCs. The results obtained in the batch experiments conducted in MFC fed sequentially with lactate at various concentrations are shown in Figure 4.3. The first two concentration profiles (Figure 4.3: Panel I; <300 h after inoculation) represent the biodegradation of lactate during the first two trials where adjustment of recirculation flowrate within the anodic chamber to the desired level of 3000 mL h^{-1} were conducted. Moreover, this period was designated as the start-up stage that allowed acclimation of microbial community and accumulation of biomass on the surface of the granules. Decrease in lactate concentration in the first run was observed without any lag phase in microbial activity. This was followed by addition of another 1000 mg L^{-1} lactate which was consumed in the same manner. Formation of biofilm, especially on the surfaces of granules close to the entry port of the recirculation loop was apparent towards the end of these two runs.

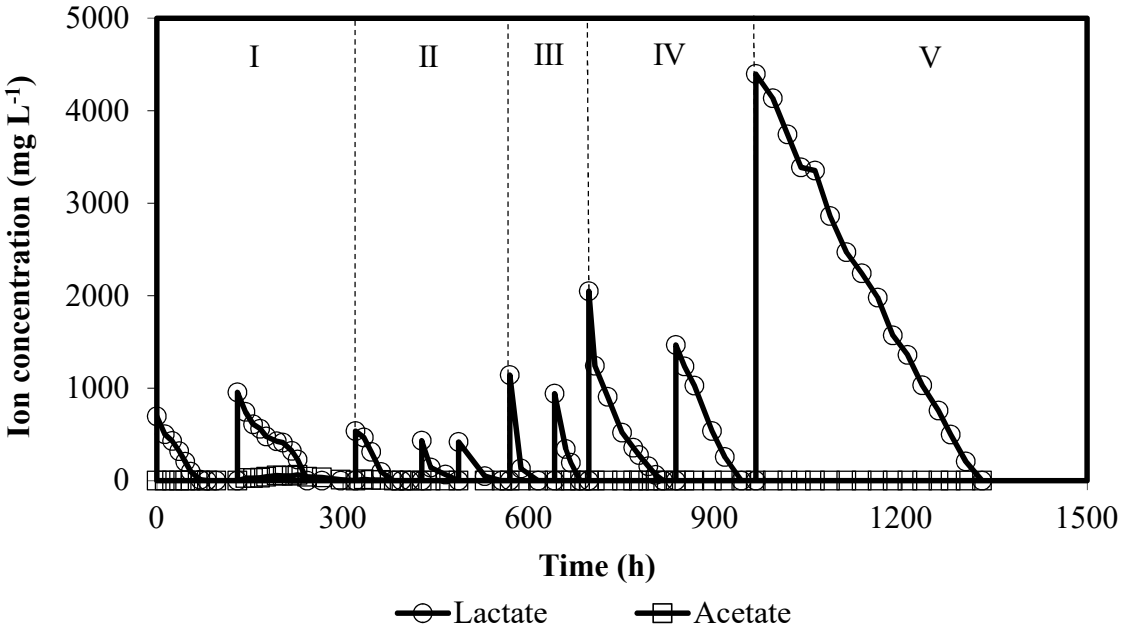

Figure 4.3 Profiles of lactate and produced acetate concentrations during the sequential degradation of lactate at various initial concentrations in MFC with granular electrodes and immobilized *P. putida* cells. Panel I: 1000 mg L^{-1} (start-up), Panel II: 500 mg L^{-1}, Panel III: 1000 mg L^{-1}, Panel IV: 2500 mg L^{-1} and Panel V: 5000 mg L^{-1} lactate.

Following the start-up period, which approximately took 250 h, actual tests were initiated by addition of 500 mg L^{-1} lactate to the anodic chamber. As with the initial start-up trials, lactate concentration began to decrease immediately after addition (Figure 4.3: Panel II). After depletion of lactate, two additional batches with 500 mg L^{-1} lactate were carried out sequentially which resulted in a similar rapid depletion of substrate until its complete exhaustion. Sequential addition of lactate at higher initial concentrations of 1000, 2000 and 4500 mg L^{-1} were then followed (Figure 4.3: Panels III, IV and V), which again resulted in fast utilization of lactate with no substrate inhibition effect even at a high concentration of 4500 mg L^{-1}. It should be pointed out that multiple sampling and the need for making up the volume of liquid contents in the anodic chamber before each experiment on occasion led to initial lactate concentrations which were slightly different from the designated values (2000 and 4500 mg L^{-1} as opposed to intended values of 2500 and 5000 mg L^{-1}).

Based on the results obtained in MFCs with single rod electrode (Chapter 3), biodegradation of lactate was expected to lead to formation and accumulation of acetate (biologically produced acetate). However, as can be seen in Figure 4.3, biodegradation of lactate did not lead to accumulation of acetate, except for a very short period during the start-up stage where acetate at very low concentrations (<65 mg L^{-1}) was detected. These low levels of biologically produced acetate were utilized immediately following the exhaustion of lactate. Overall, the rapid degradation of lactate without accumulation of acetate could be described through the complete degradation of lactate without formation of intermediates conforming to reaction 3.2 as described in Section 3.2.5. The short period where low levels of biologically produced acetate were detected shows incomplete degradation of lactate at a very slow rate and rapid utilization of biologically

produced acetate, thereby indicating that reactions 3.1, 3.2 and 3.3 were occurring at the same time.

To assess the effect of initial concentration on biodegradation of lactate in the batch MFC with granular electrode, lactate biodegradation rates were calculated by determining the slope of the linear portion of lactate concentration profiles. The average biodegradation rate of lactate at the lowest examined concentration of 500 mg L^{-1} was 7.4 ± 1.8 mg L^{-1} h^{-1}. A higher biodegradation rate of 23.1 ± 0.03 mg L^{-1} h^{-1} was achieved when the initial lactate concentration was increased to 1000 mg L^{-1}. The improved performance could be attributed to the benefits brought about by the preceding sequential batch operations which most likely enabled the microbial community to increase in population and adapt further to the granular environment. A similar improvement in lactate biodegradation was reported when adapted inoculum was used in an upflow anaerobic sludge blanket (UASB) reactor (Sorensen et al., 1990). This finding would explain the inferior biodegradation performance during the start-up period utilizing a similar initial concentration of 1000 mg L^{-1} lactate which achieved a biodegradation rate of only 7.9 ± 2.1 mg L^{-1} h^{-1} (vs. 23.1 mg L^{-1} h^{-1}).

Increase in lactate concentration to about 2,000 mg L^{-1} resulted in a lower biodegradation rate of 14.4 ± 0.3 mg L^{-1} h^{-1}. Further increase in the initial concentration to approximately 4,500 mg L^{-1} lactate led to an even lower rate of 12.3 mg L^{-1} h^{-1}. This finding was contrary to that observed in similar MFCs with rod electrodes where lactate biodegradation rate was found to increase with initial concentration. We could only speculate that some form of substrate inhibition, typical at high substrate concentrations, could have been responsible for the reduction in biodegradation rate

at the higher initial concentrations, especially when the occurring pathway of degradation was through complete lactate oxidation with no acetate production (reaction 3.2).

Lactate biodegradation in MFC with granular electrodes was generally faster when compared to those observed in MFCs with rod electrodes fed with similar lactate concentrations. A comparison of biodegradation rates achieved with rod and granular electrodes, shown in Figure 4.4, reveals that lactate biodegradation at initial concentrations of 1000 and 2500 mg L^{-1} were markedly faster in MFC with granular electrode. However, at the highest initial concentration of approximately 5000 mg L^{-1}, biodegradation rate achieved from MFC with rod electrode was higher. Additionally, in MFC with rod electrodes increase in lactate concentration led to higher rates but in MFC with granular electrodes increase in lactate concentration led the biodegradation rate to pass through a maximum. The extent that the MFC had been running prior to initiation of experiments at the higher initial concentrations, due to sequential batch operation, may have affected the effectivity of biodegradation whereas no such effect was present in MFCs with rod electrodes since biodegradation of each tested initial concentration was conducted as separate experiments. For instance, biodegradation of 5000 mg L^{-1} lactate in MFC with rod electrodes commenced after inoculation while that in the same MFC with granular electrodes was initiated 966 h after inoculation. Conditions brought about by the extent of operation including saturation of granule surface, decrease of viable microbial cells or accumulation of dead biomass creating diffusional resistance for the substrate may have affected biodegradation performance.

To date no other work has been conducted in similarly configured and operated MFC with granular electrode or immobilized cells, hence no information on lactate biodegradation in similar systems

exists in literature for comparison. In a conventional bioreactor, a faster lactate biodegradation compared to this work was achieved in an anaerobic fluidized bed reactor with porous glass beads as matrix for cell immobilization and methanogenic consortium as inoculum where 3600 mg L^{-1} (40 mM) lactate was degraded in approximately 24 h or an equivalent biodegradation rate of 150 mg L^{-1} h^{-1} (Zellner et al., 1993). The faster lactate biodegradation is due to more favourable conditions such as direct access to electron acceptor in conventional bioreactors.

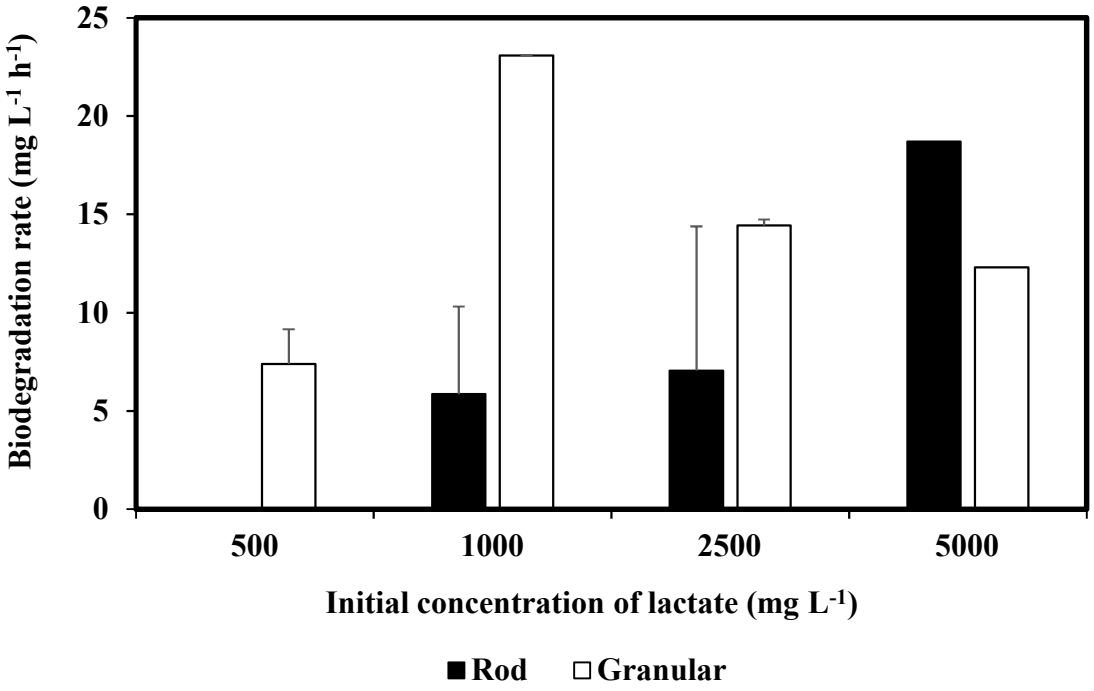

Figure 4.4 Comparison of lactate biodegradation rates achieved in batchwise operated MFCs with either single rod or granular electrode at various lactate initial concentrations.

Power, current and OCP output. The open circuit potential (OCP) of the MFC was monitored during the start-up period (i.e. immediately after addition of lactate and inoculation with microbial culture). The maximum observed OCP was approximately 200 mV which was lower compared to that from previous runs in MFC with rod electrodes fed with a similar lactate concentration of

1000 mg L^{-1} (around 500 mV). This observed difference could be due to drastic differences in the type of electrodes used in these two systems. Moreover, this level of OCP was monitored during the start-up period where immobilization of microorganisms was yet to develop and fully adapt to the granular matrix environment.

After the start-up and during the biodegradation of second batch of lactate, a low external resistance of 50 ohms was applied across the circuit to determine current and power. However, due to the relatively fast degradation of lactate, repeated removal and placing of the resistor, as carried out in MFC with rod electrodes, was not practical and the external resistance was kept in the circuit. With the relatively low applied external resistance, the resulting circuit potential as expected was low, ranging from 4 to 8 mV.

As with MFCs with rod electrodes, power and current densities were also calculated in terms of electrode surface area and anodic working volume. Using the BET analyzer, the surface area of fresh or unused graphite granules was determined as 1.1 m^2 g^{-1} which translated to a total surface area of 204 m^2, given that 185 g granules were used in the anodic chamber. Given the magnitude of BET surface area calculated, current and power densities were very low (maximum power density = 6.3×10^{-6} mW m^{-2}). These values, however, appear an underestimation and need to be treated cautiously. This is due to the fact that BET surface area includes not just the outer surface area of the granules that are accessible to bacterial cells but also the surface area created by the micronic pores that are unlikely to be colonized or populated by bacterial cells. For the reasons stated, power and current density calculated based on BET surface area potentially produce extremely skewed results and do not represent actual electrochemical output. Hence, power and

current densities from MFCs with granular electrodes were calculated based on the working volume of the anodic chamber. This is consistent with other works employing granular electrodes which reported current and power output in terms of anodic working volume only (Aelterman et al., 2006; Rabaey et al., 2006).

With the applied external resistance maintained at 50 ohms, stable circuit potential measured during each set of sequential runs corresponding to each tested initial lactate concentration of 500, 1000, 2000 and 4500 mg L^{-1} were 4.2, 4.7, 6.1 and 8.0 mV, respectively. The equivalent power densities were calculated as 3.8, 4.9, 8.3 14.3 mW m^{-3}, while the corresponding current densities were 922.2, 1046.7, 1360.0 and 1782.2 mA m^{-3}, respectively. These results reveal that power and current output improved with increase in initial lactate concentration as sequential operation of MFC progressed. Comparable results were obtained in MFCs equipped with rod electrodes where power, current and most notably OCP were higher in MFCs operated with higher initial lactate concentration. The higher electrochemical output achieved at higher lactate concentrations could be explained by Gibb's free energy where substrate with higher anodic (negative) potential contains higher capability to donate electrons to an electron acceptor. Higher lactate concentrations result to higher anodic potentials which consequently provide higher electron content for transfer to the electrode and movement through the circuit.

In relation to associated biodegradation performance, the increasing trend of power and current output with initial lactate concentration did not conform to the corresponding trend of biodegradation rates. As has been discussed previously in Section 3.3, higher power and current output in MFCs with rod electrodes was associated with higher biodegradation rates and CE. With

granular electrodes, after attaining its highest at 1000 mg L^{-1} of lactate, biodegradation rate declined with further increase in initial concentration while corresponding power and current output continued to increase. These findings were further attested by looking into the efficiency of energy recovery as revealed by the associated coulombic efficiencies. Calculated CE values were higher with increase in initial concentration from 1000-4500 mg L^{-1} with 1.2, 2.5 and 4.2%, respectively. The lowest CE of 1.2% at 1000 mg L^{-1}, where biodegradation rate was fastest, indicates that even with breakdown of electron donor at a higher rate, recovery of released electrons for generation of current was low. CE increased with initial concentration, despite decline in biodegradation rate, resulting to corresponding increase in power and current output. It could be speculated that conditions brought about by the granular system led to power and current generation being governed more by the electrochemical processes working in the system than the effectiveness of biodegradation, especially when changes that could affect the electrochemical environment was minimized by keeping the applied external resistance constant throughout the operation of MFC. Value of CE obtained at the lowest lactate concentration of 500 mg L^{-1} was within the calculated range with 3.6%.

When compared to similarly operated MFCs with rod electrodes and freely suspended cells, electrochemical output from the system with granular electrode was significantly higher. In the former system, the highest current density was approximately 10 times lower with only 177.8 mA m^{-3}, and power was also lower at 11.5 mW m^{-3}. Finally, overall CE in case of MFC with granular electrode was higher (0.2-1.7% vs 1.2-4.2%). These findings indicate the superior performance, in terms of electrochemical output, in the use of granules over rod as electrode in similarly operated MFCs. The increased surface area with the use of granules could have enhanced the capacity to

transfer electrons leading to higher CE which consequently minimized the effect of lower biodegradation performance. Potentially higher electrochemical output could have been measured if a higher external resistance was applied and more accurately if a quick monitoring tool, such as a potentiostat, was utilized. Unfortunately, a potentiostat was not available during the operation of sequential batch experiments but this became available in the latter parts of the work and used during the experiments in continuous flow MFCs.

Continuously operated MFCs. After completion of all batch experiments with lactate, the MFC with granular electrode was switched to continuous mode of operation to assess the performance of MFC in the continuous flow mode and to investigate the effect of lactate concentration and loading rate on performance of the MFC in terms of biodegradation and electrochemical outputs. The MFC was subjected to a wide range of loading rates by varying either the flowrate of the feed (from 2-400 mL h^{-1}) or feed lactate concentration (1000, 2500 or 5000 mg L^{-1}). It is important to point out that with each feed lactate concentration, a range of flow rates were applied. Experiments started with a lactate feed concentration of 1000 mg L^{-1} and a low flowrate of approximately 2 mL h^{-1}. The steady state concentration profiles of lactate and corresponding accumulated acetate obtained in these runs are shown as a function of dilution rate in Figure 4.5 panels A, B, C for 1000, 2500 and 5000 mg L^{-1} lactate feed, respectively.

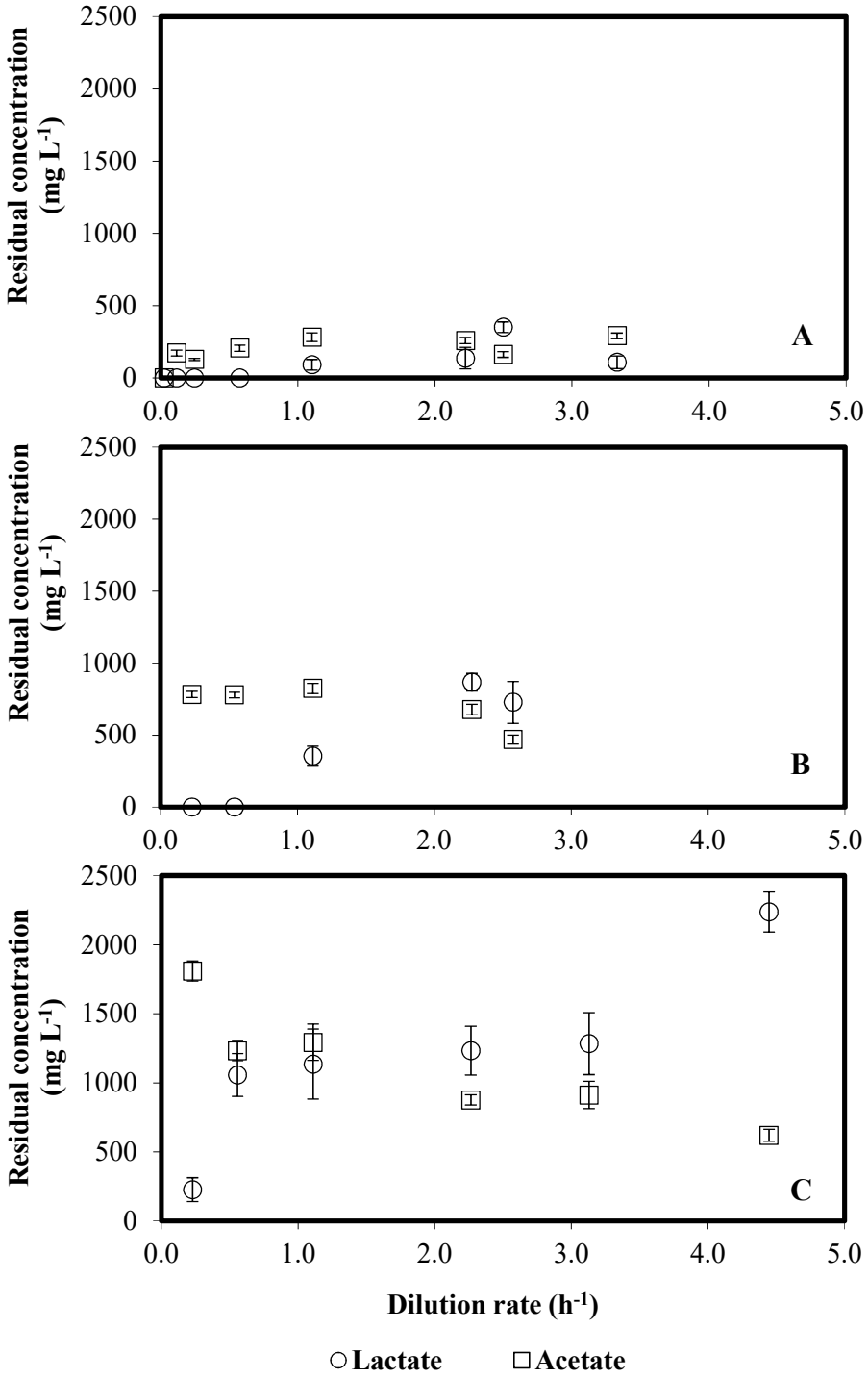

Figure 4.5 Steady state profiles of lactate and accumulated acetate concentrations as a function of dilution rate in a MFC with granular graphite electrodes operated continuously with feeds containing different levels of lactate: A) 1000, B) 2500 and C) 5000 mg L^{-1} lactate. Error bars represent standard deviation of steady state residual lactate and acetate concentrations.

At the lowest lactate feed concentration of 1000 mg L^{-1} (Figure 4.5A), effectiveness of the MFC was apparent at the lower dilution rates up to 0.6 h^{-1} (HRT=1.7 h) where complete degradation of lactate was achieved and low levels of residual acetate concentration (<207 mg L^{-1}) were detected. As dilution rate was increased, incomplete degradation of lactate was observed but residual lactate concentration remained considerably low with a maximum value of 350.8 mg L^{-1} or about 35.4% of the influent concentration observed at a considerably high applied dilution rate of 2.5 h^{-1}. Similar residual lactate and acetate concentration profiles were observed when the concentration of lactate in the feed was increased to 2500 mg L^{-1} (Figure 4.5B).

With the highest lactate feed concentration of 5000 mg L^{-1}, residual concentrations of both lactate and accumulated acetate were generally high at all applied dilution rates (Figure 4.5C), especially when compared to those from previous runs with lower lactate feed concentrations. To be more specific, residual lactate concentration increased gradually with increase in dilution rate and reached to a maximum value of 2236.9 mg L^{-1} (45.5% of feed concentration) at a dilution rate of 4.4 h^{-1}. The corresponding residual concentration of accumulated acetate slowly decreased with increase in dilution rate. This makes sense as one could expect a lower concentration of accumulated acetate when the extent of lactate biodegradation is decreased (i.e. lower biodegradation of lactate results in lower acetate production). As shown in Figure 4.5C, residual lactate concentration at dilution rates above 2.3 h^{-1} became more pronounced than acetate with difference between the diverging residual concentrations observed to widen with increase in dilution rate. As higher dilution rates were applied, the effectiveness of the MFC in degrading lactate gradually deteriorates resulting to lower lactate utilization (as shown in the increasing residual lactate concentration) and hence leading to lower conversion to acetate. As biodegradation

of lactate becomes more challenging with increase in concentration, its conversion to acetate is diminished thereby decreasing the accumulation of acetate and thus lower residual acetate concentrations.

Overall, when compared to the previous continuous MFC with single rod electrode, the range of dilution rates over which the MFC with granular electrode was able to degrade lactate and accumulated acetate was remarkably higher (0.02-4.45 h^{-1} vs 0.01-0.96 h^{-1}). With the scope of lactate concentrations used in the feed, the applied dilution rates had equivalent lactate loading rates ranging from 20 to 21,900 mg L^{-1} h^{-1}. A comparison of the steady state concentration profiles of lactate and accumulated acetate throughout the range of applied loading rates between the different lactate feed concentrations is shown in Figure 4.6. It can be observed that higher residual concentrations of both lactate and accumulated acetate were obtained when feed applied contained higher concentration of lactate. This increase was more evident in accumulated acetate concentrations which is likely attributed to the higher amounts of lactate available for conversion to acetate. As expected, residual lactate concentration increased with loading rate regardless of feed concentration. On the contrary, residual concentration of accumulated acetate showed no increase with loading rate.

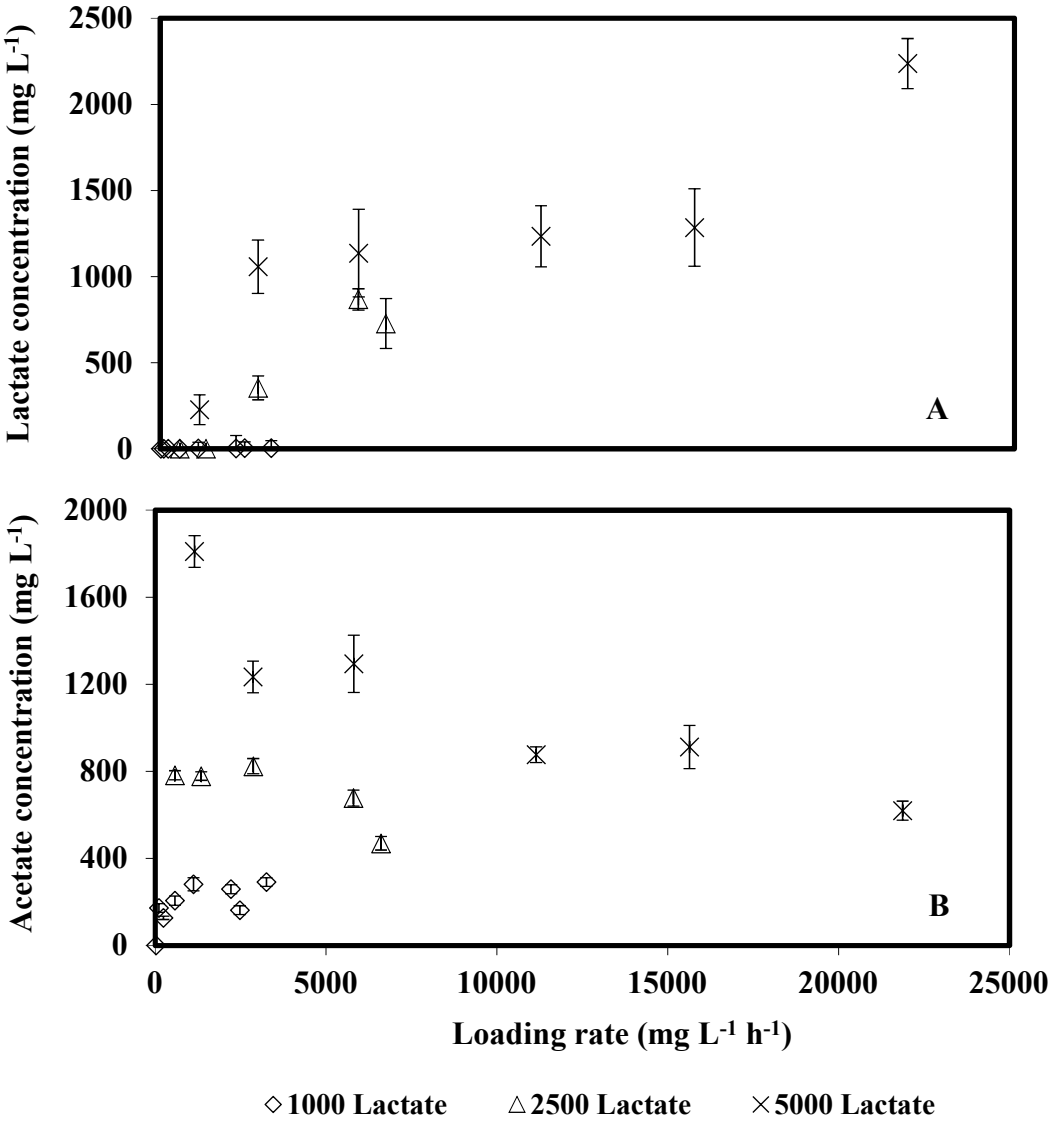

Figure 4.6 Steady state concentration profiles of lactate (panel A) and accumulated acetate (panel B) as a function of loading rate in MFC with granular graphite electrodes fed continuously with either 1000, 2500 or 5000 mg L^{-1} h^{-1} lactate.

Figure 4.7 shows the biodegradation rate of lactate as well as accumulation rate of biologically produced acetate as a function of loading rate in the continuously operated MFC with granular electrode provided with either 1000, 2500 or 5000 mg L^{-1} lactate in the feed. Also, included in the figure are the corresponding removal percentages of lactate for the entire range of applied loading rates. Overall, it can be observed that the profiles of lactate biodegradation rate and removal

percentage as well as accumulation rate of acetate was considerably consistent in following their respective trends indicating that concentration of lactate in the feed did not affect the biodegradation rate and conversion patterns.

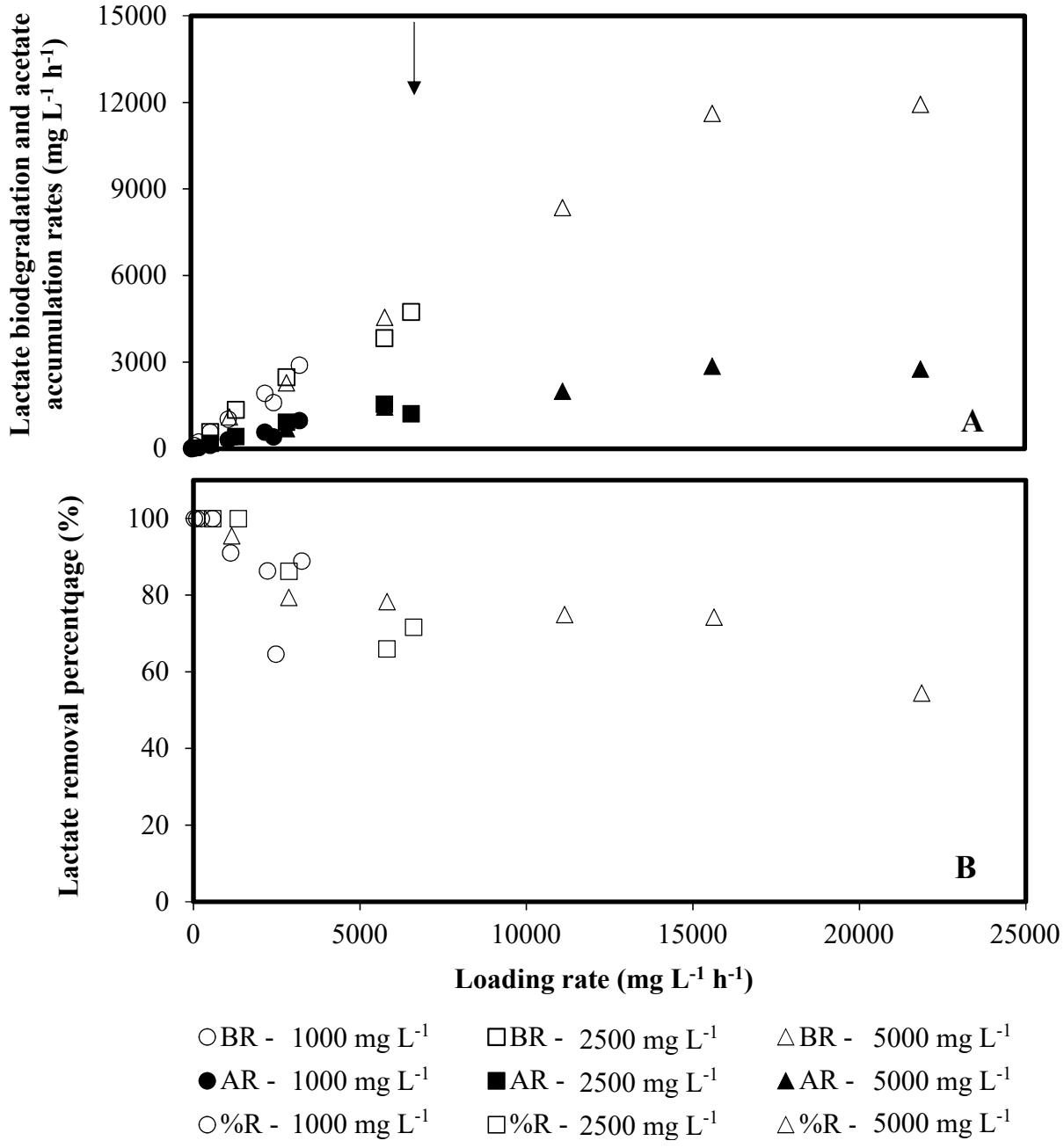

Figure 4.7 Biodegradation rate (BR) of lactate and accumulation rate (AR) of acetate (panel A) as well as the corresponding removal percentages (%R) of lactate (panel B) as a function of loading rate in continuously operated MFC with granular electrode fed with either 1000, 2500 or 5000 mg L^{-1} lactate. Arrow indicates results from additional run.

At the lowest lactate loading rate of 22.2 mg L^{-1} h^{-1} (HRT=41.4 h), complete degradation of lactate was achieved and no acetate accumulation was detected. Complete removal of lactate was achieved with loading rates up to 576.3 mg L^{-1} h^{-1} (HRT=4.3 h), after which residual lactate started to appear and its concentration slowly increased with increase in loading rate. As higher loading rates were applied, gradual increase in acetate accumulation rate was observed. For loading rates up to 1344.3 mg L^{-1} h^{-1} (HRT= 1.8h), removal percentage of lactate was still high and above 91%. Further increase in loading rate resulted in a slow decrease in removal percentage, while lactate biodegradation continued to improve.

Lactate biodegradation rate continued to increase, at a relatively rapid rate, up to a loading rate of 15636.5 mg L^{-1} h^{-1} (HRT=0.32 h) with the corresponding lactate biodegradation being 11617.9 mg L^{-1} h^{-1}. The highest accumulation rate of acetate (2853.0 mg L^{-1} h^{-1}) was also achieved at the same loading rate. Further increase in loading rate to the maximum applied of 21874.7 mg L^{-1} h^{-1} (HRT=0.22 h), resulted in a decrease in acetate accumulation rate to 2757.6 mg L^{-1} h^{-1} and significant slowdown in lactate biodegradation rate, which also corresponded to further decrease in removal percentage falling down to 54.5%. The lactate biodegradation rate observed under this condition (11925.7 mg L^{-1} h^{-1}) was slightly higher than that observed in the previous applied loading rate, indicating a levelling off trend and slow deterioration in performance of the system. With the system undergoing diminished performance as well as logistical and reactor capacity constraints, further experiments at higher lactate loading rates were not pursued. Throughout experiment, a greater portion of the entire duration was operating at a relatively high removal efficiency with an average of 84.8% ± 14.3%.

If trendlines are projected on data profiles shown in Figure 4.7, a slight deviation from the respective profiles of lactate biodegradation and acetate accumulation rates and especially in removal percentage could be observed at loading rates of 2476 mg L^{-1} h^{-1} (1000 mg L^{-1} lactate feed) and 5801 mg L^{-1} h^{-1} (2500 mg L^{-1} lactate feed). These were results from additional runs (repeated experiments) conducted after completion of continuous biodegradation tests with acetate as original substrate in the same MFC, as presented in succeeding section 4.3.2. Lower levels of biodegradation and accumulation rates and particularly removal percentage were observed at these loading rates. This finding likely resulted from hysteresis effect and stress imposed on the cells emanating from the additional runs, especially when a wide range of flowrates together with varied concentrations of lactate in the feed were implemented throughout the experiment. These additional runs were conducted for three reasons: 1)-to assess the hysteresis effect (i.e. to verify whether results obtained at the earlier parts of the experiments can be replicated, given the stress that biofilm had experienced); 2)-to allow the system to recover from deterioration in performance due to the utilization of acetate as substrate and previous operation at high lactate loading rates (i.e. high flow rates and substrate concentration); 3)-to have the opportunity to take representative granule samples for the SEM and BET examinations. Another additional run was carried out by further increasing the loading rate to 6600 mg L^{-1} h^{-1} and the corresponding points of lactate biodegradation and acetate accumulation rates as well as removal percentage appeared to have improved their fit in their respective profiles indicating the recovery of the continuous system (indicated by arrow in Figure 4.7).

As discussed earlier, residual lactate is present when lactate is not completely degraded. High level of residual lactate signifies low biodegradation performance and corresponding removal

percentage. The extent of lactate degradation clearly affects the production and accumulation of acetate. To represent the degree of acetate accumulation as an intermediate of lactate biodegradation, specific accumulation rate of acetate in the continuous system was defined and used. The specific acetate accumulation rate was defined as the ratio of the accumulation rate of biologically produced acetate over the lactate loading rate.

The specific acetate accumulation rates calculated throughout the range of applied loading rates as well as the corresponding lactate removal percentages are shown in Figure 4.8 as function of lactate loading rate. At the lower lactate loading rate range (22.2 to 1344.3 mg L^{-1} h^{-1}, Figure 4.8A) complete degradation of lactate was achieved (i.e. 100% lactate removal), which corresponded to a considerable rise in specific acetate accumulation rate as lactate loading rate was increased. In other words, increase in specific acetate accumulation rate was observed with increase in loading rate when removal percentage of lactate was relatively high (>91%). As removal percentage of lactate decreased due to increase in loading rate (from 2220.3 to 5812.3 mg L^{-1} h^{-1}, Figure 4.8B), the specific acetate accumulation rate correspondingly decreased. Further reduction in specific acetate accumulation rate was observed as lactate removal percentage continued its decline (Figure 4.8 panel C).

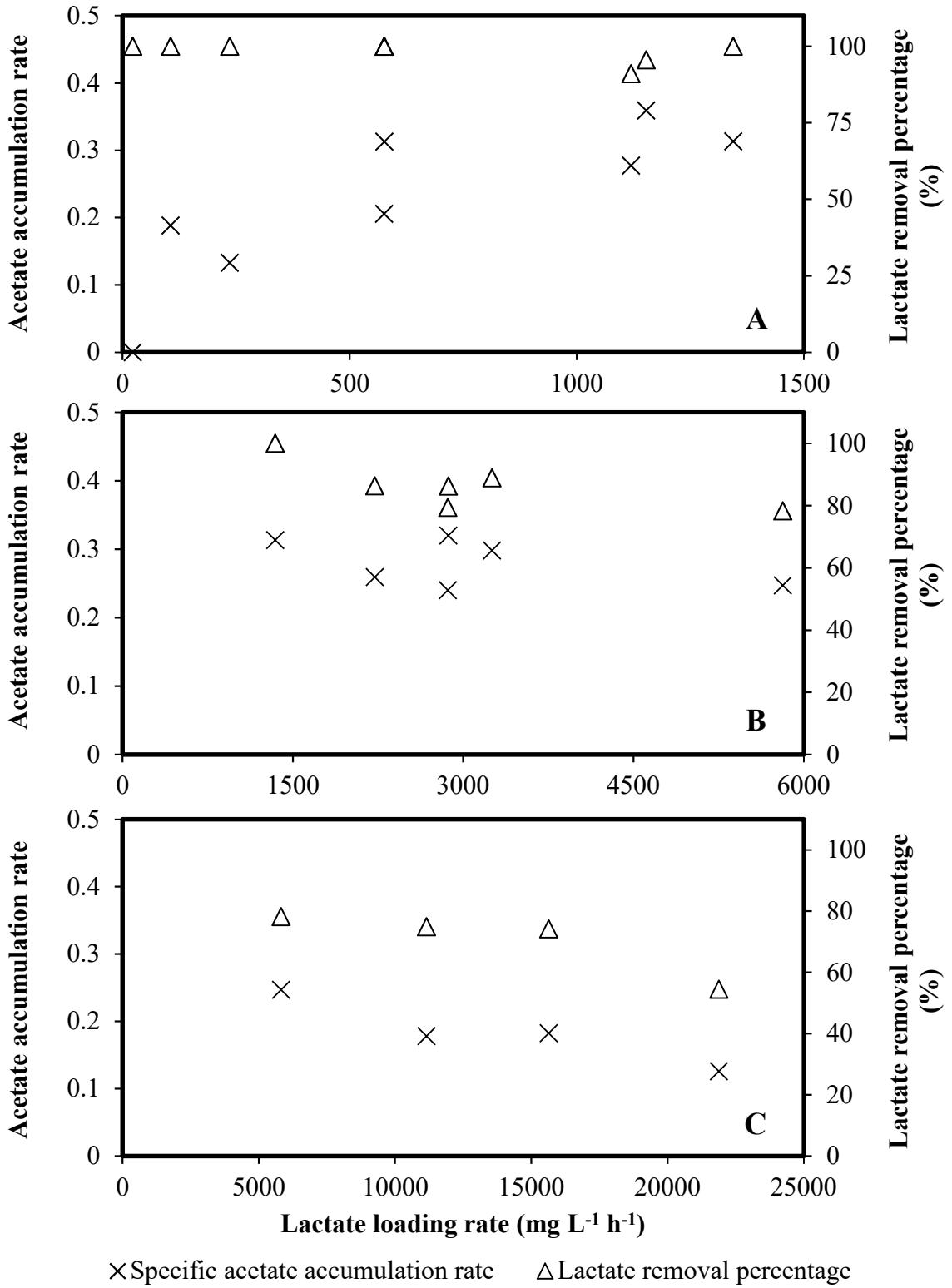

Figure 4.8 Specific accumulation rate of acetate and corresponding lactate removal percentage as a function of lactate loading rate in a MFC with granular electrodes fed continuously with lactate. Each panel shows results covered within a different range of loading rates.

The findings observed from this analysis show that lactate biodegradation with corresponding high removal levels results in specific acetate accumulation rate that increases with loading rate. However, when corresponding lactate removal percentage decreases, the specific acetate accumulation rate begins to decline and further decreases as lactate removal deteriorates even when higher amounts of available lactate are continuously provided as the loading rate increases. Lower lactate removal efficiency indicates lower lactate utilization which results to lower amounts of processed lactate available for conversion to acetate, hence resulting to a decline in the accumulation of the formed intermediate.

The highest specific acetate accumulation rate achieved by the system, which was 0.36 (mg L^{-1} h^{-1} acetate per mg L^{-1} h^{-1} lactate), was achieved at a lactate removal efficiency of 96%. This was obtained at the loading rate of 1152.7 mg L^{-1} h^{-1} where the corresponding lactate biodegradation rate and acetate accumulation rate were 1101.0 and 414.0 mg L^{-1} h^{-1}, respectively. These rates were substantially lower than the maximum lactate biodegradation and acetate accumulation rates (11925.7 and 2853.0 mg L^{-1} h^{-1}, respectively) which were achieved at significantly higher loading rates above 15600 mg L^{-1} h^{-1}. At these high loading rates, removal percentage was lower with <75% and thus resulting to substantially lower specific acetate accumulation rate of only 0.18. These findings show that specific acetate accumulation rate is highest when lactate is being degraded at high removal efficiency which does not necessarily correspond to the highest lactate biodegradation rate. This observation suggests that degree of acetate accumulation is influenced more considerably by the lactate removal efficiency than the biodegradation rate. It should be noted that no intermediate other than acetate was detected during the analysis of samples making acetate the only intermediary product of the biodegradation process. Monitoring of the specific

accumulation rate of intermediary product/s could be useful in indicating effectivity in the biodegradation of primary carbon sources especially if biodegradation of said substrate cannot be readily determined. Such potential can be applicable in wastewater treatment where monitoring of known intermediary product/s could be utilized in determining efficiency of the treatment system.

As shown in Figure 4.9, lactate biodegradation rates as well as acetate accumulation rates achieved in the continuous MFC with granular electrodes were substantially higher than those in a continuous flow MFC with single rod electrodes for the entire range of applied loading rates. With the use of granular electrode, the continuous system was able to operate at loading rates as high as 21874.7 mg L^{-1} h^{-1} before deterioration in biodegradation performance was detected as compared to only 4054.7 mg L^{-1} h^{-1} in the MFC system with single rod electrodes. At these respective loading rates, the maximum lactate biodegradation rate in the system with granular electrodes was 7 times higher than with rod electrodes (11925.7 vs 1668.2 mg L^{-1} h^{-1}) and at a hydraulic residence time which was approximately 6 times shorter (0.22 vs 1.23 h). Similar observations were found with regard to acetate accumulation where the maximum rate was 9 times higher in the system with granular electrode (2853.0 vs 316.1 mg L^{-1} h^{-1}). These findings indicate the superiority of the system with granular electrode over that with single rod electrode in the continuous biodegradation of lactate. Moreover, lactate biodegradation rates achieved in the continuous system were significantly higher than those from the batch operated MFCs with granular electrode. To be specific, the maximum biodegradation rate attained in the batch system was at least 125 times lower than in the continuous system fed with the same concentration of lactate (23.1 vs 2890.5 mg L^{-1} h^{-1} with 1000 mg L^{-1} lactate).

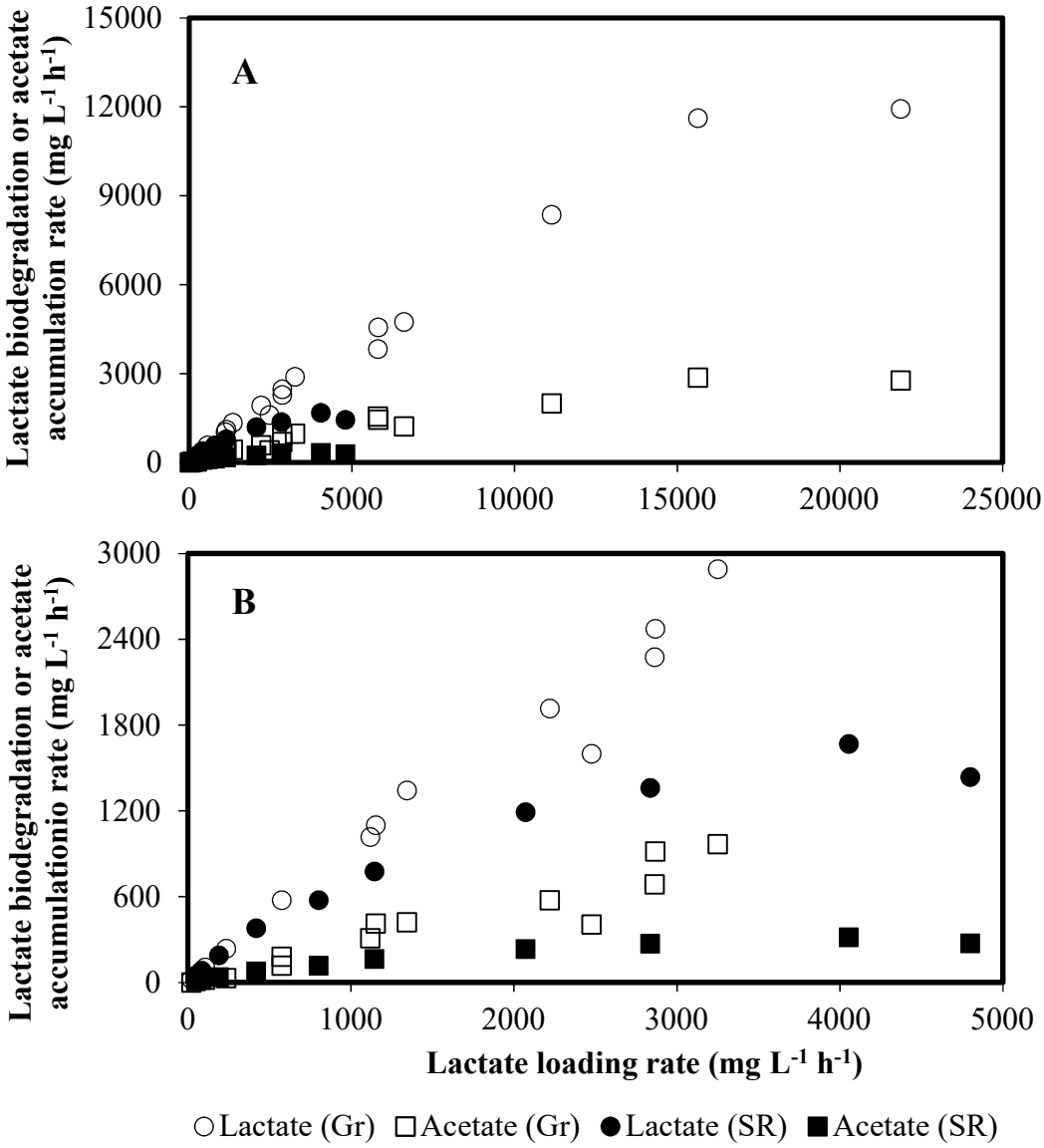

Figure 4.9 Comparison of lactate biodegradation and acetate accumulation rates in continuously operated MFCs equipped with either granular (Gr) or single rod (SR) electrodes and fed with lactate. Panel A shows the corresponding rates throughout all applied loading rates while panel B shows more detailed comparison at loading rates below 5000 mg L^{-1} h^{-1}.

Superiority of continuously operated MFC with granular electrodes, due to large surface area available for cell immobilization and formation of biofilm, was observed visually as the build-up of biomass in the anodic chamber was more evident. Although measurement of optical density became unfeasible, which would have provided a more quantitative representation of biomass

growth, the presence of biomass build-up became more apparent as the experiment proceeded. As shown in Figure 4.10 white streaks in the anodic chamber can be easily observed in the granules especially near the inlet of the recirculation loop. These white streaks of biomass seemed to follow the flow of anodic liquid passing through the granules. The streaks of biomass that were observed on the outer parts of the granules most likely were also present inside the graphite bed as well. Additionally, immobilization of cells likely minimized cell washout, which is typically observed in free cell suspension bioreactors, thereby enabling the granular system to operate a higher range of loading rates.

Figure 4.10 Biofilm formation (white streaks – as shown by arrow) around graphite granules in the anodic chamber of MFC fed continuously with lactate. Photo is taken after the continuous system had been running for around 120 days.

To have a better understanding of the potential changes in the physical condition of granules including their surface characteristics (i.e. surface area and pore volume), BET and SEM analyses were conducted on representative samples collected immediately after the continuous experiment with lactate as sole carbon source was completed. Samples of fresh (unused) granules were also subjected to the same analyses. Results generated from these analyses allowed us to assess the immobilization of cells on the graphite granules. Through BET analysis, pore volume and surface area of both fresh and exposed granules were measured and compared. The pore volume of the fresh (unused) granule of 0.0032 $cm^3 g^{-1}$ was more than twice that of the exposed granule which was only 0.0014 $cm^3 g^{-1}$. In terms of BET surface area, the fresh unused granules had a surface area of 1.10 $m^2 g^{-1}$ which was significantly higher than 0.38 $m^2 g^{-1}$ measured for the exposed granules. The substantially lower pore volume and BET surface area of the exposed granules suggested that the surface and voidages of granules were populated by biomass and associated extracellular polymeric substances (EPS) secreted by cells and therefore an evidence of successful cell immobilization.

Presence of cells and associated EPS on the surface of the granules was also confirmed by SEM examination of fresh and used granules. Figure 4.11 shows the scanning electron micrographs of an exposed granule collected from the MFC after completion of the continuous experiment with lactate as sole substrate, as well as that of a fresh granule. The set of images, at two different magnifications, clearly shows marked differences between the surfaces of the exposed and unused granules.

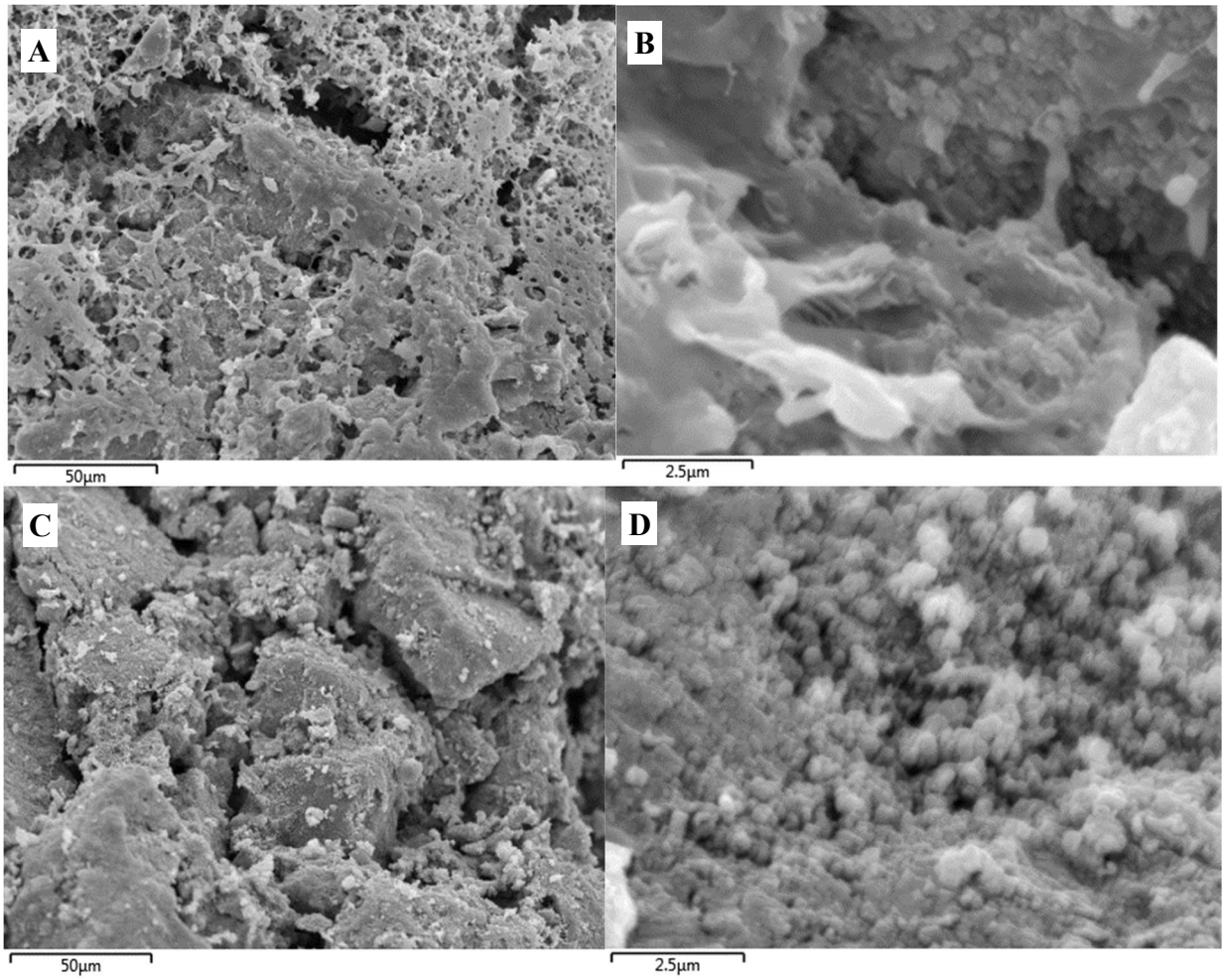

Figure 4.11 SEM photos of the surfaces of an exposed graphite granule (A and B) from an MFC fed continuously with lactate as sole carbon source, and that of a fresh (unused) graphite granule (C and D). In each case two different magnifications are provided.

At the lower magnification, the image of the exposed granule (Figure 4.11A) shows its surface covered with layers of biomass material which are not present on the surface of the unused granule (Figure 4.11C). Thickness of the biofilm is evident with trenches on the surface filled with layers forming on top of each other. Looking more closely on the surface (Figure 4.11B) shows the thickness of the biofilm as indicated in the wide range of light intensity (light to dark) covered in the image. Moreover, the biofilm appears to be smooth and slimy resembling a layer of EPS, while sharp edges are observed in the fresh granule (Figures 4.11 A and C, respectively). The EPS

produced by *P. putida* was described by Read and Costerton (1987) as substance which appears to form a "cocoon" surrounding microbial cells, mediating contact with solid surfaces and functions in forming the structural scaffolding of the biofilm matrix. The considerable thickness of EPS layer on the surface of the exposed granule most likely masked the *P. putida* cells being well embedded into the biofilm making them not clearly distinguishable.

Power and current output

A potentiostat was used to conduct linear sweep voltammetry analysis on the MFC which allowed the generation of polarization and power curves following procedures described in Section 4.2.4. The analyses were conducted for a range of lactate loading rates including 22.2, 1118.9, 1152.7, 2220.3 and 6607.5 mg L^{-1} h^{-1} where the corresponding biodegradation rates were 22.2, 1018.5, 1101.0, 1916.8, and 4735.4 mg L^{-1} h^{-1}, respectively. Additional analysis was also conducted during one of the additional runs at a loading rate of 12697.3 mg L^{-1} h^{-1} (corresponding biodegradation rate: 5162.5 mg L^{-1} h^{-1}). The generated polarization and power curves at each tested loading rate are shown in Figure 4.12. The polarization curve was used to determine the open circuit potential (OCP) and the resulting power curve was used to calculate the maximum power and corresponding current measured throughout the potential sweep. From the polarization curve, OCP was determined as the potential at a current of zero, while the resulting peak in the power curve was determined as the maximum power. The resulting OCP, maximum power and corresponding current densities obtained from all generated polarization and power curves are plotted in Figure 4.13 as a function of corresponding biodegradation rates, specifically 22.2, 1018.5, 1101.0, 1916.8 and 4735.4 mg L^{-1} h^{-1} as well as that from the additional run of 5162.5 mg L^{-1} h^{-1}, to identify possible relation with biodegradation performance.

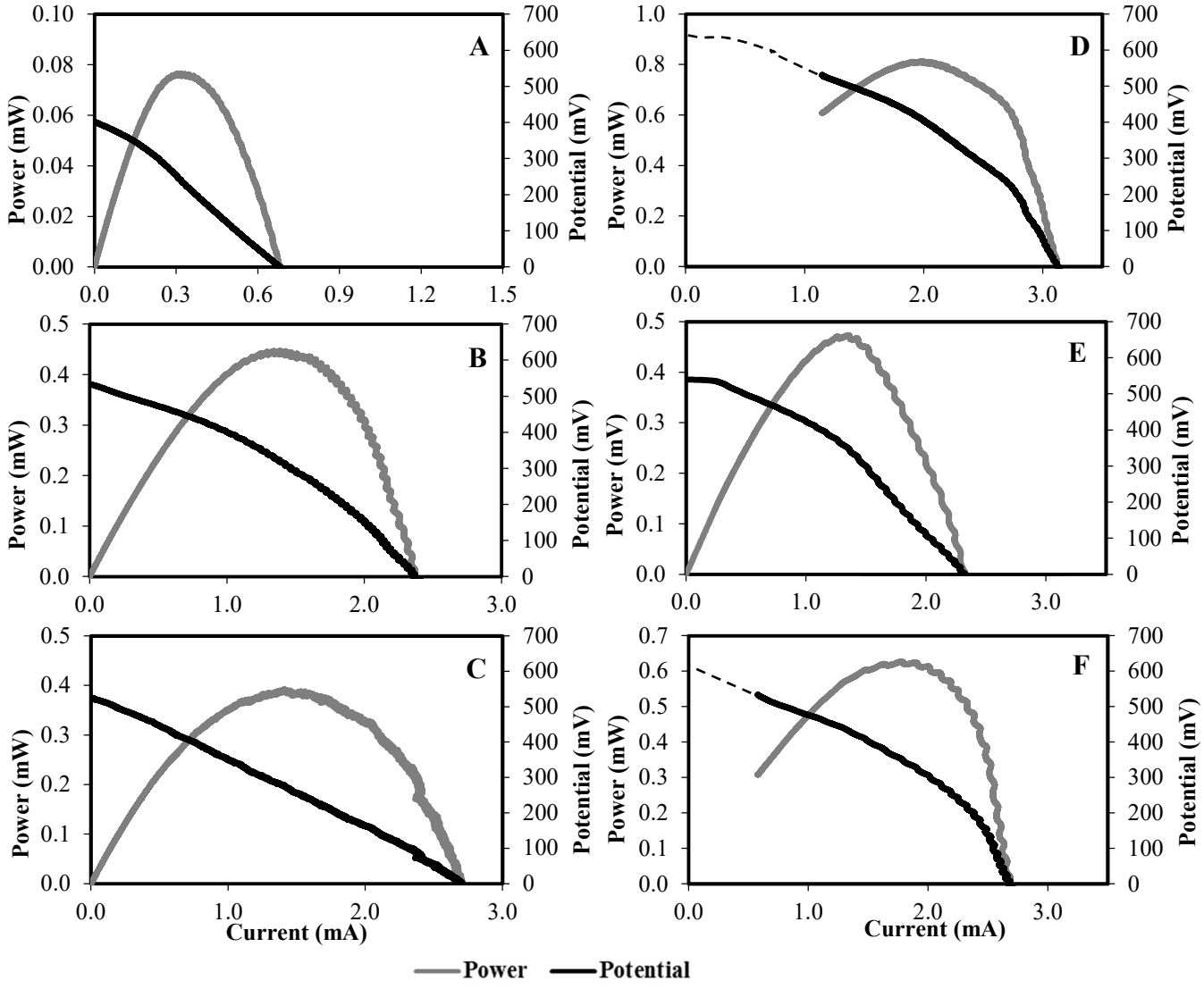

Figure 4.12 Polarization and power curves generated from MFC with granular electrodes when fed continuously with lactate at loading rates of: A) 22.2, B) 1118.9, C) 1152.7, D) 2220.3, E) 6607.5 and F) 12697.3 mg L^{-1} h^{-1}.

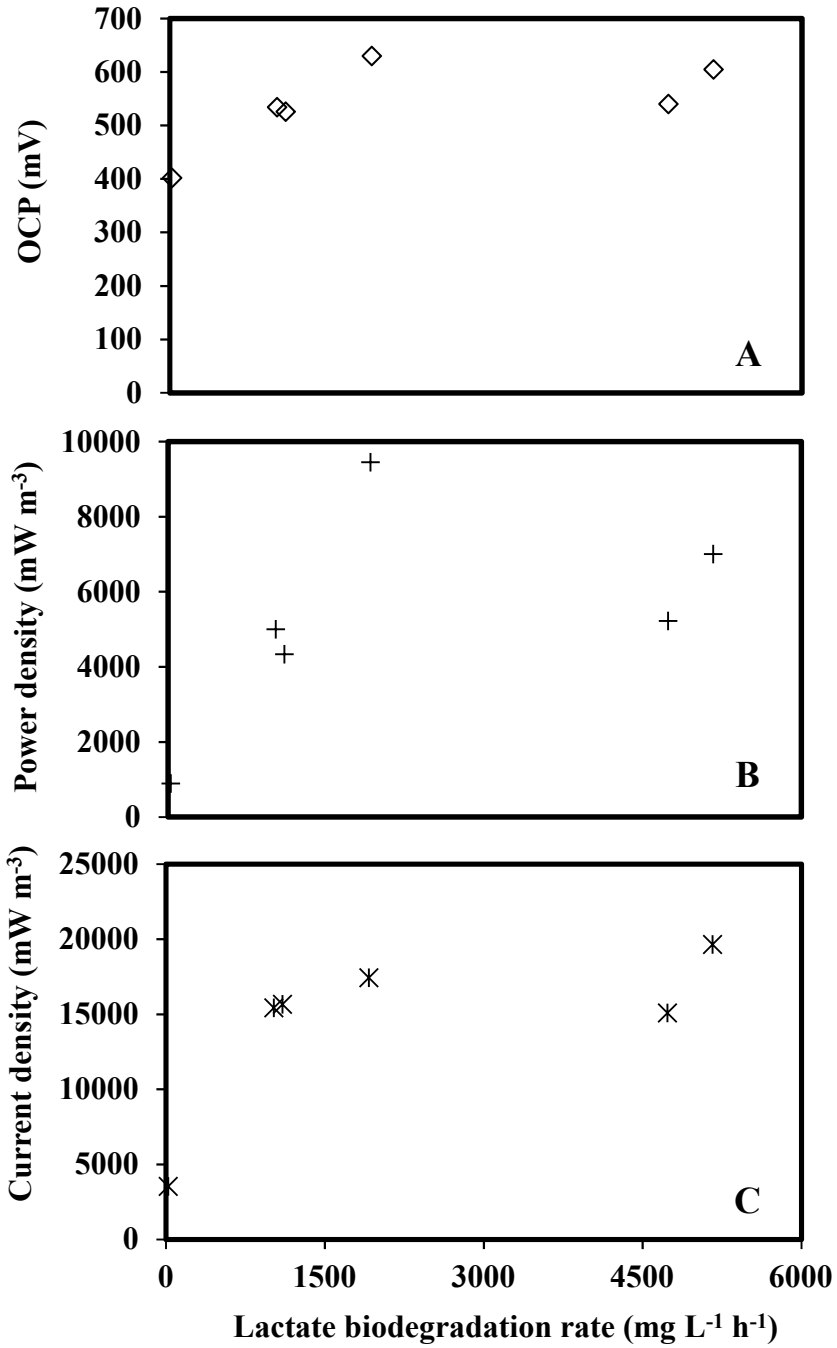

Figure 4.13 Variation of OCP (A), maximum power density (B), and current density (C) with lactate biodegradation rate obtained from polarization and power curves generated from continuously operated MFC with granular electrode and fed with lactate as sole carbon source. Corresponding lactate loading rates in sequential order are: 22.2, 1118.9, 1152.7, 2220.3, 6607.5 and 12697.3 mg L^{-1} h^{-1}.

Results from polarization curves showed that the lowest OCP of 402 mV was measured when the corresponding biodegradation rate was at the lowest value of 22.2 mg L^{-1} h^{-1} (Figure 4.13A). As higher biodegradation rates were achieved, increase in OCP was observed but this improvement appeared to reach a peak at around 630 mV. The OCP started to plateau at biodegradation rates over 1000 mg L^{-1} h^{-1} at levels which fluctuated between 526 to 630 mV. Similar patterns were observed with regard to profiles of power and current outputs (Figure 4.13B-C). Power and current densities were at the lowest levels of 888.9 mW m^{-3} and 3555.6 mA m^{-3}, respectively, when the lactate biodegradation rate was the lowest. As biodegradation performance improved, significant increase in power and current densities were observed. Throughout this period, MFC was operating at considerably high lactate removal efficiencies fluctuating between 86.3% to 95.5%. After reaching peak at biodegradation rate of approximately 2000 mg L^{-1} h^{-1}, power and current densities declined with further increase in biodegradation rate but still significantly higher than their initial levels. This decline in power and current output coincided with a decline in removal efficiency down to 71.7%.

The effect of removal efficiency was more evident on the efficiency of electron recovery as indicated by corresponding coulombic efficiencies. The highest CE value of 4.48% was attained when lactate removal efficiency was 100%. Reduction in removal efficiency resulted to lower CE, such as when removal efficiency fluctuated between 86.3-95.5% the corresponding range of CE was noticeably lower with 0.26-0.43%. An even lower CE value of 0.09% was obtained with further reduction in removal efficiency to 71.7%. The electrochemical output generated from the additional run did not show significant deviation from the trend of OCP, power and current density profiles which further attests to the observed relation of biodegradation performance and energy

output. The maximum power and current densities achieved during continuous degradation of lactate in the MFC with granular electrode were 9444.4 mW m^{-3} and 19666.7 mA m^{-3}, respectively.

The pattern of resulting profiles of OCP and especially power and current output with respect to lactate biodegradation rate were found to conform to previously observed trend of increase in energy output with biodegradation performance, such as those in results from previous batch degradation of lactate in MFCs with rod electrodes. It should be pointed out the increasing trend of power and current was observed to level off at higher loading rates that corresponded to higher biodegradation rates possibly due to a lower removal percentage of lactate. When compared to the same MFC operated batchwise, power and current output in the continuous system were significantly higher by at least one order of magnitude (9444.4 vs 14.3 mW m^{-3}; 19666.7 vs 1782.2 mA m^{-3}). Given that a potentiostat was not available during the experiments in MFCs with rod electrodes and a different method for measurement of power was used it is not practical to compare the power output measured in the systems with rod and granular electrodes.

Energy output from continuously operated MFCs with granular graphite as matrix in the anodic chamber are consistent with those reported in the literature. A baffled air-cathode MFC with graphite granules as matrix was able to produce a maximum power density of 10700 mW m^{-3} using corn stover steam process liquid as substrate, while achieving 89.1% COD removal rate (Feng et al., 2010). The same MFC was able to generate 15200 mW m^{-3} with glucose as substrate with 88% removal rate. At a slightly lower removal percentage of 85%, a power output of 13600 mW m^{-3} was achieved in a four-air cathode single-chamber MFC with packed bed graphite granules in the anodic chamber fed continuously with a glucose-based synthetic wastewater (Tremouli et al.,

2016). One of the highest energy producing MFC was constructed using graphite granules in the anode in a tubular air cathode MFC. This system was fed continuously with glucose-based substrates and was able to generate a maximum power density of 50200 mW m^{-3} at a current density of 216000 mA m^{-3} (You et al., 2007). In a similar tubular configuration, a single-chamber MFC was able to continuously utilize glucose and produce a maximum power density of 38000 mW m^{-3} while a higher output of 48000 mW m^{-3} was achieved with domestic wastewater although at a removal rate of only 22% (Rabaey et al., 2005b). Together with findings from other studies, the results from the current work show the superiority of graphite granules in harvesting of energy from the degradation of substrates in a MFC.

4.3.2 Biodegradation of acetate

Batch systems. After completion of experiments with lactate, sequential batch tests were conducted in the MFC with granular graphite electrode with acetate as the substrate. Results of biodegradation of acetate at different initial concentrations of 1000, 2500 and 5000 mg L^{-1} are shown in Figure 4.14. Sequential experiments were started with the lowest initial concentration of approximately 1000 mg L^{-1}. Rapid decrease in concentration of acetate was observed immediately after its addition into the anodic chamber and complete degradation of 1000 mg L^{-1} acetate was achieved in approximately 24 h. Addition of 1000 mg L^{-1} acetate was repeated and similar results were observed. Sequential addition of higher acetate concentrations was conducted and complete depletion of substrate was achieved in a considerably short degradation period of approximately 24 h even at the highest tested concentration of approximately 5000 mg L^{-1} acetate. This result was unexpected since acetate biodegradation in MFCs with rod electrode and freely suspended cells was found to be extremely slow, especially when compared with lactate degradation.

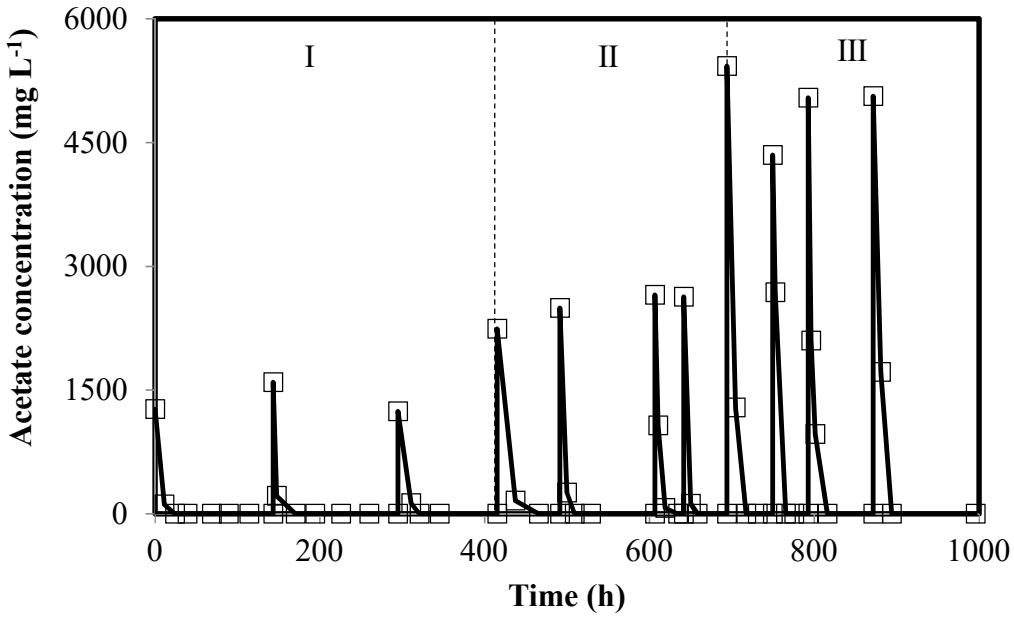

Figure 4.14 Profile of acetate concentration during the sequential degradation of acetate at various initial concentrations in MFC with granular electrode and immobilized *P. putida* cells. Panel I: 1000 mg L^{-1}, Panel II: 2500 mg L^{-1} and Panel III: 5000 mg L^{-1} acetate.

The calculated average biodegradation rates of acetate at initial concentrations of approximately 1000, 2500 and 5000 mg L^{-1} were 47.8±5.0, 133.1±64.7 and 219.1±32.5 mg L^{-1} h^{-1}, respectively. As shown in Figure 4.15, acetate biodegradation rate improved with increase in its initial concentration. Improvement in acetate biodegradation at increasing initial concentrations was not observed in similarly operated MFCs with rod electrodes and freely suspended cells. Remarkable differences in degradation of acetate in MFC systems equipped with single rod and granular electrodes were observed. Specifically, at all evaluated concentrations, biodegradation rate of acetate in MFC with granular electrode and immobilized cells was significantly faster, at least 13 times, than that in MFC with single rod and freely suspended cells (maximum biodegradation rates: 252.1 vs 3.6 mg L^{-1} h^{-1}).

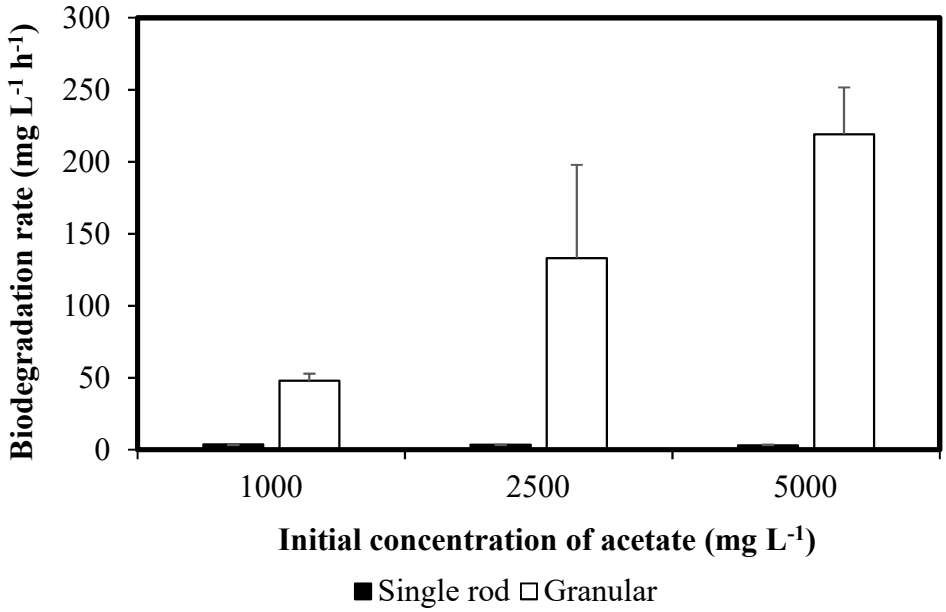

Figure 4.15 Comparison of acetate biodegradation rates achieved in MFCs with single rod and granular electrodes fed with acetate at various initial concentrations. Error bars represent standard deviation of biodegradation rates from sequential tests in each tested concentration.

As shown in Figure 4.16, acetate biodegradation rates in the MFC with granular electrodes were 2-18 times faster than those obtained for lactate attained in the same MFC with granular electrodes, depending on the applied initial concentration. This finding was contrary to that observed in previous experiments conducted in MFCs with rod electrodes and freely suspended cells where acetate biodegradation was much slower than that of lactate. Moreover, significant improvement in acetate biodegradation was observed with increase in initial concentration which was not the case with lactate where biodegradation rate deteriorated at the higher initial concentrations. These results could be attributed to the conditions in the anodic chamber of the MFC during experiments with acetate whereby a much higher biomass hold-up was present. This was due to the fact that experiments (batch and continuous) with lactate were conducted first, which took about 260 days, and the same MFC with granular electrodes was then used to conduct experiments with acetate.

Hence, higher biomass hold up and consequently higher microbial activity was observed. A much higher biomass presence most certainly resulted in significant improvement in acetate biodegradation during the batch experiments in the MFC with granular electrode.

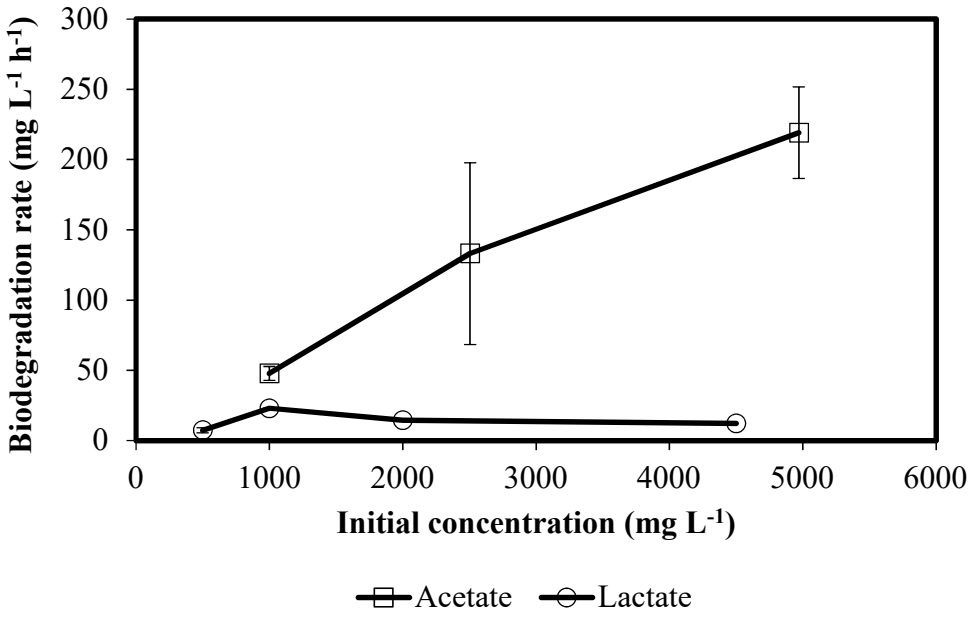

Figure 4.16 Biodegradation rates of lactate and acetate at different initial concentrations in MFC with granular electrodes operated batchwise. Error bars represent standard deviation of biodegradation rates from sequential tests in each tested concentration.

A number of studies dealing with the use of acetate as carbon source in batch operated MFCs have been conducted but limited information is available with regard to acetate biodegradation rate especially with immobilized cells. A single chamber MFC was reported to successfully utilize graphite granules in the degradation of an acetate-based synthetic wastewater with a concentration of around 3000 mg COD L^{-1} (Pandit et al., 2014). The only related biokinetic information reported in this work was removal efficiency of 77-79% achieved during batch degradation that was operated for under 65 h.

The use of a potentiostat allowed the generation of polarization curve during the batch operation of MFC with acetate. Figure 4.17 presents the polarization and power curves generated for biodegradation of 5000 mg L^{-1} acetate. The biodegradation period with this acetate concentration was long enough to allow sufficient time for conducting these tests. Using the polarization curve, the value of OCP was found to be approximately 437 mV. The maximum power density was 2222.2 mW m^{-3} and achieved at a current density of 9000.0 mA m^{-3}. This result was determined at the highest initial acetate concentration of 5000 mg L^{-1} which delivered the highest anodic potential of all tested concentrations. The resulting electrical energy output is significantly higher compared to output from previous batch degradation of acetate in MFCs with rod electrodes, although direct comparison of results is not accurate since output from previous tests was not determined using a potentiostat. With the fixed external resistance of 50 ohms, a maximum circuit potential of 14.2 mV was measured corresponding to power and current densities of 44.8 mW m^{-3} and 3155.6 mA m^{-3}, respectively. These outputs were substantially higher than the power and current densities attained from similarly operated MFCs with rod electrode fed with the same amount of acetate (5000 mg L^{-1}) which were only 4.1 mW m^{-3} and 90.1 mA m^{-3}, respectively. These findings indicate the superior performance, in terms of substrate biodegradation and corresponding energy output, of the batch operated MFC equipped with granular electrodes.

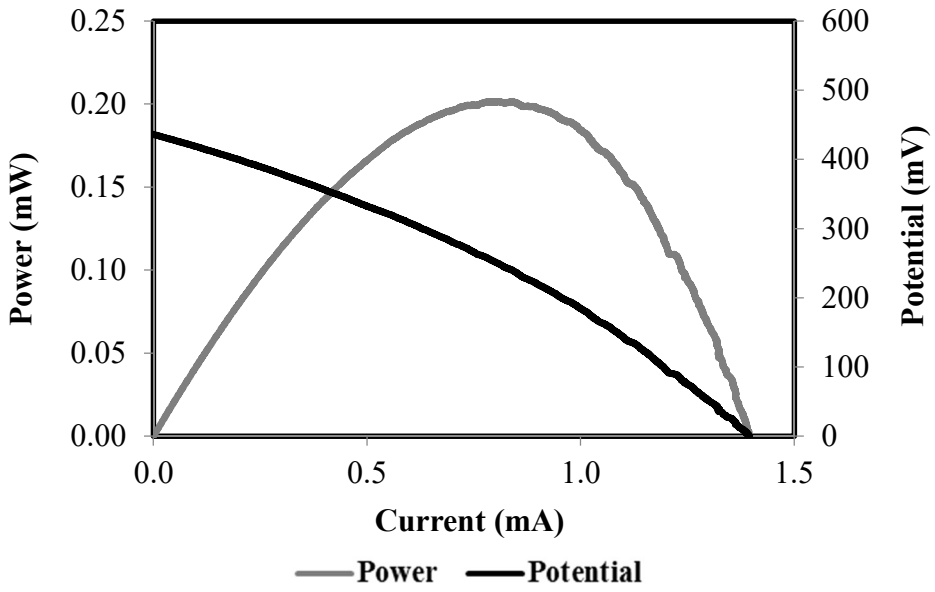

Figure 4.17 Polarization and power curves generated during batch degradation of 5000 mg L^{-1} acetate in MFC with granular electrodes.

Continuous biodegradation of acetate. With acetate as substrate, the continuously operated MFC with granular electrode was able to operate a range of dilution rates from 0.02 to 0.23 h^{-1} before system performance started to deteriorate. With approximately 1000 mg L^{-1} acetate in the feed, equivalent loading rates applied to the system ranged from 19.3-246.3 mg L^{-1} h^{-1}. The residual concentrations of acetate at steady state conditions are shown in Figure 4.18 as a function of loading rate. With loading rates up to 54.4 mg L^{-1} h^{-1}, complete degradation of acetate was achieved. Increase in loading rate to 132.5 mg L^{-1} h^{-1} resulted in partial degradation of acetate with residual acetate concentration of 342.1 mg L^{-1} (70.5% removal). Further increase in loading rate to 246.3 mg L^{-1} h^{-1} caused significant increase in the residual concentration to 845.0 mg L^{-1} which was already 79.3% of the influent concentration indicating the system encountered substantial deterioration in biodegradation performance. Even at a low feed concentration of 1000 mg L^{-1} acetate, the range of applied loading rates were certainly lower than when the same system was

fed with lactate. This finding, which is in line with the observation in the MFCs with rod electrodes and freely suspended cells, indicates the preference of the system to utilize lactate as substrate over acetate. It should be emphasized that in the system equipped with rod electrodes, degradation of acetate did not occur even at the lowest applied loading rate (5.9 mg L^{-1} h^{-1}, HRT=140 h).

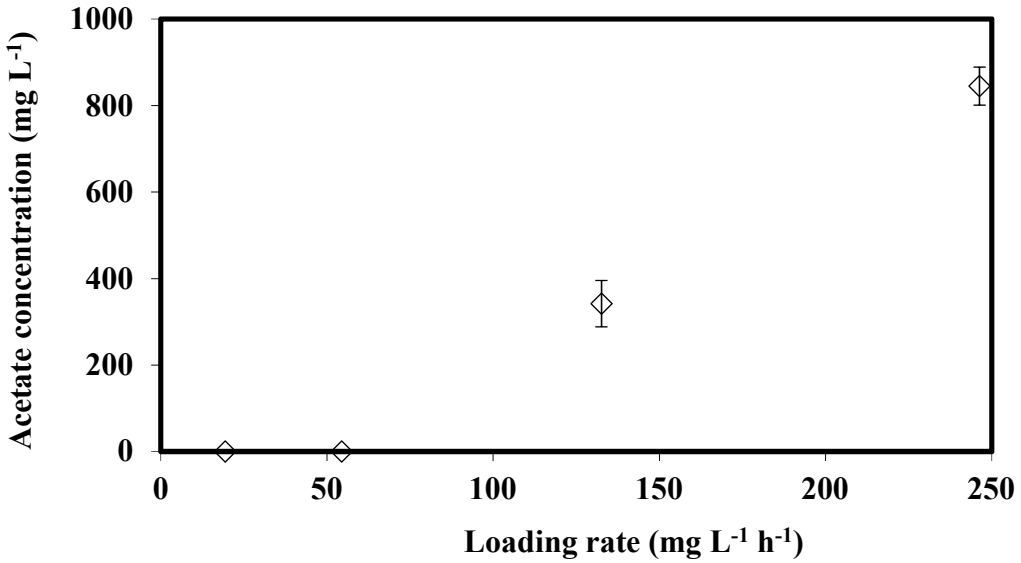

Figure 4.18 Steady state residual concentration of acetate as a function of loading rate in MFC with granular graphite electrodes fed continuously with 1000 mg L^{-1}acetate. Error bars represent standard deviation of steady state concentrations at each dilution rate.

The variation of acetate biodegradation rate with loading rate in the continuously operated MFC with granular electrodes is shown in Figure 4.19. As indicated earlier, the continuous system was only able to operate a narrow range of acetate loading rates. At the lowest loading rate (HRT=45.8 h), complete degradation of acetate was achieved as indicated by 100% removal efficiency. Complete degradation of acetate was maintained up to a loading rate of 54.4 mg L^{-1} h^{-1} (HRT=20.6 h) which corresponded to an equivalent biodegradation rate of 54.4 mg L^{-1} h^{-1}. As loading rate was increased to 132.5 mg L^{-1} h^{-1} (HRT=8.7 h), residual acetate was detected which resulted to a decrease in the removal efficiency to 70.5%, while biodegradation rate continued to increase

attaining its maximum of 93.4 mg L^{-1} h^{-1}. Further increase in loading rate to 246.3 mg L^{-1} h^{-1} (HRT=4.3 h) resulted to deterioration in MFC performance as manifested by a low acetate removal of 20.7% and a substantial decrease in biodegradation rate to 50.9 mg L^{-1} h^{-1}. At this stage, results indicated that the continuous system was already past its optimum performance and thus its operation was stopped.

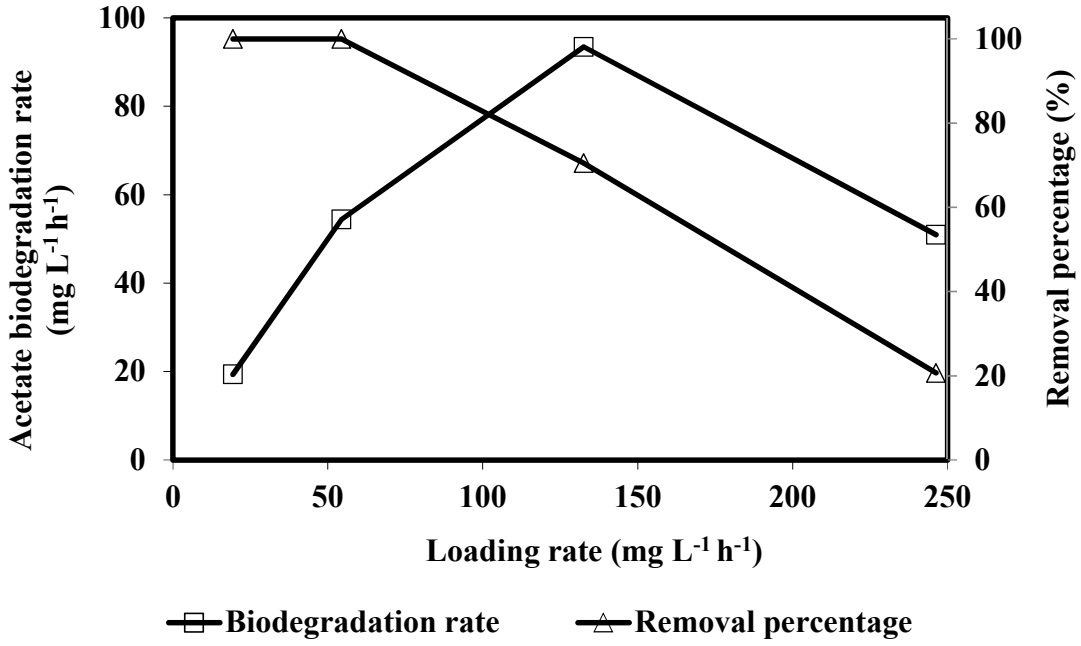

Figure 4.19 Biodegradation rates of acetate as well as corresponding removal percentages as a function of loading rate in continuously operated MFC with granular electrodes fed with 1000 mg L^{-1} acetate as substrate.

As reported earlier, experiments on the continuous biodegradation of acetate in similarly operated MFC with rod electrodes and freely suspended cells were not successful which indicate its ineffectiveness in acetate degradation. The present findings, however, show that biodegradation of acetate in a continuous system can be achieved through the utilization of granular electrodes.

Power and current output. Polarization and corresponding power curves were generated using LSV analyses conducted at acetate loading rates of 19.4, 132.5 and 246.3 mg L^{-1} h^{-1} which, as mentioned earlier, resulted to biodegradation rates of 19.4, 93.4 and 50.9 mg L^{-1} h^{-1}, respectively. The resulting polarization and power curves are shown in Figure 4.20, while profiles of OCP, power and current densities with respect to acetate biodegradation rate are shown in Figure 4.21. As shown in Figure 4.20, the generated polarization curves did not cover the range of potential that would include the OCP. Hence, projection lines were made to intersect the line of potential at zero current to estimate the OCP. Power curves were then developed using the potential and current generated from the polarization curves and resulting peak power and corresponding current were used to calculate power and current densities shown in Figure 4.21.

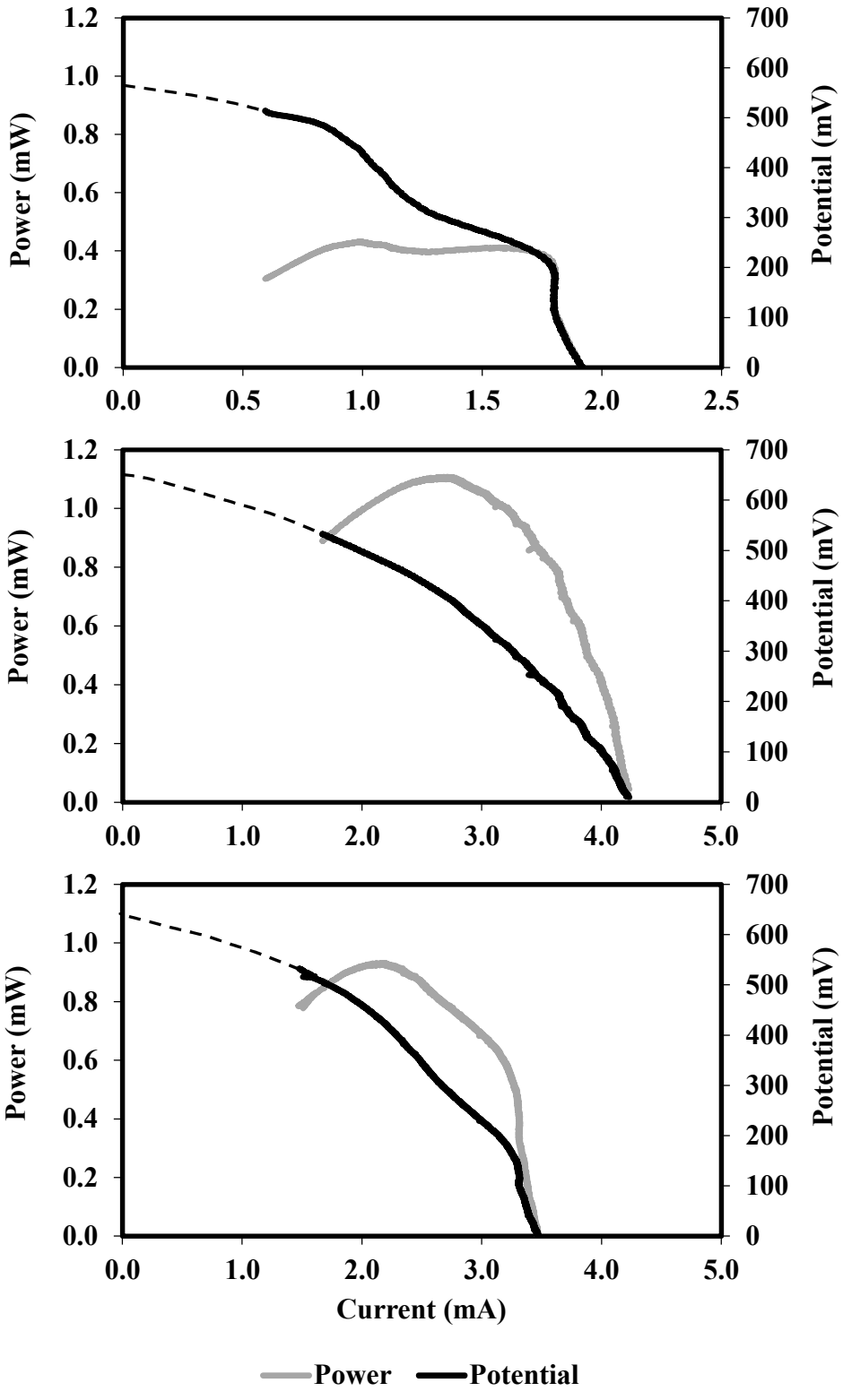

Figure 4.20 Polarization and power curves generated from MFC with granular electrode fed continuously with acetate at loading rates of 19.4 (A), 132.5 (B) and 246.3 (C) mg L^{-1} h^{-1}.

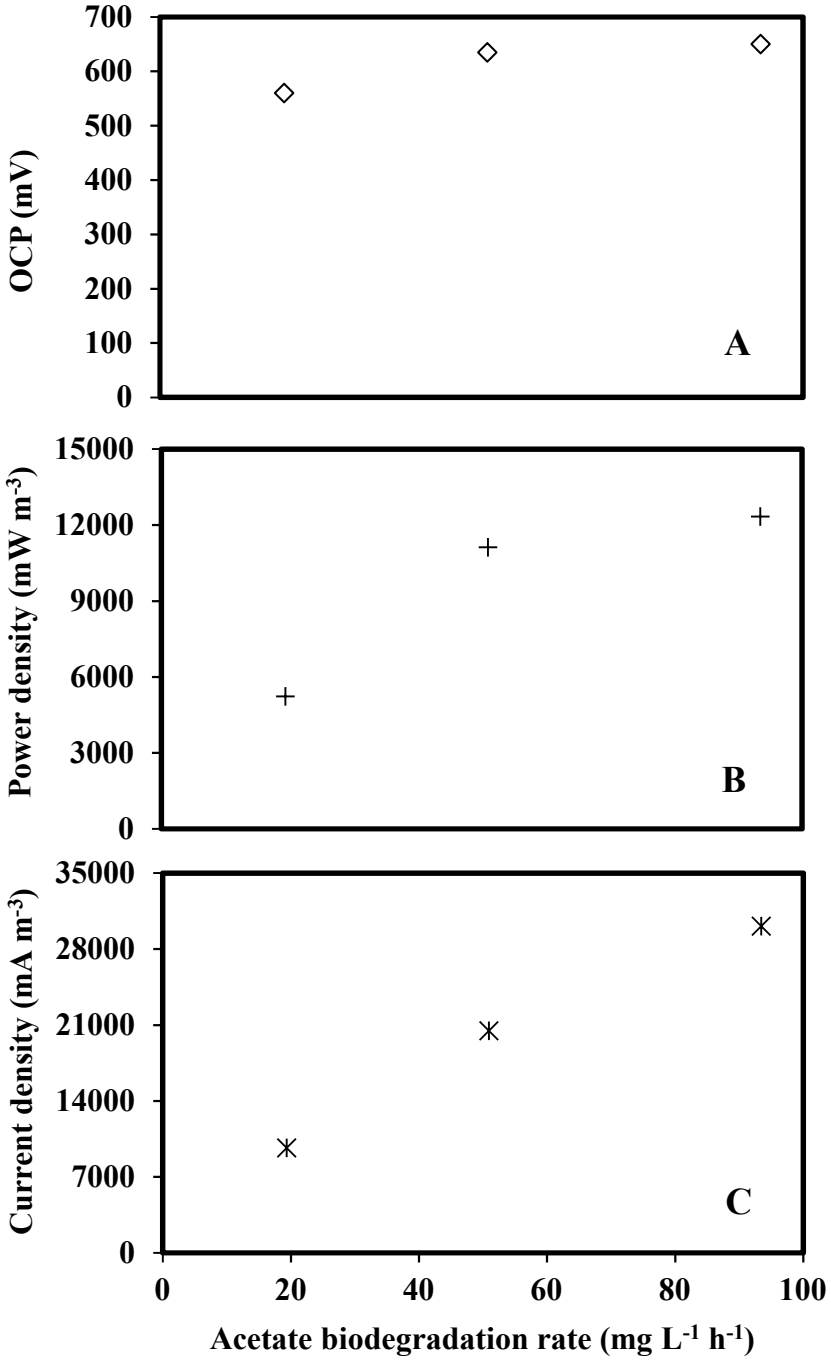

Figure 4.21 Variation of OCP (A), maximum power density (B), and current density(C) with acetate biodegradation rate obtained from polarization and power curves generated from continuously operated MFC with granular electrode and fed with acetate as sole substrate. Corresponding acetate loading rates in sequential order are: 19.4, 246.3 and 132.5 mg L^{-1} h^{-1}.

The lowest OCP, power and current densities of 560 mV, 5222.2 mW m^{-3} and 9666.7 mA m^{-3}, respectively, were attained at the lowest loading rate corresponding to the lowest acetate biodegradation rate. Improvement in biodegradation rate to its highest level of 93.4 mg L^{-1} h^{-1} as loading rate was increased yielded the highest energy output with OCP, power and current density levels of 650 mV, 12333.3 mW m^{-3} and 30111.1 mA m^{-3}, respectively. Decline in biodegradation rate with further increase in loading was accompanied by a corresponding decline in energy output with OCP, power and current densities reduced to 635 mV, 11111.1 mW m^{-3} and 20444.4 mA m^{-3}, respectively. These findings show a correlation between energy output and biodegradation activity. This was further attested by corresponding acetate removal efficiencies where decline in energy output after increase of loading rate to 246.3 mg L^{-1} h^{-1} corresponded to a decrease in removal percentage from 70.5% to 20.7%.

Overall, patterns similar to those previously observed in batch and continuously operated MFCs with either rod or granular electrodes, where higher biodegradation rate and removal efficiency resulted to higher OCP, power and current output, were also observed in this experiment. Moreover, the generated energy output from the continuous system was substantially enhanced compared to that obtained in the same MFC operated batchwise, specifically at least 5 times higher in power density and 3 time higher in current density.

4.3.3 Comparison of lactate and acetate as substrate

A comparison of lactate and acetate biodegradation rates achieved at different loading rates in the continuously operated MFC with granular electrodes is shown in Figure 4.22. At the lowest applied loading rate (approximately 20 mg L^{-1} h^{-1}), biodegradation rates of lactate and acetate were

relatively similar. In either case increase in loading rate up to a certain level led to higher biodegradation rates. However, improvement in lactate biodegradation due to increase in loading rate was more pronounced than that with acetate In fact, as revealed earlier, lactate biodegradation rate continued to increase up to a loading rate of 21874.7 mg L^{-1} h^{-1}, while acetate biodegradation rate suffered deterioration even at a much lower loading rate of only 246.3 mg L^{-1} h^{-1}. These findings further show the preference in the utilization of different types of substrate in the MFC, i.e. lactate over acetate, which is consistent with those found from previous experiments in MFCs with rod electrodes.

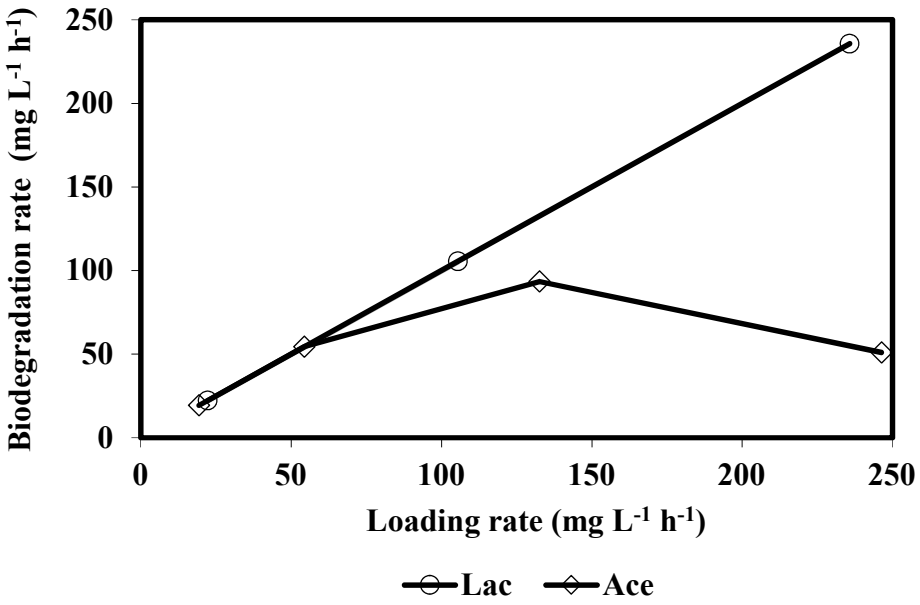

Figure 4.22 Comparison of biodegradation rates of lactate and acetate in continuously operated MFC with granular electrodes.

When comparing energy output from the same continuously operated MFC with granular electrode, OCP levels obtained with lactate and acetate as substrate were found to be similar within a range from 530 to 650 mV. However, maximum power and current densities achieved when

acetate was used as feed was considerably higher (12,333.3 vs 9,444.4 mW m^{-3} and 30,111.1 vs 19,666.7 mA m^{-3}). The superior energy output of the system was quite unexpected since stoichiometry and resulting biodegradation rates of acetate as original substrate were found to be inferior. However, looking at CE shows that electron recovery in the MFC when acetate was utilized as feed was substantially higher as indicated with the values of CE that in case of acetate were in the range 9.03-13.99%, while for lactate were substantially lower at 0.09-4.82%. We can only speculate that specific factors not observed or measured during the experiment may have influenced the energy output more significantly than the biodegradation performance. Regardless of this finding, the utilization of acetate, as one of the most common substrates used in MFCs, has been shown to result in the production of reasonably high energy output much higher than achieved in this work. For instance, the use of granular graphite matrix in the anodic chamber of a tubular single chamber MFC fed continuously with acetate led to a maximum power output of 48000 mW m^{-3} (Rabaey et al., 2005b). A similarly configured MFC bioreactor filled with graphite granules combined with an air biocathode fed continuously with acetate at a rate of 62.5 mg COD h^{-1} was able to generate an even higher maximum power production of 65000 mW m^{-3} (Clauwert et al., 2007). Results from these previous works show that considerably high power output can be achieved in MFCs equipped with graphite granules when fed with acetate as substrate.

Overall, biodegradation rates of lactate were found to be higher than those with acetate. These findings indicate that the MFC, either with rod or granular electrode, find the biodegradation of acetate more difficult than that with lactate. As has been discussed previously in Section 3.3, the lower biodegradation activity from the utilization of acetate could be attributed to its lower anodic

potential compared to lactate as indicated from Gibb's free energy. Lactate contains more electrons for oxidation and hence has higher preference to be utilized as substrate in the MFC.

4.4 Conclusions

The use of granular electrode in MFC inoculated with *P. putida* in batch and continuous systems showed effective degradation of lactate and acetate which was accompanied by rise in open circuit potential and generation of electrical energy. In batch operations, lactate biodegradation was observed to be fast without delay and no accumulation of biologically produced acetate. Among the tested initial lactate concentrations, biodegradation rate was found to peak at 1000 mg L^{-1} lactate. The biodegradation performance deteriorated with further increase in initial concentration. Overall, biodegradation rates in the granular system were higher than in similar MFC with rod electrode. Similar findings were found when acetate was utilized as original substrate where biodegradation rates were significantly higher than those achieved in similar experiments in batch MFCs with rod electrode.

In the continuous systems, the same trend was observed where peak biodegradation rates from MFC with granular electrode were significantly higher than those in the same MFC with rod electrode. With lactate, the maximum biodegradation rate obtained in the granular system of 11925.7 mg L^{-1} h^{-1}, which was obtained at a residence time of only 0.3 h, was more than 7 times faster. With acetate as substrate, the maximum biodegradation rate of 93.4 mg L^{-1} h^{-1} was a significant improvement from similar MFC with rod electrode which was unable to operate continuously. Along with improved biodegradation performance, BET analyses and SEM imaging showed successful immobilization of cells onto the surface of granules.

As observed in previous experiments in MFC with rod electrodes and suspended cells, there seems to be a correlation observed between OCP and power and current output with biodegradation activity. Electrochemical output was influenced by the biodegradation rate and substrate removal efficiency. Particularly, the substrate removal efficiency directly affected the efficiency of electron recovery whereby decrease in removal efficiency resulted to corresponding decrease in coulombic efficiency. Overall, the performance of MFC, both in terms of substrate degradation and energy output, was significantly improved when granular electrode was used (instead of rod electrode) regardless of type of substrate or feed operation (batch vs continuous). Maximum power and current densities in the granular electrode MFC reached 12333.3 mW m^{-3} and 30111.1 mA m^{-3} while the rod electrode system only achieved 49.4 mW m^{-3} and 198.1 mA m^{-3}, respectively.

Chapter 5

Biodegradation of Phenol in MFCs with Rod and Granular Electrodes

A similar version of this chapter has been published in the Environmental Technology journal: Moreno, L., Predicala, B. and Nemati (2017). Biodegradation of phenol in batch and continuous flow microbial fuel cells with rod and granular graphite electrodes. Environmental Technology 3:1-13.

The written text of the submitted manuscript was prepared by Lyman Moreno, while Dr. Mehdi Nemati and Dr. Bernardo Predicala provided editorial input.

5.1 Introduction

Different types of organic compounds are present in wastewaters including proteins, carbohydrates, fatty acids and aromatics (Tchobanoglous et al., 2003). Phenol is an aromatic compound that is commonly found in wastewaters, especially those generated from industrial operations. Phenol is a toxic compound known to impose inhibition on microbial activity even at relatively low concentrations (100 mg L^{-1}). Additionally, phenol has been shown to be a suitable model substrate for studying the kinetics of aromatic compounds degradation in conventional bioreactors (Hill and Robinson, 1975).

Most of the removal strategies for waters contaminated with phenol involve physical, chemical and biological techniques such as incineration, adsorption, chemical and photochemical oxidation, extraction by liquid membrane and advance oxidation processes utilizing UV and hydrogen peroxide (Christen et al., 2012; Antony et al., 2013; Kumar, 2010). Among the above-mentioned methods, biodegradation of phenol has received greater attention in recent years due to its ability to completely mineralize this toxic organic compound and for being environmentally friendly and economically feasible (Agarry et al., 2008; Al-Khalid and El-Naas, 2012; Christen et al., 2012).

A bioremediation technology that could effectively degrade phenol and in the process produce energy can be achieved using microbial fuel cells (MFCs). Biodegradation of phenol in MFCs can be achieved through utilization of microorganisms that can use phenol as their carbon and energy source and those that are able to release electrons to an electrode. These include a variety of microorganisms such as yeasts, fungi and bacteria that can function under either aerobic or anaerobic conditions (Agarry et al., 2008; Agarry et al., 2009; Christen et al., 2012; Pradeep et al., 2014). Pure and mixed bacterial cultures have been used in different bioreactor configurations for phenol degradation (Pradeep et. al 2014). The *Pseudomonas* genus and more specifically, *Pseudomonas putida*, is one of the most commonly used microorganism for phenol biodegradation due to its ability in effective removal of phenol (Kafilzadeh et al., 2010; Al-Khalid and El-Naas, 2012).

In this study, *P. putida* was used as the bacterial culture in MFCs for degradation of phenol and with simultaneous generation of electrical energy. Biodegradation of phenol was initially conducted in MFCs with single rod electrodes and microbial cells in suspension. After operation under batch conditions were done, MFC was switched to continuous mode. With suspended cells,

conditions were suitable for biokinetic evaluation of microbial growth and phenol biodegradation in MFC.

Experiments on phenol biodegradation in MFCs with granular graphite electrode, which promoted immobilization of cells, were also conducted. Additionally the effect of an electron mediator on the biodegradation of phenol and production of electricity was also evaluated using neutral red in MFC with granular electrode. Experiments in this system were conducted initially in MFCs operated batchwise with sequential addition of phenol. This was followed by biodegradation of phenol in continuous flow systems. In all experiments, MFC performance in terms of biodegradation and energy output was assessed.

5.2 Materials and methods

5.2.1 Experimental set-ups

Identical H-type configuration MFC bioreactors were used in all experimental runs. Set-up of MFC has been described previously in more detail in Section 3.2.2. Consistent with previous experiments, *Pseudomonas putida* was used as microbial culture (biocatalyst) in all experiments. Sub-culturing of *P. putida* including preparation of modified McKinney's growth medium and inoculum cell suspension has been described in detail in Section 3.2.1.

Two types of graphite electrodes were utilized in this study. Rod electrodes, as described in Section 3.2.2, were used to allow cells to be suspended in the anodic chamber, while granular electrodes, as detailed in Section 4.2.1, were employed to promote cell immobilization. After assembling the MFC set-up, the anodic chamber was filled with sterilized modified McKinney's medium which

was then purged with nitrogen gas (industrial grade) for about 10 minutes to ensure anoxic conditions were achieved.

Potassium ferricyanide solution, consisting of 50 mM potassium ferricyanide and 100 mM potassium phosphate buffer, was used as catholyte (cathodic chamber solution) in all experiments. Replenishment of catholyte solution was done when the cathodic potential decreased below 250 mV (approximately 25% reduction from initial potential). This was carried out to maintain a relatively constant potential in the cathodic chamber. Prior to addition of substrate and inoculation with *P. putida* cell suspension, the open circuit potential (OCP) of the MFC was monitored for about 5 hours to allow the circuit potential to stabilize and to determine the baseline OCP value. All experiments were conducted at room temperature (24±2 °C).

5.2.2. Biodegradation of phenol in MFCs with rod electrode (freely suspended cells)

Batch mode of operation: The effect of phenol concentration on biodegradation kinetics and generation of electricity was investigated in MFCs operated batchwise. Phenol concentrations of 100, 250, 500 and 1000 mg L^{-1} were evaluated in these experiments. To conduct each experimental run, approximately 200 mL of modified McKinney's medium was transferred into the anodic chamber, while a solution of potassium ferricyanide was placed in the cathodic chamber. Following establishment of anoxic conditions, a small volume of medium (1-5 mL) was withdrawn from the anodic chamber and used to dissolve the required amount of phenol for a designated concentration. The dissolved phenol solution was then injected into the anode through the sampling port of the chamber using a sterilized syringe. This was followed by immediate addition of 1 mL of a concentrated suspension of *P. putida* cells as inoculum to the anodic solution.

Addition of inoculum resulted in initial OD readings in the range of 0.09-0.18 (~ 29-64 mg cell L^{-1}). Regular sampling of the anodic chamber was done to determine phenol and biomass concentrations. Sampling was done at least once a day in experiments with lower initial phenol concentrations. At higher initial phenol concentrations, phenol degradation was slower, hence sampling was done every 2 days. Circuit potential was constantly monitored, while current and power were measured periodically, as described in Section 5.2.7.

Continuous mode of operation: Following the completion of batch experiments, biodegradation of phenol was investigated in continuously operated MFC with freely suspended cells. The experimental setup for the continuous biodegradation of phenol in the MFC with rod electrodes that was similar to that used in continuous biodegradation of lactate and acetate (Section 3.2.3) is shown in Figure 5.1. The MFC was continuously fed with modified McKinney's medium containing 100 mg L^{-1} phenol. Prior to use, feed was autoclaved at 121 °C, cooled to room temperature and then purged with nitrogen gas for about 10 minutes to ensure anoxic conditions. A variable flow peristaltic pump was used to transfer the feed continuously into the anodic chamber. The pump was pre-calibrated to determine the approximate flowrate at each pump settings. Additionally, average feed flowrate was determined during the experiment by collecting and measuring effluent volume over a specified period of time.

Initially, the continuous flow MFC was operated batchwise by adding modified McKinney's medium containing 100 mg L^{-1} phenol and inoculating it with 1 mL of *P. putida* cell suspension. Biodegradation of phenol was monitored and after complete removal of phenol, MFC was switched to continuous mode and feed was pumped into the anodic chamber at a low initial flow

rate of 1.2 mL h^{-1}. An intermediary glass for dripping the feed into the feed line was devised allowing feed to trickle down instead of a continuous flow which in turn created a space that prevented the transfer of the microorganisms through the tubing into the feed tank. Feed concentration was monitored by regular sampling from the feed line at a location very close to the anodic chamber inlet port.

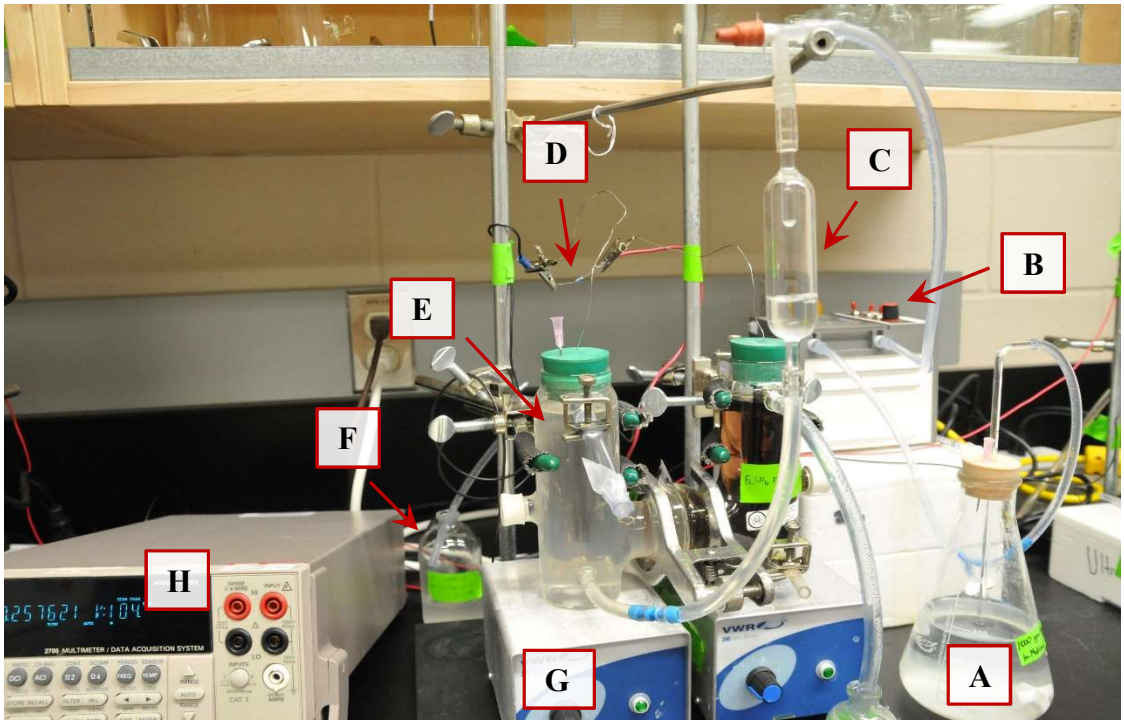

Figure 5.1 Continuous biodegradation of phenol in a MFC with single rod electrode. Feed (A) is introduced into the anodic chamber (E) using a peristaltic pump (B) passing through the intermediary device (C) used to prevent contamination of feed and exits the chamber into the effluent container (F). An external resistor (D) is attached to the anode and cathode terminals which are connected to the multimeter (H). A magnetic stirrer is used to mix the contents in the chamber (G).

The anodic chamber was sampled regularly for biomass and phenol concentrations. After establishment of steady-state conditions, flow rate of the feed was increased incrementally. Criterion for establishment of steady state conditions in continuously operated MFCs have been

described previously in Section 3.2.3. Given the slow nature of phenol biodegradation, flow rate of feed was slowly increased until MFC performance deteriorated (i.e. decrease in biodegradation rate of phenol). The highest applied flow rate in this experiment was 4.8 mL h^{-1}. Similar to batch experiments, circuit potential was constantly monitored and current and power were periodically measured.

5.2.3 Biodegradation of phenol in MFCs with granular electrode

The rationale behind the use of granular graphite electrode was: a)- to provide a matrix with large surface area for cell immobilization and formation of biofilm; b)- to increase the surface area of electrode and improve electron transfer. Both of these were expected to serve the eventual goal of enhancing phenol biodegradation and power generation.

Batch mode of operation: Production and preparation of graphite granules as electrodes have been described in detail in Section 4.2.1. Granular graphite particles were placed inside the MFC chambers (both anodic and cathodic chambers). Mixing in the anodic chamber was achieved through a recirculation loop where liquid content of the anodic chamber was withdrawn from the top and reintroduced into the bottom of the anodic chamber, using a peristaltic pump. Details of the mixing operation has also been described previously in Section 4.2.1.

Similar to previous experiments, sterile modified McKinney's medium was placed into the anodic chamber and purged with nitrogen gas. Phenol at the designated concentration was then added to the anodic chamber. This was followed by inoculation of medium with 1 mL of concentrated cell suspension of *P. putida*. As with previous batch experiments, phenol concentrations in the range

100-1000 mg L^{-1} were tested. The effect of sequential addition of phenol was also investigated. The experiment was started with the lowest phenol concentration of 100 mg L^{-1}. After complete biodegradation of phenol, another 100 mg L^{-1} phenol was added to the anodic chamber and the progress of biodegradation was monitored. This procedure was repeated with higher phenol concentrations (250 and 500 mg L^{-1}) with the exception of 1000 mg L^{-1} in which complete degradation of phenol took a long time and thus sequential addition was not carried out in this case. In all cases, the concentration of phenol was monitored regularly and corresponding MFC current and power were measured periodically.

Continuous mode of operation: Considering that conducting batch experiments promoted the formation of biofilm (i.e. cell immobilization) on the graphite particles in the anodic chamber, the same MFC was used to study biodegradation of phenol under continuous mode of operation. The experimental setup for the continuous biodegradation of phenol in the MFC with granular graphite electrode is shown in Figure 5.2. Modified McKinney's medium with 100 mg L^{-1} phenol was used as feed. Similar to previous experiments operated continuously, feed was sterilized and purged with nitrogen gas before it was used. Flowrate of feed was initially set at 1.2 mL h^{-1}. Flowrate was increased incrementally after steady-state conditions were achieved at each flow rate. In this experiment, flowrate was changed 6 times up to a maximum value of 40.6 mL h^{-1} after which performance of the system significantly deteriorated and experiment was halted.

Samples were collected regularly to monitor phenol concentration inside the anodic chamber. Sample collection was done at least once a day with frequency increasing as flow rate was increased (up to 4 times per day). Feed phenol concentration was also regularly monitored to

ensure no contamination occurred and designated phenol concentration was fed into the chamber. Circuit potential was monitored using the multimeter and datalogger. Moreover, current and power from the MFC were measured by generating polarization curves using a potentiostat. Polarization curve measurements are described in detail in Section 5.2.7. In the cathodic chamber, catholyte solution was regularly replenished to ensure that the cathodic potential did not fall below 250 mV.

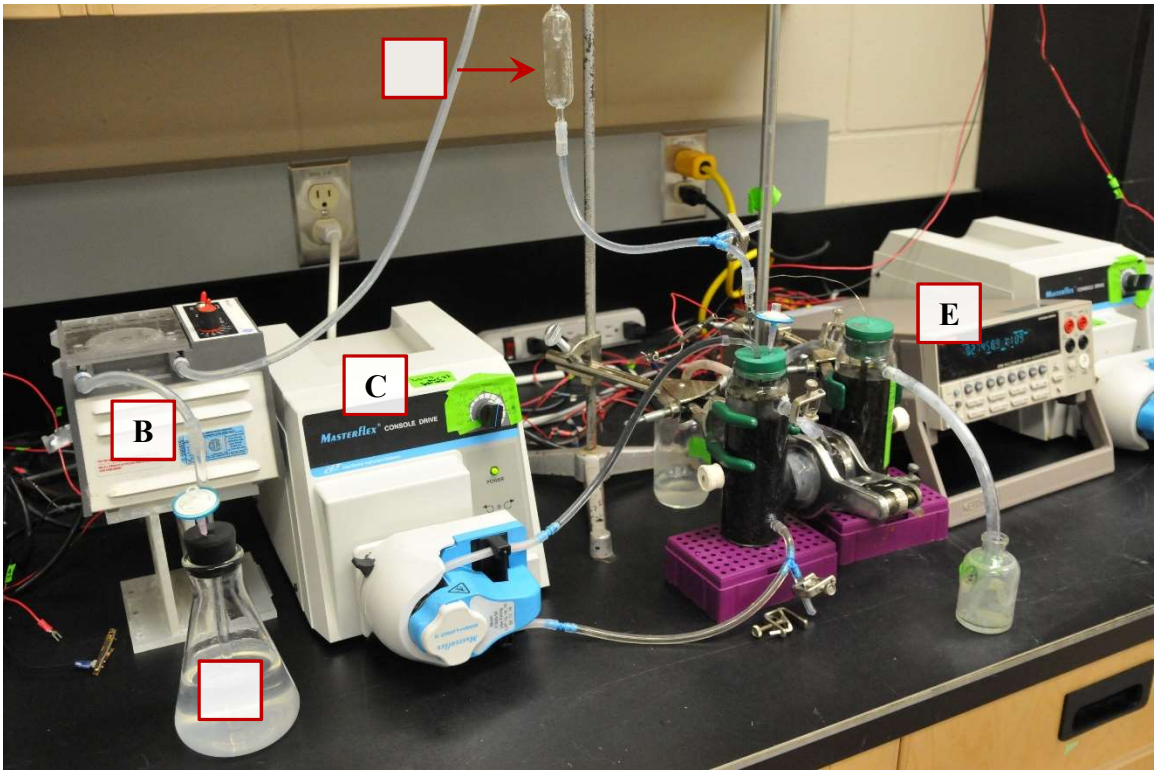

Figure 5.2 Continuous biodegradation of phenol in a MFC with granular graphite electrode. Feed (A) is drawn into the anodic chamber using a peristaltic pump (B) passing through the intermediary device (D) used to prevent contamination of feed. Another pump (C) is used to mix contents in the anodic chamber through a recirculation loop. An external resistor is attached to the anode and cathode terminals which are connected to the multimeter (E).

5.2.4 Biodegradation of phenol in MFCs with neutral red as mediator

Phenol, as an aromatic compound, is more difficult to degrade when compared to simpler organics such as fatty acids. In order to assess whether addition of a mediator (electron shuttle) could improve the biodegradation of phenol and generation of electrical energy, additional experiments were conducted in the granular graphite electrode MFCs using neutral red (NR) as the mediator. In all experiments, a NR concentration of 28.9 mg L^{-1} or 0.1 mM (Park and Zeikus, 2000) was followed.

Batch mode of operation: Modified McKinney's medium added with 28.9 mg L^{-1} NR and phenol at concentrations in the range 100-1000 mg L^{-1} was used in these set of experiments. All experimental conditions and procedure were similar to those described in Section 5.2.4. Sequential addition of phenol was also evaluated similar to previous experiments without the mediator. Figure 5.3 shows the MFC utilized for biodegradation of phenol with neutral red, where reddish stain around the anodic chamber due to the addition of neutral red can be clearly seen.

Continuous mode of operation: To investigate the effect of a mediator on the biodegradation of phenol in a continuously operated MFC, modified McKinney's medium with 100 mg L^{-1} phenol in combination with 28.9 mg L^{-1} NR was fed into the anodic chamber of the MFC (same MFC used in batch experiments) using a peristaltic pump. The experimental setup and procedures were similar to continuous MFC operation described in Section 5.2.3.

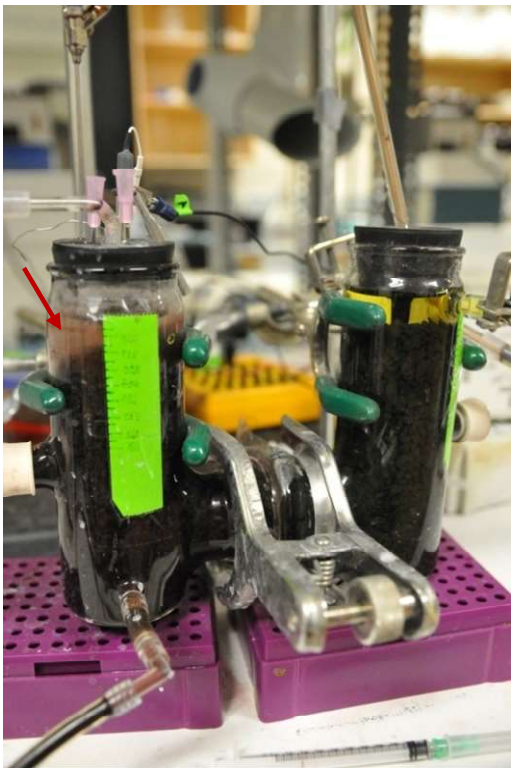

Figure 5.3 MFC with granular graphite electrode with added neutral red as mediator operated batchwise. Arrow indicates red stain around the chamber.

Initially, the MFC was fed at a relatively low rate of 1.5 mL h^{-1}. Once steady-state conditions were established, flowrate of feed was increased incrementally. The MFC was operated to a maximum flowrate of 20.0 mL h^{-1} after which performance of MFC deteriorated. Phenol concentration in the feed was regularly monitored to ensure consistent feed is introduced into the anodic chamber. Aside from regular monitoring of phenol biodegradation, circuit potential was constantly recorded. Moreover, polarization curves were developed and analysed in these experiments. All experiments were conducted at room temperature (24±2 °C).

5.2.5. Biokinetic evaluation of phenol degradation

Due to lack of detailed biokinetic model for phenol biodegradation in environmental conditions prevailing in an MFC, an attempt to model phenol biodegradation and microbial growth was

conducted following the procedures used for biokinetic evaluation of lactate and acetate in similar MFCs with suspended cells (Section 3.2.5). However, due to specific nature of phenol degradation observed in batch MFCs, whereby biodegradation occurred at a constant but slow rate (i.e. non-growth associated biodegradation) including a lag phase in microbial growth during the early stage of the process, the modelling approach used for lactate and acetate biodegradations did not lead to accurate predictions in the case of phenol (results are provided in Appendix D). This was even the case even with more sophisticated microbial growth kinetic expressions such as Haldane and Contois. A review of literature, however, revealed that a simpler approach in which a first-order rate expression as shown by Equation 5.2 (Droste, 1997) might very well describe the biodegradation of phenol in batch system.

$$-\frac{dC}{dt} = kCX \tag{5.1}$$

$$ln\ (C/C_0) = -k\ X\ t \tag{5.2}$$

Using the experimental data, $ln\ (C_0/C)$ was plotted against ($X\ t$) which resulted in a line where the slope was equivalent to the biokinetic rate constant k. Detailed calculations are shown in Appendix E.

Kinetic data generated in the continuous system together with Monod expression (Eq. 5.3) were also used to evaluate the biokinetics of microbial growth and phenol biodegradation in the continuous flow MFC. Mass balances of phenol and biomass concentrations, described below were used to accomplish this.

$$\mu = \frac{\mu_m SC}{K_s + SC} \tag{5.3}$$

Mass balance for phenol:

$$QS_{0-Phe} - QS_{Phe} - Vr_s = 0 \tag{5.4}$$

$$D = \frac{Q}{V} \tag{5.5}$$

$$r_s = \frac{Q(S_{0-Phe} - S_{Phe})}{V} = D(S_{0-Phe} - S_{Phe}) \tag{5.6}$$

Also,

$$r_s = -\frac{dS_{Phe}}{dt} = \frac{\frac{dx}{dt}}{Y_{x-Phe}} = \frac{\mu X}{Y_{x-Phe}} \tag{5.7}$$

$$D(S_{0-Phe} - S_{Phe}) = \frac{\mu X}{Y_{x-Phe}} \tag{5.8}$$

Mass balance for biomass:

$$X = \frac{DY_{x-Phe}(S_{0-Phe} - S_{Phe})}{\mu} \tag{5.9}$$

Assuming negligible biomass in the feed stream:

$$X_0 = 0$$

$$r_x = \frac{QX}{V} = DX \tag{5.10}$$

$$r_x = \mu X - K_{d-Phe}X \tag{5.11}$$

$$DX = \mu X - K_{d-Phe}X \tag{5.12}$$

$$\mu = D + K_{d-Phe} \tag{5.13}$$

Substituting μ in Equation 5.9 with Equation 5.13:

$$X = \frac{DY_{x-Phe}(S_{0-Phe} - S_{Phe})}{D + K_{d-Phe}} \tag{5.14}$$

$$DY_{x-Phe}(S_{0-Phe} - S_{Phe}) = DX + K_{d-Phe}X \quad (5.15)$$

$$\frac{(S_{0-Phe} - S_{Phe})D}{X} = \frac{D}{Y_{x-Phe}} + \frac{K_{d-Phe}}{Y_{x-Phe}} \quad (5.16)$$

Using the experimental data, one can plot $\frac{(S_{0-Phe} - S_{Phe})D}{X}$ against *D* which results in a line where slope of the line represents $\frac{1}{Y_{x-Phe}}$ and the intercept is $\frac{K_{d-Phee}}{Y_{x-Phe}Y}$.

From Equation 5.13: $D = \mu - K_{d-Phe}$

Substituting μ from Monod expression in Equation 5.3:

$$D = \frac{\mu_{max-Phe}S_{Phe}}{K_{s-Phe} + S_{Phe}} - K_{d-Phe} \quad (5.17)$$

$$D + K_{d-Phe} = \frac{\mu_{max-Phe}S_{Phe}}{K_{s-Phe} + S_{Phe}} \quad (5.18)$$

$$\frac{\mu_{max-Phe}S_{Phe}}{D + K_{d-Phe}} = K_{s-Phe} + S_{Phe} \quad (5.19)$$

$$\frac{S_{Phe}}{D + K_{d-Phe}} = \frac{S_{Phe}}{\mu_{max-Phe}} + \frac{K_{s-Phe}}{\mu_{max-Phe}} \quad (5.20)$$

Using the experimental data, one can plot $\frac{S_{Phe}}{D + K_{d-Phe}}$ against S_{Phe} which results in a line where slope of the line represents $\frac{1}{\mu_{max-Phe}}$ and the intercept is $\frac{K_{s-Phe}}{\mu_{max-Phe}}$.

5.2.6 Analyses

In MFCs with rod electrodes, biomass concentration was determined as described in Section 3.2.4. Concentration of phenol was determined using an HPLC (Agilent Technologies 1200), equipped

with a Di-Array detector (DAD) and an Eclipse Plus C-18 column (150 mm x 4.6 mm dia.). Standard solutions of phenol with concentrations in the range of 0-100 mg L^{-1} were used to develop the required calibration curve (Appendix B.4). Prior to analysis by HPLC, samples (1-1.5 mL) were centrifuged for 5 min at 10000 rpm (9180 ×g) (Microfuge 18 Centrifuge, Beckman Coulter, Fullerton, USA). The supernatant liquid was then used in analysis. Blank runs with McKinney's medium containing neutral red showed no additional peak in the resulting HPLC chromatogram indicating that the presence of neutral red did not affect the phenol measurement. Thus, HPLC was also used to determine phenol concentration in the samples from MFCs operated with neutral red.

In all cases, MFC circuit potential was continuously monitored and recorded using Keithley 2700 multimeter, equipped with 7700 datalogger (Keithley Instruments Inc., Cleveland, USA). The associated software, ExceLINX, facilitated measurement and datalogging of circuit potential. Using a handheld multimeter (Fluke, Everett, WA, USA), cathodic potential was also measured periodically against a Calomel reference electrode dipped into the catholyte solution. External resistors in the range 50-6000 ohms (You et al., 2006) were applied during the batch biodegradation of phenol in MFCs with rod electrodes and freely suspended bacterial cells to determine the current and power output.

Polarization curves were developed using Linear Sweep Voltammetry (LSV) carried out using a Gamry R600 potentiostat as part of experiments in MFCs with granular electrodes during which potentiostat was available (Gamry Instruments, Warminster, USA). The range of the sweep was from -550 mV to 10 mV at a scan rate of 0.1 mV s^{-1}. Each measurement was done for the entire fuel cell with the anode as working electrode and cathode as both the counter and reference

electrodes. Resulting potential and current data were subsequently utilized to generate corresponding power curves. Efficiency of electron recovery by the MFC during phenol biodegradation was determined by calculating the coulombic efficiency (CE) as described in detail in Appendix H.

Additional analysis was also done to determine surface area, pore size and volume of exposed graphite granules through BET analysis. Granular graphite samples were oven dried at 110 °C overnight and then examined using an ASAP 2020 Surface Area and Porosity Analyzer (Micromeritics Instrument Corp., Norcross, GA, USA). Samples were examined using 30 relative pressure points at the mesopore range. Graphite granules, fresh and exposed, were also examined by a scanning electron microscope (SEM) similar to procedures described previously in Section 4.2.4.

5.3 Results and discussion

5.3.1 Biodegradation of phenol in single rod electrode MFC with freely suspended cells

Batch mode of operation: Figures 5.4, 5.5, 5.6 and 5.7 show the biodegradation results obtained in MFCs with single rod electrode that were operated batchwise with suspended cells and phenol at initial concentrations of 100, 250, 500 and 1000 mg L^{-1}, respectively. In terms of biomass growth, it was observed that biomass concentration increased as biodegradation of phenol proceeded. Biomass concentration profile levelled off as phenol depleted and subsequently dropped as phenol exhausted. This pattern was observed in all cases and regardless of phenol initial concentration. The main distinction among these four cases was the extended lag phases of about 60 and 300 hours which were observed with higher phenol initial concentrations of 500 and 1000 mg L^{-1}, respectively. This finding points out to the inhibitory effect of high phenol concentrations

resulting in the need for microbial cells to adapt to consumption of phenol at these high concentrations.

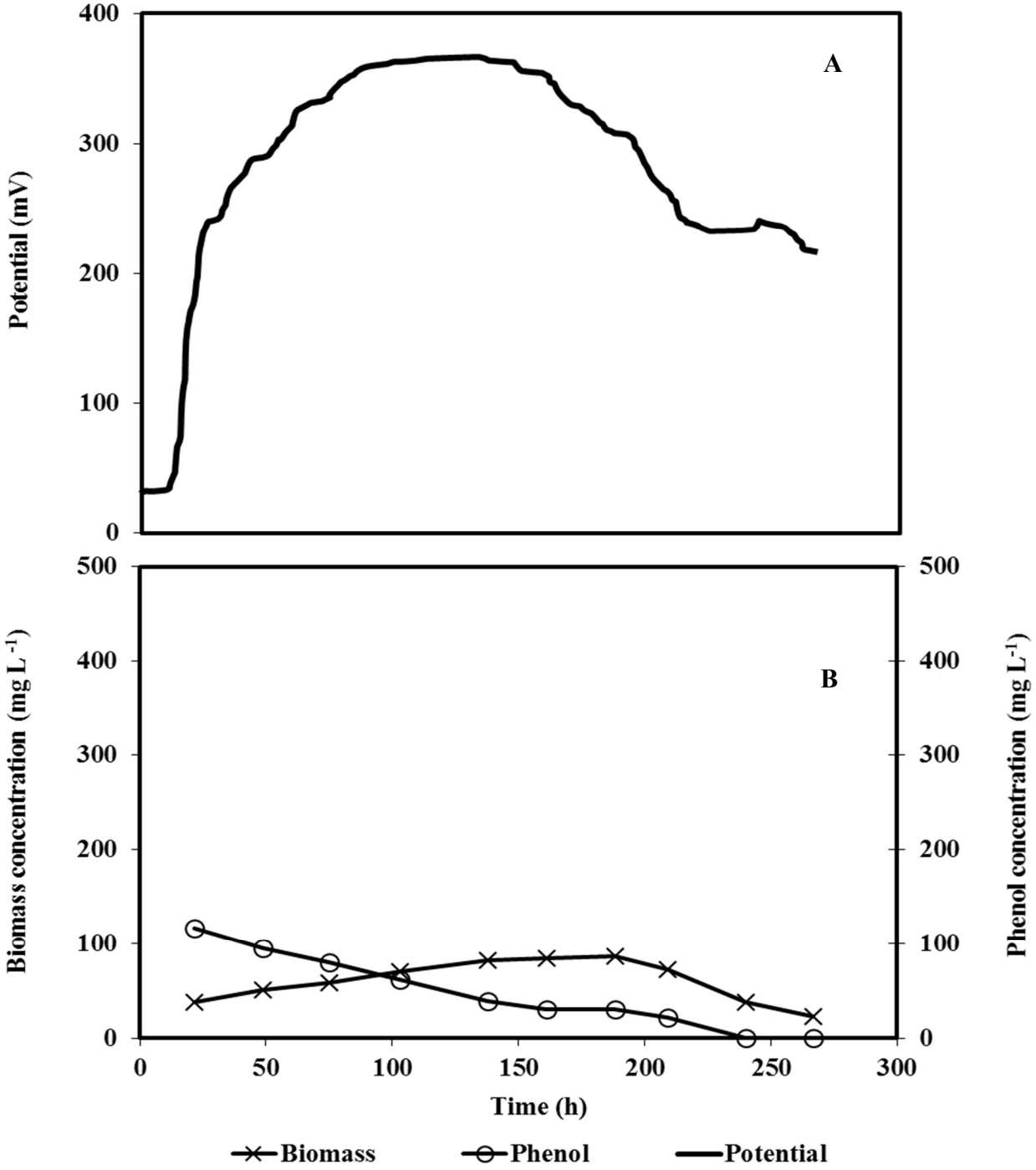

Figure 5.4 Biodegradation of 100 mg L^{-1} phenol in a batch-wise operated MFC with single rod and suspended cells of *P. putida*. A: Open circuit potential B: Phenol and biomass concentrations.

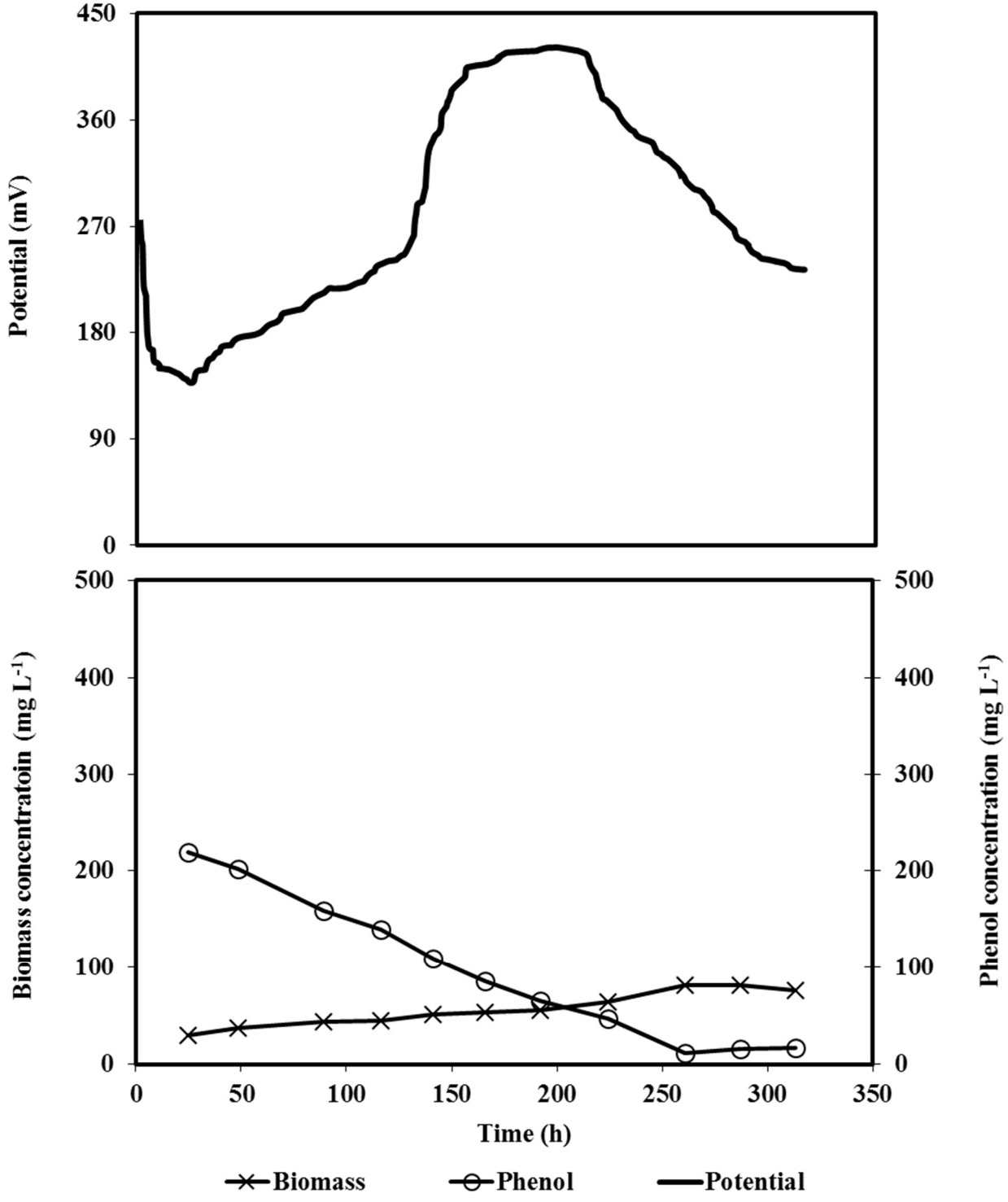

Figure 5.5 Biodegradation of 250 mg L^{-1} phenol in a batch-wise operated MFC with single rod and suspended cells of *P. putida*. A: Open circuit potential B: Phenol and biomass concentrations.

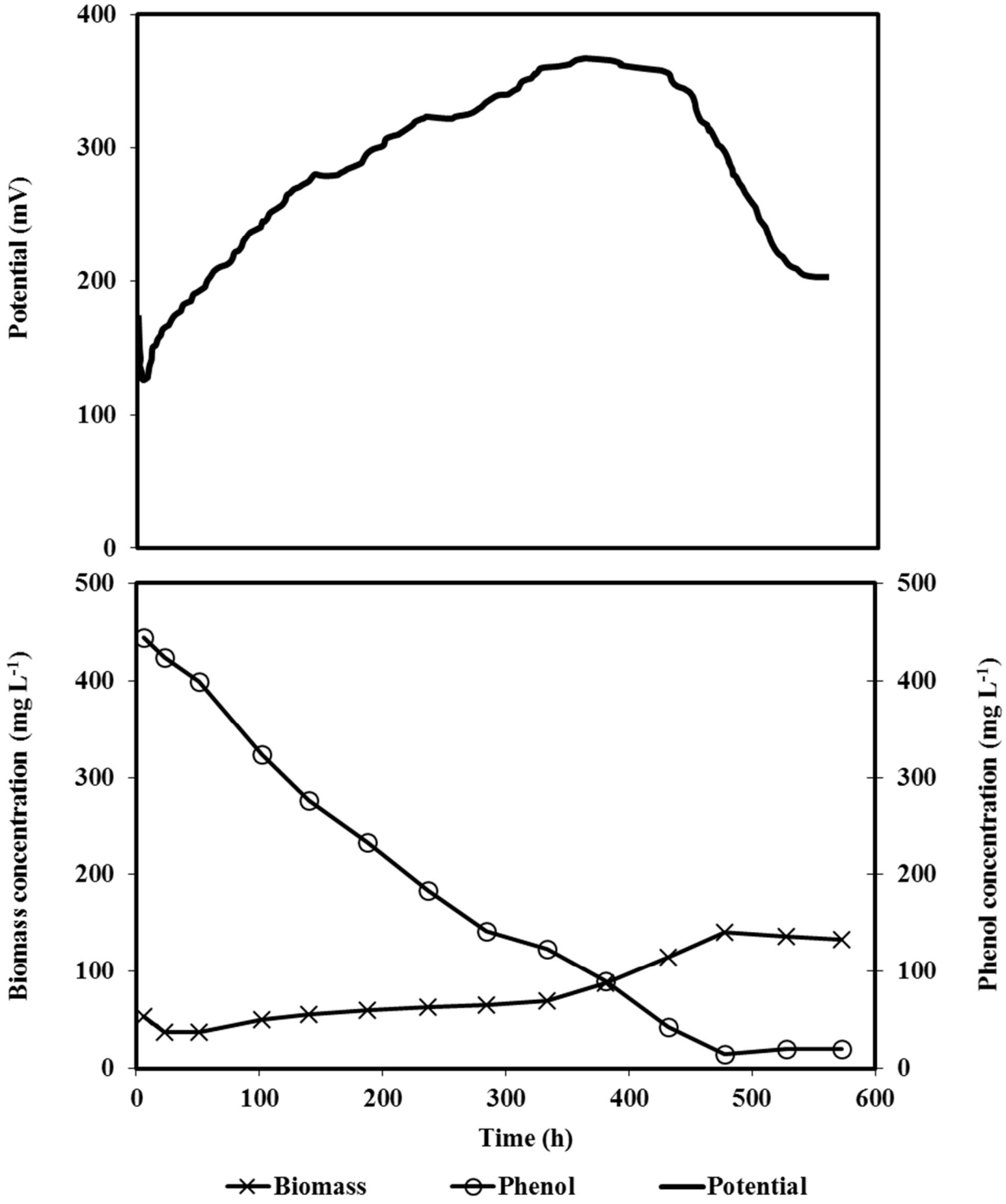

Figure 5.6 Biodegradation of 500 mg L^{-1} phenol in a batch-wise operated MFC with single rod and suspended cells of *P. putida*. A: Open circuit potential B: Phenol and biomass concentrations.

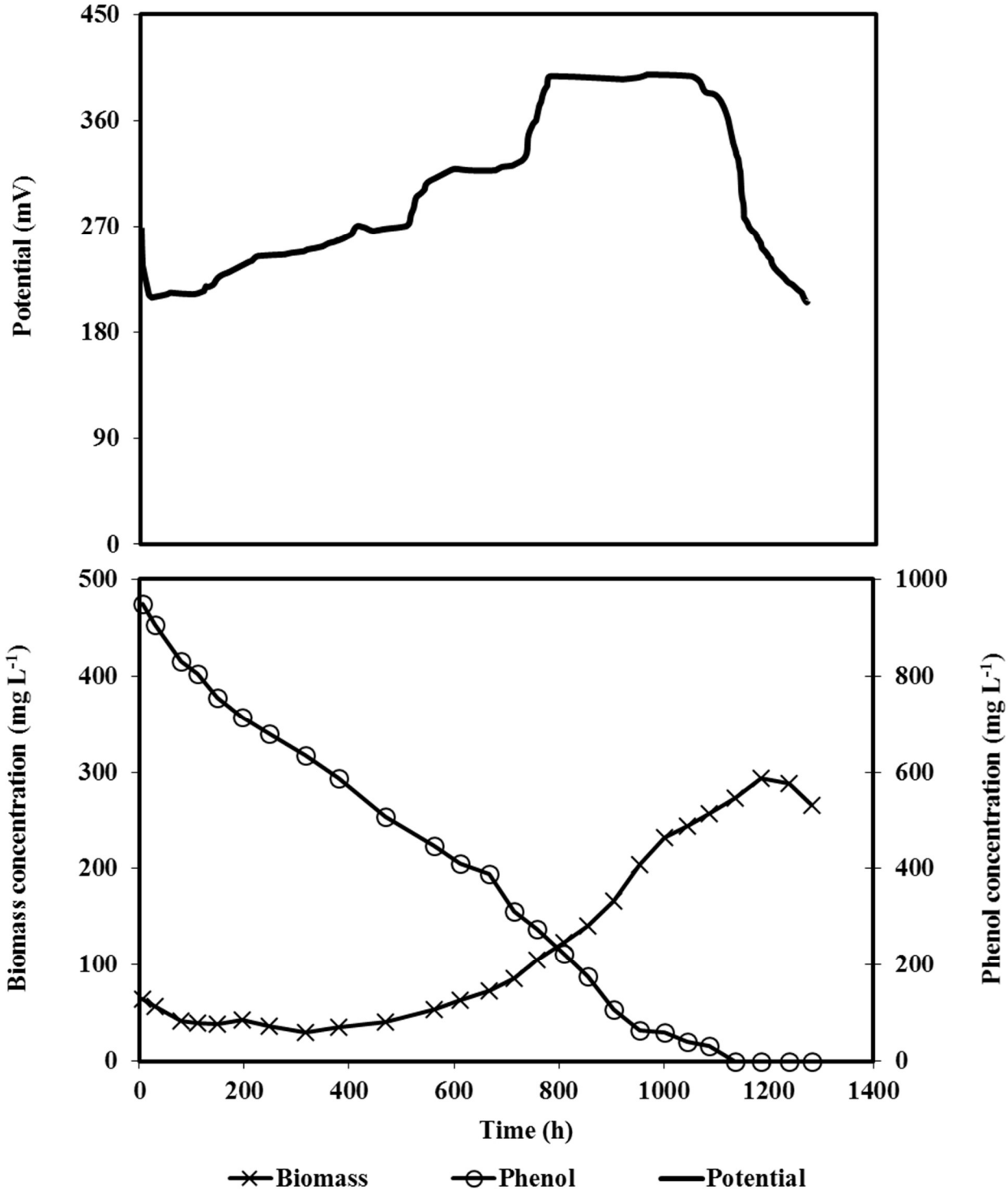

Figure 5.7 Biodegradation of 1000 mg L^{-1} phenol in a batch-wise operated MFC with single rod and suspended cells of *P. putida*. A: Open circuit potential B: Phenol and biomass concentrations.

The results further indicated the dependency of the lag phase on phenol concentration (i.e. higher phenol concentrations resulted in longer lag phases). Dapaah and Hill (1992) and Monteiro et al. (2000) have reported a similar trend in conventional bioreactors whereby lag phase tended to be longer when phenol concentration is increased in the range 60-600 mg L^{-1} and more so at higher concentrations where increase in the extent of the lag phase was reported as exponential. Using closely related strains of *Pseudomonas aeruginosa* and *Pseudomonas fluorescence*, a similar trend was also observed by Agarry et al. (2008) where increasing the initial phenol concentration from 100 to 500 mg L^{-1} extended the lag phase from 0 to 18 h and the required time for complete degradation of phenol by 72 h. As expected, application of higher phenol concentrations led to higher final biomass concentrations, with the maximum biomass concentration achieved being 86.6, 81.4, 140.5 and 293.4 mg L^{-1}, respectively. Biomass yield, however, displayed a marked decrease when concentrations of 250 mg L^{-1} and higher were applied with the values being 0.87, 0.32, 0.28 and 0.29 mg cells (mg phenol)$^{-1}$ for 100, 250, 500 and 1000 mg L^{-1} phenol, respectively. The time required for complete biodegradation of phenol which was dependent on phenol initial concentrations for 100, 250, 500 and 1000 mg L^{-1} phenol were approximately 240, 260, 480 and 1100 h, respectively.

Using the slope of the linear part of phenol concentration profile biodegradation rate of phenol at different initial concentrations were calculated. The lowest biodegradation rate of 0.5 mg L^{-1} h^{-1} was obtained in the MFC operated with an initial phenol concentration of 100 mg L^{-1} and application of higher phenol concentrations of 250, 500 and 1000 mg L^{-1} led to faster biodegradation rates of 0.9, 0.9 and 0.8 mg L^{-1} h^{-1} respectively, were achieved. This means that when cells acclimated to high phenol concentration and overcame the lag phase, phenol

concentration did not impact their activity and similar degradation rates were achieved during the exponential phase of microbial activity. When compared to similarly operated MFCs with lactate or acetate as substrate, biodegradation of phenol was substantially slower with lactate and acetate biodegradation rates being at least 3 times higher (5.7-17.3 and 3.1-3.6 mg L-1 h^{-1}, respectively).

In terms of open circuit potential (OCP), in all cases potential started to rise as microbial activity occurred. The rise in OCP continued during phenol degradation and reached its peak when biomass growth reached the stationary phase and biomass concentration profile levelled off. It was further observed that with higher concentrations of phenol, it took longer for the OCP to reach its maximum value. To be more specific the peak values of OCP with 100, 250, 500 and 1000 mg L^{-1} (361, 420, 363 and 393 mV) were achieved after 140, 210, 380 and 1000 h, respectively. As indicated earlier the increasing trend of OCP levelled off due to shift of microbial growth to its stationary phase (i.e. exhaustion of phenol) which was followed by a decrease in OCP.

During each set of experiments, external resistors were applied to measure power and current generated from the MFC. Maximum power and current densities achieved in MFC with 100 mg L^{-1} phenol of 0.01 mW m^{-2} and 2.77 mA m^{-2}, respectively, were considerably low. On the other hand, at the higher phenol concentrations of 250, 500 and 1000 mg L^{-1}, higher power and current densities of 2.08, 2.02, 1.07 mW m^{-2} and 19.58, 36.90 and 25.92 mA m^{-2} were observed, respectively. The equivalent power and current densities in terms of working volume were 0.07, 9.9, 10.4 mW m^{-3} and 4.8 mW m^{-3} and 16.4, 93.0, 166.3 and 115.4 mA m^{-3}, at 100, 250, 500 and 1000 mg L^{-1}, respectively.

The extent of power generated in MFC operated with different initial concentrations of phenol appears to correlate with the biodegradation rate. In other words, power and current generated in MFC operated with higher phenol concentrations (250-1000 mg L^{-1}), which displayed faster biodegradation rates, were markedly higher than those in the same system operated with 100 mg L^{-1} which represented the lowest biodegradation rate. This trend was previously observed in similarly operated MFCs with either lactate or acetate as substrate. Moreover, power and current output were also influenced by the efficiency in recovery of electrons as shown by the calculated coulombic efficiencies. The lowest CE of 0.38% was attained with 100 mg L^{-1} phenol, where corresponding biodegradation rate was the lowest, while higher CE values of 1.55%, 2.30% and 1.63% were achieved at the higher initial concentrations of 250, 500 and 1000 mg L^{-1} phenol. The influence of CE was even more pronounced when energy output was compared to those from lactate and acetate biodegradation in similarly operated MFCs. Despite significantly lower biodegradation rates, power and current output from phenol was essentially comparable to those from lactate and acetate. This result was likely due to the higher CE values calculated with phenol as compared to lactate and acetate which ranged from 0.17-1.71% and 0.51-1.14%, respectively. These results indicate that power and current output was affected by the biodegradation rate and CE.

Improved energy output coupled with higher phenol biodegradation has also been reported in other MFC systems. Luo et al. (2009) used a dual chamber MFC with an air cathode equipped with carbon paper as electrodes and mixed aerobic and anaerobic sludge as inoculum. This system with larger electrode surface area and a cathode coated with a platinum catalyst achieved a phenol biodegradation rate of 2.65 mg L^{-1} h^{-1} and accordingly produced a power density of 6.0 mW m^{-2}.

A higher phenol biodegradation rate of 9.5 mg L^{-1} h^{-1} and power density of 31.1 mW m^{-2} was obtained by Song et al. (2014) using a single chamber MFC with carbon felt anode and carbon cloth cathode containing platinum catalysts and anaerobic sludge as inoculum. It should be pointed out that faster removal of phenol reported in this system could be due to a gradual acclimation of bacterial culture to phenol using glucose as the initial carbon source. Subjecting a system to an acclimation period involves a series of phenol degradation stages typically in combination with a more simple structured organic such as glucose. During this period, phenol concentration in the mixture is gradually increased as the concentration of the paired organic is slowly reduced.

A single chamber air-cathode MFC operated in batch mode was used by Buitron and Moreno-Andrade (2014) to degrade phenol at various concentrations ranging from 25-200 mg L^{-1} with municipal wastewater as inoculum. These authors reported a biodegradation rate of 4.4 mg L^{-1} h^{-1} and a generated power output of 54 mW m^{-2}. Air-cathode MFCs typically have lower internal resistance than dual-chamber MFCs such as those used in the present work. Coating of cathode with a platinum catalyst in this particular system could be the other reason for better results in this work. Moreover, Buitron and Moreno-Andrade (2014) used 100 mg L^{-1} acetate as co-substrate with phenol which could have promoted faster phenol degradation. One should note that a simple MFC configuration (rod electrodes with freely suspended cells) was used in the current work to allow a better understanding of intrinsic biokinetics and the primary objective was not to produce high power output. Moreover, phenol biodegradation rates obtained in an MFC under anaerobic/anoxic conditions are expected to be lower than that in conventional reactors operated under aerobic conditions. Pazarlioglu and Telefoncu. (2005), Goudar et al. (2000) and Kumar et al. (2005) reported phenol biodegradation rates of 42, 10 and 6.1 mg L^{-1} h^{-1}, respectively. These

results were achieved in batch systems subjected to an acclimation period and under aerobic conditions.

5.3.1.1 Biokinetic evaluation based on the data from batch system

As indicated earlier biodegradation kinetics of phenol biodegradation in MFCs with rod electrode and suspended cells operated in batch mode was described by a first order kinetic expression (Eq. 5.2). Figure 5.8 shows the goodness of fit for a first order reaction rate expression with the experimental data obtained with 100, 250, 500 and 1000 mg L^{-1} phenol with the associated regression coefficient (R^2 values) in all cases being in the range 0.96-0.99. Using the slope of the lines, biodegradation rate constants were determined to be 9×10^{-5}, 20×10^{-5}, 5×10^{-5} and 1×10^{-5} L mg $cells^{-1}$ h^{-1} for phenol initial concentrations of 100, 250, 500 and 1000 mg L^{-1}, respectively. As seen the rate constants for phenol degradation at higher concentrations (500 and 1000 mg L^{-1}) were considerably lower which could suggest the inhibition effect of phenol at these concentrations. A simpler first-order kinetic evaluation for biodegradation of phenol in a batch operated MFC was carried out by Song et al. (2014). Given the rate expression used by Song et al. (2014) did not accurately describe the biokinetics of phenol degradation in an MFC, due to exclusion of the effect of biomass concentration, comparison of rate constants became impractical and thus was not carried out.

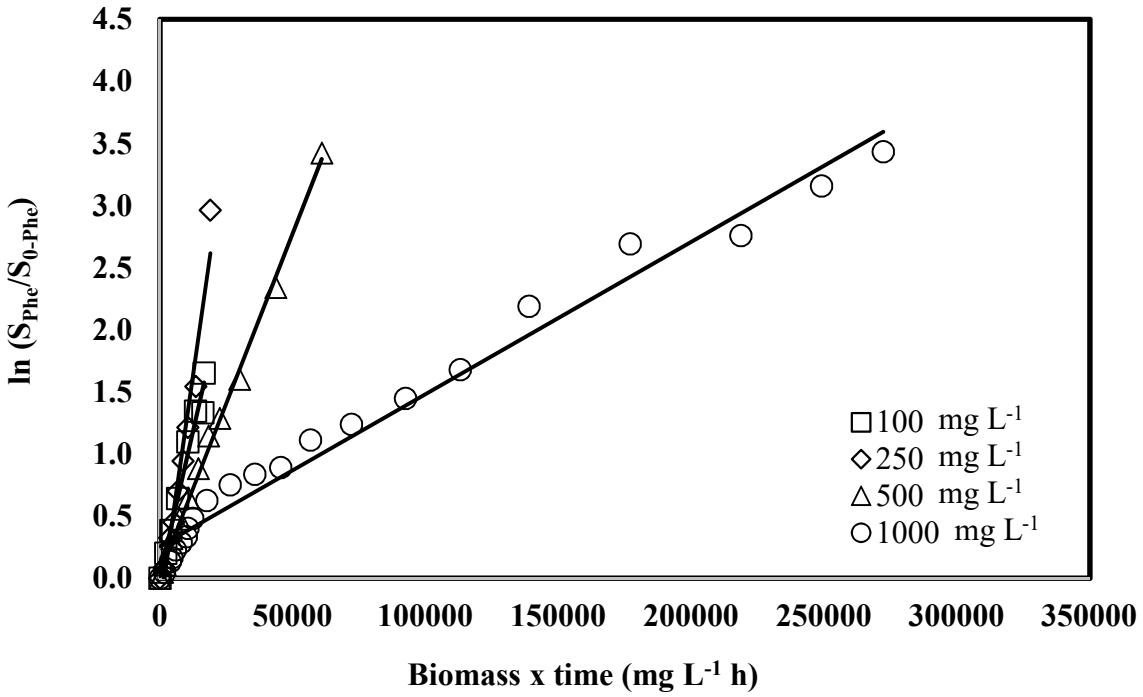

Figure 5.8 Goodness of fit of experimental data obtained during biodegradation of 100, 250, 500 and 1000 mg L^{-1} phenol in the MFCs operated batchwise with a first-order rate expression. This figure is derived in part from an article published in Environmental Technology Mar 2017 Taylor & Francis, available online: http://dx.doi.org/10.1080/09593330.2017.1296895.

Continuous mode of operation: Results for biodegradation of phenol in a MFC with rod electrodes under continuous mode of operation which include steady state profiles of biomass and phenol concentrations as a function of dilution rate are shown as in Figure 5.9. As seen the flow rate of the feed and consequently dilution rate was increased by small increments. This was employed to ensure that changes in the flow rate would only incur minimal disruption in the microbial environment given the sensitivity of the system to large changes in flow rate as a result of difficulty of phenol biodegradation. Moreover, reported observation by other researchers that large increment in flow rate or loading rate can result in inability of cells to utilize phenol and can lead to system failure (Allsop et al, 1993), was also taken into account.

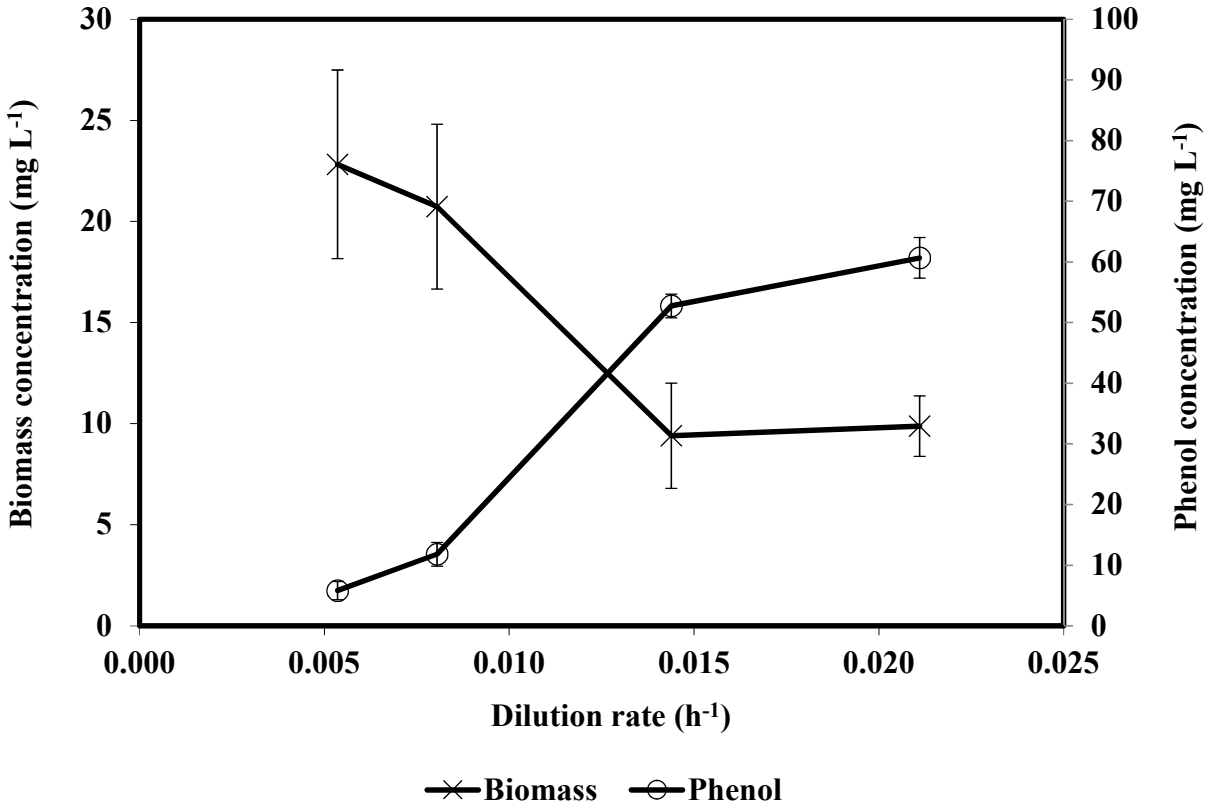

Figure 5.9 Steady state profiles of biomass and phenol concentrations as a function of dilution rate in a continuously operated MFC with single rod electrode inoculated with *P. putida* and fed with 100 mg L^{-1} phenol. Error bars represent standard deviation associated with biomass and phenol concentrations. This figure is derived in part from an article published in Environmental Technology Mar 2017 Taylor & Francis, available online: http://dx.doi.org/10.1080/09593330.2017.1296895.

Typical to what is expected in a continuous flow system, phenol residual concentration increased as dilution rate was increased. For instance, a sudden rise in phenol residual concentration from 11.8 to 52.8 mg L^{-1} was noticed when dilution rate was increased from 0.008 to 0.014 h^{-1} and this was accompanied by a sudden decrease in biomass concentration from 20.7 to 9.4 mg L^{-1}. Further increase in the dilution rate to 0.021 h^{-1} resulted in similar level of biomass concentration, indicating no significant improvement in biomass growth. Consequently, degradation of phenol showed no progress instead a further increase in the concentration was observed. At this stage, the

residual phenol concentration in the MFC was already 61% of the feed concentration when the flowrate was only 4 times the initial applied flow rate. Results showed that even at the lowest phenol concentration tested (100 mg L^{-1}) and with small incremental increases in flowrate, these changes were enough to create an arduous environment for the bacteria to function. This was in contrast to what was observed in a similar MFC with rod electrodes operated with lactate where the system was able to handle much higher dilution rates of up to 0.96 h^{-1}. Additionally, at comparable dilution rates (0.005-0.021 h^{-1}) biomass concentration in the similar system with lactate was approximately 4 times higher.

Figure 5.10 shows the phenol biodegradation rate and the corresponding removal percentage as a function of phenol loading rate. At the lowest loading rate of 0.5 mg L^{-1} h^{-1}, 94.2% of phenol fed into the MFC was removed. A slight increase in the loading rate from 0.5 to 0.8 mg L^{-1} h^{-1} resulted in a decrease in the removal percentage to 87.4%, while the biodegradation rate slightly increased from 0.5 to 0.7 mg L^{-1} h^{-1}. A more pronounced decrease in the removal percentage to 45.6% was observed when the loading rate was increased to 1.4 mg L^{-1} h^{-1} which consequently resulted to a decrease in the biodegradation rate to 0.6 mg L^{-1} h^{-1}. Further increase in the loading rate to 2.1 mg L^{-1} h^{-1} resulted in a biodegradation rate of 0.8 mg L^{-1} h^{-1}, with the corresponding removal percentage being 39.2%. The range of phenol biodegradation rates achieved in this experiment (0.5-0.8 mg L^{-1} h^{-1}) was narrow indicating that there was no significant improvement in the removal of phenol at all loading rates tested. Given the significant decrease in removal percentage as loading rate was slowly increased, the experiment was halted. Throughout the experiment, measured pH was in the range of 6.5-6.7.

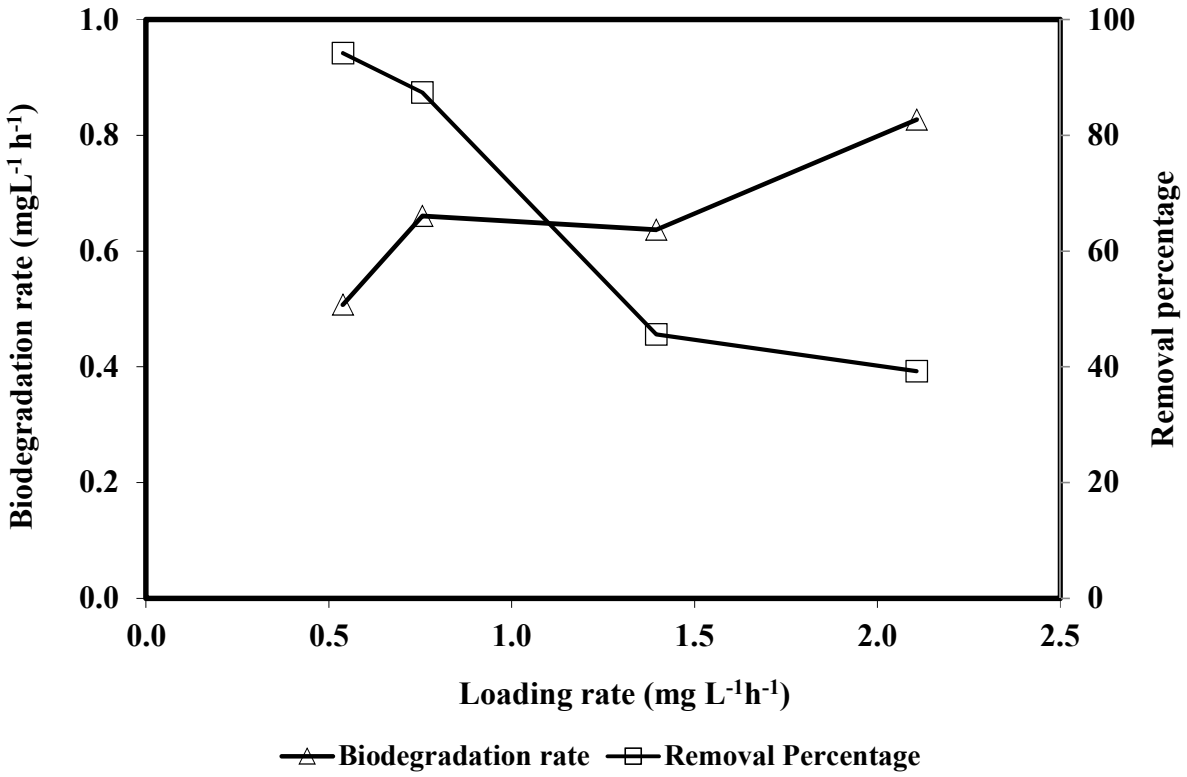

Figure 5.10 Biodegradation rate and percentage removal of phenol as a function of its loading rates in a continuously operated MFC with single rod electrode inoculated with *P. putida***.** This figure is derived in part from an article published in Environmental Technology Mar 2017 Taylor & Francis, available online: http://dx.doi.org/10.1080/09593330.2017.1296895.

There is no literature data regarding biodegradation of phenol in continuous flow MFC systems operated with freely suspended cells. Successful biodegradation of phenol by *P. putida* in conventional bioreactors operated continuously have been reported previously. Molin and Nilsson (1985) reported a phenol biodegradation rate of 230 mg L^{-1} h^{-1} in a continuously stirred tank reactor operated with an influent phenol concentration of 2500 mg L^{-1} at a hydraulic residence time (HRT) of 2.2 h (1136 mg L^{-1} h^{-1} loading rate). Mordocco et al (1999) achieved a phenol biodegradation rate of 42 mg L^{-1} h^{-1} at HRT of 1.7 h (60 mg L^{-1} h^{-1} loading rate) in a fluidized glass bioreactor. Gonzalez et al (2001) showed over 90% removal of phenol and a biodegradation rate of 133.3 mg

L^{-1} h^{-1} achieved at a HRT of 7.2 h (139 mg L^{-1} h^{-1} loading rate) in a continuous stirred tank reactor fed with 1000 mg L^{-1} phenol. These reported phenol biodegradation rates by *P. putida* were expected to be higher since these were conducted in conventional bioreactors under aerobic conditions.

When compared to the similar MFC with rod electrodes operated continuously with lactate as substrate, biodegradation rates of phenol were substantially lower. As reported earlier in Section 3.3.3, the biodegradation rates achieved from the continuous degradation of lactate ranged from 83.4-1668.2 mg L^{-1} h^{-1} which are several orders of magnitude higher when compared to those for phenol. The difference in magnitude of biodegradation rates indicate the recalcitrant nature of phenol as substrate, as compared to lactate, in a continuous MFC.

As indicated earlier, toward the end of batch operation (corresponding to complete exhaustion of phenol) and prior to switching the MFC to continuous mode, OCP was around 200-220 mV. As shown in Figure 5.11, when the initial loading rate of 0.5 mg L^{-1} h^{-1} was applied, a rise in OCP was observed. Increasing the loading rate to 0.8 and 1.4 mg L^{-1} h^{-1} resulted in a continued rise in OCP which reached its peak at approximately 420 mV. However, OCP started to fall as loading rate was further increased to 2.1 mg L^{-1} h^{-1}, a change which also resulted in the deterioration of MFC performance in terms of phenol biodegradation. Furthermore, a few sudden drops in the OCP are seen in this figure which are the result of incidental decrease in phenol concentration in the feed due to microbial contamination of the feed container. Nevertheless, the sudden decreases in OCP did not influence its overall trend and OCP recovered as soon as the contaminated feed was replaced.

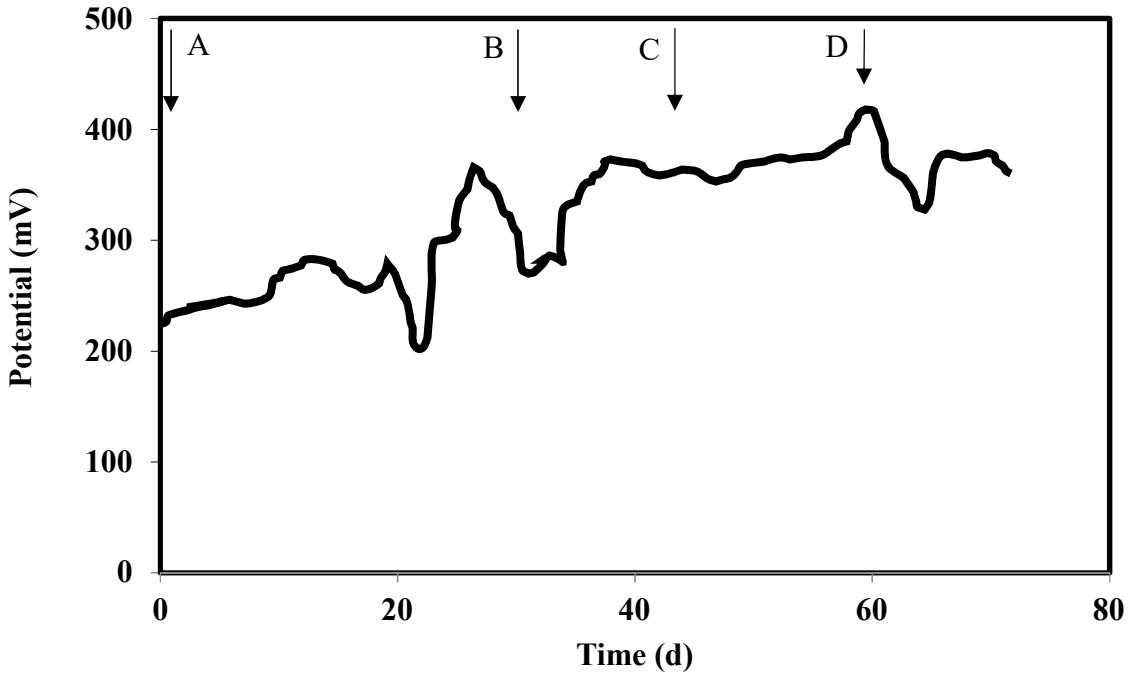

Figure 5.11 Open circuit potential in the continuously operated MFC with single rod electrode inoculated with *P. putida* fed with 100 mg L^{-1} phenol**.** Arrows indicate time when flow rates of (A) 1.2, (B) 1.8, (C) 3.2 and (D) 4.8 mL h^{-1} (corresponding loading rates of 0.5, 0.8, 1.4, 2.1 mg L^{-1} h^{-1}, respectively) were applied. This figure is derived in part from an article published in Environmental Technology Mar 2017 Taylor & Francis, available online: http://dx.doi.org/10.1080/09593330.2017.1296895.

In terms of energy output, maximum power and current densities achieved from the continuous MFC were 0.06 mW m^{-2} and 2.27 mA m^{-2}, respectively, which were achieved when biodegradation rate was at the maximum level. The equivalent power and current densities in terms of anodic chamber working volume were 0.8 mW m^{-3} and 37.3 mA m^{-3}, respectively. At the same phenol concentration (100 mg L^{-1}), power output produced from the MFC operated continuously was much higher, specifically 8 folds, than that from the similar system operated batchwise. However, when compared to the similar continuous MFC operated with lactate as substrate, these maximum power and current densities were substantially lower (lactate maximum power and current

densities: 8.1 mW m^{-2} and 43.0 mA m^{-2}, respectively). Lower energy output from the continuous biodegradation of phenol would again confirm the relationship among power and current densities and extent of biodegradation. In other words, given higher biodegradation rate in case of lactate (1668 mg L^{-1} h^{-1}), one could expect higher current and power outputs with this substrate. Coulombic efficiencies attained from continuous phenol biodegradation (0.14-0.31%) were considerably higher compared to lactate, attaining only a maximum of 0.04%, but the extremely faster biodegradation rates likely resulted to higher energy output from lactate biodegradation.

5.3.1.2 Biokinetic evaluation based on the data from continuous system

For the MFC with rod electrodes and suspended cells operated continuously, Monod kinetics was used to evaluate the microbial growth kinetics of the system as described in Section 5.2.6. Experimental data was fitted into the developed linear equations (Equations 5.13 and 5.20) to determine various biokinetic coefficients including $Y_{x\text{-}Phe}$ (biomass yield), $K_{d\text{-}Phe}$ (endogenous rate constant), $\mu_{max\text{-}Phe}$ (maximum specific growth rate) and $K_{s\text{-}Phe}$ (saturation constant). In other words $(S_{0\text{-}Phe}\text{-}S_{Phe}).DX^{-1}$ was plotted against the dilution rate, D to yield a line wherein the slope and intercept were equivalent to $Y_{x\text{-}Phe}^{-1}$ and $K_{d\text{-}Phe}Y_{x\text{-}Phe}^{-1}$, respectively. From Figure 5.12, $Y_{x\text{-}Phe}$ was determined to be 0.25 mg cell (mg phenol)$^{-1}$ and $K_{d\text{-}Phe}$ was calculated to be 3.7×10^{-4} h^{-1}. Similarly, plotting $S_{Phe}.(D+K_{d\text{-}Phe})^{-1}$ against phenol concentration, S_{Phe}, resulted in a line where the slope corresponded to $\mu_{max\text{-}Phe}^{-1}$ and the intercept was equivalent to $K_{s\text{-}Phe}\,\mu_{max\text{-}Phe}^{-1}$. The resulting line shown in Figure 5.13 was used to determine $\mu_{max\text{-}Phe}$ and $K_{s\text{-}Phe}$ as 0.03 h^{-1} and 24.2 mg L^{-1} phenol, respectively.

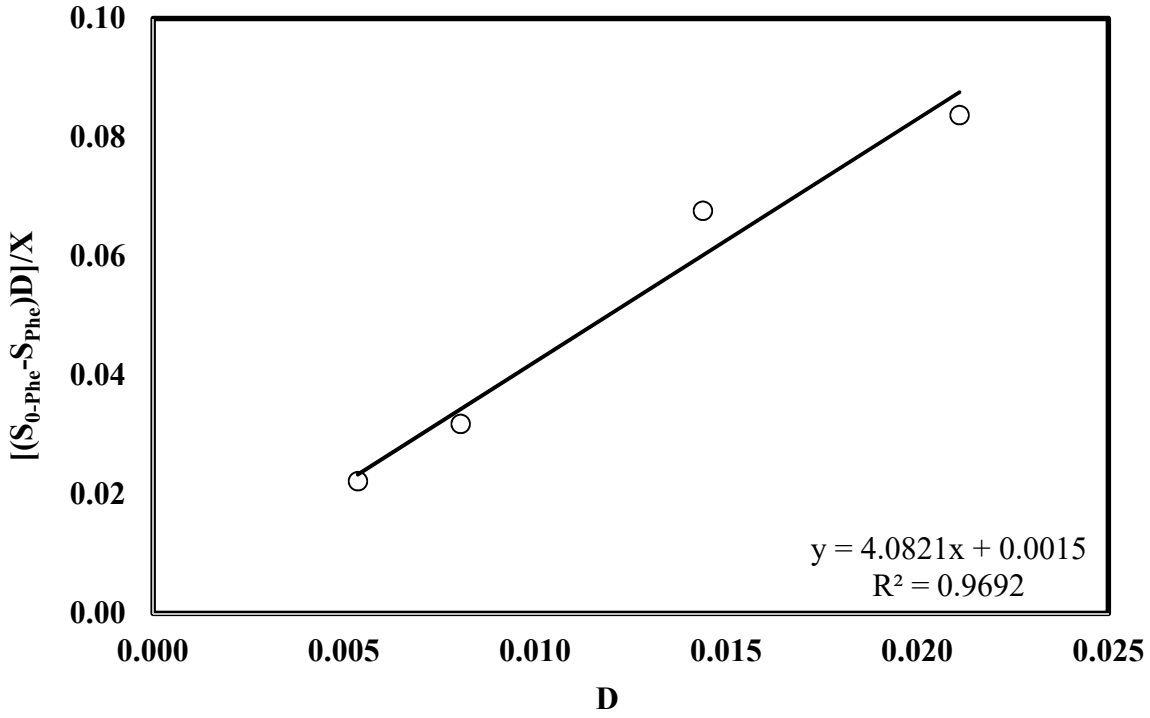

Figure 5.12 Linear plot of $\frac{(S_{0-Phe} - S_{Phe})D}{X}$ against *D*.

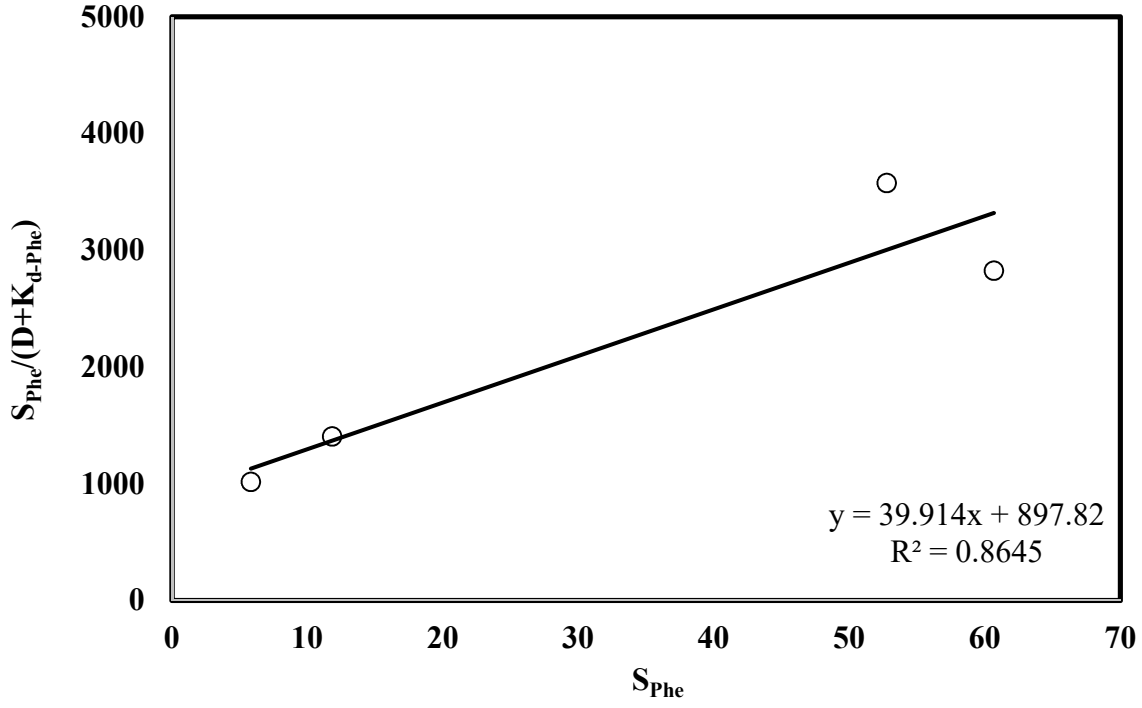

Figure 5.13 Linear plot of $\frac{S_{Phe}}{D + K_{d-Phe}}$ against S_{Phe}.

Generally, there is very little information available on the microbial growth and biodegradation kinetics and associated coefficient for biodegradation process in an MFC. Of the few biokinetic studies conducted in MFCs, these were done using simple-structured model organic compounds such as lactate and acetate, as has been discussed in Section 3.3. No biokinetic model or even simple first-order kinetic model have been evaluated for the biodegradation of phenol in an MFC operated continuously.

5.3.2 Biodegradation of phenol in MFC with granular electrodes

Batch mode of operation: The results on the biodegradation of phenol in MFC with granular electrodes are shown in Figure 5.14. The experiment was started with the lowest phenol concentration of 100 mg L^{-1}. Concentration of phenol was monitored and it was found that complete removal of phenol was achieved within 28 h. The duration of phenol degradation was much shorter than that observed in similar MFC with rod electrodes which took about 218.3 h. To verify this performance, three sequential additions of 100 mg L^{-1} phenol were conducted. These sequential runs confirmed the earlier results with the average time required for removal of phenol being 28.3 ± 5.5 h. Profiles of phenol concentration show immediate biodegradation and no indications of a slowdown in the removal of phenol. Although determination of biomass concentration was not possible due to added turbidity from the granules and potential presence of attached biomass, phenol concentration profiles suggested that biodegradation proceeded with minimal or no lag phase in microbial activity. Using the slope of the phenol concentration profiles, average phenol biodegradation rate was calculated as 3.5 ± 0.3 mg L^{-1} h^{-1}.

Sequential addition of phenol at higher concentrations of 250 and 500 mg L^{-1} was also carried out and average biodegradation rates of 3.8 ± 0.4 and 4.8 ± 0.9 mg L^{-1} h^{-1} were achieved, respectively. At the highest tested concentration of 1000 mg L^{-1}, no sequential addition was done since complete degradation of phenol needed approximately 9.2 days. The corresponding biodegradation rate with 1000 mg L^{-1} phenol was of 4.6 mg L^{-1} h^{-1}. Results from this experiment revealed that biodegradation rate increased as the initial phenol concentration was increased from 100 to 500 mg L^{-1} (Figure 5.15). However, increasing the initial concentration to 1000 mg L^{-1} did not improve the biodegradation rate indicating possible inhibition effects of phenol at high concentration. The standard deviation calculated for biodegradation rates were relatively low (0.3-0.9 mg L^{-1} h^{-1}) indicating repeatability of the results obtained during the sequential addition of phenol.

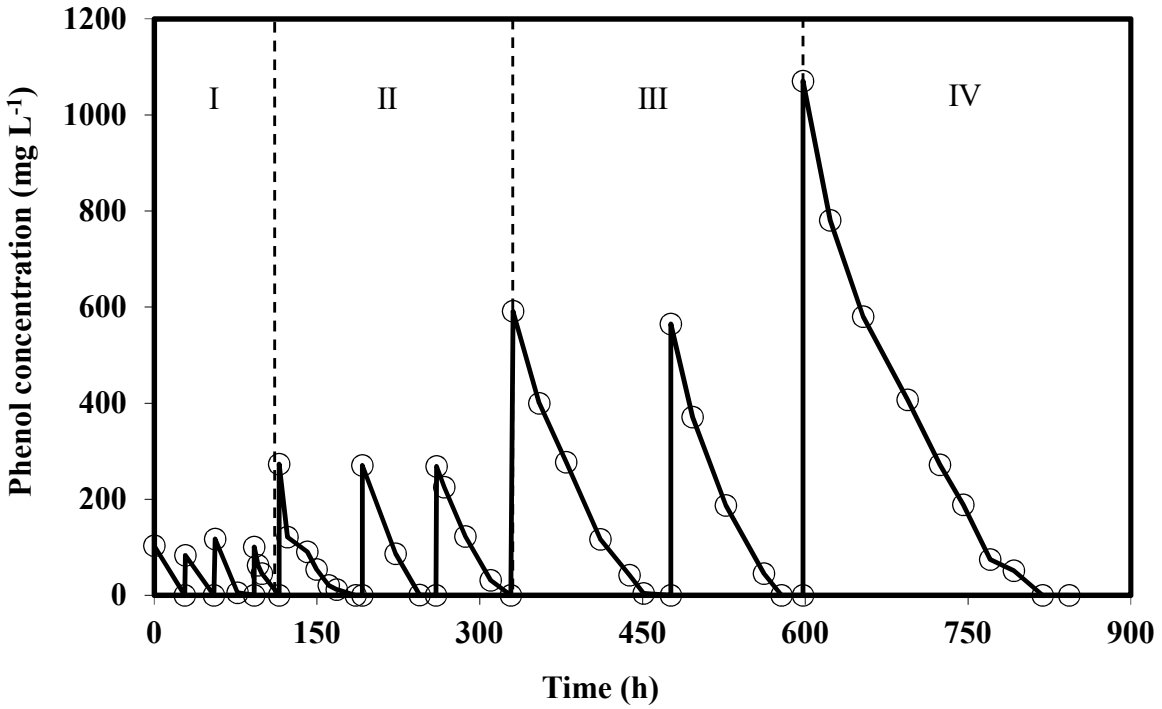

Figure 5.14 Sequential biodegradation of phenol in MFC with granular electrodes and *P. putida*. Panel I: 100 mg L^{-1} phenol, Panel II: 250 mg L^{-1} phenol, Panel III: 500 mg L^{-1}, and Panel IV: 1000 mg L^{-1}. This figure is derived in part from an article published in Environmental Technology Mar 2017 Taylor & Francis, available online: http://dx.doi.org/10.1080/09593330.2017.1296895.

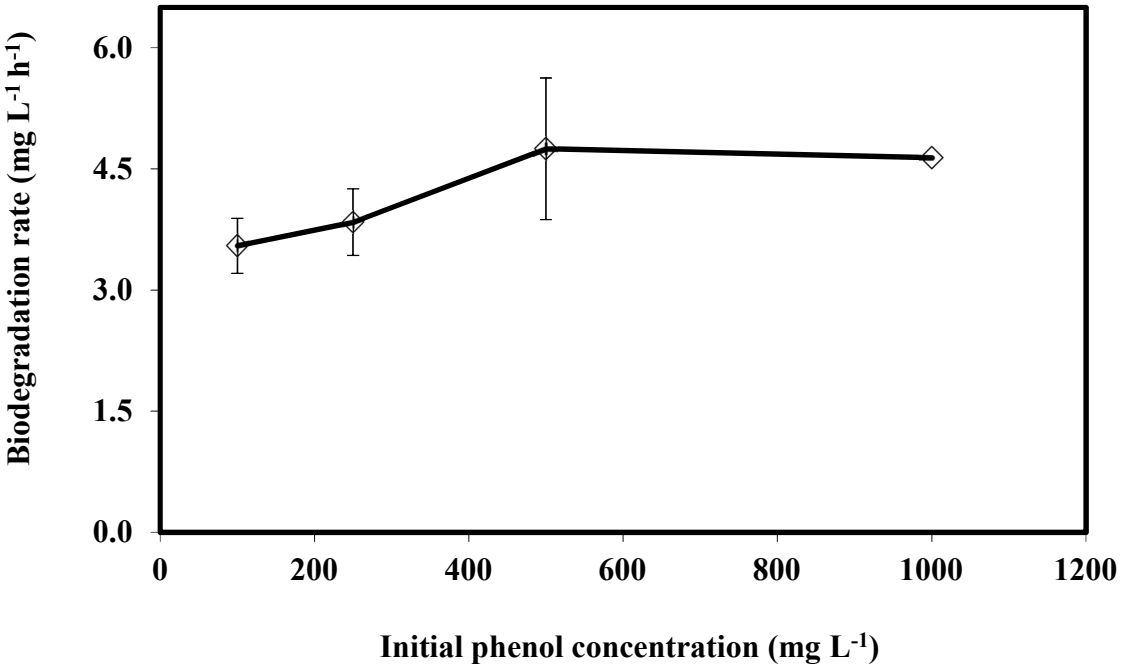

Figure 5.15 Biodegradation rate of phenol at different initial concentrations in an MFC with granular graphite electrodes. Error bars represent standard deviation of biodegradation rates from sequential tests in each tested concentration.

Biodegradation of phenol in MFC with granular electrode was found to be substantially faster than that in MFCs with rod electrodes. With an initial concentration of 1000 mg L^{-1}, complete phenol biodegradation took 47.3 days in the MFC with rod electrodes, which was more than 5 times longer than that observed in MFC with granular electrodes. Moreover, biodegradation rates obtained in MFCs with rod electrodes for phenol concentrations of 100, 250, 500 and 1000 mg L^{-1} (0.5, 0.9, 0.9 and 0.8 mg $L^{-1}h^{-1}$, respectively) were 4-6 times lower than those in an MFC with granular electrodes (3.5, 3.8, 4.8 and 4.6 mg $L^{-1}h^{-1}$, respectively). These results in general showed that biodegradation of phenol is improved significantly when granular graphite is used as electrode as opposed to graphite rod.

An MFC system with granular graphite as packing material was used by Luo et al. (2009) to degrade 1000 mg L^{-1} phenol. These authors achieved 90% phenol removal within 48 h with a corresponding biodegradation rate of 18.8 mg L^{-1} h^{-1}. The higher biodegradation rate obtained in this system could be attributed to the use of pre-acclimated bacteria from the anode of an aqueous air cathode MFC that had been running in fed batch mode for over 5 months and the employment of recirculation streams in both the anode and cathode. These authors did not attempt to evaluate the kinetics of phenol biodegradation in detail. Unfortunately there is no other reported work on degradation of phenol in an MFC with granular electrode operated batchwise. So further comparison of the current work is not possible.

Conventional batch bioreactors operated under aerobic conditions using immobilized cells of *P. putida* have achieved significantly higher phenol biodegradation rates than those in MFC systems. Pazarlioglu and Telefoncu (2005) immobilized *P. putida* in Zr-activated pumice as supporting material to degrade 1000 mg L^{-1} phenol. Batch operation of this system resulted in a biodegradation rate of 45.4 mg L^{-1} h^{-1}. El-Naas et al (2009) employed *P. putida* immobilized in polyvinyl alcohol gel pellets to degrade 75 mg L^{-1} phenol in a batch bubble column bioreactor and reported a maximum biodegradation rate of approximately 48 mg L^{-1} h^{-1}. Both systems were subjected to an acclimation period, using glucose as a co-substrate with phenol, which could have greatly contributed to these high biodegradation rates. Gonzalez et al (2001) used *P. putida* immobilized in calcium alginate directly (i.e. with no acclimation) for biodegradation of 1000 mg L^{-1} phenol. A phenol biodegradation rate of 3.5 mg L^{-1} h^{-1} was reported by these authors which is comparable with the rates achieved in the granular electrode MFC of the current work which also did not undergo an acclimation period. To compare the efficiency in the degradation of phenol in

conventional reactors, Annadurai et al (2002) compared effectiveness of *P. putida* freely suspended and immobilized and cells for degradation of 100-400 mg L^{-1} phenol in combination with 500 mg L^{-1} glucose in shake flasks and, as expected, reported that the immobilized cells were far superior when compared with the freely suspended cell.

When compared to similarly batch operated MFC with granular electrodes provided with lactate or acetate as substrate, rates of phenol biodegradation were found to be lower. At comparable initial concentration of 1000 mg L^{-1}, biodegradation rates of lactate and especially acetate were substantially faster (7.4 and 47.8 mg L^{-1} h^{-1}, respectively). Again, this finding indicates the challenging nature of phenol as a recalcitrant compound, as compared to the fatty acids.

In MFC with granular electrodes, a low external resistance (load) of 50 ohms was applied in all experimental runs. Similar to previous batch operated MFC with granular electrodes fed with lactate, the external resistance was not removed or replaced with a different resistance throughout the experiment. Application of the resistor, as expected, resulted in a low circuit potential in the range of 4.1-8.2 mV. Calculation of power and current output resulted to power and current densities of 4.8 mW m^{-3} and 1165.7 mA m^{-3}, respectively. Potentially higher power output could have been measured if higher resistances were applied or a potentiostat was utilized for more accurate results. Unfortunately, potentiostat was not available at that time to conduct linear sweep voltammetry (LSV) analysis for generation of polarization curve. Nevertheless, the resulting power density was comparable to those attained from the biodegradation of phenol in similar MFCs with rod electrodes, while current density was approximately 7 times higher. This higher

output from the granular electrode MFC was corresponded with a CE of 4.63% which was higher compared to those from the previous batch experiments in MFCs with rod electrodes (0.38-2.30%).

Compared to other batch MFCs using phenol as substrate, the only system with granular electrodes reported in literature to date was able to generate a significantly higher power output of 9100 mW m^{-3} (Luo et al., 2009). As described earlier, the superior performance of this system could be attributed to the use of pre-acclimated bacteria in the anode and the employment of recirculation streams in both the anodic and cathodic chambers.

Continuous mode of operation: The experiment in granular electrode MFC operated continuously was conducted with a feed containing 100 mg L^{-1} phenol. Similar to the previous experiment in MFC with rod electrodes, initial flowrate was set at 1.2 mL h^{-1} corresponding to a dilution rate of 0.013 h^{-1}. Figure 5.16 presents the steady state profile of phenol concentration as a function of dilution rate. No profile for biomass concentration is included since majority of cells were in the attached state. Furthermore, optical density could not be used as an accurate representation of suspended biomass concentration due to the turbidity that was created by fine particles of graphite.

At the lowest dilution rate of 0.01 h^{-1}, all phenol from the feed was removed and concentration of phenol in the anodic chamber was zero. Increasing the dilution rate to 0.03 and then 0.06 h^{-1} did not affect the biodegradation process negatively and phenol residual concentration maintained at zero. This was quite distinct from the continuous system with single rod electrodes, where there was a considerable increase in the phenol residual concentration (>50%) in the anode even at a

lower dilution rate of 0.01 h^{-1}. In the system with granular electrodes, increase in residual phenol concentration occurred when dilution rate was increased to 0.10 h^{-1} and this increasing trend continued for the entire range of higher dilution rates tested. At the highest dilution rate of 0.45 h^{-1}, phenol concentration in the anode was around 73.8 mg L^{-1} which was around 74% of the feed concentration (i.e. 36 % phenol removal). The range of dilution rates over which the system with granular electrode was able to achieve phenol biodegradation was certainly higher than those in a similar system with rod electrodes (0.01-0.45 h^{-1} vs 0.005-0.02 h^{-1}).

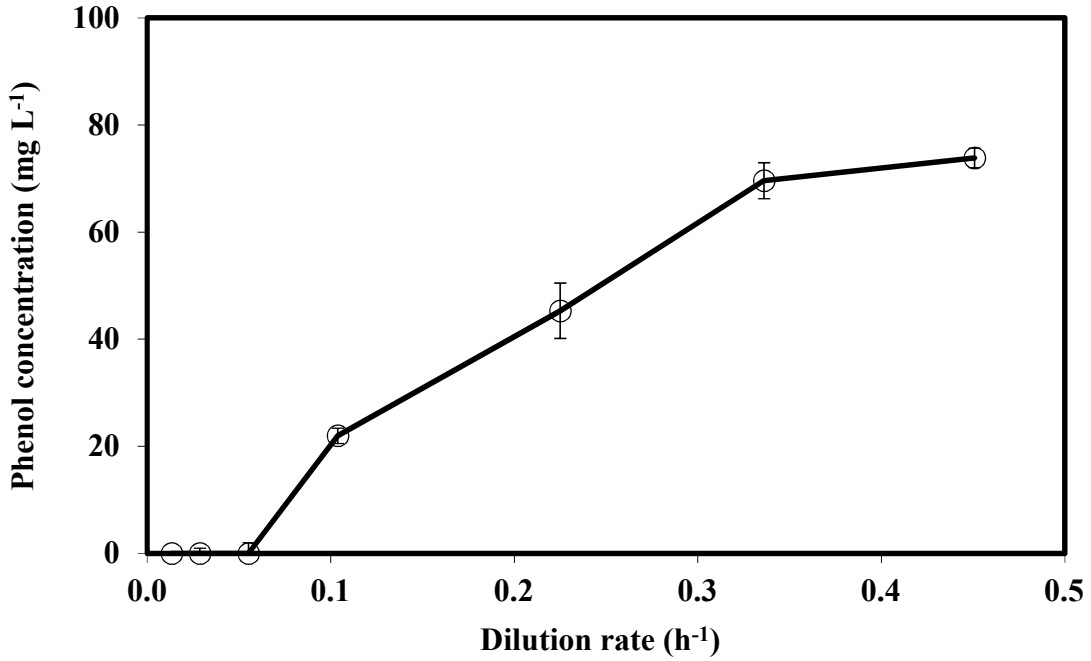

Figure 5.16 Steady state profile of phenol concentration as a function of dilution rate in a continuously operated MFC with granular graphite electrodes with immobilized *P. putida*.

Phenol biodegradation rate and its corresponding removal percentages as a function of phenol loading rate achieved in the MFC with granular electrodes is shown in Figure 5.17. The removal percentage was 100% at the lowest loading rate of 1.4 mg L^{-1} h^{-1} (HRT = 75.3 h) and complete phenol removal was maintained up to a loading rate of 5.5 mg L^{-1} h^{-1}. Subsequently, increase in

biodegradation rate was highest during this period. With 100% removal, the biodegradation rates were essentially equal to the loading rates at 1.4, 2.8 and 5.5 mg L^{-1} h^{-1}, respectively. When loading rate was increased to 10.2 mg L^{-1} h^{-1} (HRT = 9.6 h), removal percentage decreased to 77.6%, while biodegradation rate continued to increase to 7.9 mg L^{-1} h^{-1}. However, the rate of increase in biodegradation rate started to slow down to approximately 43.5% (i.e. the increasing trend of removal rate levelled off). Increasing the loading rate to 21.7 mg L^{-1} h^{-1} (HRT = 4.4 h) led to a maximum biodegradation rate of 11.5 mg L^{-1} h^{-1}, while the removal percentage decreased to 53.0%. This maximum biodegradation rate which was achieved at a residence time of 4.4 h was 3.3 times higher than the biodegradation rate of 3.5 mg L^{-1} h^{-1} obtained in a similar MFC with granular electrode operated under batch conditions. As loading rate was further increased to 33.9 mg L^{-1} h^{-1} (HRT = 3.0 h), the biodegradation rate decreased to 10.5 mg L^{-1} h^{-1}, while the removal percentage continued to decline at 31.0%. This finding indicates that the MFC was already passed its optimum performance in the biodegradation of phenol. Nonetheless, a higher loading rate of 44.4 mg L^{-1} h^{-1} (HRT = 2.2 h) was tested and results showed further deterioration in the removal percentage down to 25.1%. Given this deterioration at this stage the experiment was culminated.

For similar or comparable loading rates, the resulting removal percentages and phenol biodegradation rates obtained in MFC with granular electrodes were markedly higher than that in the MFC with rod electrodes. For instance, at loading rates of 1.4 and 2.1 mg L^{-1} h^{-1}, the MFC with rod electrodes achieved biodegradation rates of 0.64 and 0.83 mg L^{-1} h^{-1}, respectively, which were at least two times lower than those obtained with granular electrodes at the same loading rates. No comparison can be made at loading rates above 2.1 mg L^{-1} h^{-1} since this loading rate corresponded to the maximum value that the MFC with rod electrodes was able to operate. Moreover, the maximum biodegradation rate achieved in the granular system

was approximately 14 times faster than that in the system with rod electrodes and attained at a residence time that was 10 times shorter (4.4 vs 47.4 h).

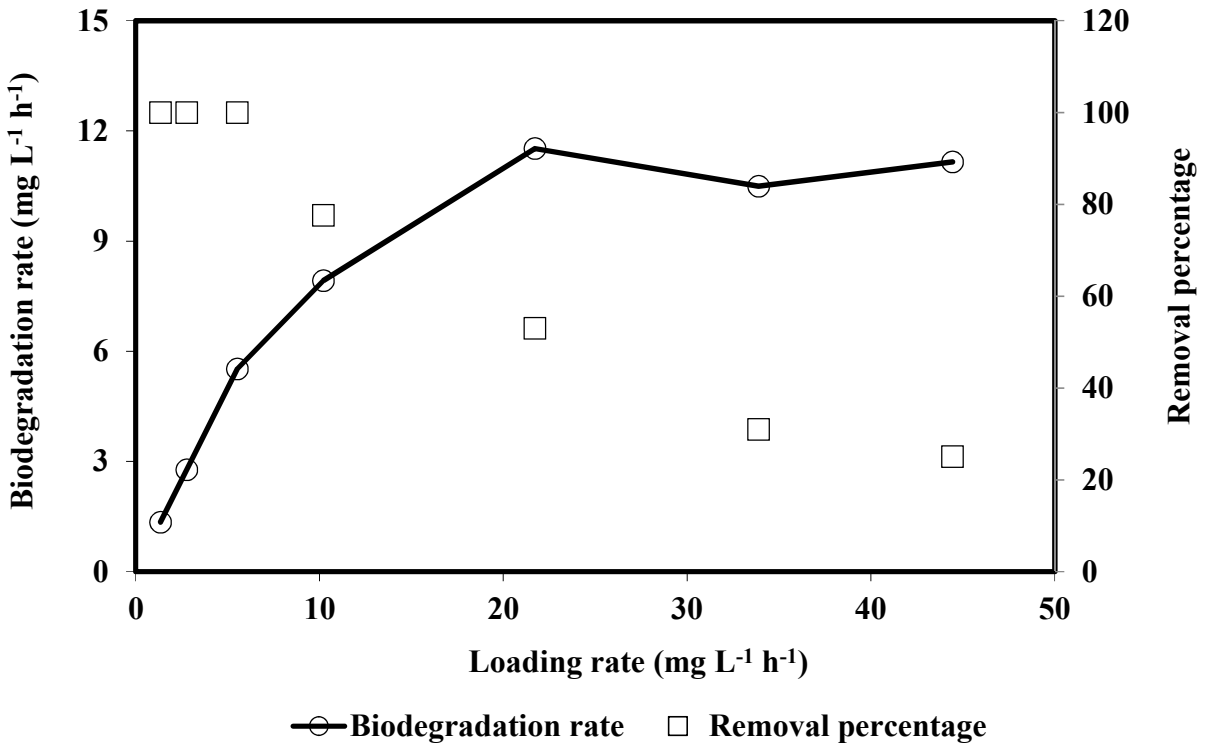

Figure 5.17 Biodegradation rate and removal percentage of phenol as a function of its loading rate in a continuously operated MFC with granular graphite electrode with immobilized *P. putida* fed with 100 mg L^{-1} phenol**.** This figure is derived in part from an article published in Environmental Technology Mar 2017 Taylor & Francis, available online: http://dx.doi.org/10.1080/09593330.2017.1296895.

As the experiment progressed, it was observed that biomass layer was slowly building up on the surface of the granules, especially in the region around the entry port of the recirculation loop (Figure 5.18). As observed with the lactate fed MFC with granular electrode, streaks of biomass were observed to follow the flow of liquid passing through the recirculation loop notably in the vicinity of the entry port. However, the amount of accumulated biomass in the system with phenol

was visibly lower than that in the system operated with lactate (Figure 4.10). One reason is that with the lactate as the substrate, the MFC was operated at a much wider and higher loading rates (i.e. longer period of operation) before deterioration in performance was observed (24.2-22238.8 mg L^{-1} h^{-1}).

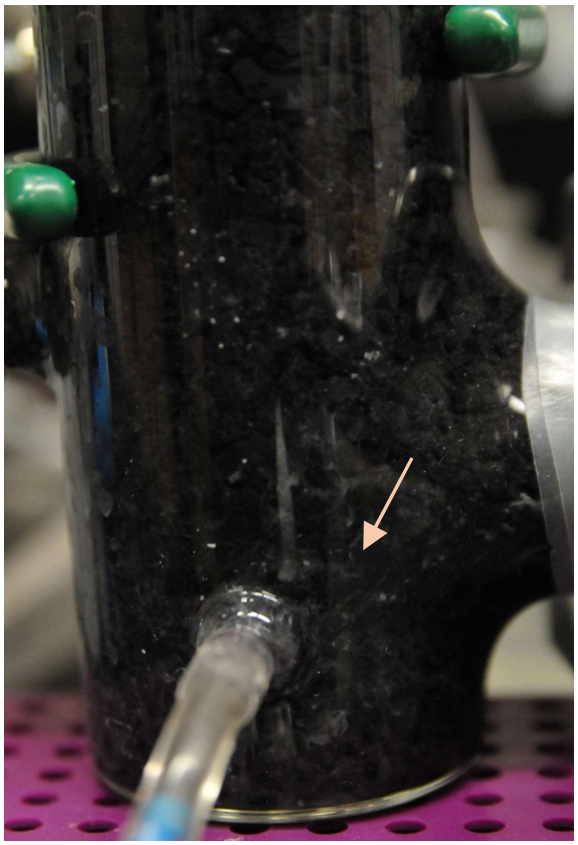

Figure 5.18 Biofilm formation on granular graphite electrode is prominently visible around the inlet of the recirculation loop of a MFC operated continuously with phenol as feed.

As with the batch experiments in MFC with granular electrodes, a low external resistance of 50 ohms was applied across the circuit and as a result the circuit potential was relatively low (<5 mV). To measure current and power produced from the MFC, we relied on development of polarization curves using linear sweep voltammetry (LSV). Polarization curves were developed during the operation of MFC at loading rates of 21.7 and 44.4 mg L^{-1} h^{-1} where the highest phenol

biodegradation rates were achieved. Figure 5.19 shows the polarization and power curves obtained for the MFC with granular electrodes fed continuously with 100 mg L^{-1} phenol. At the loading rate of 21.7 mg L^{-1} h^{-1}, the value of OCP was determined as 390 mV, while in the second test which was carried out at a higher loading rate of 44.4 mg L^{-1} h^{-1} an OCP of 244 mV was measured. From the power curves, the maximum power produced from the system operated at a loading rate of 21.7 mg L^{-1} h^{-1} was 0.07 mW measured at a current of 0.31 mA (Figure 5.19A). This translated to volumetric power and current densities of 777.8 mW m^{-3} and 3444.4 mA m^{-3}, respectively. As indicated earlier, this result was obtained at the loading rate where the maximum biodegradation rate of 11.5 mg L^{-1} h^{-1} was achieved. At the higher loading rate of 44.4 mg L^{-1} h^{-1}, the maximum power output and corresponding current were lower with 0.02 mW and 0.15 mA, respectively (Figure 5.19B). This was equivalent to power and current densities of 205.6 mW m^{-3} and 1611.1 mA m^{-3}, respectively. Corresponding CE confirmed this trend where CE value of 3.75% at the loading rate of 21.7 mg L^{-1} h^{-1} was higher than 1.87% attained at the higher loading rate.

Results from polarization curve measurements show that higher power output was produced when MFC was operating at its maximum performance with regard to phenol biodegradation. This finding, again, suggests that power output is correlated with biodegradation rate. As MFC performance declined, biodegradation rate decreased which resulted in a lower power output from the system. Similar with power output, a decline in OCP was also observed when the biodegradation rate decreased due to application of higher loading rate. When compared to power output from similar MFC with lactate, at the lowest feed flow rate of 2.2 mL h^{-1} (loading rate of 24.2 mg L^{-1} h^{-1}), the maximum power (0.08 mW) measured was still higher than what was produced from phenol. This finding shows that power output from an MFC operated with a

recalcitrant substrate, such as phenol, is lower compared to a substrate such as lactate which is amenable to biodegradation.

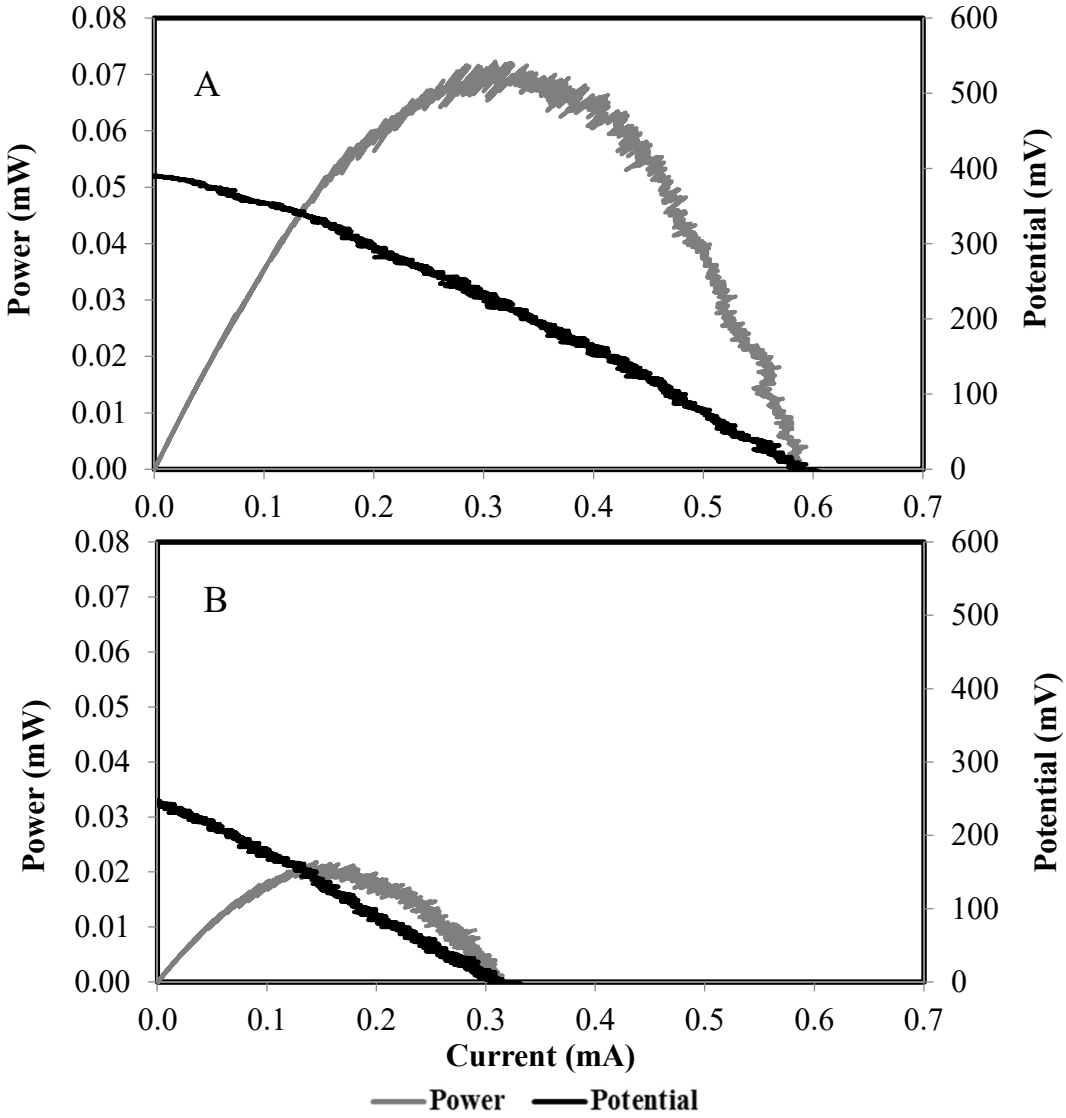

Figure 5.19 Polarization and power curves generated for a continuously operated MFC with granular graphite electrode and immobilized *P. putida* fed with phenol. Phenol loading rate (A): 21.7 mg L^{-1} h^{-1}, and (B): 44.4 mg L^{-1} h^{-1}.

Currently, no study has reported on the biodegradation of phenol using immobilized cells in a continuously operated MFC. Hence, comparison of MFC performance in this experiment are only

carried out with conventional reactors. A fermenter equipped with stainless steel baffle which allowed formation of *P. putida* biofilm achieved a high biodegradation rate of 720 mg L^{-1} h^{-1} at residence time of 0.7 h when continuously fed with 2500-3000 mg L^{-1} phenol (Molin and Nilsson, 1985). Mordocco et al. (1999) immobilized *P. putida* into 2 mm diameter alginate beads and packed them in a bubble column bioreactor operated under aerobic conditions without an acclimation period. With a feed containing 100 mg L^{-1} phenol a high biodegradation rate of 58.5 mg L^{-1} h^{-1} achieved at a residence time of 1.7 h. The continuous system used by Gonzalez et al (2001) attained a biodegradation rate of 166.7 mg L^{-1} h^{-1} at HRT of 4.8 h using a feed containing 1000 mg L^{-1} phenol. Without an acclimation period, the continuous system utilized by Pazarlioglu and Telefoncu (2005) was able to achieve a much higher biodegradation rate of approximately 725 mg L^{-1} h^{-1} at a loading rate of 800 mg L^{-1} h^{-1} with feed concentrations of up to 820 mg L^{-1} phenol. The above-mentioned systems evidently achieved much higher biodegradation rates than the current MFC system which are expected in systems operated under aerobic conditions. Moreover, similar to our findings with the MFC, these systems show that biodegradation rates in immobilized cell systems are considerably higher than those achieved with suspended cell bioreactors (Molin and Nilsson,1985; Mordocco et al.,1999; Gonzalez et al., 2001; Lee et al., 2009). Additionally, it has been reported that continuous cultures with biofilms could tolerate higher phenol concentrations than non-biofilm systems (Molin and Nilsson, 1985).

5.3.3 Biodegradation of phenol in MFC with neutral red

Batch mode of operation: After the completion of experiments focusing on continuous biodegradation of phenol in the MFC with granular electrode, the same system was used to evaluate biodegradation of phenol in the presence of a mediator, specifically neutral red. Similar

to previous experiments operated batch-wise, the experiment was started with the biodegradation of 100 mg L^{-1} phenol. The profiles of phenol concentration during this experiment is shown in Figure 5.20. As seen in this figure, complete degradation of phenol was achieved within 38 h. Complete removal of phenol could have occurred faster, however, since this fast degradation was not expected only two samples were taken within this period. To determine whether phenol concentration dropped to zero at an earlier time, another 100 mg L^{-1} phenol was added to the anodic chamber and more frequent sampling conducted. This frequent sampling revealed that complete degradation of phenol indeed just needed 18 h.

Sequential addition of phenol at higher concentrations was also conducted. Phenol at concentration of approximately 250 mg L^{-1} was completely removed within 25.9 ± 6.9 h, while at the higher concentrations of 500 and 1000 mg L^{-1}, complete removal of phenol was achieved within 38.0 ± 8.1 h and 54.4 ± 7.4 h, respectively. In similar experiments in MFC without neutral red, complete removal of phenol at 250, 500 and 1000 mg L^{-1} were achieved within 69.0, 123.4 and 221.0 h, respectively. These results indicate that phenol degradation in a MFC, especially at the higher concentrations (250-1000 mg L^{-1}) was faster when neutral red was present.

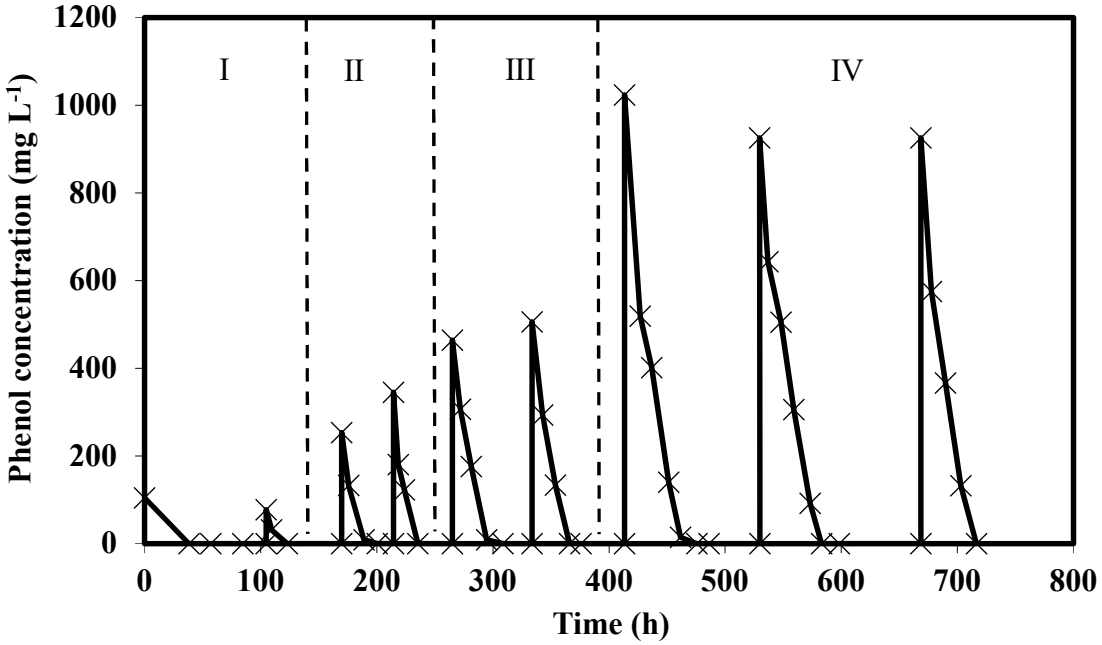

Figure 5.20 Sequential biodegradation of phenol in MFC with granular electrodes, immobilized *P. putida* cells and neutral red as mediator. Panel I: 100 mg L^{-1} phenol, Panel II: 250 mg L^{-1} phenol, Panel III: 500 mg L^{-1} and Panel IV: 1000 mg L^{-1}. This figure is derived in part from an article published in Environmental Technology Mar 2017 Taylor & Francis, available online: http://dx.doi.org/10.1080/09593330.2017.1296895.

The biodegradation rate of phenol at different initial concentrations in MFC with granular electrode and neutral red was calculated and shown in Figure 5.21. At the lowest initial concentration of 100 mg L^{-1} phenol, an average biodegradation rate of 3.3 ± 0.8 mg L^{-1} h^{-1} was achieved. At higher initial concentrations of 250, 500 and 1000 mg L^{-1} phenol, much faster biodegradation rates of 11.4 ± 4.8, 13.0 ± 3.3 and 17.1 ± 1.4 mg L^{-1} h^{-1}, were attained, respectively. This pattern is similar to that from the identical MFC without neutral red where biodegradation rates increased as initial concentration of phenol was increased, except at 1000 mg L^{-1} where possible inhibition effect was noted. This trend is also consistent with previous results in the batch biodegradation of lactate in an MFC with single rod electrodes where biodegradation rates was higher with increasing initial concentration of substrate.

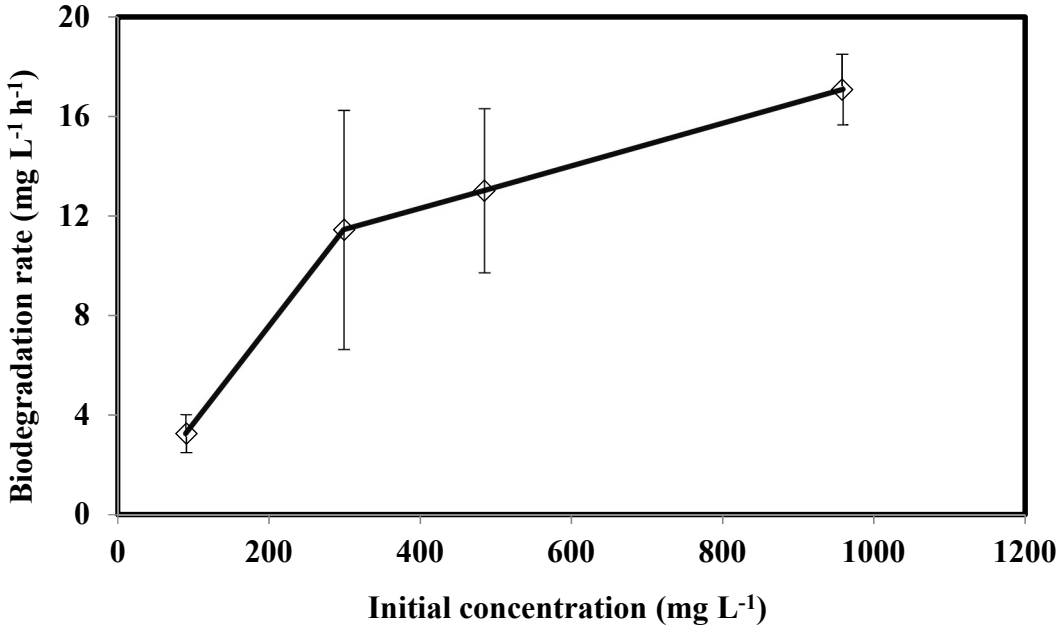

Figure 5.21 Biodegradation rates of phenol at different initial concentrations in an MFC with granular graphite electrodes, immobilized *P. putida* with neutral red as mediator.

A comparison of biodegradation rates of phenol achieved in a granular electrode MFC with and without neutral red as well as in the previous system with rod electrodes without neutral red is made in Figure 5.22. It can be observed that biodegradation rates in MFC with neutral red were generally higher compared to those from MFCs without neutral red. To be specific in MFCs with granular electrodes, biodegradation rates in the presence of neutral red were approximately 3-4 times higher than those in the system without neutral red except at the lowest initial concentration of 100 mg L^{-1} where biodegradation rate was slightly lower. In MFCs with suspended cells and single rod electrodes, biodegradation rates were 4-7 times lower than those from the granular electrode MFC without neutral red and remarkably slower at approximately 7-21 times lower than those from the MFC with neutral red.

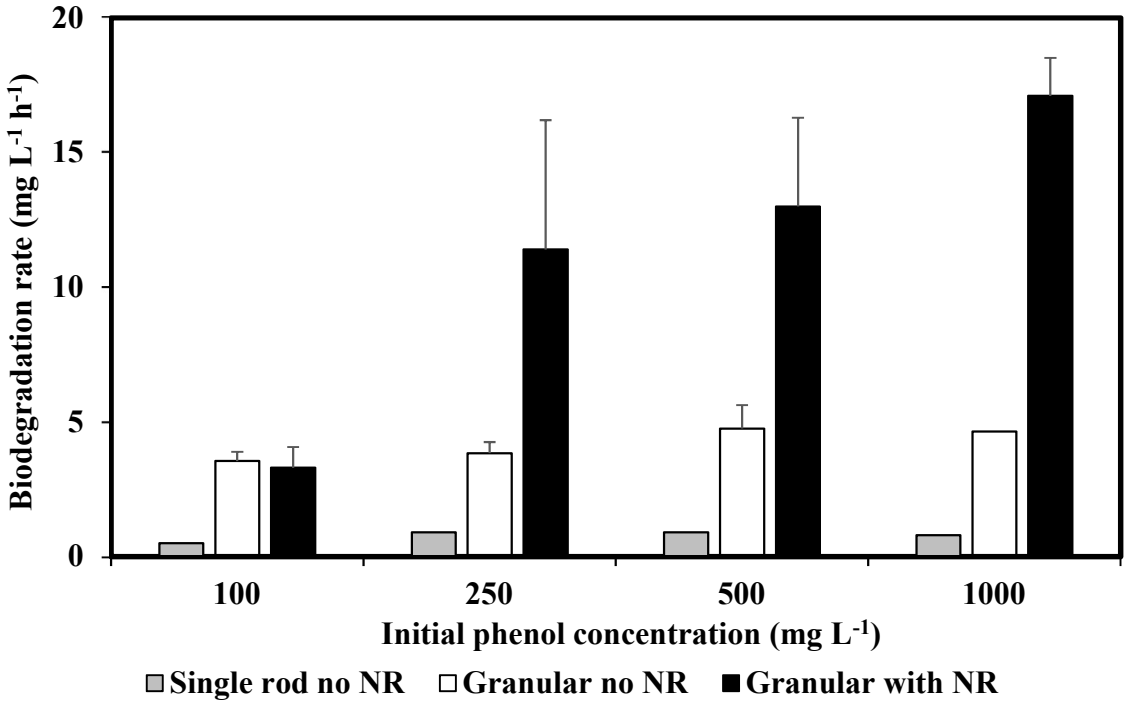

Figure 5.22 Biodegradation rates of phenol at different initial concentrations in MFCs with single rod, and granular graphite electrodes with and without neutral red**.** This figure is derived in part from an article published in Environmental Technology Mar 2017 Taylor & Francis, available online: http://dx.doi.org/10.1080/09593330.2017.1296895.

A trend was also observed where biodegradation rates from the MFC with neutral red increased as initial concentration of phenol was increased. This pattern was not consistent with that in MFCs without neutral red for both granular and single rod electrodes where biodegradation rates appeared to deteriorate as initial concentration was increased to 1000 mg L^{-1}. This finding resembles substrate inhibition effect typically observed with phenol especially at high concentrations. The results obtained from experiments with MFCs operated under batch conditions suggest that the addition of neutral red enhanced biodegradation of phenol and contributed to alleviating the inhibition effects of phenol especially at high concentrations.

As indicated earlier, in the MFC with granular electrodes, the application of a 50 ohm resistor across the circuit resulted in very low potential readings. With the maximum circuit potential of 4.06 mV, the calculated power and current densities from the system were 4.7 mW m^{-3} and 1160.0 mA m^{-3}, respectively, which were considerably comparable to the output from similar MFC without neutral red. For a more appropriate measurement of current and power output, an LSV was carried out during the operation of MFC with 1000 mg L^{-1} phenol. The resulting polarization and power curves are shown in Figure 5.23. From the polarization curve, it can be observed that the OCP was approximately 302 mV, while the power curve shows the MFC produced a maximum power of approximately 0.03 mW at a current of 0.16 mA. In terms of power and current density, the equivalent output per anodic volume was calculated to be around 428.6 mW m^{-3} and 2285.7 mA m^{-3}, respectively. The calculated CE of 0.70% was substantially lower than in the similar MFC without neutral (4.63%) which could potentially explain the comparable power and current output between the two systems despite the superior biodegradation rates in the MFC with neutral red.

Continuous mode of operation: After batch experiments with neutral red was completed in granular electrode MFC, the system was switched to continuous operation and fed with modified McKinney's medium containing 100 mg L^{-1} phenol and 28.9 mg L^{-1} neutral red. Feed was introduced into the anodic chamber at a relatively low flowrate of 1.9 mL h^{-1} (equivalent dilution rate: 0.03 h^{-1}). Residual concentration of phenol was regularly monitored and after the system reached steady state conditions, the flowrate was increased incrementally. Flowrate was continually increased up to 20.1 mL h^{-1}, after which the system performance displayed deterioration.

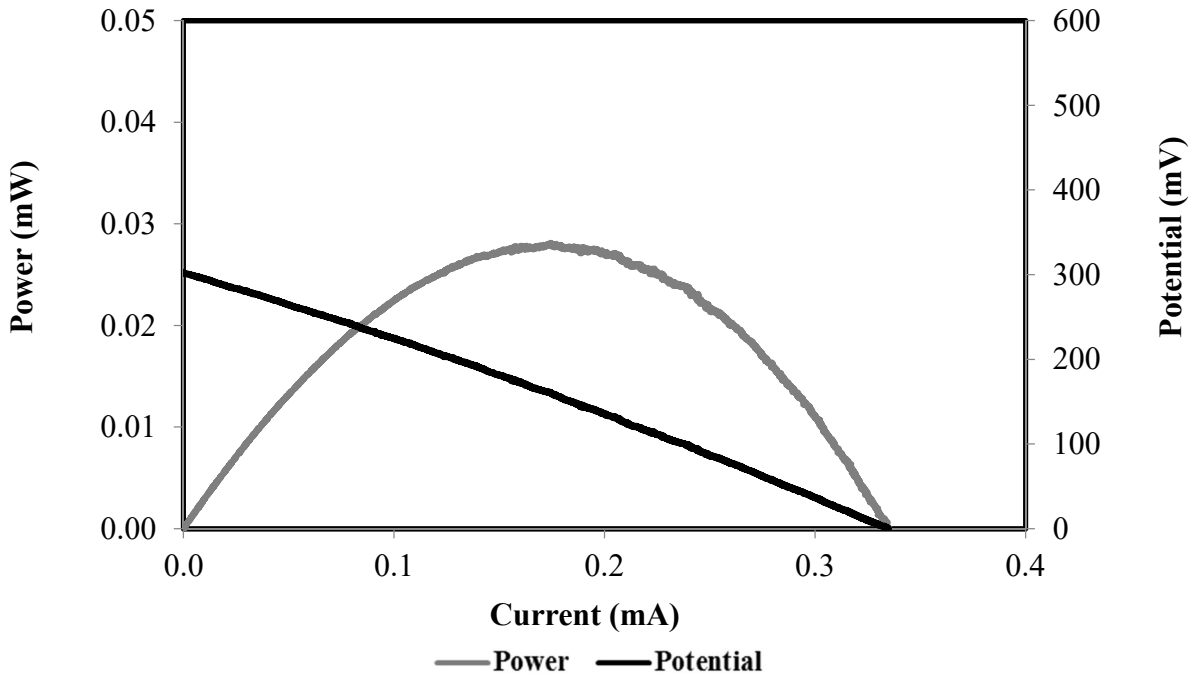

Figure 5.23 Polarization and power curves developed during biodegradation of 1000 mg L^{-1} phenol in an MFC with granular graphite electrodes, immobilized *P. putida*, and neutral red operated batch-wise.

Figure 5.24 shows the steady state profile of phenol concentration as a function of dilution rate. Again, due to added turbidity by granule particles and the fact that biofilm was the dominant state of microbial cells, no profile for biomass concentration is presented. At the low range of dilution rates (0.03-0.07 h^{-1}) complete biodegradation of phenol was achieved. Increasing the dilution rate to 0.17 h^{-1} resulted to an abrupt increase in the residual phenol concentration from 0 to 26.0 ± 5.6 mg L^{-1}. Further increase of dilution rate to 0.29 h^{-1} led to a residual phenol concentration of 75.7 ± 8.2 mg L^{-1}, a similar trend that observed in the MFC with granular electrode in the absence of neutral red. It can be recalled that in the former system, as dilution rate was increased to a similar level (0.34 h^{-1}), deterioration in biodegradation rate started to occur.

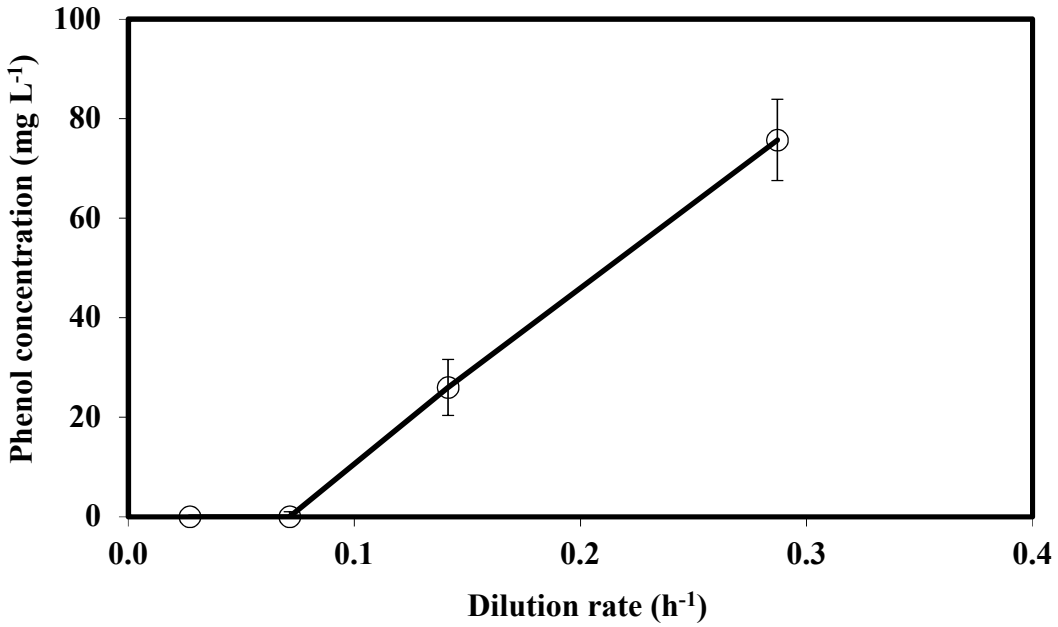

Figure 5.24 Steady state concentration profile of phenol as a function of dilution rate in a continuously operated MFC with granular electrode, immobilized *P. putida* cells, and neutral red as mediator.

The biodegradation rate of phenol and the corresponding removal percentage as a function of loading rate in this system is shown in Figure 5.25. At the lowest loading rate of 2.6 mg L^{-1} h^{-1} (HRT=36.8 h^{-1}), the removal percentage was 100%. Complete phenol removal was maintained up to a loading rate of 6.5 mg L^{-1} h^{-1} (HRT=14.0 h^{-1}), with corresponding biodegradation rate being 6.5 mg L^{-1} h^{-1}. When loading rate was increased to 14.5 mg L^{-1} h^{-1} (HRT=7.1 h^{-1}), removal percentage decreased to 74.6%, while biodegradation rate reached its maximum value of 10.6 mg L^{-1} h^{-1}. Further increase in the loading rate to 29.4 mg L^{-1} h^{-1} (HRT=3.5 h^{-1}), resulted in significant decrease in the removal percentage to 25.9% and consequently a lower biodegradation rate of 7.6 mg L^{-1} h^{-1}. At this point, the system has encountered deterioration in performance, hence the experiment was terminated. The maximum biodegradation rate achieved in this system was markedly higher than that in a similar system operated batchwise (3.3 mg L^{-1} h^{-1}) which again

supports the trend wherein biodegradation rates in the MFCs operated continuously were higher than those achieved in similar system operated batchwise.

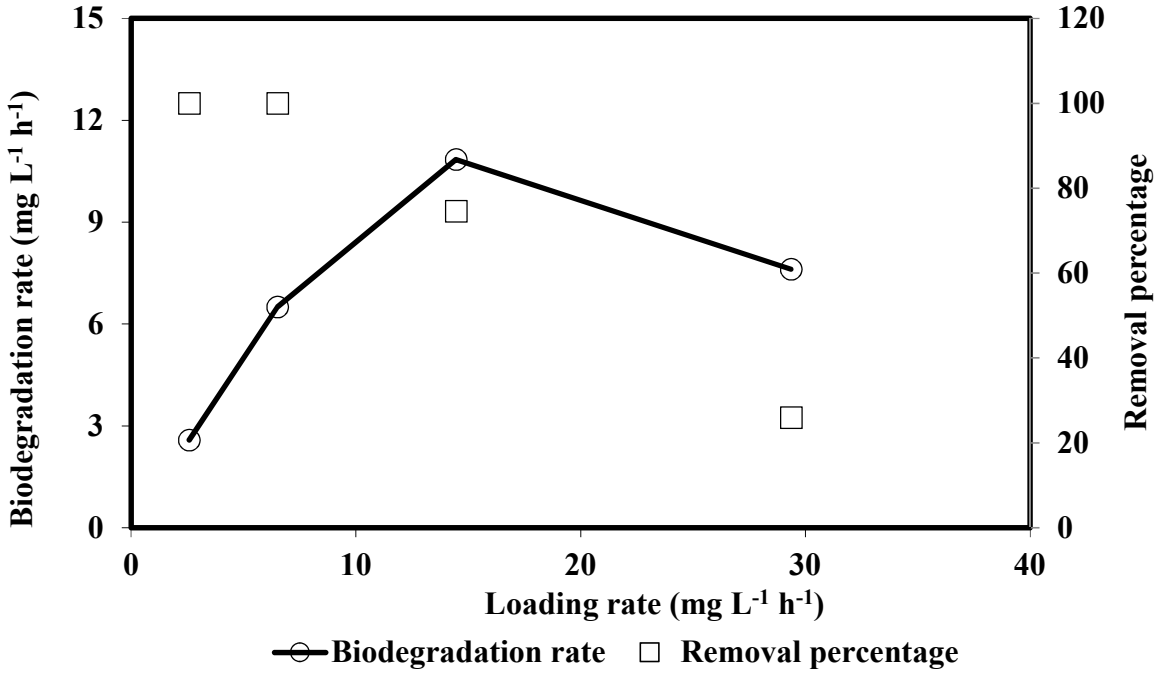

Figure 5.25 Biodegradation rate and removal percentage of phenol as a function of its loading rate in a continuously operated MFC with granular graphite electrodes, immobilized *P. putida,* and fed with 100 mg L^{-1} phenol and neutral red**.**

Figure 5.26 compares the results obtained in granular electrode MFCs operated continuously with and without neutral red, as well those in a similar MFC with single rod electrodes. Among the three evaluated systems, the performance of MFC with single rod electrode was inferior whereby its maximum biodegradation rate were at least 10 times slower than that in MFCs with granular electrodes. Granular MFC systems, in the presence or absence of neutral red, achieved almost similar biodegradation rates when phenol loading rates was below 10 mg L^{-1} h^{-1}. The maximum biodegradation rate in the system with neutral red was 10.8 mg L^{-1} h^{-1} which was slightly lower than 11.5 mg L^{-1} h^{-1} obtained in a similar system without neutral red. Moreover, a much longer residence time of 7.1 h was needed for the system with neutral red to attain its peak biodegradation

rate than in a similar system without neutral red which only required 4.4 h. These results indicate that, unlike in batch operated MFCs, the addition of neutral red did not enhance the biodegradation rate of phenol in the continuously operated MFC. This finding is consistent with that observed in the batch systems fed with the same phenol concentration of 100 mg L^{-1} where biodegradation rates in MFCs with granular electrode with or without neutral red were similar. Additionally, these biodegradation rates were markedly higher than that achieved in a similar MFC with rod electrodes.

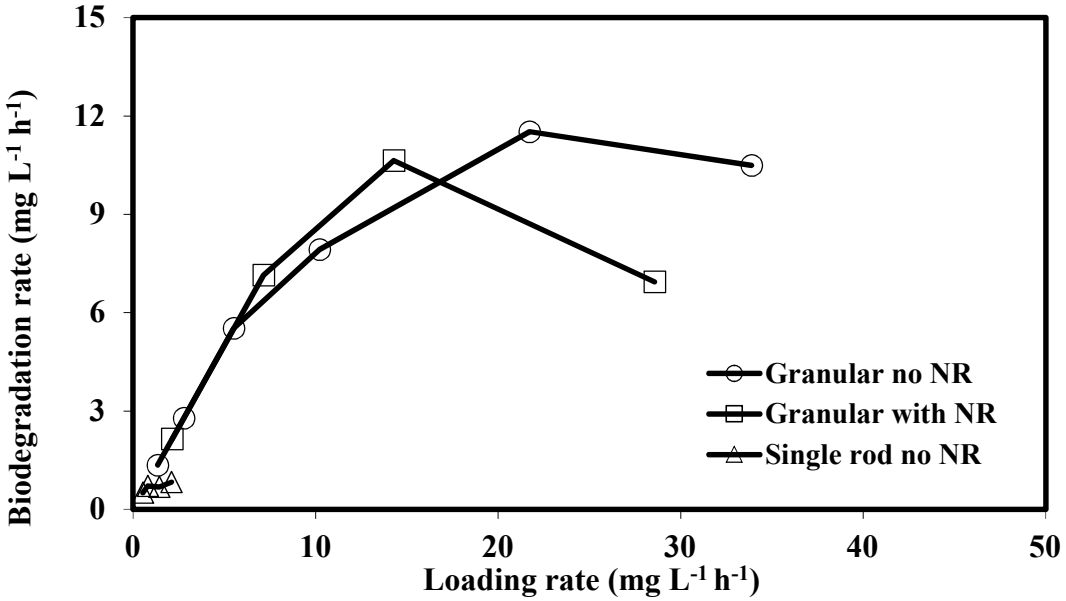

Figure 5.26 Biodegradation rate of phenol as a function of its loading rate in continuously operated MFCs with single rod or granular graphite electrodes fed with 100 mg L^{-1} phenol with or without neutral red**.** This figure is derived in part from an article published in Environmental Technology Mar 2017 Taylor & Francis, available online: http://dx.doi.org/10.1080/09593330.2017.1296895.

BET analysis was conducted to gain an insight on the surface area and porosity of graphite granules at the end of experiments. Results of these examinations suggested successful immobilization of microbial cell on the surface of graphite granules. This was evident through comparison of pore

volumes and surface areas of fresh (unused) granules with those of the exposed (used) granules. The pore volume for the fresh granules was 0.0032 $cm^3 g^{-1}$, while with the used granules a much lower pore volume of 0.0007 $cm^3 g^{-1}$ was measured. Moreover, BET surface area of the same used granules was substantially lower at 0.05 $m^2 g^{-1}$ as compared to that value for fresh granules that was 10 $m^2 g^{-1}$. These findings could be interpreted as population of granule voidages by biomass and secreted extracellular polymeric substances (EPS) and an evidence of cell immobilization and formation of biofilm.

As indicated earlier fresh and exposed granules were also examined by scanning electron microscopy. Figure 5.27 shows the surfaces of a fresh and unused graphite granule as well as that for an exposed granule taken from the MFC at the end of experiments with neutral red. Comparison of photos of fresh and exposed granules at low magnification (A and C) clearly shows formation of biomass layer or the EPS associated with biofilm on the surface of exposed granule which is absent on the surface of unused granule. Looking more closely into these surfaces as depicted in SEM photos of higher magnification (B and D), one can clearly see numerous rod shape cells on the surface of the used granule which are not present on the surface of the unused granule. The shape characteristics of these cells resemble to those of *Pseudomonas putida* (Flemming, 2009).

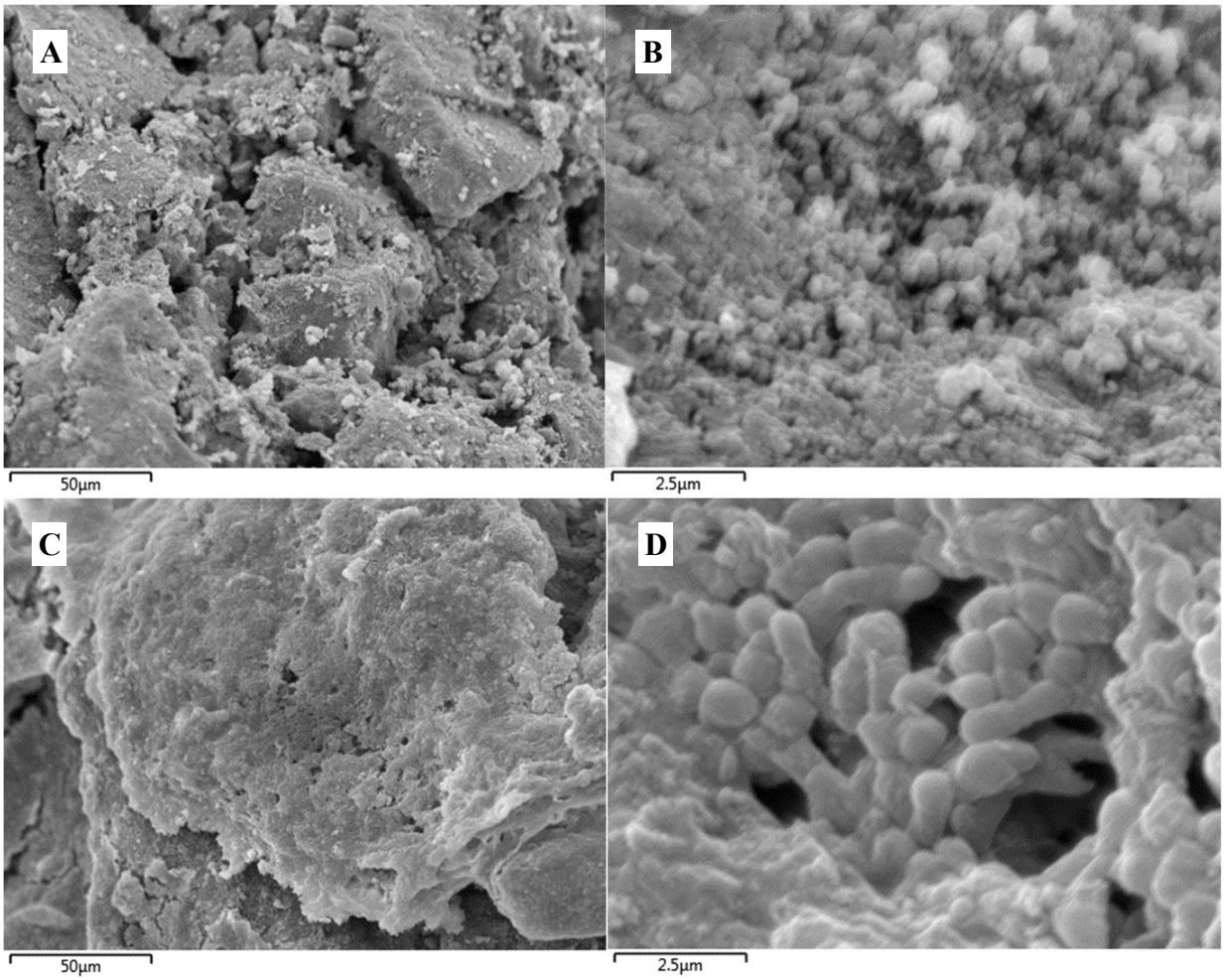

Figure 5.27 SEM photos of the surface of a fresh and unused graphite granule (A and B) and an exposed graphite granule (C and D) from an MFC operated with neutral red. In each case two different magnifications are provided. This figure is derived in part from an article published in Environmental Technology Mar 2017 Taylor & Francis, available online: http://dx.doi.org/10.1080/09593330.2017.1296895.

Figure 5.28 shows the polarization and power curves generated at various phenol loading rates in the continuously operated granular electrode MFC with neutral red. The maximum power and OCP determined from these curves are summarized and compared in Figure 5.29. The corresponding biodegradation rates achieved at the different loading rates are presented in the figure as well. The maximum power produced at phenol loading rates of 2.6, 6.5, 14.5 and 29.4 mg L^{-1} h^{-1} were 0.01, 0.07, 0.10 and 0.02 mW, respectively. The corresponding currents were 0.11, 0.27, 0.40 and 0.24

mA, respectively. These measurements translated to power densities of 142.9, 971.4, 1428.6 and 242.8 mW m^{-3}, and current densities of 1571.4, 3857.1, 5714.3 and 3428.6 mA m^{-3}, respectively.

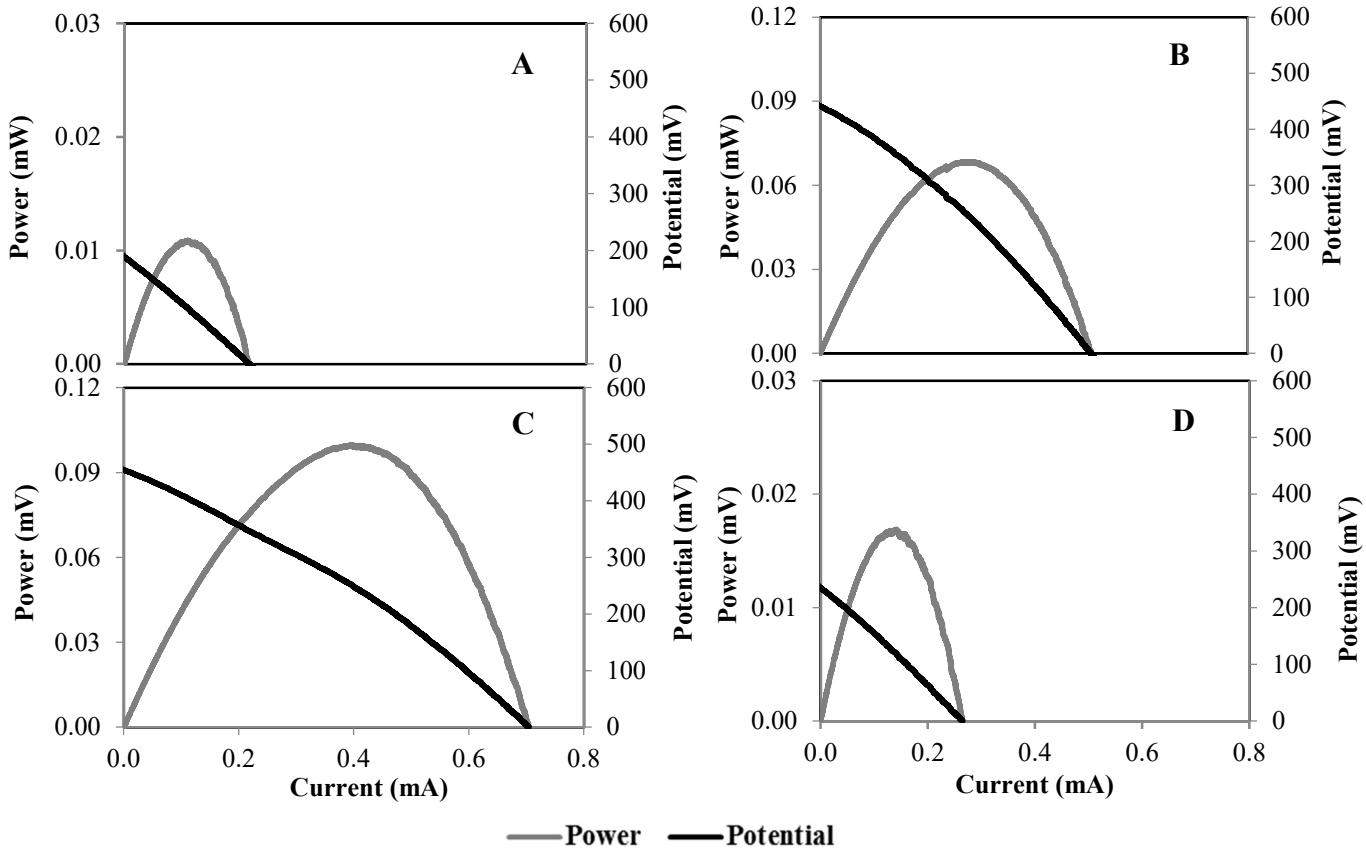

Figure 5.28 Polarization and power curves generated for a continuously operated MFC with granular graphite electrodes fed with phenol and neutral red at various phenol loading rates; A) 2.6 B) 6.5 C) 14.5 and D) 29.4 mg L^{-1} h^{-1}.

For loading rates up to 14.5 mg L^{-1} h^{-1}, power and OCP along with biodegradation rate increased as loading rate was increased (i.e. dependency of power and OCP on biodegradation rate). Further increase in loading rate led to decrease in all three parameters. This finding suggests that the extent of power produced in a granular electrode MFC is influenced by the biodegradation rate. In other words, a higher biodegradation rate would result in higher power and the decline in the rate would lead to a decrease in power. A similar trend was also observed in the MFC with granular electrodes

operated without neutral red where the maximum power density of 777.8 mW m^{-3} was achieved at a loading rate (21.7 mg L^{-1} h^{-1}) at which the maximum biodegradation rate of 11.5 mg L^{-1} h^{-1} was achieved.

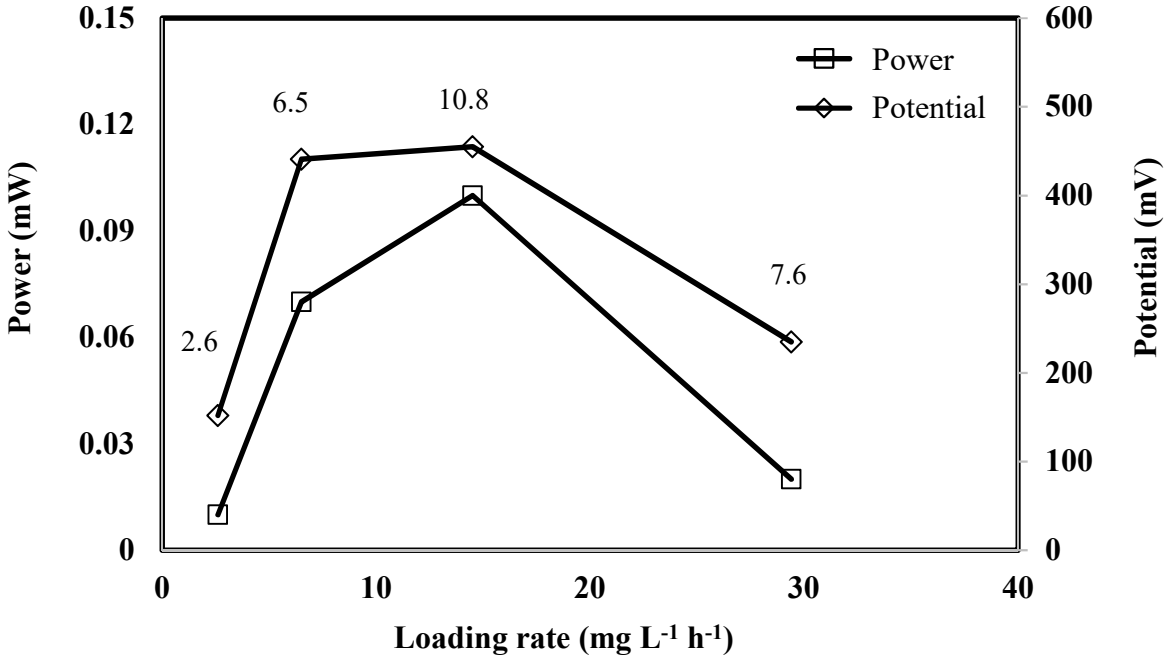

Figure 5.29 Maximum Power and OCP obtained from polarization curves at various phenol loading rates in an MFC with granular graphite electrodes fed with phenol and neutral red. Numbers on each point represent biodegradation rate (mg L^{-1} h^{-1}) achieved at the corresponding loading rate.

When comparing the two similar MFCs with granular electrodes, the maximum power output generated in the system with neutral red was substantially higher even when its corresponding biodegradation rate (10.8 mg L^{-1} h^{-1}) was lower than in the system without neutral red. This result suggests than the presence of neutral red enhances the power output of the MFC even without a significant improvement in the biodegradation rate. This observation was further attested by corresponding CE which were at least 2 times higher when neutral red was present (5.65-7.62% vs 1.87-3.75%). Comparing the mode of operations for the MFCs with granular electrode and

neutral red, the system operated batchwise generated much lower power and current outputs than that from a similar system operated continuously. This was consistent with the finding in the MFCs with rod electrodes when their performances in the batch and continuous modes of operation were compared.

5.4. Conclusions

Results of this study have shown that biodegradation of phenol with concomitant generation of energy can be achieved successfully in microbial fuel cell type bioreactors. Being an aromatic compound, phenol is more difficult to degrade than simple-structured compounds such as fatty acids, hence lower concentrations of phenol (100-1000 mg L^{-1}) were tested in these experiments. During the batch experiments in MFCs with single rods and suspended cells the biomass concentration increased as biodegradation of phenol proceeded. Biodegradation of phenol experienced a lag phase which was found to be dependent on the phenol initial concentration (i.e. higher phenol concentrations resulted in longer lag phases). Contrary to what observed with lactate no improvement in the biodegradation rate was observed when phenol concentration was increased above 250 mg L^{-1}. These findings show the inhibition effect of phenol at high concentrations on microbial growth.

In terms of energy output, faster biodegradation rates led to higher power and current. Biodegradation of phenol in a continuous flow MFC appeared challenging and operation of MFC was only possible at low phenol loading rates (< 2.1 mg L^{-1} h^{-1}). Even with these low loading rates residual phenol concentration in the system was relatively high and corresponding biodegradation

rates were considerably low (<0.9 mg L^{-1} h^{-1}). Power output produced from this system was significantly higher than that in the batch system fed with the same phenol concentration.

The use of MFC with granular electrode significantly improved the biodegradation of phenol in both batch and continuous systems. Biodegradation rates were 4-6 times higher in MFCs operated batchwise and 14 times faster in systems operated continuously which were achieved at HRTs of at least 10 times shorter than in similar MFCs with single rod electrodes. Furthermore, no lag phase was observed in the biodegradation of phenol in any of concentrations evaluated in the batch systems which was confirmed also as part of sequential batch experiments. Slight increases in the biodegradation rate was observed as initial concentration of phenol was increased up to 500 mg L^{-1}, after which no improvement was found when initial concentration was further increased to 1000 mg L^{-1} that again can be attributed to the inhibition effects of phenol at these levels. Moreover, granular electrodes promoted and maintained a high level of biomass in the anodic chamber. Immobilization of cells on and in the granules was confirmed through reduction of pore space and surface area of granules as determined through BET analysis, as well as from SEM images showing bacterial cells and the EPS layers covering the surface of the granule. As expected, power and current output from MFCs with granular electrode were higher than that in similar systems with rod electrodes.

The addition of neutral red as electron mediator in MFCs operated batchwise significantly improved the overall biodegradation of phenol. There was an increase in biodegradation rate as initial phenol concentration was increased and no indication of phenol inhibition even at a high concentration of 1000 mg L^{-1} was observed. However, unlike in batch systems, similar MFC with

added neutral red operated continuously did not show improved phenol biodegradation and resulting biodegradation rates that were comparable to those in a system without the mediator. This was a similar finding observed in the batch system at an identical concentration of 100 mg L^{-1} phenol where no significant difference in the biodegradation rates was found in both systems with or without neutral red. In terms of energy output, the addition of neutral red enhanced the power output of the MFC in both batch and continuous systems. As with previous systems, energy output in the continuous system was substantially higher than in the batch system. In fact, the highest power and current output in the biodegradation of phenol was achieved in the MFC with neutral red operated continuously.

In all evaluated conditions (suspended vs immobilized cells, batch vs continuous systems, with or without mediator), a correlation between biodegradation rate and levels of OCP and energy output generated from the MFC was evident. To be specific, higher biodegradation rates resulted in higher OCP, power and current which were further corroborated with higher CE. A better performing MFC would be able to degrade phenol faster and at the same time generate higher energy output. When compared to fatty acids, such as lactate, the biodegradation of phenol in MFCs was shown to be slower and hence corresponding biodegradation rates and power output were lower as well.

In MFCs with suspended cells, results of biokinetic evaluation of microbial growth and phenol degradation using a simple first-order kinetics in the batch systems and Monod kinetics in continuous systems were able to describe the experimental results with reasonable accuracy. Relevant biokinetic parameters were determined, specifically biodegradation rate constants in the batch systems and coefficients of specific growth rate, biomass yield, saturation constant and

endogenous rate constant for the continuous flow MFC. Currently, there is very limited information, if any, on the biokinetics of microbial growth and biodegradation of phenol, and other various types of substrates in general, based on the data generated in an MFC. Hence, no relevant comparison of biokinetic constants generated from the growth kinetic models and overall performance of phenol biodegradation in MFCs can be conducted. Understanding the biokinetics is a vital aspect of the technology since performance of an MFC is influenced not only by electrochemical processes but also diverse biological processes that occur in such systems.

CHAPTER 6

Co-biodegradation of Lactate and Phenol in MFCs with Rod and Granular Graphite Electrodes

6.1. Introduction

Phenol, as an aromatic compound, has been previously shown to be more difficult to degrade than simple structured compounds such as fatty acids in MFCs. Biodegradation of phenol was successfully conducted in batch and continuously operated MFCs using either freely suspended or immobilized cells. Similarly, the same MFC system has also been shown previously to effectively treat simple structured organic compounds specifically fatty acids such as lactate and acetate. It was then logical to evaluate the co-biodegradation of the two types of organic compounds together as co-substrates in an MFC to create a scenario which is closer to practical cases.

Evaluation of the co-biodegradation of phenol and lactate in MFCs specifically aimed to elucidate on two fundamental questions or possibilities. First, to determine whether the presence of lactate would facilitate and promote biodegradation of phenol (i.e. faster biodegradation of phenol in the presence of lactate). It is believed that presence of a compound which is more amenable to biodegradation (i.e., lactate) could potentially promote an environment conducive for improved biomass growth and release of enzymes that are required for biodegradation which could indirectly contribute to faster degradation of recalcitrant compounds such as phenol. Second, to determine if

phenol would impose inhibition effects on biodegradation of lactate. Additionally and as indicated earlier, the use of a mixture of organic compounds of different structures is a step closer to mimicking the treatment of actual wastewaters which contain different types of organics.

Utilization of an electron mediator (neutral red) in the biodegradation environment as a means of improving the biodegradation rate and electrochemical output was also investigated and performances of MFC with granular electrodes in the absence and presence of the mediator were compared. As with previous cases, these experiments were conducted in both batch and continuous modes of operation.

6.2. Materials and methods

6.2.1. Experimental set-ups

The co-biodegradation of phenol and lactate in MFC systems were conducted using experimental set-up and procedures that are essentially similar to previous experiments with phenol as sole substrate as presented in Section 5.2. In all experiments, *P. putida* was utilized as the biocatalyst. The procedures for maintenance of culture and preparation of cell suspension for inoculation has been described in detail in Section 3.2.1, while assembly and preparation of H-type MFCs equipped with rod or granular electrodes has been presented in Section 3.2.2 and Section 4.2.1.

Establishment of essential conditions immediately prior to inoculation of MFCs with *P. putida*, specifically anoxic conditions in the anodic chamber and stabilization of open circuit potential (OCP), were similar to previous cases as described in detail in Section 3.2.1. Moreover, the use of potassium ferricyanide as electron acceptor at the same concentration and regime of replenishment

as with previous experiments along with the equipment and procedures for monitoring of circuit potential were similar to previous cases and are not repeated here. All experiments were conducted at room temperature (24 ± 2 °C).

6.2.2. Co-biodegradation of Phenol and Lactate in MFCs with single rod electrodes (freely suspended cells)

Batch mode of operation: To assess whether the presence of lactate would promote faster biodegradation of phenol and to evaluate the potential inhibitory effect of phenol on the biodegradation of lactate, different combinations of phenol and lactate concentrations were evaluated in MFCs with rod electrodes operated with freely suspended cells. Phenol at concentration of 100 mg L^{-1} was combined with lactate at concentration of either 1000, 2500 or 5000 mg L^{-1}. Another set of experiments was also conducted where 500 mgL^{-1} lactate in combination with 100, 250 or 500 mg L^{-1} phenol underwent biodegradation. To be more specific a total of six phenol and lactate combinations were tested in MFCs with single rod electrodes and freely suspended cells.

After establishment of anoxic conditions in the anodic chamber containing modified McKinney's medium, addition of specified amounts of phenol and lactate as well as inoculation with *P. putida* cell suspension were carried using sterile syringes. After the experiment was initiated, regular sampling of the anodic chamber was carried out to determine phenol, lactate and biomass concentrations over time. Sample collection was done at least once a day. Moreover, circuit potential was monitored constantly, while current and power were measured periodically, as described in Section 6.2.5.

Continuous mode of operation: Results from batch experiments showed significant deterioration in phenol biodegradation when combined with lactate. Considering this and the fact that continuous biodegradation of phenol as sole substrate in MFCs with rod electrodes (Section 5.3.1) was not as effective as expected with the maximum possible loading rate being only 2.1 mg L^{-1} h^{-1}, experiment aiming at continuous co-biodegradation of phenol and lactate was not pursued in MFC with single rod electrode and freely suspended cells.

6.2.3. Co-biodegradation of Phenol and Lactate in MFCs with granular electrodes

The use of granular electrode in MFCs was shown in previous experiments to enhance phenol biodegradation rates and led to higher power outputs when compared with MFCs with rod electrodes. The graphite granules were employed with the aim of increasing the surface area available for better electron transfer and providing a matrix for cell immobilization and formation of biofilm. Preparation and specifications of granules have been described previously in Section 4.2.1. In summary prior to setting up of MFC, graphite granules were disinfected with bleach and thoroughly rinsed with reverse osmosis (RO) water. Graphite granules were then placed in the anodic and cathodic chambers occupying around 220 mL of each chamber volume. Approximately 85 mL of modified McKinney's medium was needed to sufficiently submerge all granules in the anodic chamber (i.e. anodic chamber working volume was 85 mL). As with previous experiments in MFCs with granular electrodes, a recirculation loop was devised to mix the liquid content in the anodic chamber using a peristaltic pump that provided a recirculation flow rate of approximately 3000 mL h^{-1}. The cathodic chamber was also charged with graphite granules and approximately 85 mL of potassium ferricyanide solution was added.

Batch mode of operation: The co-biodegradation of phenol and lactate in batch MFCs was investigated at concentrations of 100, 250 or 500 mg L^{-1} phenol in combination with 1000 mg L^{-1} lactate. After establishing anoxic conditions in the anodic chamber, small amount of concentrated solutions of phenol and lactate were added to the anodic chamber to provide the intended concentrations. This was followed immediately by the inoculation with microbial culture by injecting approximately 1 mL of a concentrated suspension of *P. putida* cells. Sequential addition of the mixture (repeated batches) was conducted with each designated combination. Co-biodegradation experiments started with the lowest concentration of phenol. Regular sampling of the anodic chamber was conducted, at least once daily, to monitor phenol and lactate concentrations as well as accumulation of biologically produced acetate. Biomass concentration could not be measured, as expected, due to the added turbidity by particles from the granules. Throughout the experiment, circuit potential was constantly monitored and current and power were measured periodically as described in Section 6.2.5. As with previous experiments, potassium ferricyanide solution in the cathodic chamber was regularly replenished to maintain the level of potential in the cathode.

Continuous mode of operation: Following the completion of sequential batch experiments, continuous co-biodegradation of combined phenol and lactate was investigated in MFC with granular electrodes. The anodic chamber of the MFC was fed continuously with modified McKinney's medium containing different combinations of phenol and lactate concentrations using a variable flow peristaltic pump. Feed combinations include either of 100, 250 or 500 mg L^{-1} phenol with 100, 250, 500 or 1000 mg L^{-1} lactate (i.e. 7 combinations in total). Similar to previous experiments in the continuous MFC systems, feed was autoclaved at 121 °C, cooled to room

temperature and then purged with nitrogen gas for about 10 minutes prior to its use. With each combination of feed different loading rates of phenol and lactate were achieved and evaluated by varying the flow rate of the feed into the anodic chamber. The experiment was started at an initial feed flow rate of approximately 2.0 mL h^{-1}. A relatively low initial flow rate was applied considering the slow and difficult biodegradation process of phenol as found in previous experiments. To measure phenol and lactate concentrations, regular sampling was conducted using a syringe. Sampling of the anodic chamber was done at least once daily, with more frequent sampling done in experiments with lower phenol and lactate concentrations given the faster biodegradation expected at lower concentrations. Along with lactate, concentration of accumulated acetate, produced during lactate biodegradation, was also determined.

At each flow rate, sufficient time was given until steady state conditions were attained. As with previous continuous experiments, steady state conditions were assumed when there was less than 10-15% variation in the residual concentrations of phenol and lactate in the anodic chamber. After the establishment of steady state conditions, MFC was operated at the same feed flow rate for at least three additional residence times before the next flow rate was applied. The average value of the data obtained as part of these samplings and associated standard deviations were used in presenting the results. The incremental increase in the feed flowrate was followed to flow rates as high as 200 mL h^{-1}, where MFC performance declined. In some cases experiments was stopped when the biodegradation rate of phenol deteriorated and in other occasions experiments were continued despite insignificant phenol degradation in order to generate data at loading rates similar to those applied in case of lactate as the sole substrate (Chapter 4) to allow comparison and verification of the effect of phenol on lactate biodegradation.

To ensure correct levels of feed concentration into the anodic chamber, sampling of the feed line in close proximity of the inlet port was done regularly. Moreover, actual flowrate during the experiments was monitored by collecting and measuring effluent volume over a specified period of time. In terms of cathodic solution replenishment, it was found that more frequent replacement of potassium ferricyanide solution was needed in these experiments as compared to previous ones (every 1-2 days). Throughout the experiment, circuit potential was constantly monitored and current and power were measured periodically. Figure 6.1 shows the continuous flow MFC with granular graphite electrodes and recirculation loop used for co-biodegradation of phenol and lactate.

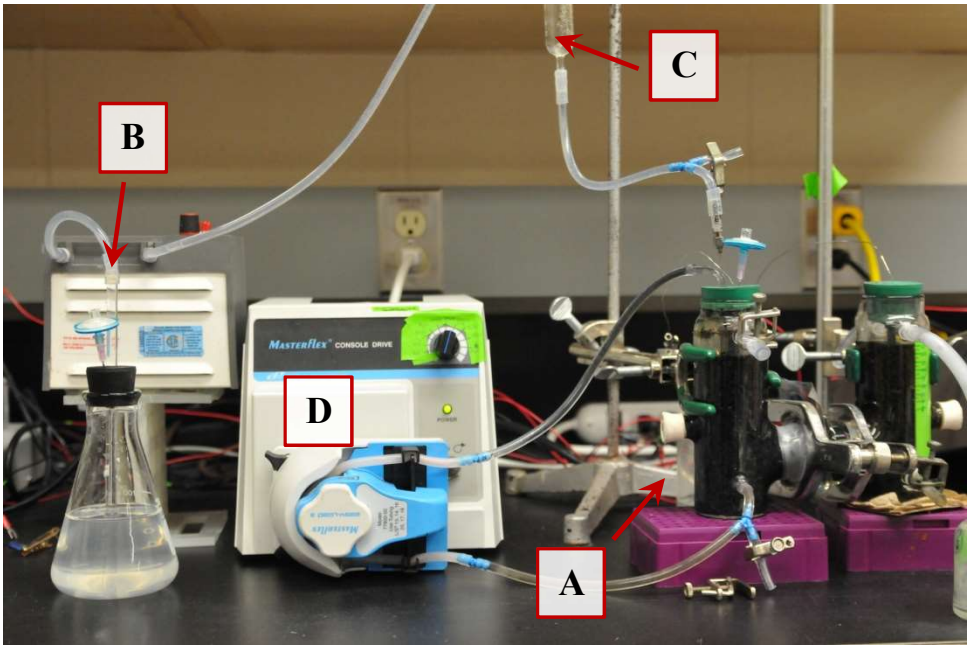

Figure 6.1 Experimental system used in continuous co-biodegradation of phenol and lactate in an MFC with granular electrodes. Feed is drawn into the anodic chamber (A) using a peristaltic pump (B) passing through the intermediary glass device (C) used to prevent contamination of feed. A second peristaltic pump (D) was used to recirculate the anodic liquid.

6.2.4. Co-biodegradation of Phenol and Lactate in MFCs with Neutral Red as Mediator

Batch mode of operation: As presented in Chapter 5, experiments in batch MFCs with phenol and neutral red revealed that the use of neutral red (NR) as electron mediator significantly improved the biodegradation of phenol. Thus, additional experiments aiming to study the effect of NR on the co-biodegradation of phenol and lactate in MFC with granular electrode were conducted. Phenol at concentration of either 100, 250 or 500 mg L^{-1} in combination with 1000 mg L^{-1} lactate underwent sequential batch biodegradation in order of increasing phenol concentration. Designated amounts of phenol and lactate along with 28.9 mg L^{-1} (0.1 mM) NR (Park and Zeikus, 2000) were added into the anodic solution using a sterile syringe. This was followed by inoculation of anodic chamber with 1 mL of *P. putida* cell suspension. Regular sampling of the anodic chamber was done to monitor concentrations of phenol and lactate, as well as that of accumulated acetate. Moreover, circuit potential of MFC was constantly monitored and current and power output were measured as described in Section 6.2.5.

Continuous mode of operation: After completion of sequential batch co-biodegradation of phenol and lactate in MFC with granular electrode and NR as mediator, the same MFC was switched to continuous mode of operation to investigate the effect of NR on the continuous co-biodegradation of phenol and lactate. Feed composition was similar to those used in the batch experiments consisting of McKinney's medium added with designated amounts of phenol, lactate and NR. Specifically, either 100, 250 or 500 mg L^{-1} phenol was combined with 1000 mgL^{-1} lactate and 28.9 mg L^{-1} NR. Initially, the peristaltic pump was set at a relatively low flow rate of 1.5 mL h^{-1}. Monitoring phenol, lactate and acetate concentrations were conducted to determine when steady state conditions have been attained, after which the flow rate of feed was increased

incrementally. Increase in flow rate was done multiple times until performance of MFC started to deteriorate. To ensure consistent levels of phenol and lactate in the feed, regular sampling of the feed line was conducted. Constant monitoring of circuit potential and measurement of current and power from the MFC at various loading rates were performed as described in Section 6.2.5.

6.2.5. Analyses

As part of experiments in MFCs with rod electrodes, biomass concentration was determined by measuring the optical density (OD) at 620 nm and then converting it to biomass concentration (mg cell-dry weight L^{-1}) using a calibration curve (Appendix A). Similar to previous experiments, supernatant liquid extracted from the samples were collected for analysis of phenol, lactate and acetate using an HPLC (Agilent Technologies 1200), equipped with a Di-Array detector (DAD) and an Eclipse Plus C-18 column (150 mm x 4.6 mm dia.).

In terms of circuit potential, MFC was continuously monitored and recorded using Keithley 2700 multimeter, equipped with 7700 datalogger (Keithley Instruments Inc., Cleveland, USA). With the use of the handheld multimeter, cathodic potential was monitored against a Calomel reference electrode dipped into the cathodic solution. Similar procedures in the measurement of power and current output from the previous experiments were followed by application of external resistors in the range 50-6000 ohms (You et al., 2006). In the latter experiments with granular electrodes, polarization curves were developed using Linear Sweep Voltammetry (LSV) using a Gamry R600 potentiostat (Gamry Instruments, Warminster, USA) as detailed in Section 4.2.4. Open circuit potential of the MFC was allowed to stabilize before conducting potential sweep and external resistance was re-applied immediately after measurement. Coulombic efficiency (CE)

was calculated as described in Appendix H.

Additional analysis was also done to determine surface area, pore size and pore volume of graphite granules used in the experiments through BET analysis. Moreover, surface of exposed and fresh granules was also analyzed using a scanning electron microscope (SEM). These analyses have been described previously in more detail in Section 4.2.4.

6.3. Results and discussion

6.3.1. Co-biodegradation of Phenol and Lactate in MFCs with single rod electrodes Lactate with varying phenol concentrations: Experiments on the co-biodegradation of lactate and phenol in MFCs with single rod electrodes were conducted to assess whether the presence of lactate would promote faster biodegradation of phenol, and to evaluate the potential inhibitory effect of phenol on the biodegradation of lactate. Batch experiments in MFC were started by adding relatively low concentrations of phenol (100 mg L^{-1}) and 500 mg L^{-1} lactate, with the biodegradation results being presented in Figure 6.2. After inoculation, biodegradation of lactate started immediately, while phenol was practically not utilized. Biomass concentration increased as a result of lactate utilization. As lactate was about to be depleted, phenol biodegradation started and proceeded at a relatively slow rate. It was only after complete exhaustion of lactate that the decrease in phenol concentration becomes notable. This finding suggests that utilization of phenol became significant when no other substrate was available for microbial community to utilize. Biomass concentration increased and reached its peak and then declined as phenol was depleted. The time required for biodegradation of 100 mg L^{-1} phenol was almost twice that of lactate.

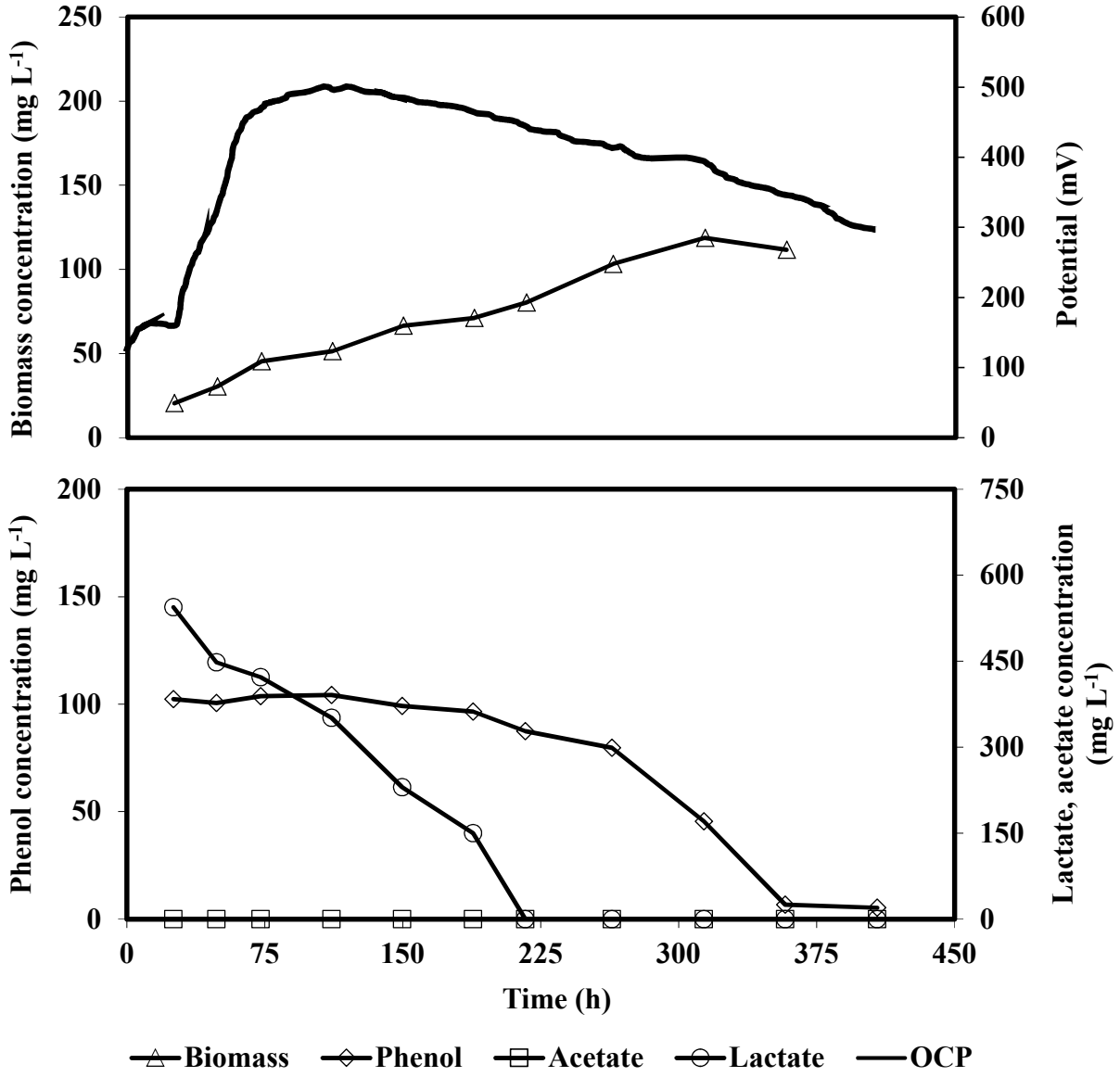

Figure 6.2 Profiles of biomass, phenol, lactate, and acetate concentrations and open circuit potential (OCP) during the co-biodegradation of 100 mg L^{-1} phenol and 500 mg L^{-1} lactate in batch MFC with single rod electrodes.

Another set of experiments was conducted in similar MFCs with higher concentration of phenol, specifically 250 and 500 mg L^{-1} in combination with 500 mg L^{-1} lactate. Culture developed in the previous experiment (i.e. co-biodegradation of 100 mg L^{-1} phenol and 500 mg L^{-1} lactate) was used as inoculum in these experiments. Results of these experiments are shown in Figure 6.3 and

6.4, respectively. Unlike in the previous experiment with 100 mg L^{-1} phenol and 500 mg L^{-1} lactate, biodegradation of both phenol and lactate occurred simultaneously and without any delay. To be more specific decrease in phenol concentration occurred along with lactate utilization without a noticeable lag phase. It could be speculated that the lag phase encountered in the previous experiment with 100 mg L^{-1} phenol and 500 mg L^{-1} lactate was due to a substantial period needed for acclimation of the microbial community to the use of phenol as substrate and that the improvement in the succeeding experiments with higher phenol concentrations was the result of to the use of this acclimated culture.

Simultaneous biodegradation of lactate and phenol led to an increase in biomass concentration from initial values in the range 24.7-34.9 mg L^{-1}. Biomass growth profile appeared to have a very brief delay, identified by the arrow in both Figures, once lactate was exhausted, possibly due to the fairly rapid change in substrate composition where the more complex and potentially growth inhibiting substrate (i.e. phenol) was the only available substrate. Exhaustion of lactate was completed well ahead of phenol at 136 and 354 h after inoculation in experiments with 250 and 500 mg L^{-1} phenol, respectively. Biomass growth continued during the biodegradation of remaining phenol and stopped once phenol was depleted. Compared to lactate, depletion of phenol took longer and completed at 600 and 800 h after inoculation with 250 and 500 mg L^{-1} phenol, respectively. Upon completion of this part 500 mg L^{-1} lactate in combination with either 250 or 500 mg L^{-1} phenol was added to each respective MFC to assess the effect of sequential addition on co-biodegradation of the combined substrates. As shown in Figures 6.3 and 6.4, in both experiments, complete degradation of lactate was achieved in a much shorter period in the subsequent batch operation (approximately 100 and 140 h with 250 and 500 mg L^{-1} phenol,

respectively). On the other hand, phenol biodegradation did not show a marked improvement. As expected, the provision of additional of phenol and lactate resulted in further biomass growth.

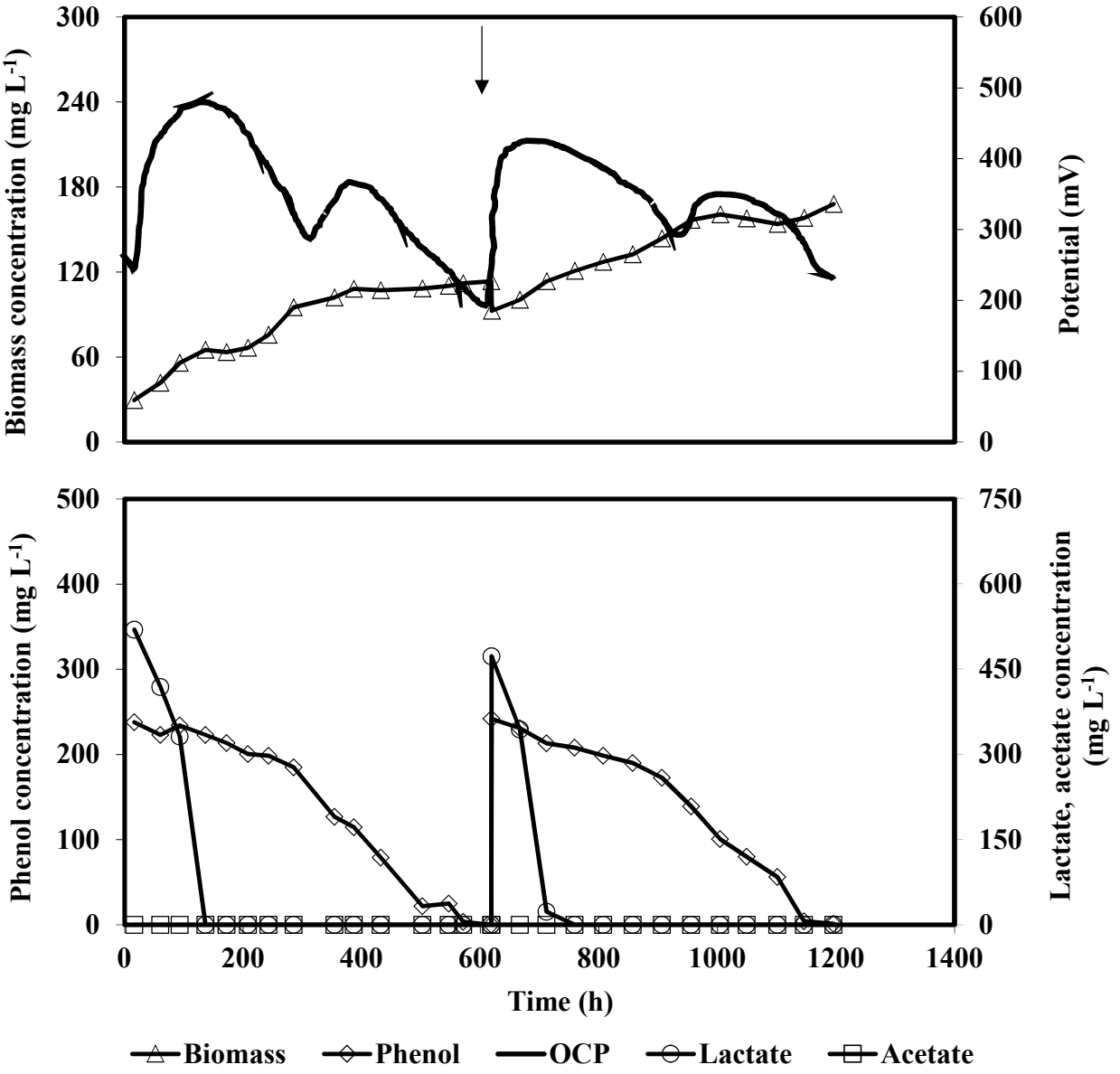

Figure 6.3 Profiles of biomass, phenol, lactate, and acetate concentrations and open circuit potential (OCP) during the co-biodegradation of 250 mg L^{-1} phenol and 500 mg L^{-1} lactate in batch MFC with single rod electrodes. Arrow indicates sequential addition of phenol and lactate.

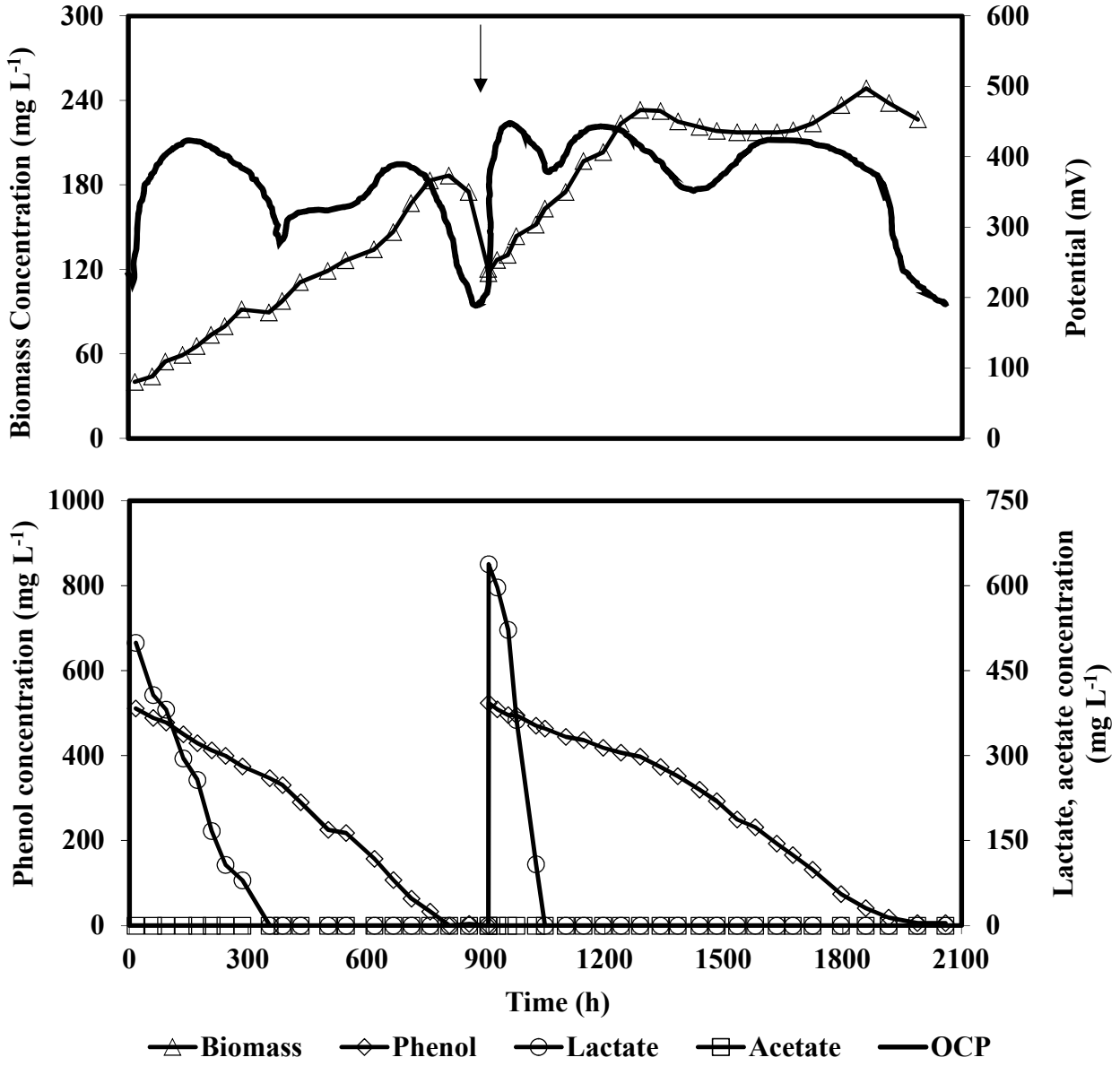

Figure 6.4 Profiles of biomass, phenol, lactate, and acetate concentrations and open circuit potential (OCP) during the co-biodegradation of 500 mg L^{-1} phenol and 500 mg L^{-1} lactate in batch MFC with single rod electrodes. Arrow indicates sequential addition of phenol and lactate.

As reported in Section 3.3.1, biodegradation of lactate as the sole substrate at concentrations of 1000-5000 mg L^{-1} resulted in the accumulation of acetate (i.e. biologically produced acetate) which was found to be a consistent occurrence regardless of applied lactate concentration. However, in these experiments with 500 mg L^{-1} lactate in combination with a range of phenol concentrations,

acetate was not detected in any of the tested conditions. The concentration of lactate (500 mg L^{-1}) utilized in these experiments was lower than those used in experiments with lactate as the sole substrate and thus might not have been sufficient to produce detectable levels of acetate, or it could have been produced at very low amounts and was degraded immediately. In all experiments, complete biodegradation of lactate occurred faster and ahead of phenol suggesting lactate as the preferred substrate.

Finally, since complete biodegradation of 500 mg L^{-1} phenol required more than 800 h and that biodegradation of higher phenol concentrations (e.g. 1000 mg L^{-1}) would have required even longer period, experiment with combined 500 mg L^{-1} lactate and 1000 mg L^{-1} phenol was not conducted.

Phenol with varying lactate concentrations. To further evaluate the capacity of lactate in promoting phenol biodegradation and to investigate possible inhibition effect of phenol, another set of experiments was conducted in MFCs with rod electrodes and freely suspended cells whereby in contrast to previous experiments, phenol concentration was maintained at 100 mg L^{-1}, while lactate at different concentrations of 1000, 2500 and 5000 mg L^{-1} was used. As shown in Figure 6.5, the combination of phenol with the lowest initial lactate concentration (1000 mg L^{-1}) resulted in a delay not just in phenol removal but more importantly in lactate degradation. This delay was not observed in the preceding co-biodegradation experiments with 100-500 mg L^{-1} phenol and 500 mg L^{-1} lactate where biodegradation of lactate was practically instantaneous. The initial sluggish reduction in lactate concentration persisted for about 190 h. Phenol degradation also encountered a lag phase concurrent with that of lactate albeit a shorter period (~100 h). This pattern that was

not observed in previous experiments with 100 mg L^{-1} phenol and 500 mg L^{-1} lactate nor when lactate or phenol were used as the sole substrate (Sections 3.3 and 5.3, respectively) suggests that increase of lactate concentration in the mixture could affect the microbial activity negatively and that an adaptation period longer than that with lower lactate concentration of 500 mg L^{-1} or when phenol or lactate was provided as sole substrate would be required. A similar result was reported by Polymenakou and Stephanou (2005) where cells of *Pseudomonas* sp. experienced a lag phase for adaptation in utilizing supplementary substrates combined with phenol that was not observed when degrading phenol as the sole substrate.

Following the lag phase, substantial decrease in phenol and especially lactate concentrations was observed along with increase in biomass concentration. At the same time, formation and accumulation of acetate was observed. As with previous results from similarly operated MFCs with lactate as sole substrate, accumulation of acetate continued as lactate biodegradation proceeded and reached its peak as lactate was utilized completely. After complete exhaustion of lactate accumulation of acetate ceased and decrease in its concentration observed. This confirmed the earlier speculation that high concentrations of lactate (i.e. 1000 mg L^{-1} and higher) were required for an appreciable level of acetate accumulation. Simultaneous with lactate degradation and acetate accumulation, reduction in phenol concentration proceeded at a rate that was relatively constant. Upon exhaustion of acetate phenol removal became more pronounced resulting in significant decrease in its concentration. Utilization of phenol led the biomass concentration to its peak that consequently declined due to complete exhaustion of phenol.

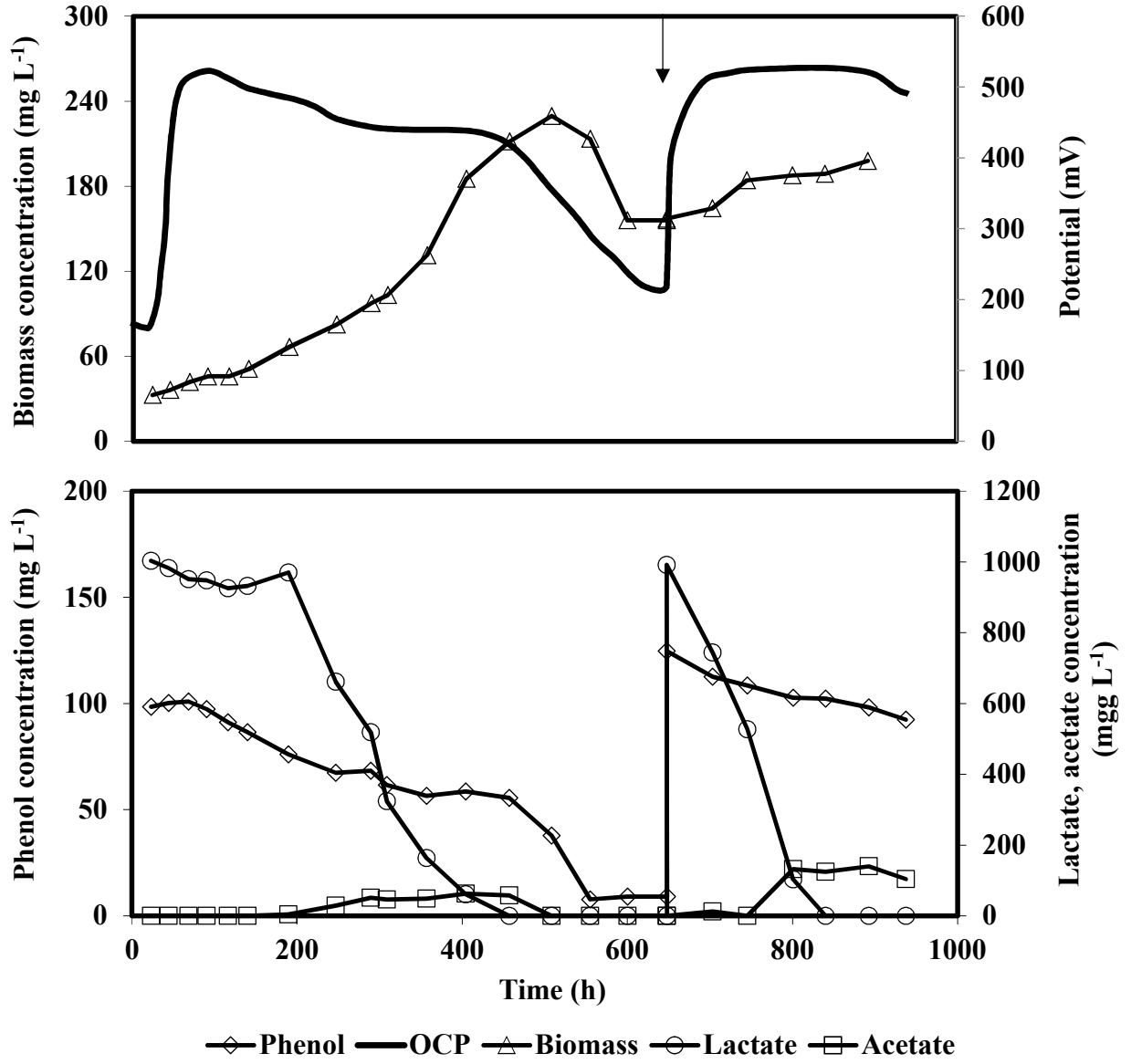

Figure 6.5 Profiles of biomass, phenol, lactate, and acetate concentrations and open circuit potential (OCP) during the co-biodegradation of 100 mg L^{-1} phenol and 1000 mg L^{-1} lactate in batch MFC with single rod electrodes. Arrow indicates sequential addition of phenol and lactate.

Before evaluating other combinations, another batch of 100 mg L^{-1} phenol and 1000 mg L^{-1} lactate was added to the MFC to assess if sequential addition would enhance biodegradation such as those found in previous experiments with lactate or phenol as sole substrate (Sections 3.3 and 5.3). In contrast with findings from the first run, biodegradation of both substrates was instantaneous and

no lag phase was observed. One could speculate that the microbial community had adapted to utilization of combined substrate as part of the first run and as a result no lag phase was observed in the subsequent run. The resulting concentration profiles from the second test are included in Figure 6.5 show that the utilization of lactate occurred simultaneously with phenol degradation and led to formation of acetate and increase in biomass. Acetate reached its peak concentration once lactate concentration dropped to zero and underwent degradation while utilization of phenol and increase in biomass concentration continued.

As indicated earlier two other experiments with 100 mg L^{-1} phenol in combination with lactate at higher concentrations of 2500 and 5000 mg L^{-1} were conducted in two MFCs run in parallel with the results presented in Figures 6.6 and 6.7, respectively. Similar to findings from the previous experiment with 100 mg L^{-1} phenol and 1000 mg L^{-1} lactate, biodegradation of phenol and lactate experienced a lag phase with the lag phase with 2500 mg L^{-1} lactate being considerably shorter than that with 5000 mg L^{-1} (45 vs 190 h). Moreover, formation and accumulation of acetate was again observed and its subsequent utilization occurred only after lactate was depleted.

With higher lactate concentrations of 2500 and 5000 mg L^{-1}, concentration of accumulated acetate was higher with the maximum amounts of 474 and 1076 mg L^{-1}, respectively, as opposed to only 140 mg L^{-1} observed with 1000 mg L^{-1} lactate. The biodegradation of accumulated acetate was observed to progress at a steady but slow rate simultaneously with phenol degradation and biomass growth. Combined with findings from earlier co-biodegradation experiment with 1000 mg L^{-1} lactate, it appeared that utilization of accumulated acetate slowed down the removal of phenol.

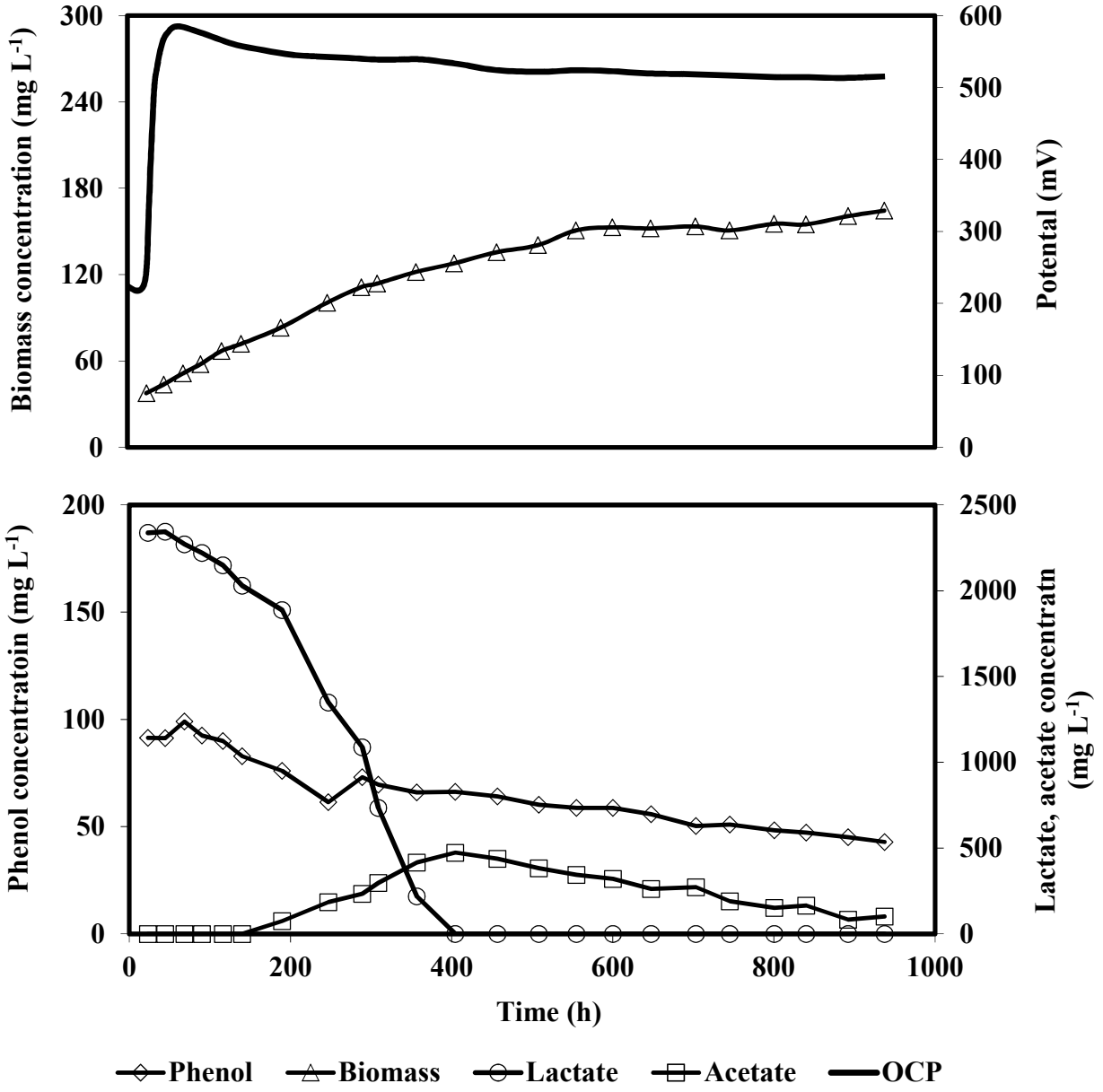

Figure 6.6 Profiles of biomass, phenol, lactate, and acetate concentrations and open circuit potential (OCP) during the co-biodegradation of 100 mg L^{-1} phenol and 2500 mg L^{-1} lactate in batch MFC with single rod electrodes.

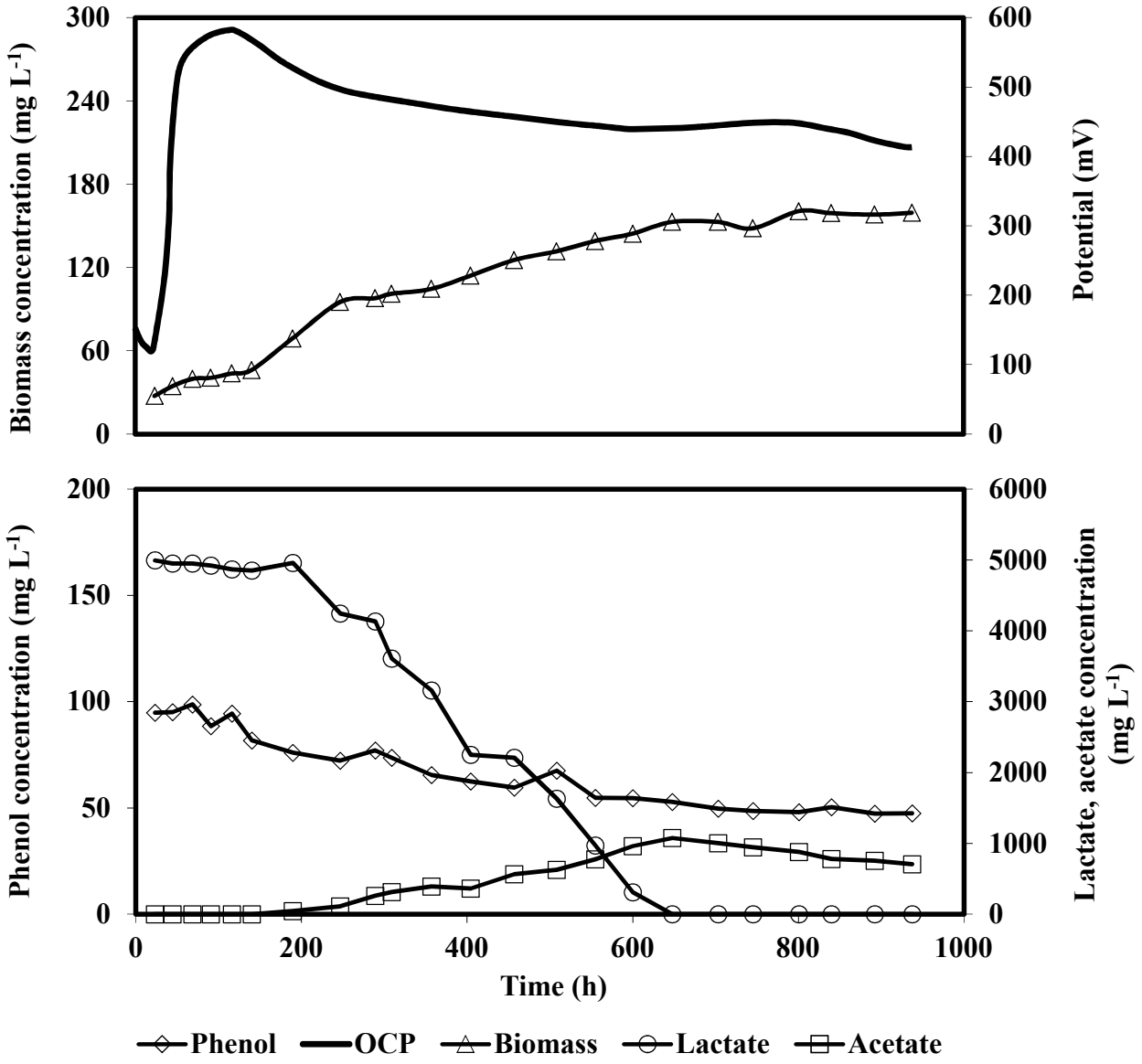

Figure 6.7 Profiles of biomass, phenol, lactate, and acetate concentrations and open circuit potential (OCP) during the co-biodegradation of 100 mg L^{-1} phenol and 5000 mg L^{-1} lactate in batch MFC with rod electrodes.

It has been observed in results from the initial run of sequential tests with 100 mg L^{-1} phenol and 1000 mg L^{-1} lactate that acetate depletion had to be complete before phenol exhaustion. Even after 937 h (39 d) into the experiment (Figures 6.6 and 6.7), or roughly 747 h (31 d) since detection of

biologically produced acetate, biodegradation of accumulated acetate was still ongoing. Consequently, no substantial decrease in phenol concentration was observed and residual phenol concentrations were still almost half of its original amounts (42.9 and 47.4 mg L^{-1} in tests combined with 2500 and 5000 mg L^{-1} lactate, respectively). Given the steady rate in reduction of phenol and accumulated acetate concentrations and the predictability of the ongoing biodegradation process, a significant amount of time would have been required for complete removal of phenol. Hence, at this point, both experiments were terminated. Overall, in all evaluated combinations, lactate was found to be the more amenable substrate and was completely removed. Furthermore, a pattern of sequential utilization of available substrates was observed where lactate was depleted first followed by accumulated acetate and lastly by phenol.

Biodegradation rates of phenol, lactate and accumulated acetate (when present) were determined using the slope of the linear part of their respective concentration profiles. The biodegradation rates of phenol achieved from the experiments in MFCs with rod electrodes and freely suspended cells with combination of 500 mg L^{-1} lactate and either 100, 250 or 500 mg L^{-1} phenol were 0.37, 0.44 ± 0.02 and 0.57 ± 0.11 mg L^{-1} h^{-1}, respectively. Results showed that phenol biodegradation rate increased slightly when higher phenol concentrations was used. This was similar to the trend observed in the previous experiments with phenol as sole substrate in similarly operated MFC where biodegradation rates with 100, 250 and 500 mg L^{-1} phenol were 0.5, 0.9 and 0.9 mg L^{-1} h^{-1}, respectively (Section 5.3). Comparison of these results show that the addition of lactate did not enhance the biodegradation of phenol and in fact presence of a more favourable substrate like lactate led to lower phenol biodegradation rates.

Biodegradation rates were also determined for the set of experiments conducted in batch operated MFCs where phenol concentration was maintained at 100 mg L^{-1} and lactate was added at various concentrations. When combined with 1000 mg L^{-1} lactate, the resulting phenol biodegradation rate was 0.15 mg L^{-1} h^{-1} which was significantly lower compared to 0.37 mg L^{-1} h^{-1} achieved from the previous test where 100 mg L^{-1} phenol was combined with a lower lactate concentration of 500 mg L^{-1}. Further increase in the concentration of lactate to 2500 and 5000 mg L^{-1} resulted in lower phenol biodegradation rates of 0.06 mg L^{-1} h^{-1} in both experiments. These results revealed a trend where phenol biodegradation rate decreased as the concentration of lactate as the co-substrate was increased. It could be speculated that biodegradation of lactate, as the more amenable substrate, is preferred by microorganisms over phenol and only after complete lactate degradation that phenol utilization proceeds with a notable rate.

With higher lactate concentrations (1000-5000 mg L^{-1}), formation and subsequent utilization of acetate was observed which resulted in further decrease in the biodegradation of phenol. A preference in utilization of acetate by microorganisms over phenol was observed similar to that with lactate over phenol. Combination of lactate at higher concentrations resulted in formation of higher amounts of biologically produced acetate which in turn required more time for degradation and consequently causing further slowdown in phenol utilization. Hence, the resulting biodegradation rates of phenol were considerably lower in experiments where higher concentrations of lactate was used. A similar sequential pattern of substrate degradation was reported by O'Sullivan (1998) from utilization of phenol-glucose mixtures where glucose biodegradation preceded that of phenol.

Similar trend has been reported in conventional bioreactors. For example batch biodegradation of 200 mg L^{-1} phenol combined with various concentrations of glucose, conducted in 250 mL flasks with a mixed microbial culture consists of *Pseudomonads* and *Actinomycetes* was investigated by O'Sullivan, 1998 who reported that the rate of phenol biodegradation decreased with increasing the glucose concentration. In another batch system, the addition of either lactate, glucose, benzoate or succinate to phenol reduced the rate at which phenol was degraded by freely suspended *Aureobasidium pullulans* FE13 (dos Santos et al., 2009). Polymenakou and Stephanou, 2005 reported that the combination of supplementary substrates (toluene, *o*-cresol and naphthalene) decreased the biodegradation rate of phenol by *Pseudomonas* sp. cells by a factor of 8 as compared to the rate with phenol as the sole substrate.

In terms of lactate biodegradation, the combination of 500 mg L^{-1} lactate with 100 mg L^{-1} phenol resulted in a biodegradation rate of 2.6 mg L^{-1} h^{-1}. Increasing initial lactate concentration to 1000, 2500 and 5000 mg L^{-1} while maintaining phenol at 100 mg L^{-1} showed higher biodegradation rates of 3.72, 6.80 and 10.96 mg L^{-1} h^{-1}, respectively. These results were consistent with the trend observed in the experiments with lactate as sole substrate where lactate biodegradation rate improved with increase in lactate initial concentration. Moreover, at the same initial concentration, lactate biodegradation rates from the previous experiments without phenol were higher (5.73, 10.08 and 17.33 mg L^{-1} h^{-1} at concentrations of 1000, 2500 and 5000 mg L^{-1}, respectively). These results indicate that the presence of phenol negatively affects the degradation of lactate. Being a recalcitrant compound, the presence of phenol could have created a more challenging environment for microorganisms to utilize lactate effectively.

During the co-biodegradation of 500 mg L^{-1} lactate with 250 and 500 mg L^{-1} phenol, lactate biodegradation rate improved slightly to 3.97 mg L^{-1} h^{-1} when combined with 250 mg L^{-1} phenol but decreased to 2.98 mg L^{-1} h^{-1} when phenol concentration was further increased to 500 mg L^{-1} h^{-1}. The perceived decrease in lactate biodegradation rate as phenol was increased to 500 mg L^{-1} could be attributed to inhibition effects of phenol especially at the higher concentrations. A similar finding was observed from the study by O'Sullivan (1998) in conventional bioreactors where glucose biodegradation deteriorated when combined with 2-, 3-, 4-chlorophenol and phenol.

Similar to previous experiments in MFCs operated with lactate as the sole substrate, accumulation of biologically produced acetate was observed in co-biodegradation experiments with higher lactate concentrations (1000-5000 mg L^{-1}) with accumulation rates comparable to those from experiments in the absence of phenol. At an initial concentration of 1000 mg L^{-1} lactate with 100 mg L^{-1} phenol the biodegradation rate of accumulated acetate was 0.60 mg L^{-1} h^{-1} which was comparable to those in similar experiments with lactate as sole substrate (average rate: 0.85 ± 0.59 mg L^{-1} h^{-1}). Moreover, it was observed that biodegradation of accumulated acetate proceeded at a much slower rate than that of lactate.

To date no other study has been conducted that attempted to investigate the effects of combining a more amenable substrate with phenol in an MFC with freely suspended cells operated batchwise. The batch experiments conducted by Song et al. (2014) in a single-chamber MFC combined glucose, sodium acetate or sodium propionate with phenol but the main reason for the use of these substrates was the acclimation of bacterial culture to phenol utilization and no information on the effect of the added substrates on phenol biodegradation was presented in that work.

OCP, power and current: The combination of 100, 250 and 500 mg L^{-1} phenol with lactate at a concentration of 500 mg L^{-1} produced relatively similar maximum open circuit potentials (OCP) of 501, 495 and 497 mV, respectively. In experiments with 100 mg L^{-1} phenol in combination with higher lactate concentrations of 1000, 2500 and 5000 mg L^{-1}, higher maximum OCPs of 524, 589 and 583 mV were obtained. These results suggest that the increase in lactate concentration could contribute to raise the OCP. In terms of power output, the combination of 100-500 mg L^{-1} phenol with 500 mg L^{-1} lactate produced power and current densities in the range of 0.008-0.05 mW m^{-2} and 2.58-3.46 mA m^{-2}, respectively. In terms of anodic working volume, equivalent power and current densities were 0.06-0.33 mW m^{-3} and 18.07-25.72 mA m^{-3}, respectively. Higher electrochemical output was achieved when higher lactate concentrations (1000-5000 mg L^{-1}) were combined with 100 mg L^{-1} phenol with power and current densities in the range of 0.02-0.25 mW m^{-2} and 1.78-21.95 mA m^{-2}, respectively. Equivalent power and current densities in terms of anodic volume were 0.11-5.07 mW m^{-3} and 13.04-140.90 mA m^{-3}, respectively.

The higher power and current output from MFCs operated with phenol and lactate at higher concentrations is consistent with the higher lactate biodegradation rates achieved in these systems. Overall, the power and current densities achieved in all combinations of phenol and lactate were markedly lower than those with phenol or lactate as sole substrates. This was consistent with the biodegradation rates that in case of phenol and lactate as sole substrate were much higher than the biodegradation rates when combination of these substrates were evaluated. These findings once again conformed to the trend where higher biodegradation rates result in higher power and current output, as has been discussed previously in Sections 3.3, 4.3 and 5.3.

6.3.2. Co-biodegradation of Phenol and Lactate in MFCs with granular electrodes

Batch mode of operation: Batch experiments including sequential addition of substrate were conducted in MFC with granular electrodes in a manner similar to those for lactate and phenol as sole substrates (Sections 4.3.1 and 5.3.2, respectively). Co-biodegradation of phenol and lactate in combinations of 1000 mg L^{-1} lactate with either 100, 250 or 500 mg L^{-1} phenol were evaluated. Measurement of the actual initial phenol and lactate concentrations, however, showed deviation from their designated concentrations with the measured initial concentrations of lactate and phenol in sequence of operation were approximately 650 and 60, 770 and 140 instead of 1000 and 100 mg L^{-1}; 600 and 300, 650 and 450 instead of 1000 and 250 mg L^{-1}, and finally 1100 and 200, 900 and 650 mg L^{-1}, instead of 1000 and 500 mg L^{-1}, respectively. Although calculations and procedures for adding the designated substrates into the anodic chamber were identical to previous experiments somehow accurate adjustment of concentrations of both substrates was not possible even with repeated attempts. A potential reason could be the porous structure of granules that affected the effective volume of anodic liquid leading to inaccurate estimations. Given this it was decided to go ahead with experiments and to evaluate the biodegradation pattern despite the deviation of initial concentrations from the designated values.

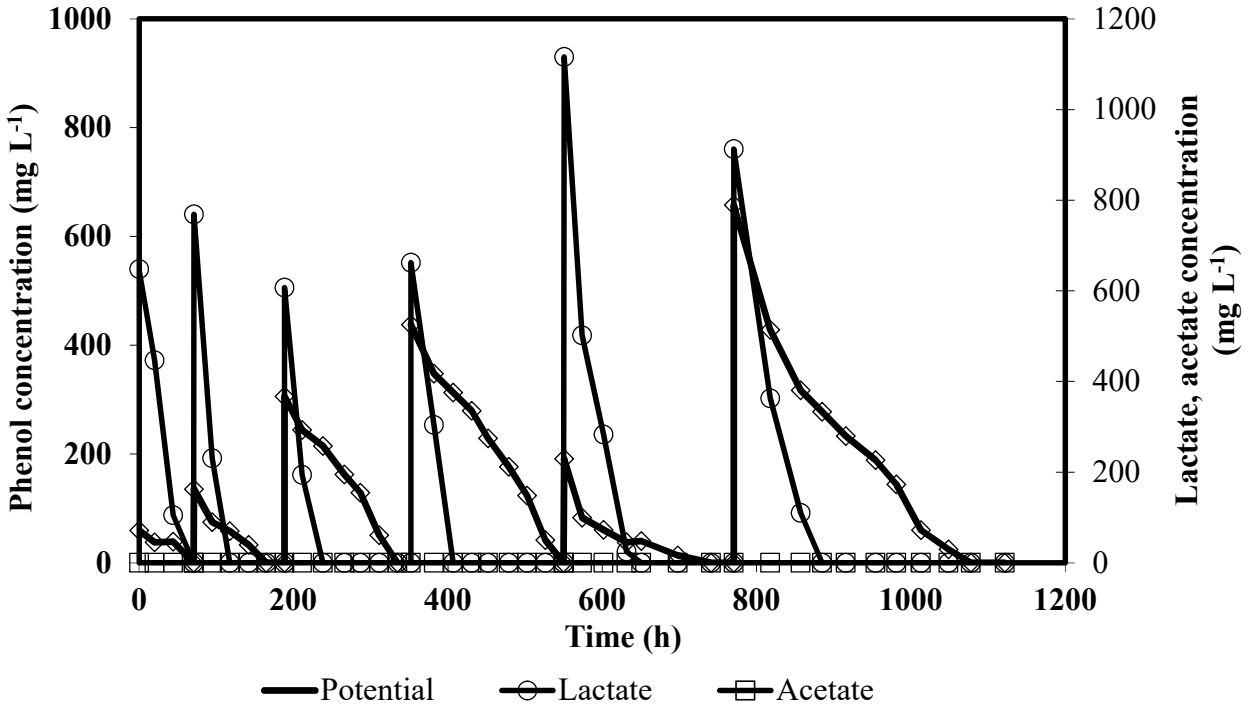

Figure 6.8 Co-biodegradation of phenol and lactate in an MFC with granular electrode operated batchwise and inoculated with *P. putida* fed sequentially with phenol and lactate at various initial concentrations.

Results of sequential batch experiments for various combinations are presented in Figure 6.8. In all cases, simultaneous biodegradation of phenol and lactate occurred immediately after initiation of experiment and unlike the previous experiments in MFCs with rod electrodes, the lag phase in co-biodegradation of phenol and lactate was not observed even at the highest tested phenol concentration of approximately 650 mg L^{-1}. Moreover, the biodegradation of phenol and lactate occurred simultaneously though lactate biodegradation occurred at faster rates. This pattern was observed in all combinations and regardless of phenol and lactate initial concentration. To be more specific in MFCs with rod electrodes, preference in utilization of the more amenable substrate was observed where lactate and subsequently accumulated acetate were utilized ahead of phenol, while in MFC with granular electrodes degradation of phenol and lactate occurs simultaneously but depletion of the more amenable substrate (lactate) is completed faster, even at concentrations more

than twice of the recalcitrant substrate (phenol). A similar trend was reported in an MFC with granular graphite as packing material used for degradation of phenol where the biodegradation of 1000 mg L^{-1} phenol was delayed when combined with 500 mg L^{-1} glucose suggesting the preferential use of glucose by microbial culture (Luo et al., 2009).

In terms of lactate biodegradation, resulting profile of lactate concentration resembled that observed in an MFC with granular electrodes degrading lactate as sole the substrate (Section 4.3). The most notable similarity is the absence of formation or accumulation of biologically produced acetate which was in contrast with the pattern observed in MFCs with rod electrodes where biodegradation of lactate at initial concentrations of 1000 mg L^{-1} and higher in combination with 100 mg L^{-1} phenol resulted in formation of acetate. One could attribute the absence of acetate formation to either formation of a small amount of acetate and its immediate and fast biodegradation or that lactate degradation proceeded through a complete degradation pathway that does not involve any intermediate product (Reaction 3.2).

Biodegradation rates of phenol and lactate: Using the slope of phenol and lactate concentration profiles, biodegradation rates of phenol and lactate at different combinations of phenol (60-650 mg L^{-1}) and lactate (600-1100 mg L^{-1}) were calculate and presented as a function of phenol initial concentration in Figure 6.9. As seen in this figure phenol biodegradation rate had the lowest value of 0.76 mg L^{-1} h^{-1} at the lowest initial concentration of 60 mg L^{-1} and increased from 0.76 to 2.15 mg L^{-1} as phenol concentration was increased in the range 60 to 450 mg L^{-1}. Further increase in phenol concentration to 650 mg L^{-1} led to a lower rate of 1.93 mg L^{-1}. This observed trend was comparable to those achieved in the batch experiments in similarly operated MFCs with phenol as

sole substrate which, again, indicates the potential inhibition effects of phenol at high concentrations. Application of granular electrodes as expected enhanced the biodegradation rate and the results obtained with granules were at least two-fold faster than those in a similarly operated MFCs with rod electrodes (0.37-0.57 mg L^{-1} h^{-1}). However, when compared to an MFC system with granular electrode operated with phenol as sole substrate (Section 5.3), the biodegradation rates in the mixture were considerably lower (3.5-4.8 vs 0.76-2.15 mg L^{-1} h^{-1}). These results again suggest that the presence of a more amenable substrate, such as lactate, negatively affected the biodegradation of phenol.

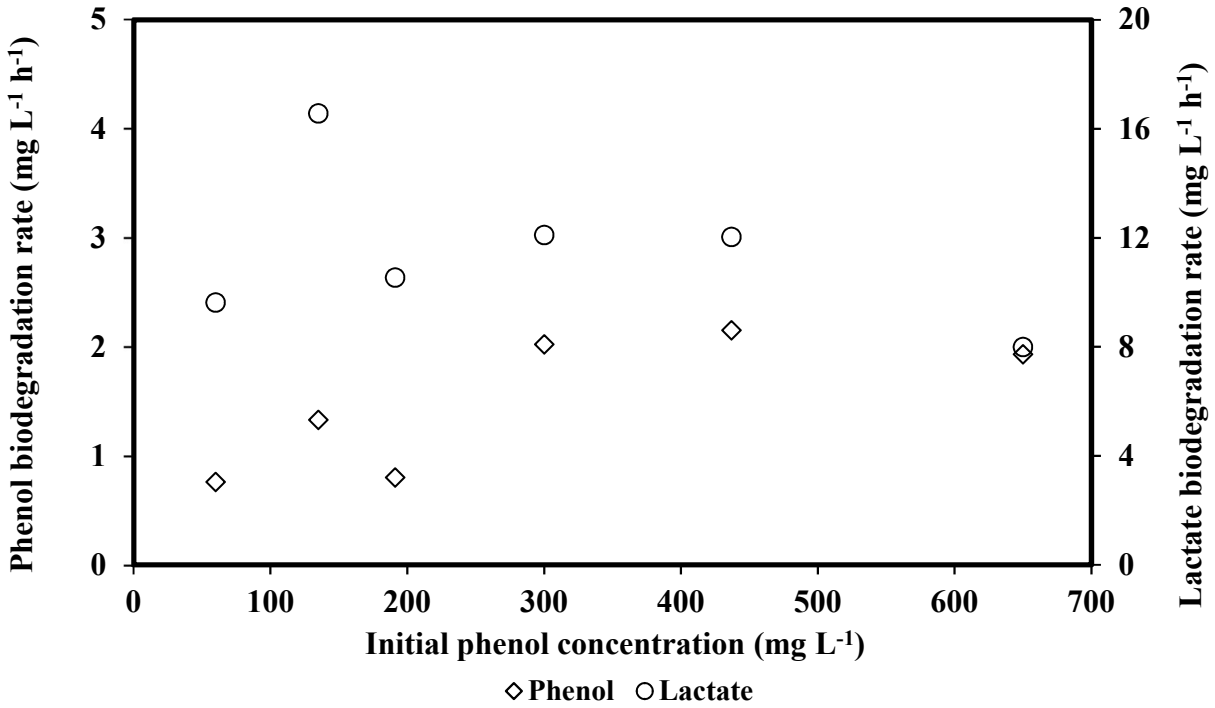

Figure 6.9 Biodegradation rates of phenol and lactate achieved in MFC with granular electrodes operated batchwise and inoculated with *P. putida* fed sequentially with different combinations of phenol (60-650 mg L^{-1}) and lactate (600-1100 mg L^{-1}).

Similar findings were observed by Luo et al. (2009) in batch operated MFC with granular graphite used for biodegradation of phenol as sole substrate and co-biodegradation of phenol and glucose

whereby biodegradation rate of phenol was decreased from 22.2 to 16.7 mg L^{-1} h^{-1} when glucose was added as the co-substrate. Similar trends were also reported from batch experiments in conventional bioreactors inoculated with *P. putida* where the presence of glucose or sodium glutamate both hindered the removal of phenol (Rozich and Colvin, 1986; Wang et al., 1996; Wang and Loh, 1999).

Biodegradation of lactate exhibited a trend where lactate biodegradation rates were generally higher at the lower initial phenol concentrations (≤ 300 mg L^{-1} h^{-1}) and decreased as phenol concentration was increased. Lactate biodegradation rates calculated from these sequential batch experiments were in the range of 7.99-16.56 mg L^{-1} h^{-1} with the lowest rate attained at the highest combined initial phenol concentration of 650 mg L^{-1} h^{-1}. This resulting trend is consistent with the pattern observed in MFCs with rod electrodes fed with different combinations of phenol and lactate and could be attributed to the inhibitory effect of phenol especially at high concentrations. In other words, the increased inhibitory effect with increasing phenol concentration could be responsible for the deterioration in the biodegradation of the more amenable substrate similar to that described in the study by O'Sullivan (1998).

The average biodegradation rate of lactate from all evaluated combinations (11.47 ± 2.93 mg L^{-1} h^{-1}) was substantially lower compared to that achieved in similarly operated MFC with granular electrodes fed with lactate as sole substrate with an average biodegradation rate of 23.08 ± 0.03 mg L^{-1} h^{-1} (Section 4.3). Again, this finding suggests that the presence of phenol, being the more difficult substrate to degrade and a compound known to impose inhibitory effect on microbial activity, negatively affects the ability of microorganisms to utilize lactate, thereby resulting to

lower biodegradation rates. When compared to MFCs with rod electrodes fed with similar combinations of phenol and lactate, improved performance of MFC with granular electrode was clear. Lactate biodegradation rates were 3-5 times higher when granular electrodes were used.

Power and current output: Similar to previous experiments in MFC with granular electrodes, a 50 ohm resistor was applied across the circuit of the MFC without replacement for the duration of all experimental runs. The application of low external resistance resulted in an expected low circuit potential (<6.5 mV) throughout the experiments. Using the maximum potential of the MFC the power and current densities were calculated as 9.64 mW m^{-3} and 1505.88 mA m^{-3}, respectively. These values were markedly higher than those generated from similarly operated MFCs with rod electrodes (6.93 mW m^{-3} and 179.54 mA m^{-3}). Moreover, these higher power and current densities corresponded to the substantially higher phenol and lactate biodegradation rates achieved when granular electrodes were used.

When compared to the similar granular electrode MFC fed with phenol as sole substrate, the measured power and current outputs during the co-biodegradation of phenol and lactate were higher (9.64 mW m^{-3} and 1505.88 mA m^{-3} vs 4.80 mW m^{-3} and 1165.70 mA m^{-3}). This was despite a lower phenol biodegradation rates that were achieved during co-biodegradation of phenol and lactate. These results indicate that the presence and biodegradation of lactate had a more pronounced effect on the power and current output and dictated the outcome. When compared to power and current densities in the MFC with granular electrodes fed with lactate as sole substrate (14.22 mW m^{-3} and 1777.78 mA m^{-3}), power and current output during the co-biodegradation of

phenol and lactate were lower which, again, could be a consequence of differences in corresponding lactate biodegradation rates.

Continuous mode of operation: Feed containing phenol and lactate as combined substrate was fed into the anodic chamber of the MFC with granular electrodes at various flowrates ranging from 2 to 100 mL h^{-1}, which were equivalent to dilution rates of 0.03-1.4 h^{-1}. To cover a diverse and wide range of loading rates, different concentrations of phenol and lactate were tested throughout the applied flowrates as shown in Table 6.1. With the applied flowrates and varied concentrations of co-substrates, loading rates of phenol and lactate being in the range of 2.9-804.5 and 7.7-2674.8 mg L^{-1} h^{-1}, respectively.

Table 6.1. Combinations of phenol and lactate concentrations utilized in the feed of continuously operated MFC with granular electrodes at various flowrates.

Flowrate (mL h^{-1})	Phenol (mg L^{-1})	Lactate (mg L^{-1})
2	100	1000
5	100	100, 250, 500, 1000
10	100	1000
20	100, 250, 500	1000
50	100	1000
100	100, 250, 500	1000

The removal percentages and biodegradation rates of phenol as a function of its loading rate are shown in Figure 6.10, while the corresponding results for biodegradation of lactate is shown in Figure 6.11. As seen in Figure 6.10 effective phenol biodegradation was only achieved at lower loading rates in the range 2.9-15.7 mg L^{-1} h^{-1} (Figure 6.10A) and with the lowest initial phenol

concentration of 100 mg L^{-1} in the feed mixture. For the loading rates above 15.7 mg L^{-1} h^{-1}, decrease in phenol concentration was practically marginal as shown in the poor removal percentages of only 2.1-7.3%. Removal percentages from degradation of combined substrate with higher phenol concentrations of 250 and 500 mg L^{-1} also fell in this range. By contrast, for the entire range of applied lactate loading rates the MFC functioned effectively as practically 100% of lactate was removed (Figure 6.11A). An exception to this was the result when feed contained the highest phenol concentration of 500 mg L^{-1} where removal percentages of 70.8% and 40.5% were attained at a high loading rate. These results show that efficiency of removing either phenol or lactate is decreased when concentration of phenol in the feed is high, which is an indication of the inhibitory effects of phenol at these concentrations.

With lower loading rates where considerable utilization of phenol took place, resulting phenol biodegradation rates were relatively low in the range of 2.1-6.7 mg L^{-1} h^{-1} (Figure 6.10B). With the lowest loading rate that led to complete removal of phenol a biodegradation rate of 2.9 mg L^{-1} h^{-1} attained at the longest HRT of 34.8 h. Small improvements in biodegradation rate was observed with increase in loading rate achieving its peak of 6.7 mg L^{-1} h^{-1} at a loading rate of 7.6 mg L^{-1} h^{-1} (HRT = 13.0 h). Although further increase in loading rate led to a slight improvement in phenol biodegradation rate this was associated with very low removal efficiencies. By contrast, effective utilization of lactate for most of the applied loading rates resulted in continued improvement in lactate biodegradation rate with increase in loading rate (Figure 6.11B). An exception to this finding was observed when feed contained the highest combined phenol concentration (500 mg L^{-1}) that caused the lowest removal percentages and low corresponding biodegradation rates (outlier

points in the resulting biodegradation-loading rate trend). Again, this confirmed the negative effect of high phenol concentration on the lactate biodegradation.

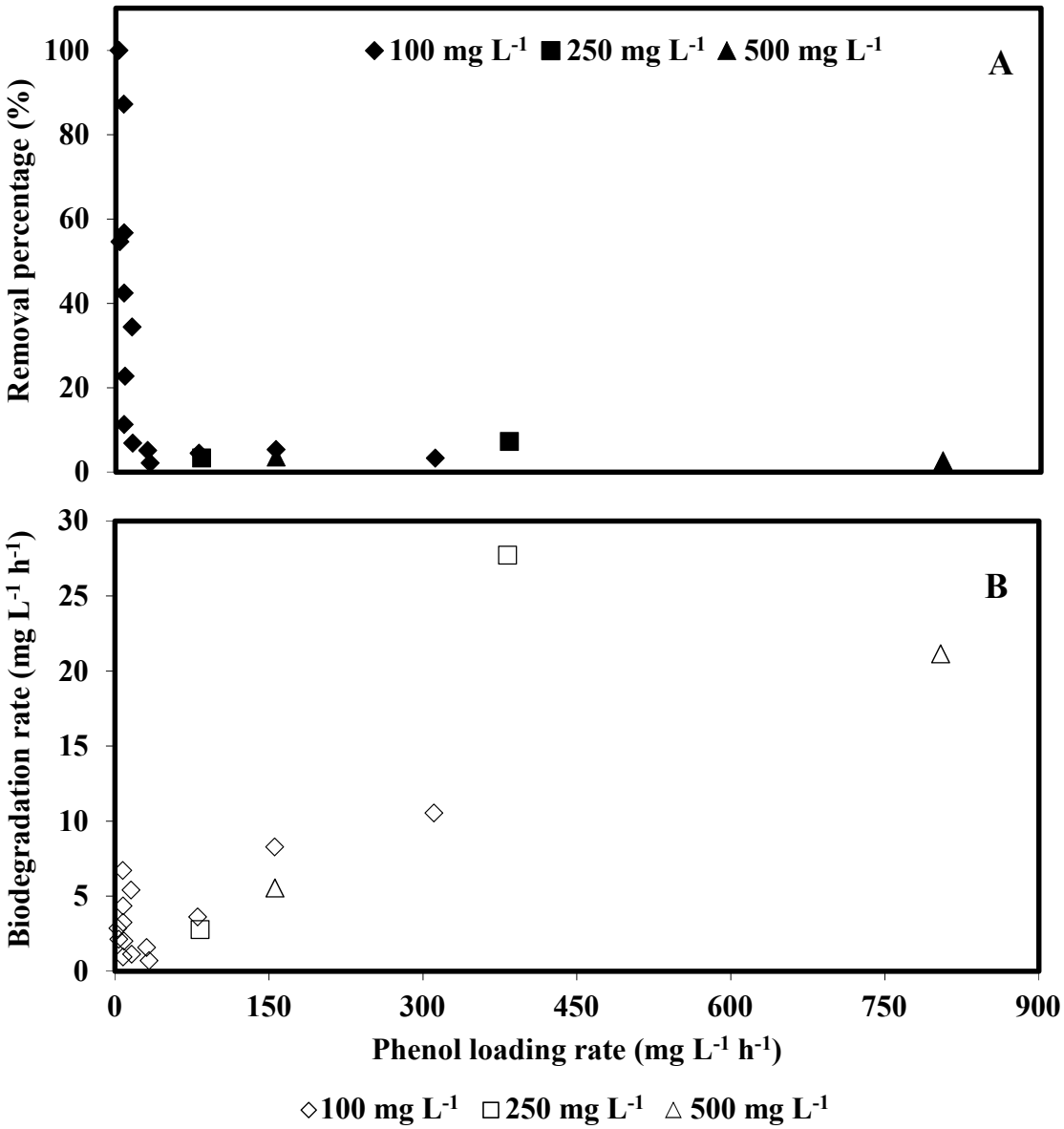

Figure 6.10 Removal percentage (panel A) and biodegradation rate (panel B) of phenol as a function of its loading rate in MFC with granular electrodes fed continuously with lactate in combination with either 100, 250 or 500 mg L^{-1} phenol**.**

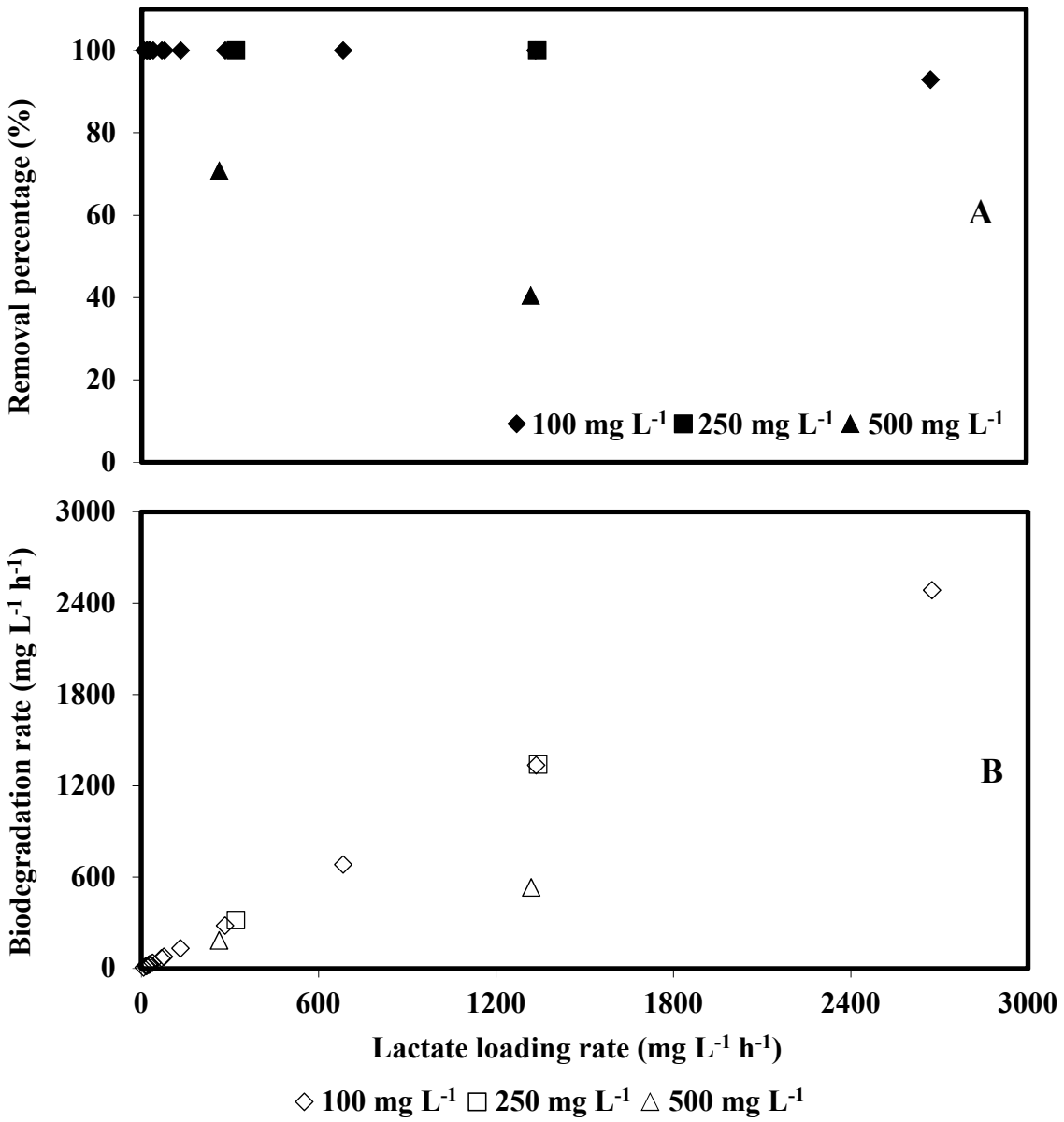

Figure 6.11 Removal percentages (panel A) and biodegradation rates (panel B) of lactate as a function of its loading rate in MFC with granular electrodes fed continuously with lactate in combination with either 100, 250 or 500 mg L^{-1} phenol**.**

To assess the effect of initial lactate concentration on continuous phenol biodegradation, experiments were conducted by combining 100, 250, 500 or 1000 mg L^{-1} with l00 mg L^{-1} phenol, while maintaining feed flowrate constant at approximately 5 mL h^{-1}. These combinations led to lactate loading rates in the range of 7.7-76.8 mg L^{-1} h^{-1} that fall in the loading rate range evaluated

in the previous experiments. Results from these runs that are presented in Figure 6.12 reveal that removal efficiency of phenol (panel A) decreased with increase in initial concentration of lactate. This led to a decline in corresponding phenol biodegradation rates from 6.7 mg L^{-1} h^{-1} with 100 mg L^{-1} lactate to 1.0 mg L^{-1} h^{-1} at the highest lactate concentration of 1000 mg L^{-1}. These findings confirmed the negative effect of higher lactate concentrations on phenol biodegradation that was observed during batch co-biodegradation of phenol and lactate. As far as lactate is concerned increase in lactate initial concentration and its loading rate led to increase in lactate biodegradation rates as observed in previous experiments with lactate as sole substrate.

Figure 6.13 compares the results of biodegradation of phenol as the sole substrate and co-biodegradation of phenol and lactate in terms of phenol removal percentage and biodegradation rate as a function of phenol loading rate. It is important to note that data is presented for the lower range of applied loading rates (7.7-35.5 mg L^{-1} h^{-1}) in which phenol removal was achieved. Included in the figure are also average values of phenol removal percentage and biodegradation rate obtained at different initial lactate concentrations while maintaining phenol loading rate at 7.8 mg L^{-1} h^{-1} with corresponding standard deviations shown as the error bars.

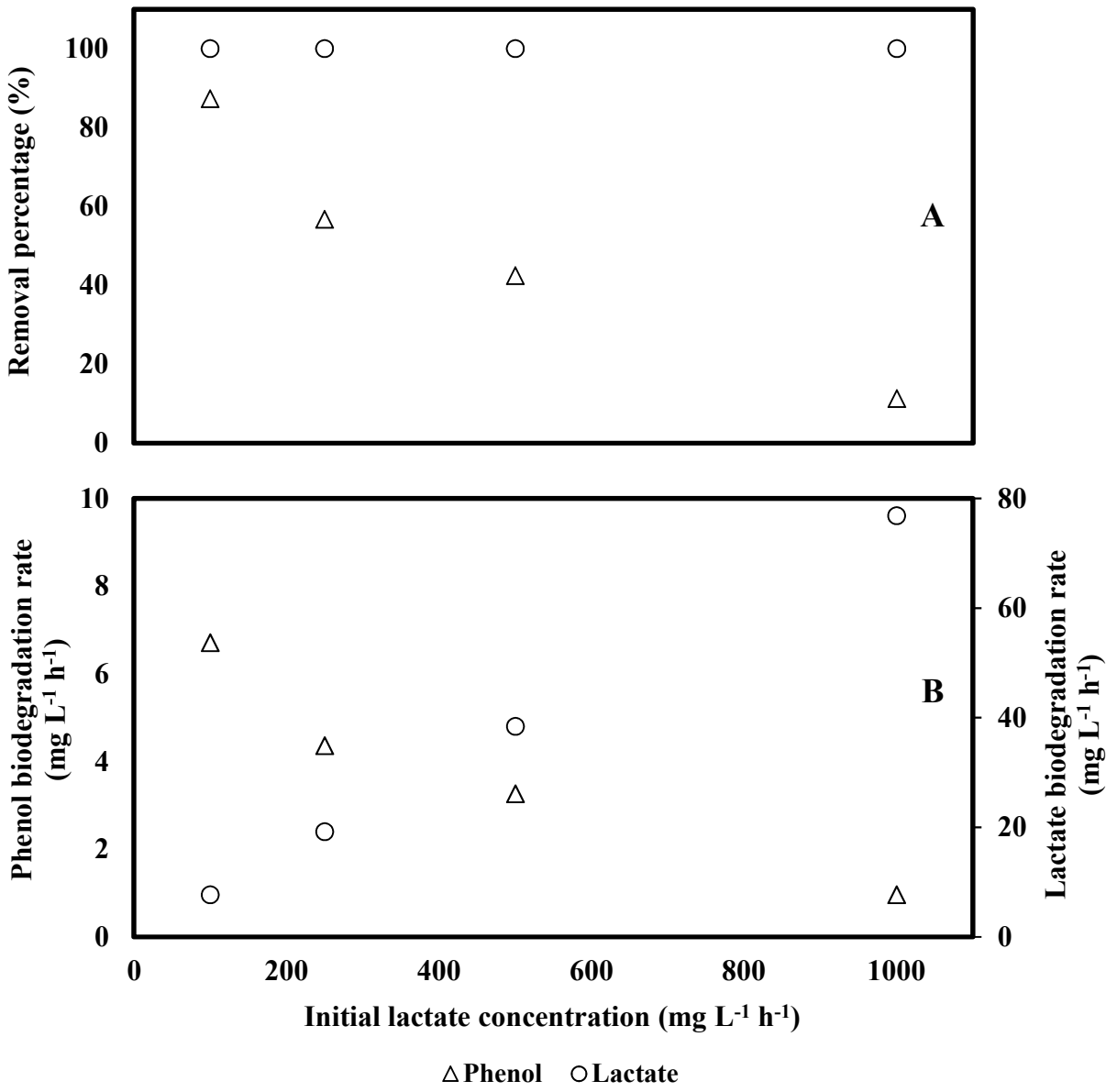

Figure 6.12 Removal percentages (panel A) and biodegradation rates (panel B) of 100 mg L^{-1} phenol attained during co-biodegradation with different initial concentrations of 100, 250, 500 or 1000 mg L^{-1} lactate, in the continuously operated MFC with granular electrodes. Corresponding removal percentages and biodegradation rates of lactate are shown as well.

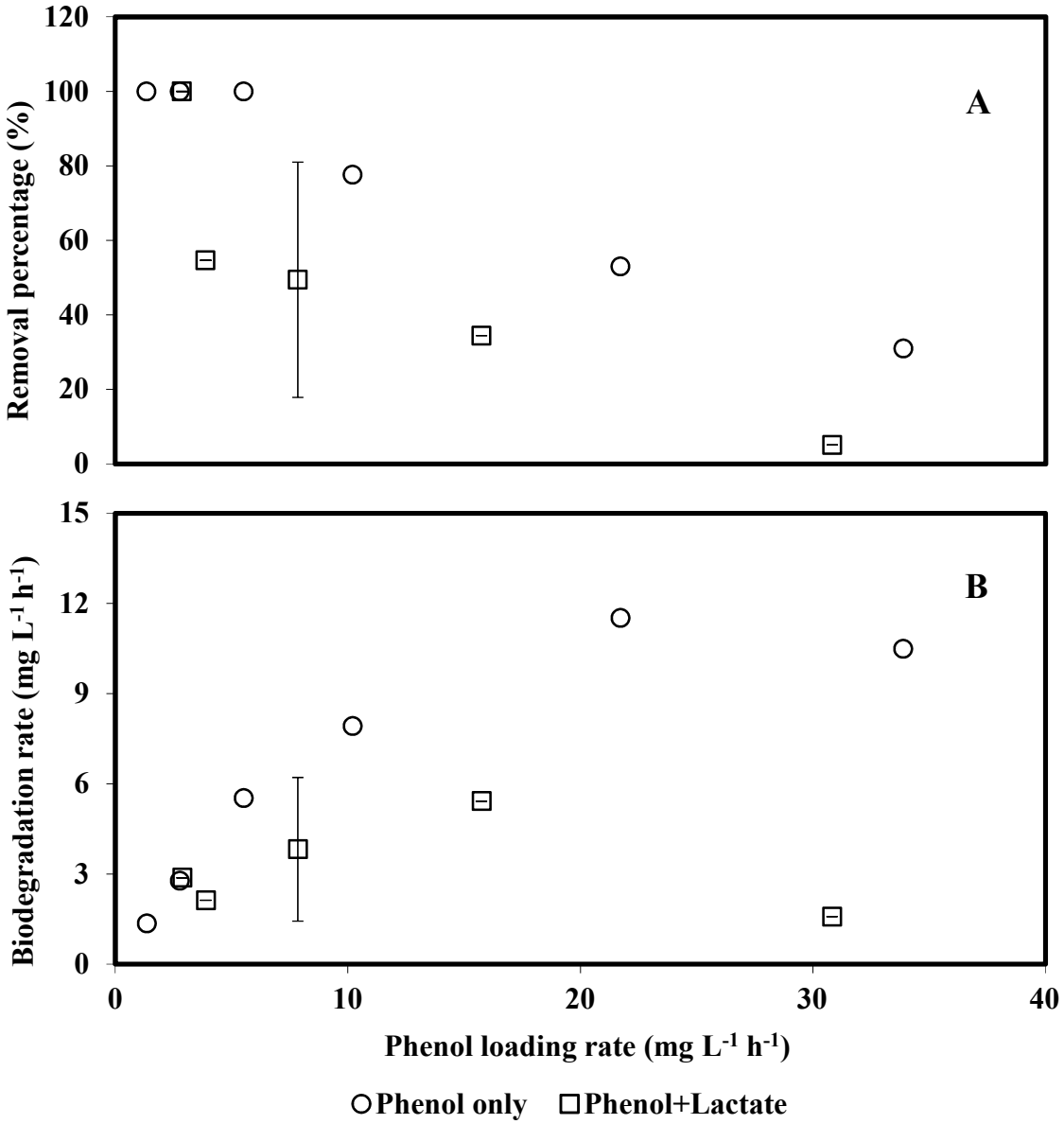

Figure 6.13 Removal percentages (A) and biodegradation rates (B) of phenol as a function of its loading rates in MFC with granular electrodes fed continuously with either phenol as sole substrate or in combination with lactate**.**

As seen in either case (i.e. phenol alone or in combination with lactate) phenol biodegradation rate increased as its loading rate was increased, reached the maximum level and then decreased. However, in terms of magnitude, phenol biodegradation rates achieved during co-biodegradation of phenol with lactate were lower than those with phenol alone, especially at the higher loading

rates (Figure 6.13B). Similarly, phenol removal efficiencies in the presence of lactate was lower than that with phenol alone (Figure 6.13A). This phenomenon that is consistent with what was observed in batch experiments in the MFCs with either rod or granular electrodes, indicates that contrary to expectations, presence of a compound more amenable to biodegradation (i.e. lactate) not only does not enhance the degradation of the recalcitrant compound (i.e. phenol) but due to preferential use of the more amenable substrate by microbial community, the degradation of recalcitrant compound is negatively impacted (i.e. lactate, as the more amenable substrate, is exclusively utilized while phenol is being ignored).

The removal percentages and biodegradation rates of lactate as well as the accumulation rates of biologically produced acetate obtained in MFCs fed continuously with lactate as sole substrate and in combination with phenol are shown and compared in Figure 6.14. Overall the results indicate that lactate biodegradation in granular electrode MFC fed continuously with various combinations of phenol and lactate was largely effective throughout the applied loading rates similar to those observed in identical MFC system fed with lactate as sole substrate. In both systems, lactate biodegradation rate improved with increase in loading rate at relatively the same rate. However, lower removal efficiencies and lactate biodegradation rates were observed at loading rates of 263.1 and 1318.7 mg L^{-1} h^{-1} that could be attributed to the use of 500 mg L^{-1} phenol in the feed mixture. Again, this could be an indication of the inhibitory effects of phenol at high concentrations.

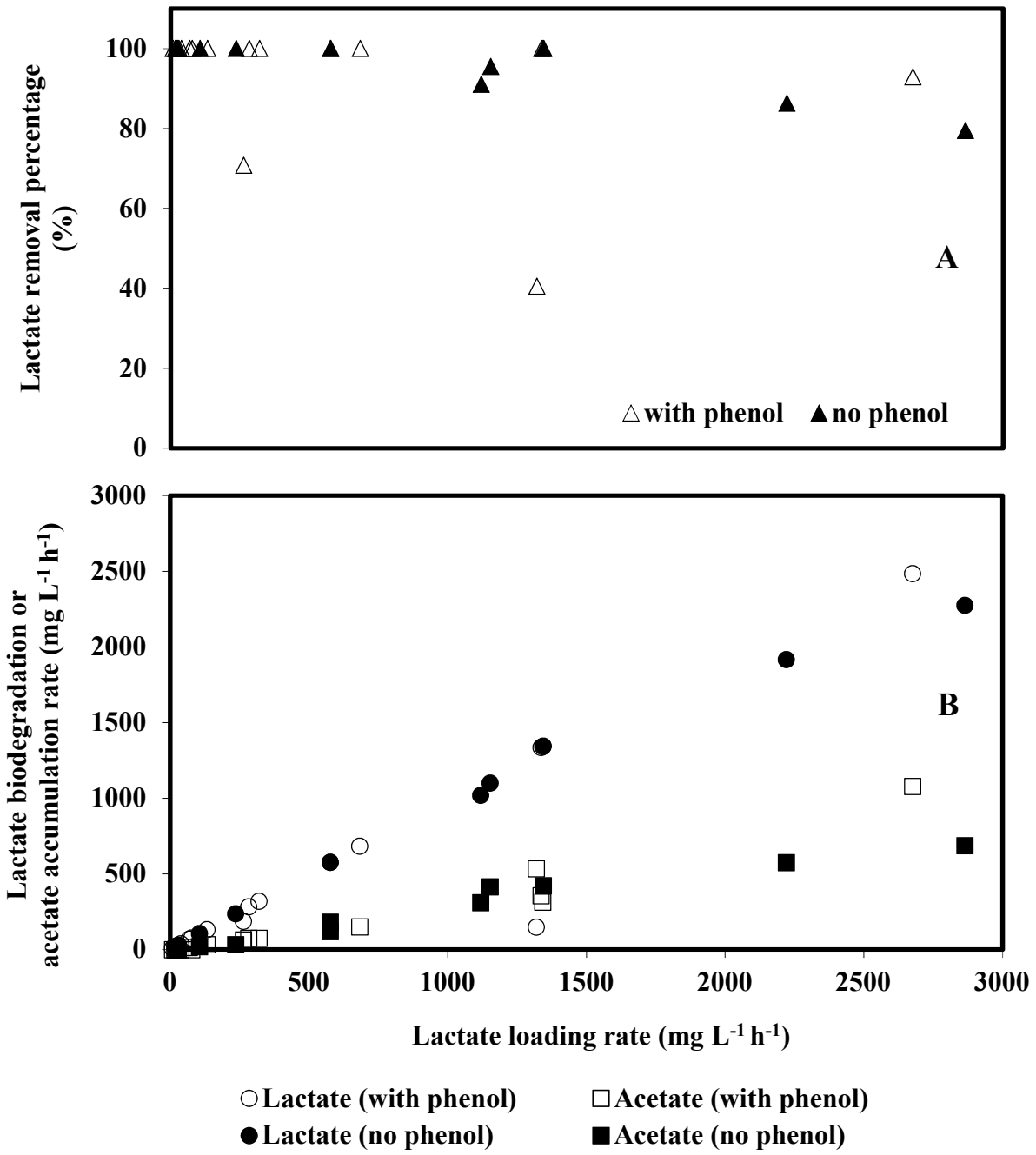

Figure 6.14 Removal percentages (panel A) and biodegradation rates of lactate as well as accumulation rates of acetate (Panel B) as function of lactate loading rates in MFC with granular electrodes fed continuously with lactate alone or in combination with phenol.

Profiles of acetate formation and the associated rate (acetate production rate) were also close in the presence and absence of phenol. In the presence of phenol, biologically produced acetate was

detected when lactate loading rate of 68.12 mg L^{-1} h^{-1} was applied. With increase in loading rate, accumulation rate of acetate increased as well and the highest accumulated acetate concentration of 387.7 mg L^{-1} was observed at the highest applied lactate loading rate of 2674.8 mg L^{-1} h^{-1}. Comparison of data shown in Figure 6.14 reveals that the degradation of lactate and accumulation of biologically produced acetate in continuously operated MFC with granular electrodes were not affected by the presence of phenol except when phenol concentration in the feed was high at 500 mg L^{-1}.

Power and current output: The power and current output from the continuously operated MFC with granular electrodes were determined at different loading rates of phenol and lactate, specifically 35 and 300 (Figure 6.15A), 85 and 300 (Figure 6.15B), 150 and 300 (Figure 6.15C) and 300 and 2700 (Figure 6.15D) mg L^{-1} h^{-1}, respectively. At these loading rates, experiments with varying phenol concentrations in the feed mixture while maintaining feed flowrate were carried out. Figures 6.15A-C represent results when feed contained 100, 250 and 500 mg L^{-1} phenol, respectively, in combination with 1000 mg L^{-1} lactate. Figure 6.15D shows results when feed flowrate was increased to its highest level of 200 mL h^{-1} with feed containing the same phenol and lactate amounts of 100 and 1000 mg L^{-1}, respectively.

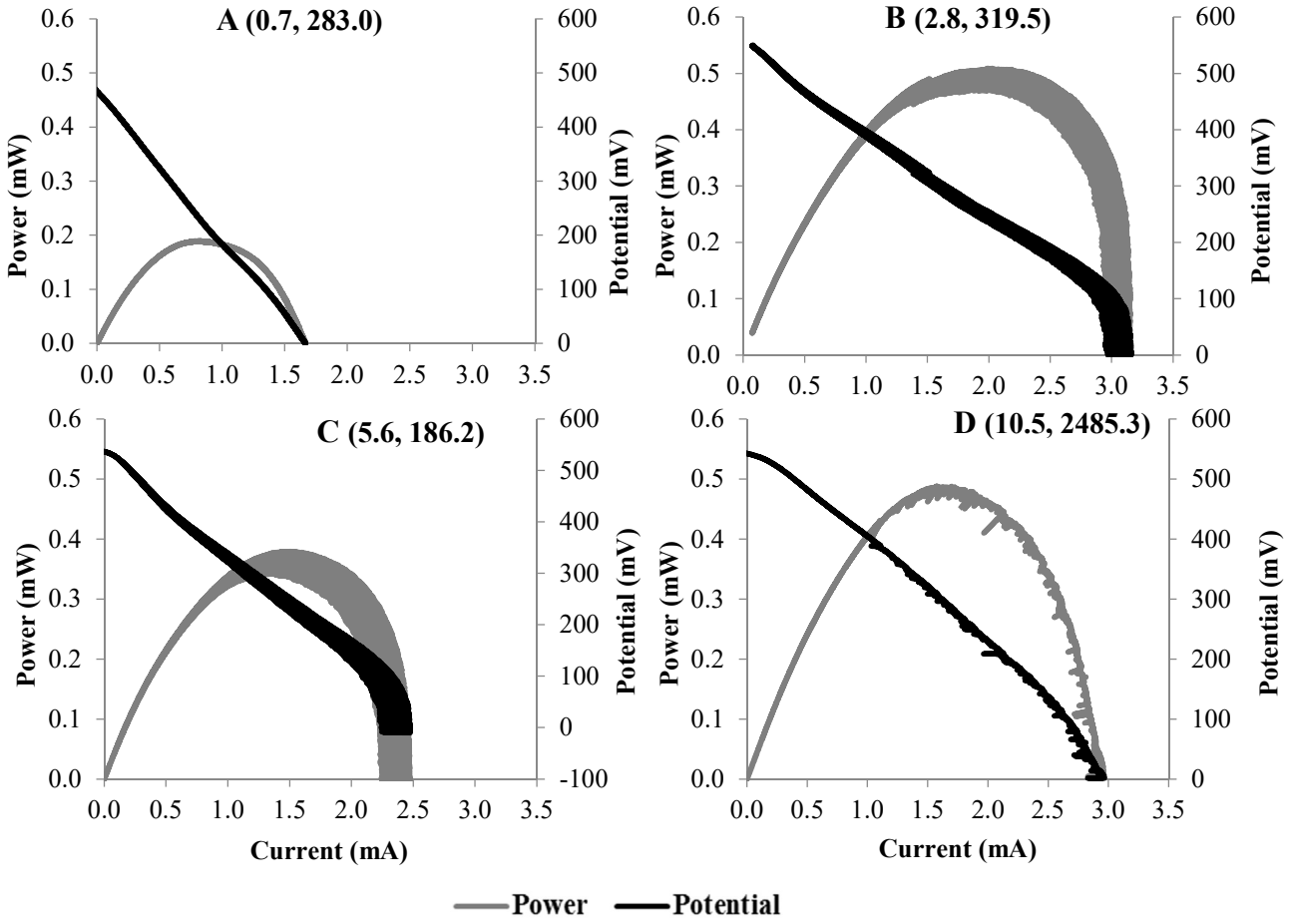

Figure 6.15 Polarization and power curves generated in a MFC with granular electrodes fed continuously with phenol and lactate at various loading rates; A 35 and 300 B) 85 and 300 C) 150 and 300 D) 300 and 2700 mg L^{-1} h^{-1}, respectively. Numbers in brackets represent respective phenol and lactate biodegradation rates in mg L^{-1} h^{-1}.

At the lower phenol and lactate loading rates (Figure 6.15A), the measured OCP was around 465 mV, while those obtained at the higher loading rates (Figures 6.15B-D) were relatively higher at approximately 550 mV. In terms of power and current, the maximum power obtained at the lowest evaluated loading rate was approximately 0.19 mW and attained a current of 0.81 mA, which translated to equivalent power and current densities of 2714.3 mW m^{-3} and 11571.4 mA m^{-3}, respectively. This output was significantly higher than those achieved in the batch systems but considerably lower at roughly half the magnitude achieved at the higher loadings rates. The highest

power density output of the continuous system was 7285.7 mW m^{-3} obtained at a current density of 28571.4 mA m^{-3} and measured when phenol and lactate loading phenol and lactate loading rates were 83.2 and 319.5 mg L^{-1} h^{-1} respectively.

Increasing the phenol loading rate to 155.9 mg L^{-1} h^{-1} with lactate loading rate at 263.2 mg L^{-1} h^{-1} resulted in lower power and current densities of 5428.6 mW m^{-3} and 21428.6 mA m^{-3}. At the highest applied loading rate of 310.7 mg L^{-1} h^{-1} phenol and 2674.5 mg L^{-1} h^{-1} lactate, power density of 7000.0 mW m^{-3} was comparable to the highest value indicated earlier but the corresponding current density was lower at 22857.1 mA m^{-3}. This output was generated when lactate biodegradation and acetate accumulation rates were at the highest. As with the batch systems, power and current output was found to have been affected considerably by the performance of MFC which was affected mainly by the extent of lactate degradation and not phenol and that both lactate removal percentage and biodegradation rate were instrumental in the MFC performance. To be more specific, the maximum power and current densities of 7285.7 mW m^{-3} and 28571.4 mA m^{-3} were obtained when lactate removal was 100% (loading and biodegradation rates: 319.5 and 319.5 mg L^{-1} h^{-1}) and lower power and current output of 7000.0 mW m^{-3} and 22857.1 mA m^{-3} occurred when lactate removal percentage was lower and around 92.9% (loading and biodegradation rates: 2674.5 and 2485.3 mg L^{-1} h^{-1}). This was despite the fact that biodegradation rate in the latter case was higher. Consistent with this trend lower power and current densities of 5428.6 mW m^{-3} and 21428.6 mA m^{-3} were attained when lactate removal percentage was only 70.8% (loading and biodegradation rates: 263.2 and 186.2 mg L^{-1} h^{-1}).

Since power and current output during co-biodegradation of phenol and lactate was dictated by the extent of lactate biodegradation, comparison to previous experiment with lactate as sole substrate was more relevant. The closest lactate loading rate where polarization and power curves were generated from the previous experiment was at 2220 mg L^{-1} h^{-1} which resulted in a higher power density of 9444.4 mW m^{-3} but a lower current density of 17444.4 mA m^{-3} compared to the power and current outputs generated during co-biodegradation. This result could indicate that outputs were within comparable range especially that lactate biodegradation and acetate accumulation rates of the two systems were comparable.

6.3.3. Co-biodegradation of phenol and lactate in the presence of neutral red

Batch mode of operation: The effect of addition of neutral red as electron mediator on the co-biodegradation of phenol and lactate was evaluated in MFC with granular electrodes. Batch experiments similar to those conducted in MFC with granular electrodes were essentially repeated but with the addition of 28.9 mg L^{-1} neutral red (Park and Zeikus, 2000). Results from the experiments in MFC with granular electrode fed sequentially with different combinations of phenol and lactate in the presence of neutral red is shown in Figure 6.16. The biodegradations of 100 mg L^{-1} phenol and 1000 mg L^{-1} lactate with neutral red occurred simultaneously and without any lag phase in microbial activity or biodegradation. Complete degradation of both substrates proceeded with lactate depletion progressing faster than that of phenol. These findings were consistent with those observed in the MFC with granular electrodes in the absence of neutral red. After complete exhaustion of phenol and lactate, another batch of 100 mg L^{-1} phenol and 1000 mg L^{-1} lactate with neutral red was added and similar findings were observed. After completion of these runs, sequential addition of higher phenol concentrations (250-500 mg L^{-1}) in combination

with the same lactate and neutral red concentrations (1000 and 28.9 mg L^{-1}, respectively) was conducted. The succeeding experiments applied with combinations containing higher initial phenol concentrations revealed similar patterns as the initial runs with 100 mg L^{-1} phenol and 1000 mg L^{-1} lactate and neutral red.

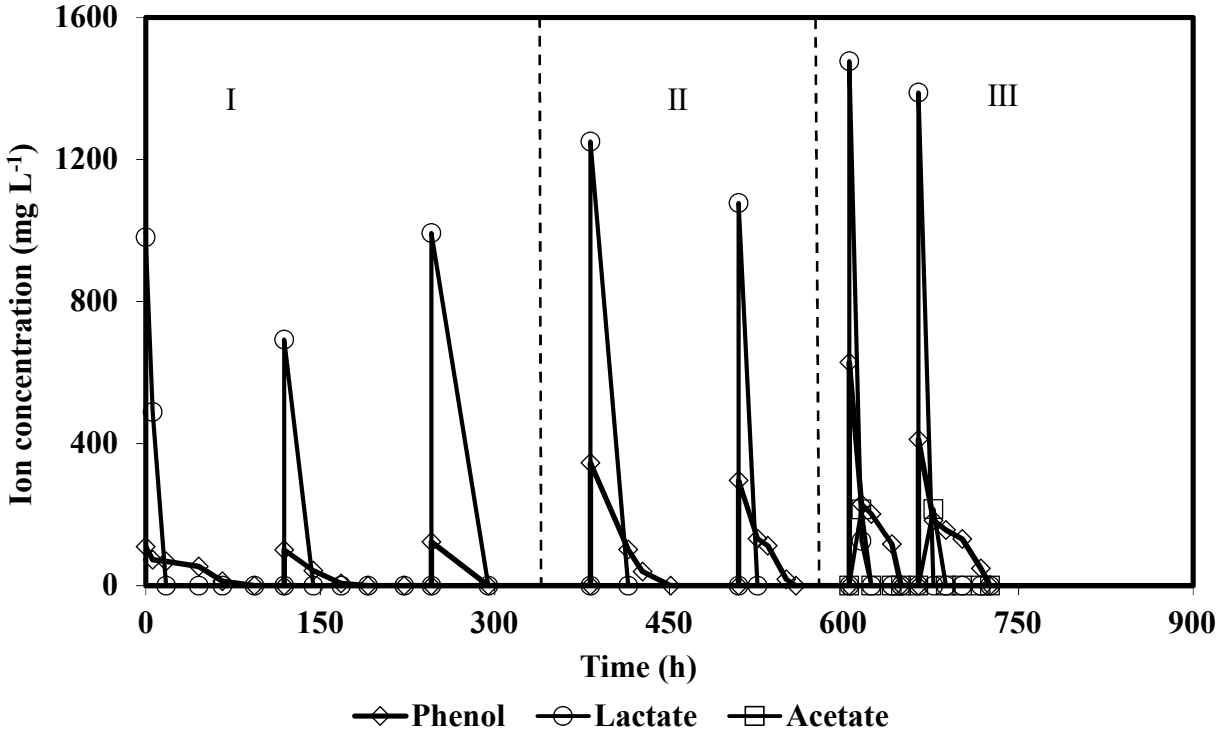

Figure 6.16 Co-biodegradation of phenol and lactate as combined substrate in an MFC with granular electrodes with 28.9 mg L^{-1} neutral operated batchwise and sequentially with approximately 1000 mg L^{-1} lactate and phenol at various initial concentrations of (I): 100 mg L^{-1} phenol; (II): 250 mg L^{-1} phenol; (III): 500 mg L^{-1} phenol.

In all evaluated combinations, simultaneous biodegradation of both substrates was achieved with lactate depletion occurring faster than phenol as observed in similar batch experiments in the absence of neutral red. This was contrary to the pattern observed in MFCs with rod electrodes, where phenol biodegradation proceeded after complete consumption of lactate and accumulated

and biologically produced acetate. This observation was particularly noticeable during the co-biodegradation of higher initial concentrations of phenol and lactate where in the presence of neutral red all available substrates, including accumulated acetate, were consumed simultaneously. It should be pointed out that accumulation of acetate was observed only with higher lactate concentrations (approximately 1400 mg L^{-1}) where the amount of lactate was high enough to allow formation of acetate at the notable levels.

Biodegradation rates of lactate and phenol: Using the slope of concentration profiles, biodegradation rates of phenol and lactate for various combinations were calculated. Average phenol biodegradation rates achieved in granular electrode MFC with neutral red with combinations of 1000 mg L^{-1} lactate and 100, 250 and 500 mg L^{-1}phenol were 1.67 ± 0.76, 5.52 ± 0.50 and 8.57 ± 4.21 mg L^{-1} h^{-1}, respectively. Similar to previous experiments involving phenol as substrate, biodegradation rate increased with increase in initial concentration of phenol from 100 to 500 mg L^{-1}, more so when neutral red was added where inhibition effect of phenol was rendered minimal or nonexistent even at the highest tested concentration. Figure 6.17 compares the biodegradation rates of phenol in various mixtures of phenol and lactate in MFCs with rod electrodes and granular electrodes in the presence or absence of neutral red. Overall and regardless of the mixture compositions, biodegradation rates in MFC with granular electrodes and neutral red had the highest values, followed by MFC with granular electrodes without neutral red while MFC with rod electrodes had the lowest rates.

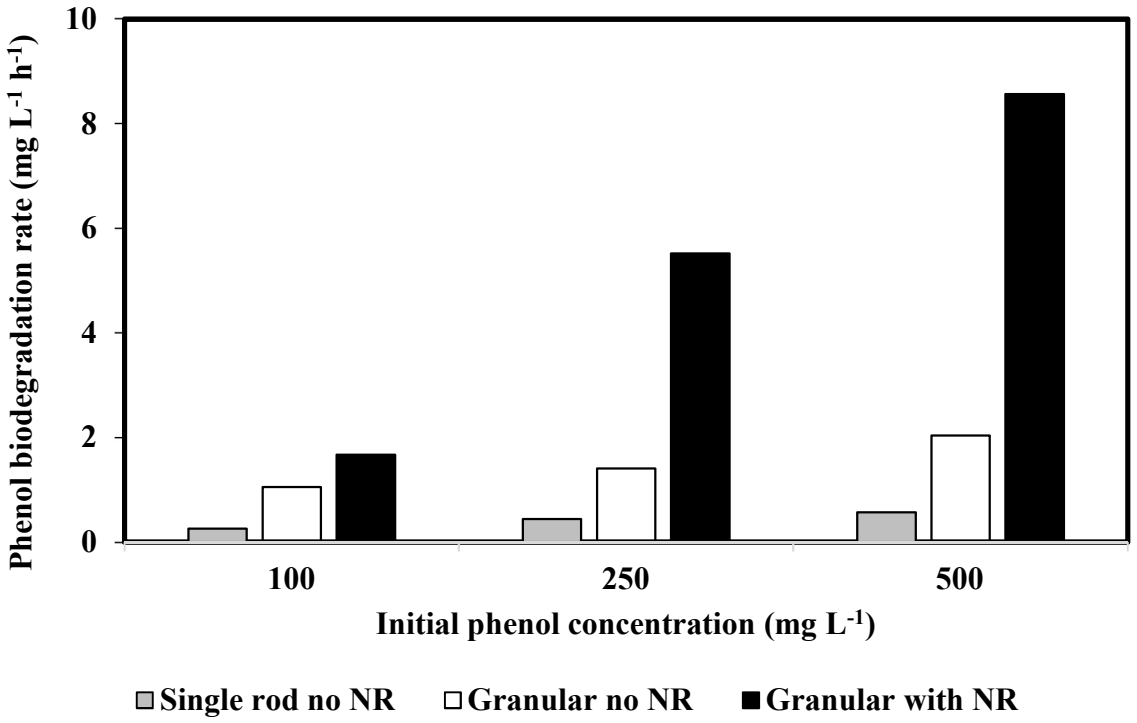

Figure 6.17 Biodegradation rates of phenol at different initial concentrations in MFCs with single rod and granular graphite electrodes with and without neutral red (NR) operated with 1000 mg L^{-1} lactate and various concentrations of phenol (100-500 1000 mg L^{-1}).

Presence of neutral red did not alleviate the negative impact of lactate on phenol biodegradation and the rates observed in the experiments with combined substrates were lower than those obtained with neutral red and phenol alone. For instance, at a phenol concentration of 500 mg L^{-1}, MFC with granular electrode and neutral red achieved a biodegradation rate of 13.0 mg L^{-1} h^{-1} compared with a rate of 8.57 mg L^{-1} h^{-1} achieved when 500 mg L^{-1} phenol was combined with 1000 mg L^{-1} lactate. This finding confirmed the negative effect of a more amenable substrate such as lactate on phenol biodegradation regardless of the presence or absence of neutral red.

Lactate biodegradation rates in the mixture of phenol and lactate of different combinations obtained in MFCs with single rod and granular electrodes with or without neutral red are compared

in Figure 6.18. Results showed that in the presence of neutral red, increase in initial phenol concentration did not cause deterioration in lactate biodegradation rate unlike those observed in the absence of neutral red and surprisingly lactate biodegradation rate increased with increase in initial phenol concentration with the rates being 34.1 ± 17.9, 52.9 ± 20.4 and 93.3 ± 19.2 mg L^{-1} h^{-1} when lactate was combined with 100, 250 and 500 mg L^{-1} phenol, respectively. This unexpected trend could be due to the unintentional increase in initial lactate concentration when combined with phenol (i.e. average initial concentrations of lactate were 889.1, 1164.4 and 1433.0 mg L^{-1} with 100, 250 and 500 mg L^{-1} phenol, respectively).

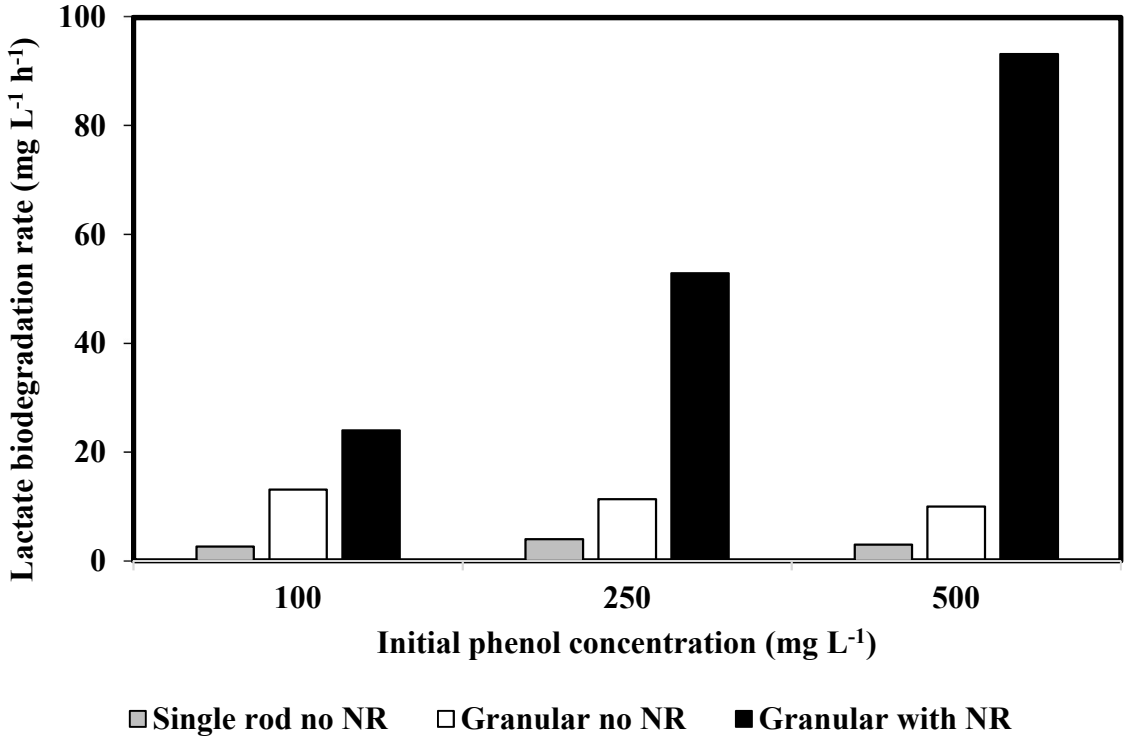

Figure 6.18 Biodegradation rates of lactate in mixture of phenol and lactate obtained in MFCs with single rod and granular graphite electrodes with and without neutral red (NR) fed with combinations of phenol and lactate**.**

Comparing results obtained in MFCs with granular electrode shows that the addition of neutral red during the co-biodegradation of phenol and lactate led to an average lactate biodegradation rate of 60.1 ± 3.2 mg L^{-1} h^{-1} which was substantially higher than the average biodegradation rate in the absence of neutral red which was only 11.5 ± 2.9 mg L^{-1} h^{-1}. Furthermore, this average lactate biodegradation rate (60.1 ± 3.2 mg L^{-1} h^{-1}) was also higher than the biodegradation rate of 23.1 mg L^{-1} h^{-1} achieved in MFC with granular electrode fed with lactate as the sole substrate and in the absence of neutral red. In MFCs with rod electrodes and no added neutral red, the average lactate biodegradation rate from the co-biodegradation of 500-1000 mg L^{-1} lactate and 100-500 mg L^{-1} phenol was substantially lower at around 3.7 mg L^{-1} h^{-1}.

Although the negative impacts of lactate on overall biodegradation of phenol is repeatedly seen in various experiments conducted in this part of the research, a closer look at phenol and lactate co-biodegradation pattern specially at high lactate initial concentrations as shown in Figure 6.19, reveals two distinct phases in phenol biodegradation. In the first stage when both lactate and phenol are present and undergo biodegradation simultaneously, phenol biodegradation is rather fast with an average rate of 27.78 ± 14.5 mg L^{-1} h^{-1}. In the second stage which starts with depletion of lactate a substantial decrease in phenol biodegradation rate (5.04 ± 1.84 mg L^{-1} h^{-1}) is observed.

One could speculate that presence of lactate as the more amenable substrate at high level creates an environment favourable for microbial activity and potentially leads to release of the enzymes that could assist with degradation of phenol and enhance the phenol biodegradation rate. One should note that the during the first stage, lactate is used preferentially and with a fast rate. Depletion of lactate could lead to deterioration of this favourable environment and thus a

slowdown in the biodegradation of the phenol. It could also be speculated that the formation of accumulated acetate could have caused the slowdown in phenol degradation. However, this effect is the least likely to have occurred since no improvement in phenol biodegradation was observed immediately after depletion of accumulated acetate. To understand this phenomenon, it is recommended to evaluate the co-biodegradation of phenol and lactate at higher lactate concentrations which would provide a longer timeframe for frequent sampling and analysis resulting in more accurate information during these two stages of biodegradation.

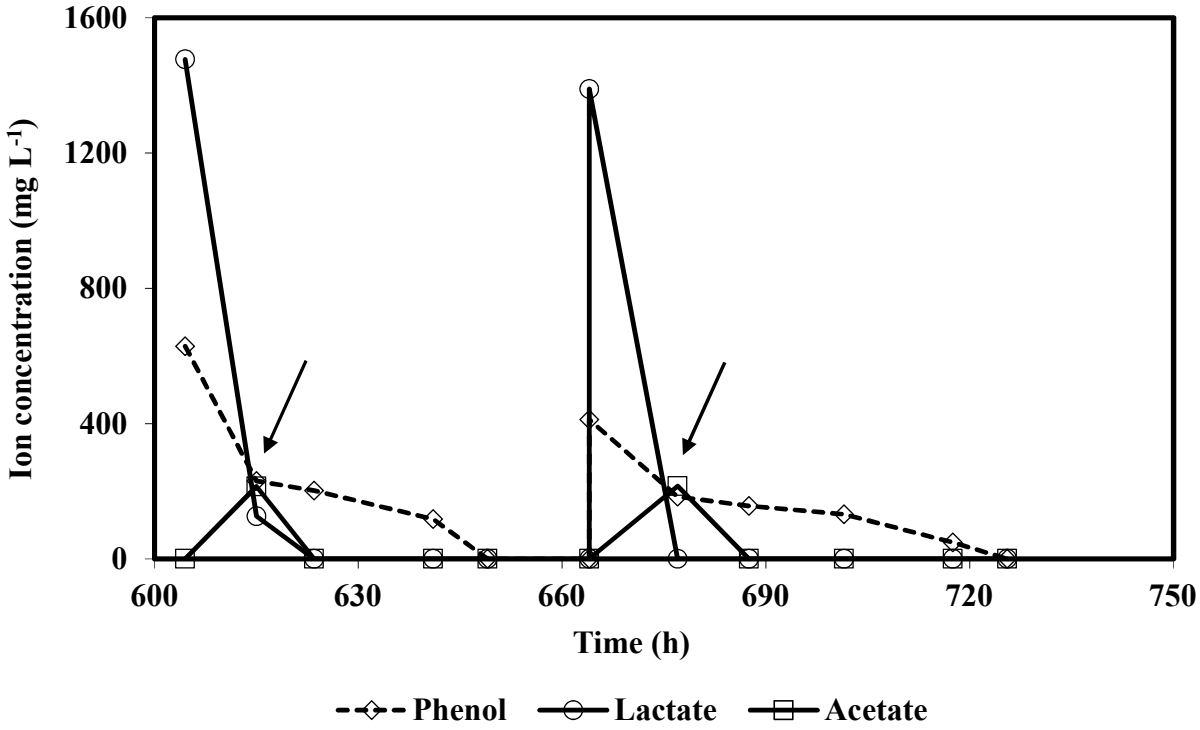

Figure 6.19 Co-biodegradation of approximately 500 mg L^{-1} phenol and 1000 mg L^{-1} lactate including acetate accumulation and biodegradation profile in an MFC with granular electrodes with added neutral red operated batchwise. Arrows indicate point of change in phenol biodegradation.

Power and current output: Similar to previous experiments in MFCs with granular electrodes, an external resistance of 50 ohm was applied across the circuit of the MFC which resulted to correspondingly low potential readings. For more appropriate determination of current and power output, polarization and power curves were generated by conducting LSV analysis using a potentiostat. The LSV runs were conducted when the MFC with granular electrodes and neutral red was operated with combinations of approximately 1000 mg L^{-1} lactate and the lowest and highest phenol concentrations of either 100 or 500 mg L^{-1}. The resulting polarization and power curves are shown in Figure 6.20. When operated with approximately 100 mg L^{-1} phenol and 1000 mg L^{-1} lactate (Figure 6.20A), the MFC generated an OCP of 537 mV, and a maximum power output of 0.19 mW attained at a current of 0.59 mA. The equivalent power and current densities were calculated to be approximately 2242.4 mW m^{-3} and 6884.7 mA m^{-3}, respectively.

The results of the second LSV run with a combination of 500 mg L^{-1} phenol and 1000 mg L^{-1} are shown in Figure 6.20B. As seen, the OCP could not be determined directly since it was beyond the range of the applied potential sweep where the upper limit set to only 540 mV. To estimate the OCP, the polarization curve that is typically linear was extrapolated and the y-axis intercept was used as the OCP. Based on this extrapolation line ($R^2 = 0.996$) the OCP was estimated as 707 mV. From the power curve, the maximum power achieved from the MFC was 0.33 mW at a current of 0.88 mA which would translate to equivalent power and current densities of 3847.2 mW m^{-3} and 10322.4 mA m^{-3}, respectively. Results show that OCP, power and current output was higher when higher concentrations of substrates were used. More importantly, the resulting higher power and current output coincide with the improved biodegradation rates of both lactate and phenol. As reported earlier, biodegradation rates of lactate and phenol were approximately 3 folds higher in

the experiment with 500 mg L^{-1} phenol due to an unintentional higher lactate concentration used in this experiment.

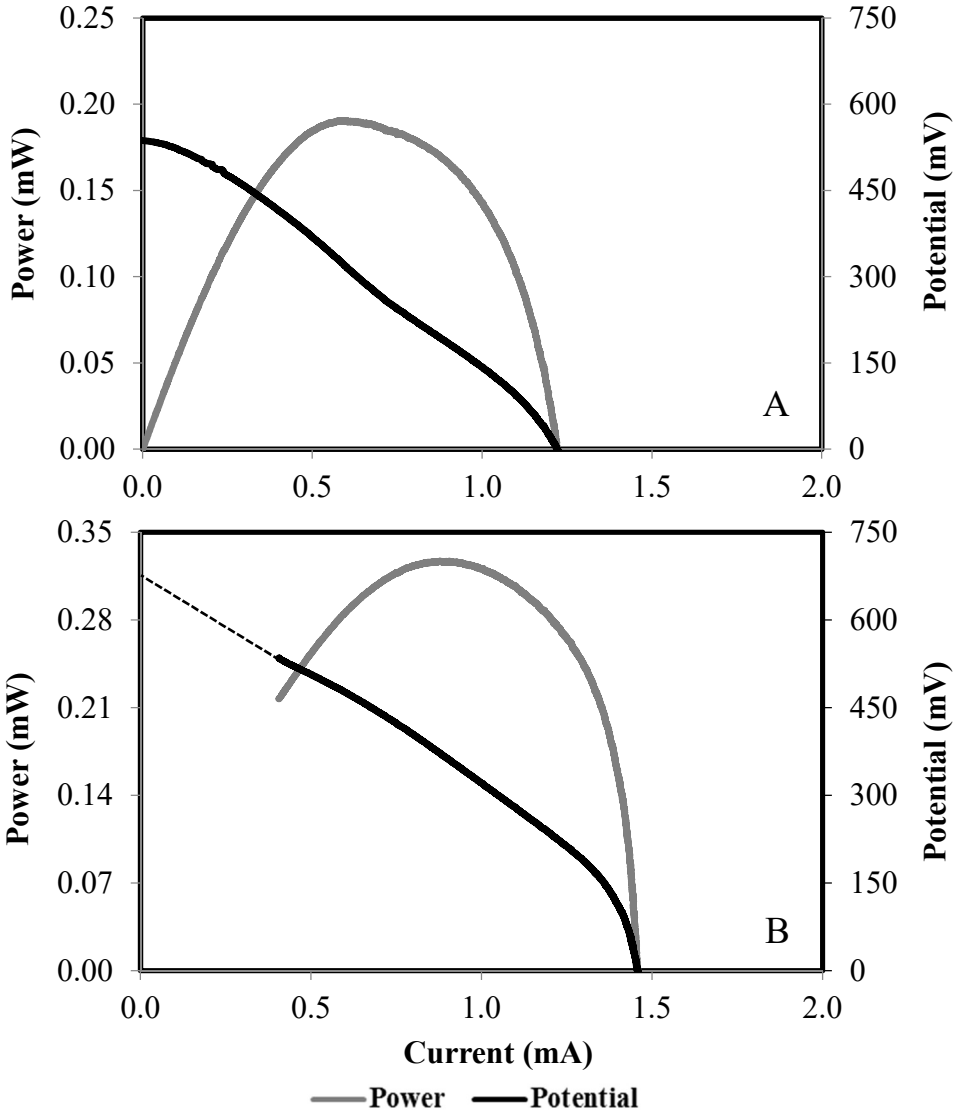

Figure 6.20 Polarization and power curves generated during batch co-biodegradation of (A) 100 mg L^{-1} phenol and 1000 mg L^{-1} lactate and (B) 500 mg L^{-1} phenol and 1000 mg L^{-1} lactate in an MFC with granular graphite electrodes and neutral red. The extrapolation line used to determine the OCP is shown as part of the polarization.

OCP, power and current output achieved when phenol and lactate were combined as substrates in the absence of neutral red were substantially higher than those obtained in a similar MFC with

neutral red and phenol (1000 mg L^{-1}) as sole substrate, with the observed values in the latter case being 302 mV, 428.6 mW m^{-3} and 2285.7 mA m^{-3}, respectively. This was despite a lower phenol biodegradation rate of 8.6 mg L^{-1} h^{-1} obtained with combined substrate as opposed to a rate of 13.0 mg L^{-1} h^{-1} achieved with phenol as the sole substrate. The presence of lactate, which has been shown to enhance power and current output during co-biodegradation in a similarly operated MFC without neutral red, could be the reason for to the improved performance. In other words, lactate appear to play a more critical role in the extent of power and current outputs in MFCs used for co-biodegradation of phenol and lactate, regardless of presence or absence of neutral red.

Continuous mode of operation: Continuous biodegradation of phenol and lactate in MFC with granular electrode and neutral red were carried out starting at a feed flow rate of about 5 mL h^{-1} that then increased to 20 and 100 mL h^{-1} or at equivalent dilution rates of 0.06 to 1.4 h^{-1}. Feed was composed of approximately 1000 mg L^{-1} lactate in combination with either 100, 250 or 500 mg L^{-1} phenol. The applied loading rates ranged from 7.4-766.0 mg L^{-1} h^{-1} for phenol and 57.6-1474.1 mg L^{-1} h^{-1} for lactate. The continuous experiment started with a feed containing 1000 mg L^{-1} lactate in combination with the lowest phenol concentration of 100 mg L^{-1}. The MFC was operated at all indicated flow rates before phenol concentration in the feed was increased. Results for biodegradation of phenol and lactate at the different applied loading rates including the corresponding removal percentages in MFC with granular electrodes and neutral red are shown in Figures 6.21 and 6.22, respectively.

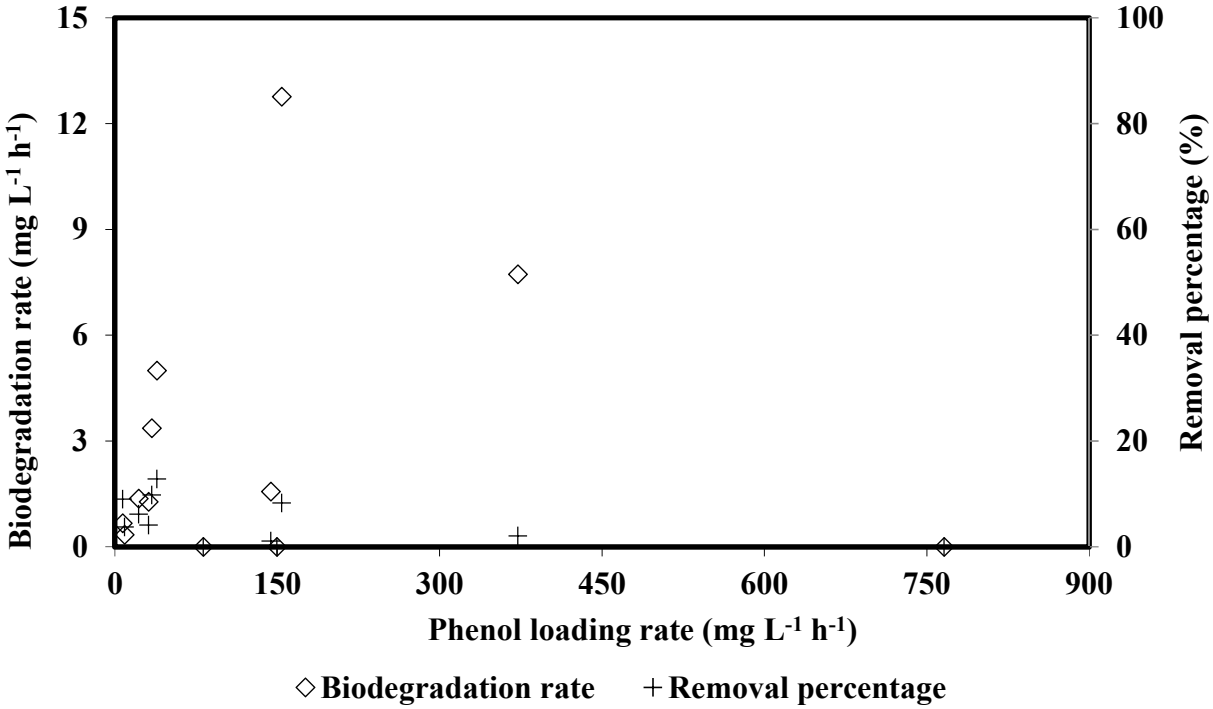

Figure 6.21 Biodegradation rate and removal percentage of phenol as a function of its loading rate in MFC with granular electrodes and neutral red operated continuously with different combinations of phenol and lactate.

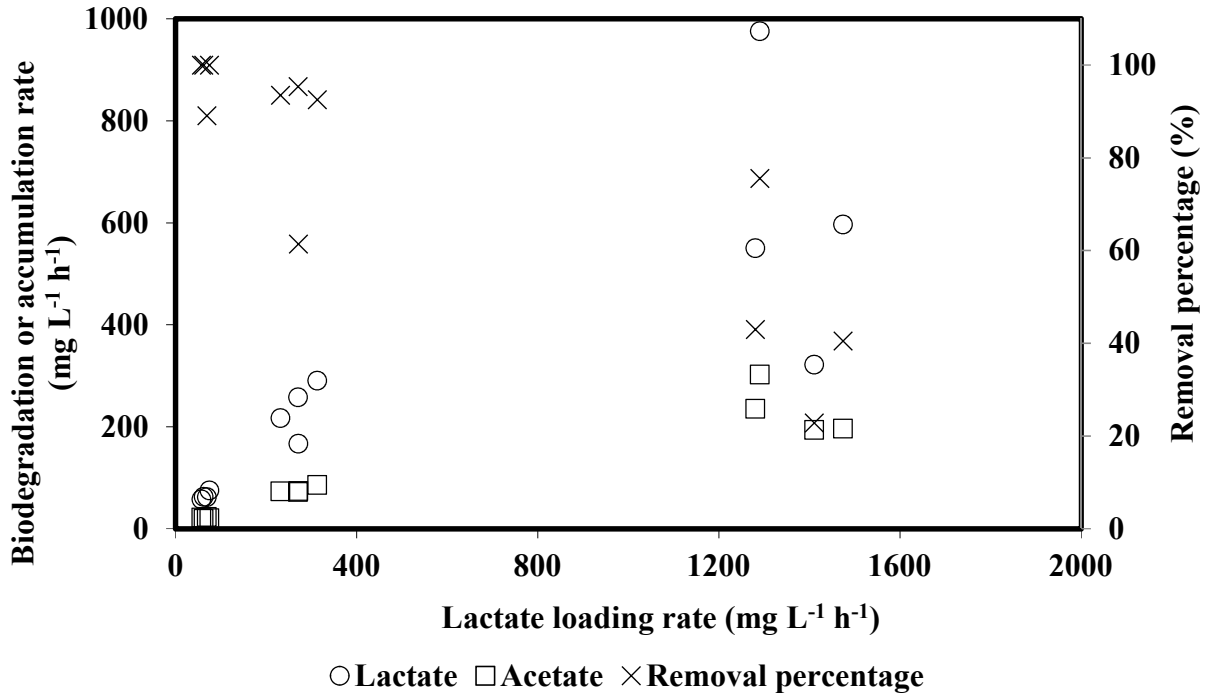

Figure 6.22 Biodegradation rate and removal percentage of lactate including accumulation rate of acetate as a function of lactate loading rate in MFC with granular electrode and neutral red operated continuously with different combinations of phenol and lactate.

At the initial feed flowrate of 4.4 mL h^{-1} corresponding to the lowest phenol loading rate of 7.4 mg L^{-1} h^{-1}, biodegradation of phenol was considerably slow with a corresponding rate of 0.67 mg L^{-1} h^{-1} and a removal percentage of only 9.0%. Simultaneous degradation of lactate resulted to a residual lactate concentration of 120.7 mg L^{-1} which translated to a lactate biodegradation rate of 62.03 mg L^{-1} h^{-1} and removal percentage of 89.1%. As loading rate was increased, similar outcomes on the biodegradation of phenol were observed throughout the applied loading rates (i.e. very low removal percentage and biodegradation rate). Difficulty in phenol biodegradation was evident at all applied loading rates regardless of initial phenol concentration and loading rate.

For the entire applied loading rate range, biodegradation of phenol was ineffective with average phenol removal percentage being around 4.8% which translates to residual phenol concentrations of 95.2, 238.0 and 476.0 mg L^{-1} for feeds containing 100, 250 and 500 mg L^{-1} phenol, respectively. The maximum phenol removal percentage was only 12.8% at a loading rate of 38.9 mg L^{-1} h^{-1} and no phenol reduction at all transpired at the higher loading rates (>373 mg L^{-1} h^{-1}). Phenol biodegradation rate was also considerably low ranging from 0-12.8 mg L^{-1} h^{-1} and an average value of only 2.8 mg L^{-1} h^{-1}. This was lower than the average rate obtained in a similarly operated MFC without neutral red (6.2 mg L^{-1} h^{-1}). This finding indicates that the addition of neutral red in a continuously operated MFC fed with various combinations of phenol and lactate did not enhance phenol biodegradation.

Despite the ineffective phenol biodegradation increases in loading rate was continued to investigate the potential inhibitory effect of phenol on the lactate biodegradation. As shown in Figure 6.22, despite the poor performance in terms of phenol biodegradation, MFC with granular

electrode and neutral red was effective in the biodegradation of lactate over the majority of the applied loading rates. Overall improvement in lactate biodegradation rate was observed as loading rate was increased.

To assess the possible inhibitory effect of phenol on lactate biodegradation, biodegradation rates of lactate and corresponding removal percentages at various lactate loading rates was plotted as a function of initial phenol concentration in the mixture (Figure 6.23). At the lowest loading rate between 63-75 mg L^{-1} h^{-1}, lactate biodegradation rate was essentially the same in the presence of all evaluated phenol concentrations. Increasing the range of loading rate to about 230-310 and 1280-1474 mg L^{-1} h^{-1} resulted to very slight differences in the biodegradation rate but in no particular order of magnitude with respect to phenol concentration. To be more clear, average lactate biodegradation and associated standard deviation at three evaluated loading rate ranges corresponding to flow rates of 5, 20 and 100 mL h^{-1}, calculated using the rates in the presence of 100, 250 and 500 mg L^{-1} phenol, were 65.9 ± 8.2, 239.8 ± 43.7, 598.6 ± 49.3 mg L^{-1} h^{-1}, respectively. The small values of standard deviation indicate that the effect of phenol on lactate biodegradation was insignificant. In terms of removal percentage, no considerable difference among the results observed with various phenol concentrations at each applied loading rate was observed.

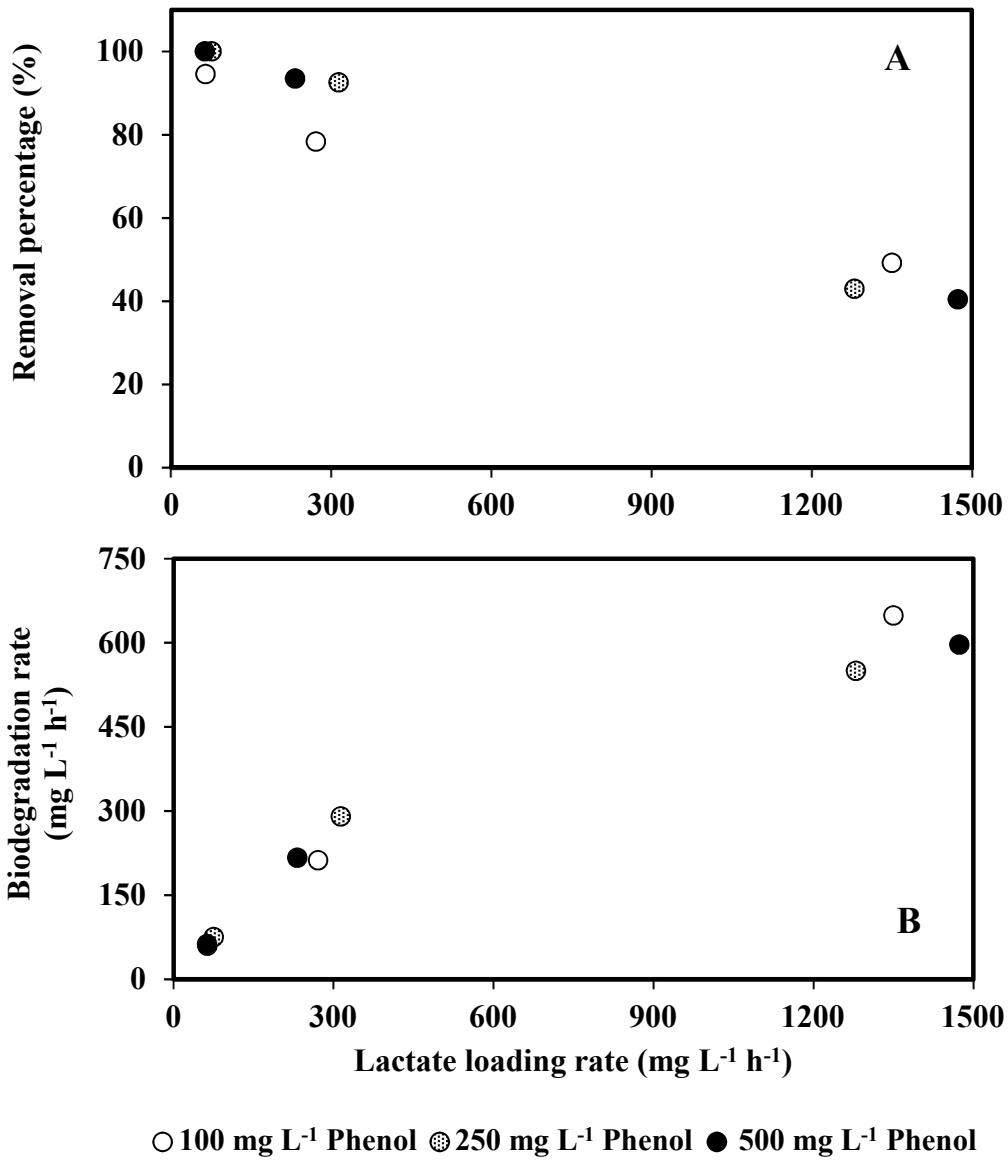

Figure 6.23 Removal percentage (A) and biodegradation rate (B) of lactate as a function of its loading rate at different phenol concentrations in MFC with granular electrodes and neutral red, fed continuously with various combinations of phenol and lactate**.**

Accumulation rate of biologically generated acetate attained at different initial phenol concentrations was also compared and as seen in (Figure 6.24) acetate accumulation rate observed at various phenol concentrations were relatively close. Overall, these findings suggest that phenol in the range 100-500 mg L^{-1} did not affect biodegradation of lactate and consequently

accumulation of acetate. Increase in loading rate from 67 to 230-310 mg L^{-1} h^{-1} and subsequently to 1280-1475 mg L^{-1} h^{-1} improved the lactate biodegradation rate and acetate accumulation rate from 64.4 and 21.2, to 232.9 and 76.2, and 611.1 and 231.9 mg L^{-1} h^{-1}, respectively. Similarly, removal percentage of lactate was decreased from 97.3 to 85.7 and then 45.5% as a result of increase in loading rate. This finding was consistent with the results obtained in similarly operated MFC without neutral red but in that case the decrease in lactate removal percentage was not as drastic and complete or high removal percentage was observed for a wider range of applied loading rates.

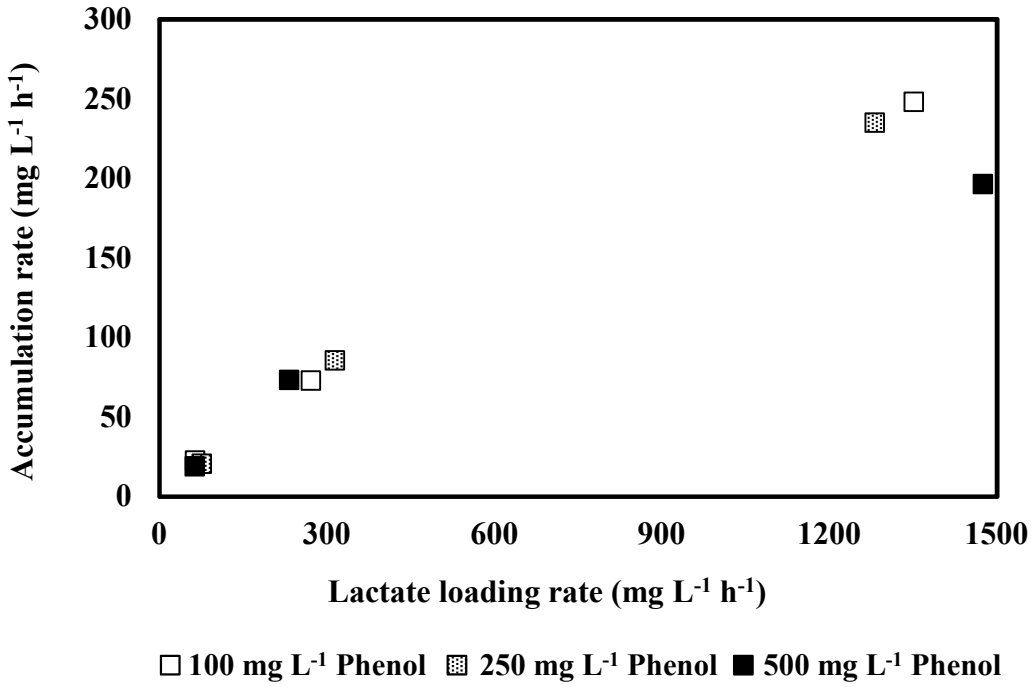

Figure 6.24 Accumulation rate of biologically produced acetate as a function of lactate loading rate at different phenol concentrations in MFC with granular electrode and neutral red fed continuously with various combinations of phenol and lactate.

Biodegradation rates and removal percentages of phenol achieved in similar loading rates in MFCs with granular electrode in the presence and absence of neutral red are compared in Figure 6.25. In the MFC without neutral red, typical biodegradation rate profile from a continuous system was observed whereby increase in loading rate increased phenol biodegradation rate which then reached a peak and decreased due to further increase in the loading rate. On the other hand, in similar MFC with neutral red, biodegradation of phenol was not effective for the most if not all applied loading rates, as reflected in the corresponding removal percentages (9% at the lowest and an average value of 4.8% for higher applied loading rates). In the system without neutral red, complete phenol removal was achieved at the lowest loading rate which eventually declined with increase in loading rate leading to gradual deterioration in biodegradation performance.

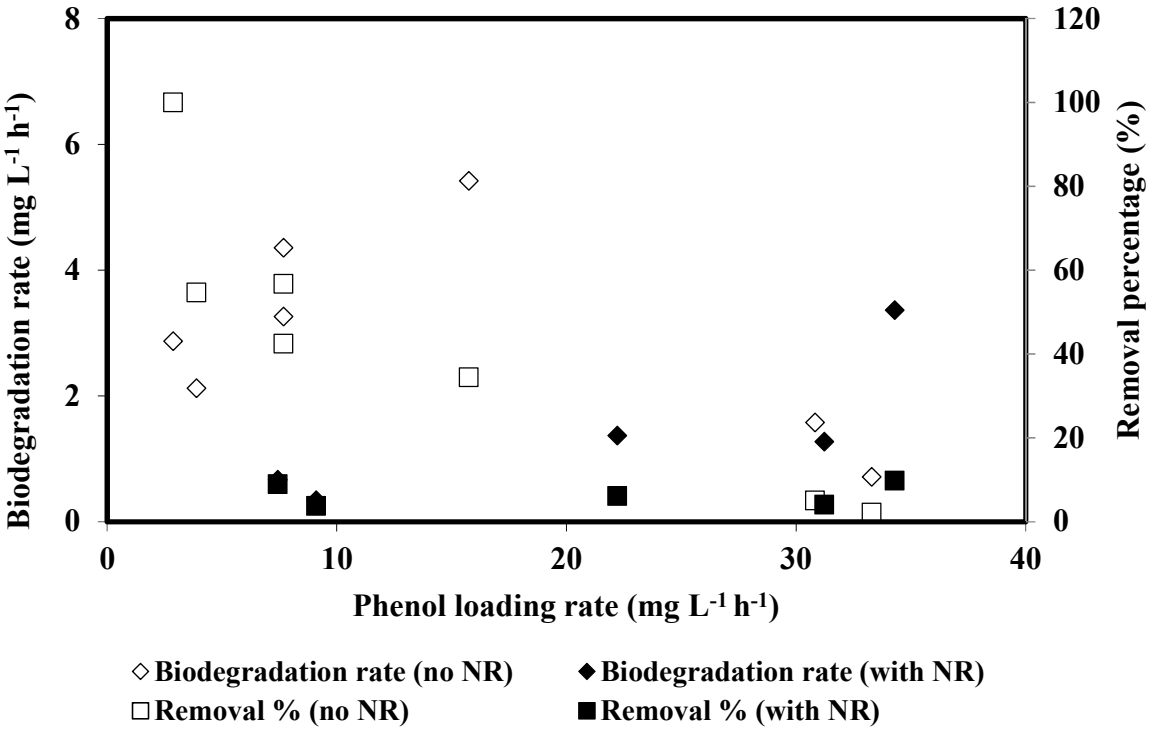

Figure 6.25 Biodegradation rates and removal percentages of phenol as function of phenol loading rate in MFC with granular electrodes inoculated with *P. putida* and fed continuously with different combinations of phenol and lactate with or without neutral red (NR).

Performance of MFC in terms of lactate biodegradation and acetate accumulation rates in the presence and absence of neutral red are compared in Figure 6.26. For the lactate loading rates up to approximately 320 mg L^{-1} h^{-1} lactate biodegradation and acetate accumulation rates of were close and almost fit the same trendlines with and without neutral red. At higher loading rates, however, both rates appeared to have been negatively affected by the presence of neutral red resulting in considerably lower values at higher loading rates.

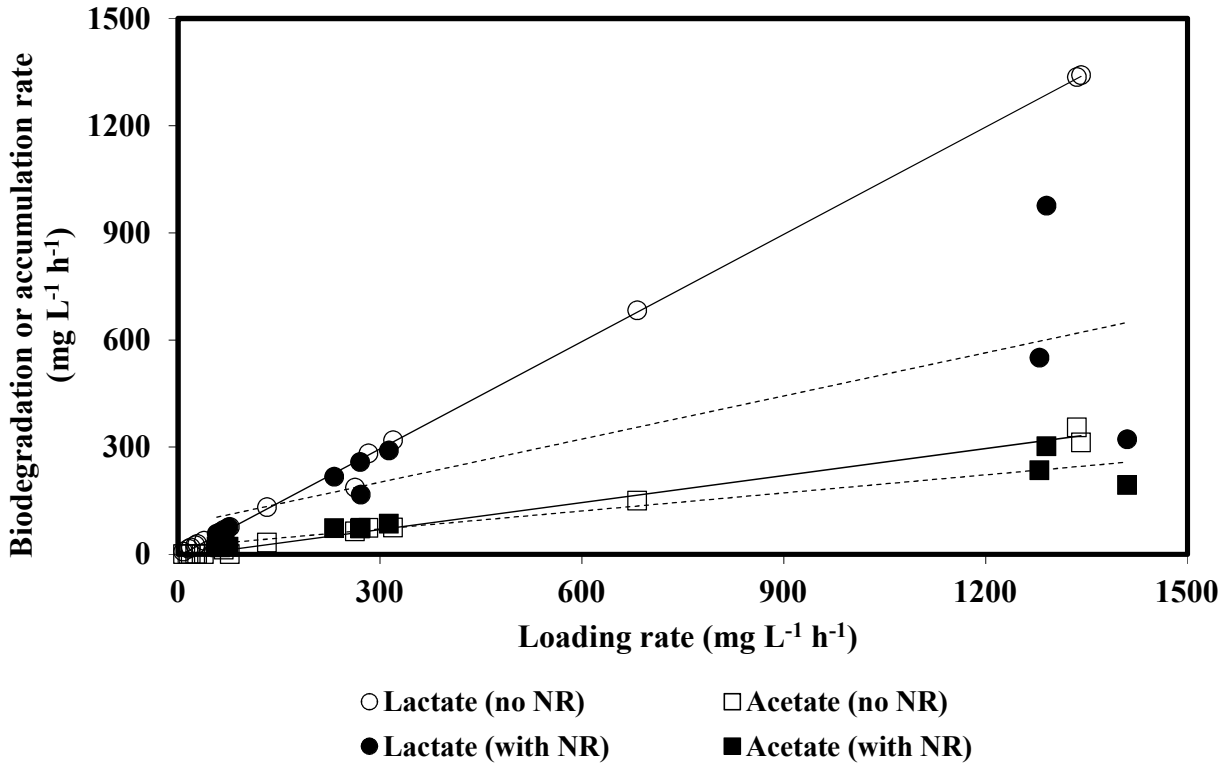

Figure 6.26 Biodegradation rate of lactate and accumulation rate of acetate as function of lactate loading rate in MFCs with granular electrode operated continuously with different combinations of phenol and lactate with or without neutral red (NR). Dashed and solid lines represent the rates trend lines in MFC with and without NR, respectively.

Power and current output: As discussed in previous parts of the results, the power and current outputs in batch or continuously operated MFCs with granular electrodes without neutral red, as well as in the batch operated MFCs with granular electrodes with neutral red were dictated mainly

by the extent of lactate biodegradation and not so much by biodegradation of phenol. This pattern was even more evident in the current set of experiments since phenol biodegradation over the most applied loading rates was ineffective. To evaluate power and current outputs, the polarization and power curves generated from the granular electrode MFC fed continuously with 1000 mg L^{-1} lactate in combination with either 100, 250 or 500 mg L^{-1} phenol at loading rates of approximately 77, 300 and 1350 mg L^{-1} h^{-1} were developed (Appendix Figure G.1-2) and the resulting OCP, maximum power and corresponding current densities are shown in Figure 6.27.

Despite the small differences in the observed value, especially at the lowest lactate loading rate, variation in phenol concentration in the range 100 to 500 mg L^{-1} did not seem to have a marked effect on electrochemical outputs. Overall, there was no definite trend in OCP, power and current output that correlated with initial phenol concentration. Thus, there was no strong evidence to indicate possible effect of initial phenol concentration on the generated energy output. This was expected since for the most applied loading rates phenol biodegradation was very low and at the same time phenol even at the highest applied concentration did not have a marked effect on lactate biodegradation (i.e. lactate biodegradation rates in the presence of different phenol concentrations were similar).

Moreover, increase in loading rate did not show considerable effect on the overall profile of OCP, power, or current density. Average power and current densities at each applied loading rate of approximately 77, 300 and 1350 mg L^{-1} h^{-1} were relatively close at 4878.8, 4764.3 and 4846.4 mW m^{-3} and 11771.4, 12085.7 and 11082.1 mA m^{-3}, respectively. Similarly, OCP levels were also= comparable with average values of 746.9, 724.4 and 713.8 mV, respectively.

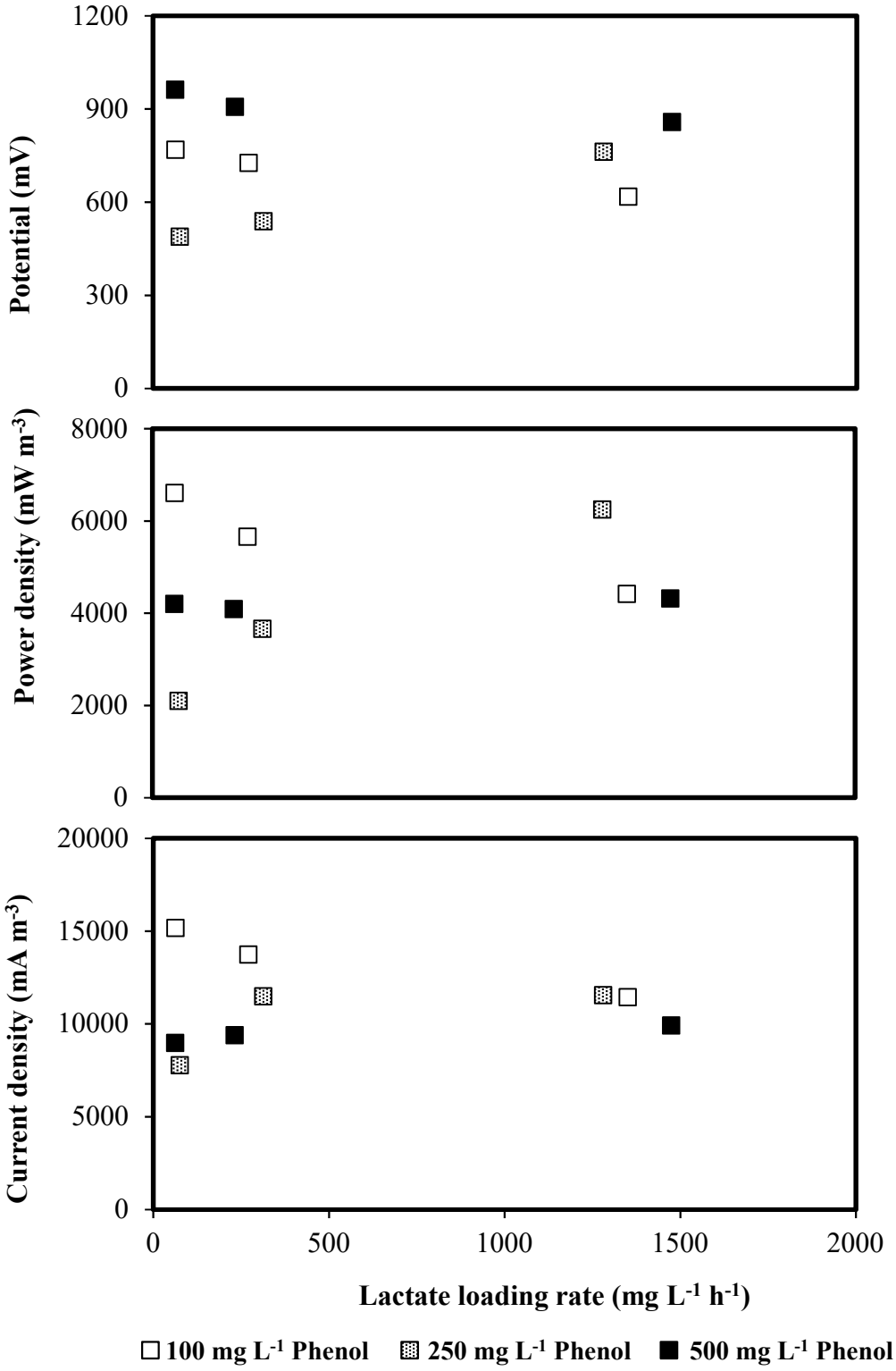

Figure 6.27 Open circuit potential (A), power (B) and current (C) densities determined in MFCs with granular electrode and neutral red, operated continuously at different loading rates with lactate in combination with either 100, 250 or 500 mg L^{-1} phenol.

Comparison of these results with those obtained in the MFC with granular electrodes operated under similar conditions in the absence of neutral red revealed that the addition of neutral red did not enhance energy generation and instead caused a decline in power and current output. In MFC system with neutral red, average power and current densities, regardless of initial phenol concentration, produced at lactate loading rate of approximately 300 mg L^{-1} h^{-1} were 4764.3 mW m^{-3} and 12085.7 and mA m^{-3}, respectively. At similar lactate loading rate, corresponding average power and current densities in MFC without neutral red was considerably higher at 5142.9 mW m^{-3} and 20523.8 mA m^{-3}, respectively.

As presented earlier, performance in terms of lactate biodegradation in MFC with neutral red was inferior when compared to MFC system without neutral red (lactate biodegradation rate and removal percentage: 232.9 mg L^{-1} h^{-1} and 85.7% vs 262.9 mg L^{-1} h^{-1} and 90.3%, respectively). Again, this finding suggests a correlation between the biodegradation performance and power and current outputs.

Examination of graphite granules: As indicated in the earlier parts following the completion of experiments, BET analysis was conducted to determine surface area and porosity of graphite granules. BET surface area and pore volume of granule samples collected at the end of continuous experiments were found to be 1.2 m^2 g^{-1} and 0.003 cm^3 g^{-1}, respectively. These results were similar to those achieved with fresh and unused granules (1.10 m^2 g^{-1} and 0.003 cm^3 g^{-1}) as presented in previous chapters (Sections 4.3 and 5.3). This finding could be interpreted as ineffective occupation of pore spaces or voidages within the granules by biomass and as one of the reason for the mediocre performance of this MFC system.

Further examination of the granule surface more closely with SEM (Figure 6.28), however, revealed the formation of biofilm and layer of extracellular polymeric substances (EPS) on the granule surface similar to those observed in other examined cases for instance with lactate as the sole substrate (i.e. Figure 4.11) but the EPS layer observed with lactate appeared to be considerably thicker and denser, reflecting superior biomass growth and substrate biodegradation. This contrast was expected since effective cell immobilization and superior lactate biodegradation was achieved in the earlier experiments. Although features of *P. putida* cells are not clearly distinguishable in the SEM photos due to amalgamation into the EPS layer, the SEM results somewhat is in contrast with BET analysis which indicated the absence of biomass in the pores and voidages. The reason could be attributed to the use of a non-representative sample in BET analysis or potentially steps required for preparation of the sample for BET analysis such as mechanical grinding and the high heat and pressure imposed during BET analysis could have caused detachment of loosely bound biomass rendering the results inaccurate.

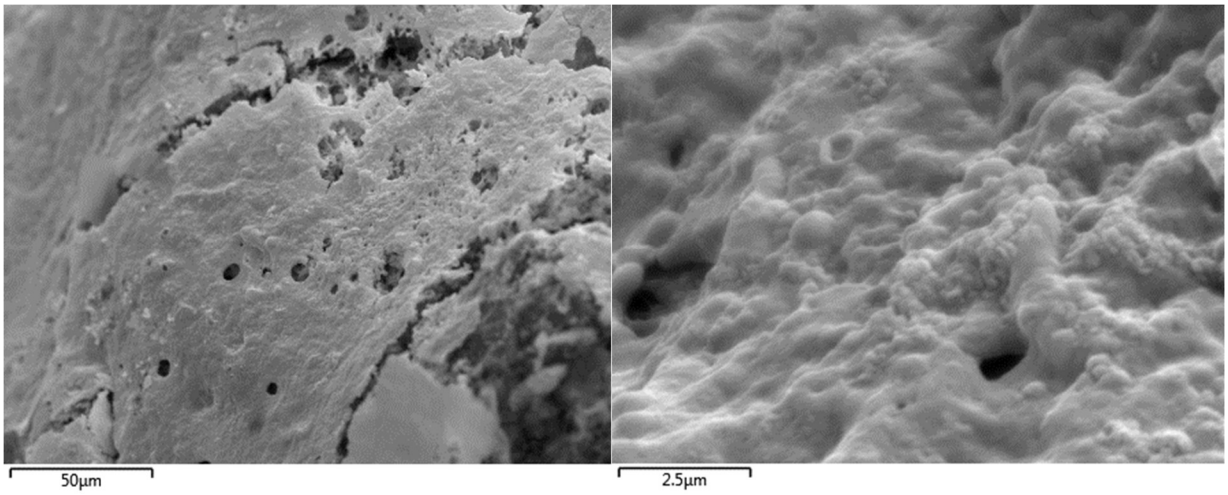

Figure 6.28 SEM photos of the surface of graphite granule used in an MFC with neutral red fed continuously with phenol and lactate taken at two different magnitudes.

Results from this experiment revealed that the addition of neutral red to a continuously operated MFC with granular electrode did not improve the performance in terms of biodegradation of either phenol or lactate, as well as energy output. This was contrary to that observed in similar MFCs operated batchwise where neutral red enhanced both phenol and lactate biodegradation rates, as well as power and current production. It is important to point that similar trend was also observed with phenol as the sole substrate in batch and continuously operated MFCs with neutral red whereby positive effect of neutral red was only observed in the batch system.

It has been reported that improved efficiency due to an electron mediators might be limited to batch systems since steady loss of mediator could occur in continuous systems (Lovley, 2006a; Schroder, 2007). However, this condition is likely to happen in a system with endogenous mediators than in those systems where mediators is continuously supplied externally and as a component of the influent. There could also be a significant concern with mediated electron transfer in the anodic chamber of an MFC in terms of diffusion of the electron shuttle in and out of the bacterial environment (Rabaey et al., 2007). The process transpiring during these conditions has not been fully understood and require additional investigation which was beyond the scope of this study.

6.4. Conclusions

Phenol, as an aromatic compound, is structurally more difficult to degrade than simple structured organic compounds such as fatty acids. In this part of the work, co-biodegradation of lactate and phenol was evaluated to assess if the presence of lactate would stimulate faster biodegradation of phenol, and to assess if the biodegradation of lactate would be negatively affected by the inhibitory

effect of phenol. Experiments in MFC with rod electrodes and freely suspended cells operated batchwise showed successful utilization of phenol and lactate with resulting biomass growth, rise in open circuit potential (OCP) and generation of current. Results showed that phenol and lactate biodegradation rates both decreased with increase in phenol concentration in the range 100-500 mg L^{-1}. This deterioration could be attributed to inhibition effects of phenol especially at the higher concentrations. During co-biodegradation with lactate concentrations higher than 500 mg L^{-1}, a lag phase in the biodegradation of both phenol and lactate was observed and subsequent biodegradation of lactate led to formation of acetate. Accumulation rate of acetate was comparable to those in similar MFCs with lactate as the only substrate.

Preferential substrate utilization was evident where lactate was consumed initially, followed by utilization of accumulated acetate after exhaustion of lactate, and finally phenol only when accumulated acetate was depleted. The utilization of higher lactate concentrations resulted in formation of higher amounts of acetate which further delayed the biodegradation of phenol. In all evaluated combinations of lactate and phenol, generated power and current densities were considerably lower when compared to those in MFCs operated with lactate as sole substrate.

In MFC with granular electrodes operated batchwise, biodegradation of phenol and lactate as combined substrate were faster than in similar MFCs with rod electrodes and proceeded with no lag phase. Moreover, biologically produced acetate was not detected which could be attributed to the substantially high biodegradation rates. Similar to results in MFCs with rod electrodes, the presence of lactate negatively affected the biodegradation of phenol and that phenol imposed an inhibitory effect on lactate biodegradation that became more pronounced as initial phenol

concentration was increased. Specifically, the biodegradation rates of phenol and lactate in mixture were lower than those in similar MFCs operated with phenol or lactate as sole substrates.

In the continuous flow MFC with granular electrodes presence of lactate negatively impacted the biodegradation of phenol. To be more specific the highest phenol biodegradation rate achieved in this system was only 5.4 mg L^{-1} h^{-1} compared to that in the similar MFC operated with only phenol as substrate that achieved a maximum biodegradation rate of 11.5 mg L^{-1} h^{-1}. By contrast, lactate biodegradation appeared not to be affected by the presence of phenol, even at phenol concentrations as high as 500 mg L^{-1}, as complete degradation of lactate was achieved practically at all applied loading rates. Unlike the batch systems, lactate biodegradation and acetate accumulation rates were essentially comparable to those obtained in a similar MFC operated with lactate as sole substrate. The resulting power and current densities correlated with lactate biodegradation performance and no effect due to changes in phenol concentration was observed. The highest power and current output was achieved when lactate removal percentage was 100%. Addition of neutral red as an electron mediator largely improved biodegradation of phenol and lactate in batch operated MFC. Results indicated the effectiveness of neutral red in the enhancement of the biodegradation of lactate, rendering the effect of phenol as an inhibitory substrate minimal. In all tested conditions, the system with added neutral red produced the highest power and current output than those obtained in the absence of neutral red which again shows the relation of electrochemical outputs and the extent of biodegradation.

In the continuous flow MFC addition of neutral red did not enhance the performance of MFC and for the entire applied loading rate range, biodegradation of phenol was essentially ineffective with

maximum phenol removal being only 12.8%. In terms of lactate biodegradation, the continuous system with neutral red did not enhance the biodegradation rate and instead led to performance deterioration at the higher loading rates. Lactate and accumulated acetate biodegradation as well as the resulting power and current output were not affected by changing initial phenol concentration in the feed. Overall, the addition of neutral red in the continuously operated MFC with granular electrode fed with various combinations of phenol and lactate did not improve performance in terms of biodegradation of either phenol or lactate as well as in energy output. The deficient performance when neutral red was added to MFC under continuous operations could be due to issues with diffusion of mediator in and out of the bacterial environment, a phenomenon that requires further investigation.

Overall the results of this part of work have shown that presence of a more amenable compound, such as lactate not only does not enhance the biodegradation of phenol but could negatively impact the biodegradation process. Effect of phenol on lactate biodegradation was largely minute with the exception of a high phenol concentration of 500 mg L^{-1}.

Chapter 7

Preliminary Study on Treatment of an Internal Process Stream Wastewater

7.1 Introduction

With their ability to simultaneously degrade organic compounds and generate electricity, microbial fuel cells (MFCs) can be utilized for the treatment of wastewaters with added benefit of generating renewable energy. Wastewaters contain large amounts of organic and inorganic matter of various types, making them very suitable substrate for utilization in MFCs. As such, treatment of wastewaters has been regarded as the most practical application of MFC technology (Logan, 2008). The surge in number of studies devoted to investigating the effectiveness of MFCs in treatment of wastewaters within the past decade supports this trend. Most of these studies, however, have prioritized the enhancement in magnitude and efficiency of electricity generation and a large number of these studies seemingly overlook or completely disregard the impact and outcome of the biodegradation process.

It is imperative that for an MFC to be a reliable technology for the treatment of wastewaters, at the very least, the degradation of organic and inorganic contaminants has to take place effectively and that the biological processes and their impact on the overall performance of such systems are fully understood. Given the completed detailed studies on biodegradation of model compounds, as the next logical step a preliminary study was conducted to assess the effectiveness of the configured

MFC in the treatment of a process stream wastewater and to gain an understanding, albeit preliminary, on the associated biokinetics.

Results from previous experiments have shown that the MFCs equipped with granular electrodes in the biodegradation of model organic compounds, specifically lactate, acetate and phenol, were effective with appreciable biodegradation rates and energy output. The same MFC setup and operational procedures were then utilized in this part of study to study the treatment of a representative wastewater and activated sludge, collected from the Saskatoon wastewater treatment plant (SWTP), utilized as substrate and inoculum, respectively. After initial start-up of MFC conducted batchwise, continuous biodegradation of process stream wastewater was monitored and power and current output were measured at selected loading rates using a potentiostat.

7.2 Materials and methods

After successful trials in biodegradation of model organic compounds with granular graphite electrodes, the same MFC setup was used to investigate the treatment of a process stream wastewater. Other than the utilization of wastewater as feed and activated sludge from a wastewater treatment plant as inoculum, preparation and operation of MFC, including sterilization of equipment and use of potassium ferricyanide as catholyte, were identical to the experiments described in previous chapters.

Wastewater collected from the fermenter (prior to the anaerobic digester) of the Saskatoon wastewater treatment plant was used. The relatively high organic content of the

stream from the fermenter allowed a longer monitoring period of the biodegradation process in the MFC. Moreover, this process stream could well represent effluent from an anaerobic treatment process of wastewater from industrial or agricultural operations. Collection of the internal process stream wastewater was done in batches using an 18 L capacity container. Freshly collected samples were stored in a temperature controlled chamber (4°C) for approximately one week. After several analyses of wastewater samples, it was found that organic concentration significantly increased with the storage time which reached relatively stable levels after one week.

At the start-up the MFC anodic chamber was filled with 70 mL of wastewater and approximately 10 mL of sludge collected from the bottom of the aeration basin of the SWTP was added as inoculum. Before using in the MFC, stored wastewater was sieved to remove larger solids. The system was operated in batch mode and the concentration of organic matter (COD) in the wastewater was monitored. After several weeks of operation in batch mode and once stable COD level was attained, the MFC was switched to continuous mode using a peristaltic pump to introduce wastewater as influent. Initial flowrate was set at 2 mL h^{-1} and then gradually increased to 5, 10, 20, 40 and 60 mL h^{-1}. The anodic chamber liquid was regularly sampled and analysed for COD contents. After increasing the flowrate to 60 mL h^{-1}, difficulty in getting consistent organic (COD) concentration in the feed was encountered which resulted in significant fluctuation in the organics (COD) loading rates. Despite acquiring new batches of wastewater from the SWTP and employing the same storage procedures, the inconsistency in organics (COD) concentration of wastewater remained. Hence, due to the inherent inaccuracy of subsequent results, the experiment was halted. All experiments were conducted at room temperature (24 ± 2 °C). The setup used in the experiment is shown in Figure 7.1.

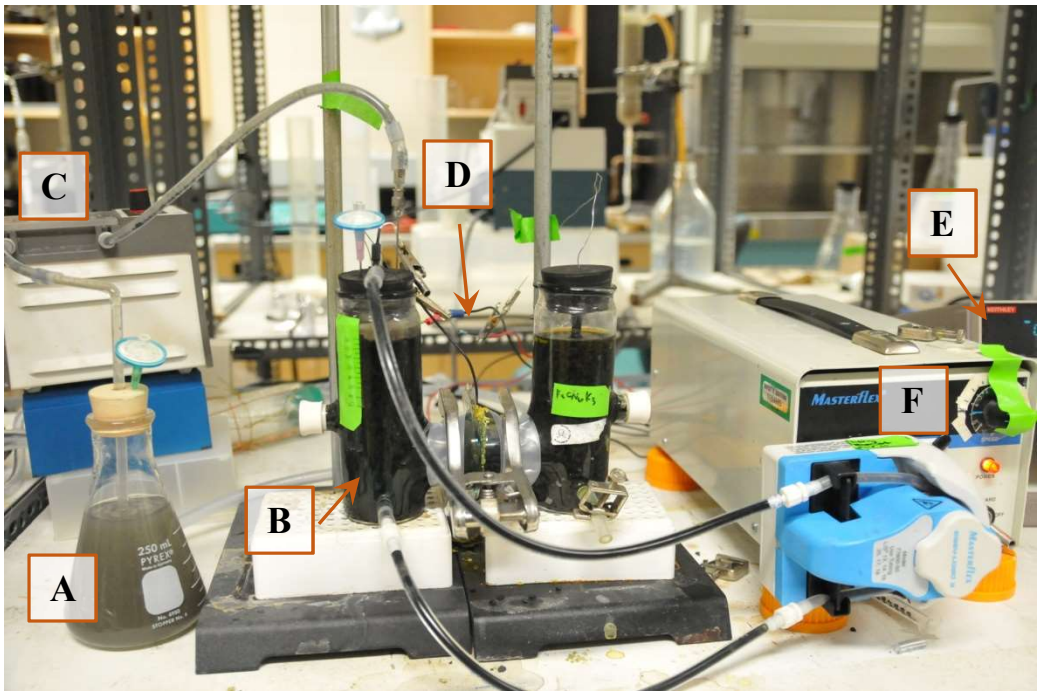

Figure 7.1 Experimental system used in treatment of internal process stream wastewater in a MFC with granular electrodes. Wastewater (A) is fed into the anodic chamber (B) using a peristaltic pump (C). An external resistor (D) is attached to the anode and cathode terminals which are connected to a multimeter (E) equipped with a datalogger. A second peristaltic pump (F) was used to recirculate the contents in the anodic chamber.

7.2.1 Analyses

To determine the dissolved organic contents of representative wastewater, chemical oxygen demand (COD) of the influent and effluent were determined following the dichromate digestion method (Boyles, 1997). This was carried out by mixing samples in Hach COD digestion reagent vials and heating them at 150 °C in a COD reactor (Hach reactor model 45600, Hach Co. Loveland, USA), after which the absorbency of the mixture was measured in a spectrophotometer (Shimadzu Uvmini 1240) at 620 nm. Optical density (OD) readings were then converted to COD using a generated calibration curve (Appendix Figure I.1.). Only the supernatant of the samples, after centrifugation at 10000 rpm

(9180 ×g) for 5 min using a microfuge (Microfuge 18 Centrifuge, Beckman Coulter, Fullerton, USA) , was used to measure the dissolved COD.

MFC circuit potential was continuously monitored and recorded, using the Keithley 2700 multimeters, equipped with 7700 dataloggers (Keithley Instruments Inc., Cleveland, USA) connected to a personal computer. Cathodic potentials were also measured occasionally against a Calomel reference electrode. Polarization curves were developed using Linear Sweep Voltammetry using a Gamry R600 potentiostat (Gamry Instruments, Warminster, USA). The applied scan rate was 0.1 mV s^{-1} covering a range from -550 mV to 50 mV. Moreover, efficiency of electron transfer, in terms of Coulombic efficiency (CE) for the biodegradation of organics in wastewater was calculated as described in Appendix H.

7.3 Results and discussion

The granular electrode MFC was initially operated in the batch mode to allow acclimation of inoculum (i.e. activated sludge) to MFC environmental conditions and to provide a period for formation of biofilm on the surface of graphite granules. Following this period (approximately 23 days after inoculation), MFC was switched to continuous mode by feeding the wastewater to the anodic chamber at a low flow rate of 2 mL h^{-1}. Subsequent monitoring of organic contents (COD) of feed wastewater (influent) showed inconsistencies or fluctuation in COD concentration. Analysis of a series of samples in the same batch of collected wastewater revealed that COD concentration increased with time due to storage. A similar pattern was also observed in other batches of wastewater collected from SWTP fermenter afterward. Close monitoring of the

wastewater indicated that COD concentration started to increase immediately after collection and storage (at 4 °C in a controlled chamber) and achieved relatively stable COD levels after a week. Thus, in the follow up experiment, wastewater samples were stored for a week before utilizing them as substrate in the MFC. This, however, did not alleviate the fluctuation in COD completely. Present solids that settled at the bottom of the container may have undergone further degradation with time, resulting in the release of dissolved organics and hence the change in dissolved COD concentration. Fluctuations in influent COD concentration was also reported by Rabaey et al. (2005) which resulted in highly variable COD removal in their MFC reactors.

Despite challenges in maintaining a consistent feed, the experiment in the MFC was conducted to evaluate its potential in biodegradation of organics and simultaneous generation of energy from an actual wastewater. The organic (COD) loading rates and corresponding biodegradation rates of organics in continuous flow MFC with granular electrodes is shown in Figure 7.2. At the lowest loading rate of 35.8 mg COD L^{-1} h^{-1} (HRT=37.5 h), a COD removal of 74.1% was attained that represented the highest value for the entire range of applied loading rate, with a corresponding biodegradation rate being 26.5 mg COD L^{-1} h^{-1}. Increase in loading rate decreased the removal percentage down to 49.3% at the highest applied loading rate of 645.3 mg COD L^{-1} h^{-1}. As was the case during the biodegradation of lactate and phenol or combination of these two, COD biodegradation rate was increased with the increase in loading rate with the highest biodegradation rate of 318.2 mg COD L^{-1} h^{-1} (HRT=1.9 h) achieved at a loading rate of 645.5 mg COD L^{-1} h^{-1} mg COD L^{-1} h^{-1}. The corresponding removal efficiency was 49.9%. It is important to point out that for the entire range of applied loading rates, average COD concentration in the influent wastewater was 1321.6 ± 170.3 mg COD L^{-1}.

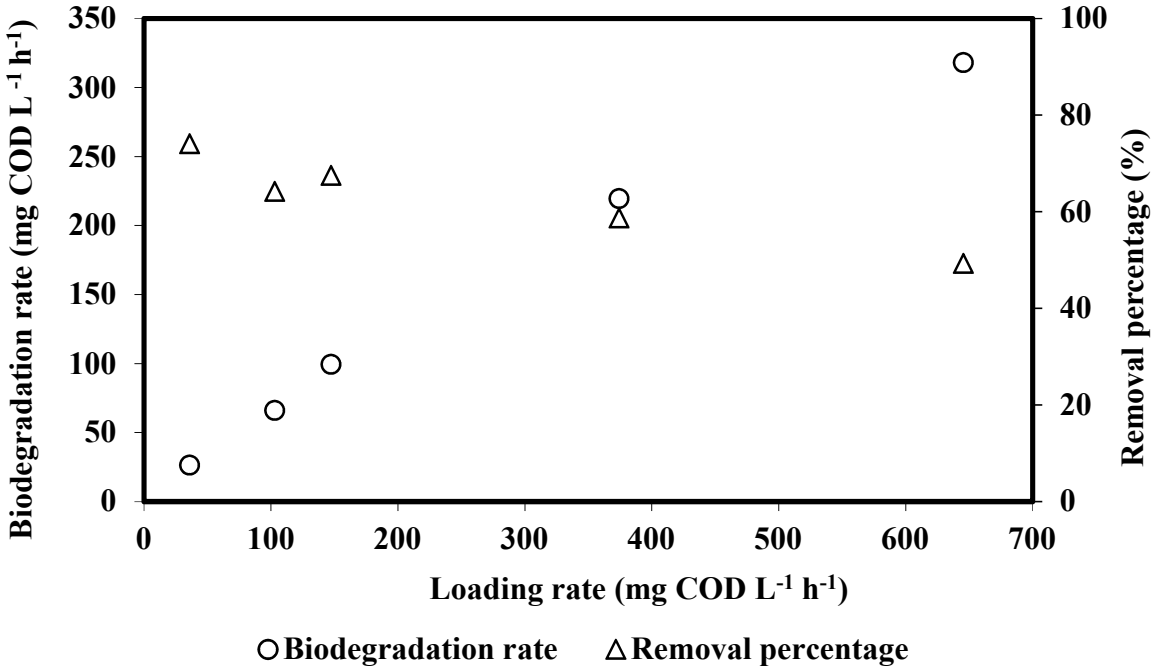

Figure 7.2 Biodegradation rate and removal percentage of COD as a function of its loading rate in continuously operated MFC with granular electrodes fed with representative wastewater.

To assess whether applying higher loading rates would result in higher COD biodegradation rate, flowrate of feed was increased to 60 mL h^{-1}. However, during this part of experiment substantial inconsistency in wastewater COD concentration was again observed (variation in influent COD concentration:116.1-1598.1 mg COD L^{-1}). As indicated earlier, this inconsistency in concentration of organics (COD) in the influent was one of the major problems encountered in the treatment of wastewater in the MFC. Moreover, at this stage of the experiment, considerable flocculation of particles in the anodic chamber which rendered proper operation of MFC at higher loading rates impractical and thus the experiment was terminated after 10 months of operation since the start-up of MFC system.

Polarization and power curves developed at different COD loading rates of 35.8, 102.9, 147.2 and 645.5 mg COD L^{-1} h^{-1} are shown in Figure 7.3. As seen, due to inconsistency in operating

conditions of MFC (i.e. fluctuation in COD contents of influent), resulting polarization and power curves showed considerable signal noise when compared to those measured in MFCs operated with model organic compounds. The reason for these differences is not clear but could possibly be due to the complex and varied organic contents of the wastewater. Open circuit potential (OCP) could not be directly determined since the potential at 0 current was not covered by the potential sweep. Extrapolating the polarization curve profiles (not shown) would roughly predict the OCP to be in the range 550-600 mV, while those at the lower loading rates were slightly higher.

In terms of power and current output, the highest power density of 6533.3 mW m^{-3}, attained with a current density of 14933.3 mA m^{-3}, was generated when MFC was operated at the lowest loading rate of 35.8 mg COD L^{-1} h^{-1} (Figure 7.3A). Increase in loading rate to 102.9, 147.2 and further to 645.5 mg COD L^{-1} h^{-1} resulted to decreases in both power and current densities to 5866.7, 4266.7 and 4533.3 mW m^{-3} and 13466.7, 11333.3 and 10400.0 mA m^{-3}, respectively. The changes in current output was also reflected in the efficiency of electron transfer in terms of CE. The highest CE value of 16.8% was attained at the initial loading rate where removal efficiency was the highest. This then was substantially diminished to 6.1% as loading rate was increased which was accompanied by corresponding decrease in removal efficiency. Values of CE further decreased to 3.4% and 1.0% at the next higher loading rates. These results indicate that power and current output was influenced more by the COD removal efficiency than COD biodegradation rate - a finding that is consistent with observations from previous experiments with model organic compounds.

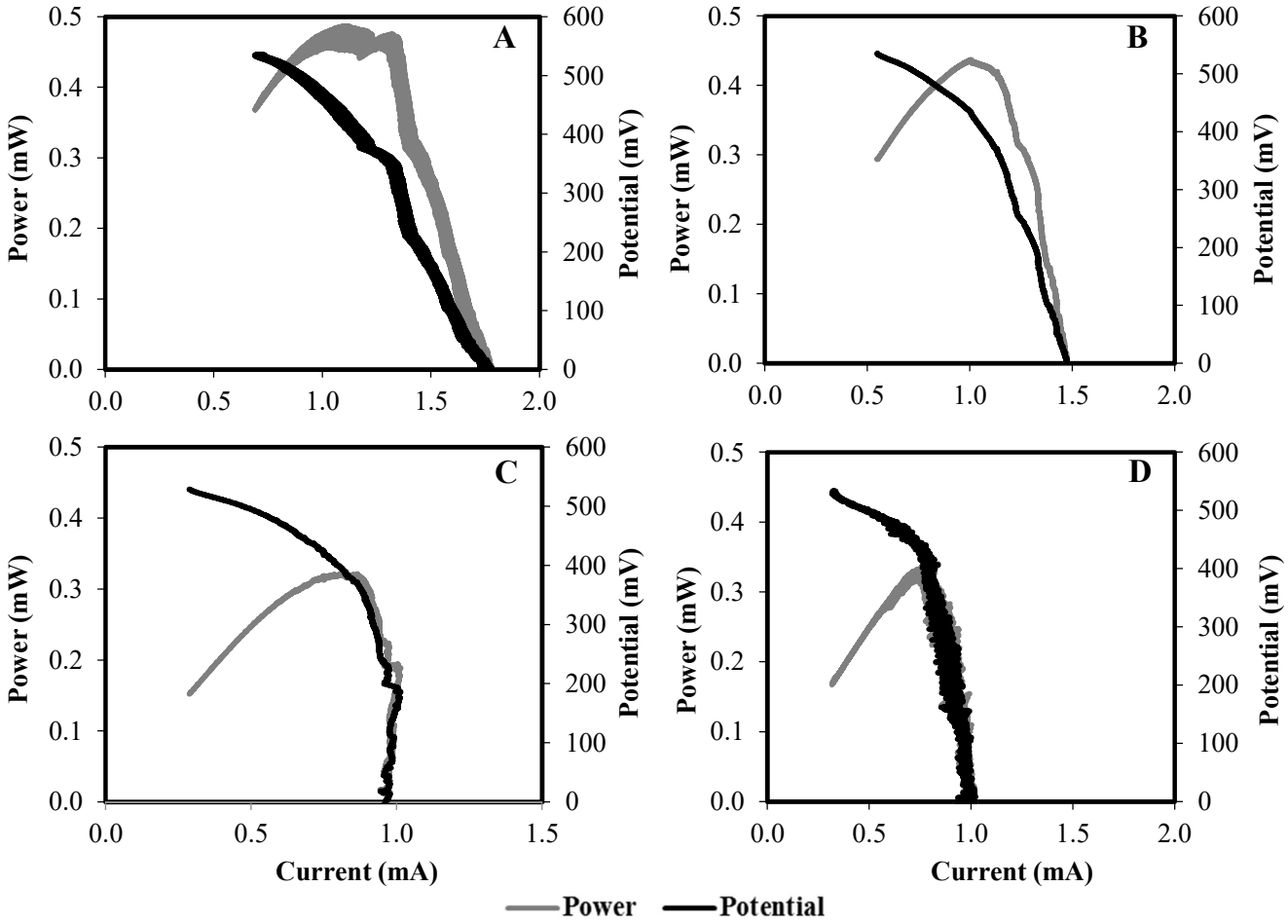

Figure 7.3 Polarization and power curves generated from granular electrode MFC operated continuously with representative wastewater at various COD loading rates. A) 35.8 B) 102.9 C) 147.2 and D) 645.5 mg COD L^{-1} h^{-1}.

The resulting COD biodegradation rates were somewhere between the rates obtained with model compounds, with phenol having the lowest, followed by wastewater and then lactate that had the highest biodegradation rate. Despite attaining higher biodegradation rates and generating higher energy output than phenol, biodegradation of wastewater was not as effective as reflected in the removal efficiency with the highest of 74.1% obtained at a COD loading rate of 35.8 mg COD L^{-1} h^{-1} as compared to that of phenol reaching 100% at phenol loading rates of up to 6.5 mg L^{-1} h^{-1}.

This finding points to the complex nature of wastewater degradation in MFC, both in terms of influent composition and inoculum, as compared to previous experiments with model organic compounds and *P. putida*.

Results of this preliminary study was comparable to other works dealing with degradation of domestic wastewater in MFCs. In fact, COD removal efficiency in the present work was considerably higher than a value of 22% achieved in the biodegradation of domestic wastewater in a tubular MFC with similar granular graphite as electrode (Rabaey et al., 2005b). On the other hand, the MFC configuration of the system used by Rabaey et al., 2005b showed superior in terms of generating higher power output of up to 48000 mW m^{-3} and a CE around 96%. With the aim of achieving high energy output, Daniel et al. (2009) treated domestic wastewater in a five-cell series-connected MFC operated with a fed-batch anode and a continuous flow cathode. Despite addition of methylene blue as electron mediator, maximum power and current densities were only 1.0 mW m^{-2} and 1.2 mA m^{-2}, respectively, while the COD removal efficiency was only 10%. Overview of these studies once again confirm the lack of focus or seemingly overlooking of the earlier works on biological processes involved in operation of MFCs and the MFC performance in terms of contaminants removal.

7.4 Conclusions

A previously evaluated MFC that was capable of effective degradation of model organic compounds, namely lactate, acetate and phenol or combination of these, was utilized in this part of the study to assess its effectiveness in treating a representative wastewater and activated sludge as inoculum. After an initial start-up stage in batch, continuously operated MFC was effective in

treatment of internal process stream wastewater with loading rates up to 645.5 mg COD L^{-1} h^{-1}. The increase in COD loading rate resulted in higher COD removal rate, with the highest removal rate of 318.2 mg COD L^{-1} h^{-1} achieved at a loading rate of 35.8 mg COD L^{-1} h^{-1} with the corresponding HRT being 37.5 h.

MFC potential in terms of COD removal rate was not attained as the experiment was terminated due to operational difficulties. Specifically, fluctuations in COD concentration of influent wastewater made biodegradation results inaccurate. Although the maximum removal efficiency of COD (74.1%) was not as high as those obtained with model organic compounds, at the highest applied loading rate the removal was still substantial (49.3%) when compared with model compounds indicating that the biodegradation rate in MFC still had room for improvement.

Increase in loading rate improved the removal rate but led to lower removal percentage and consequently coulombic efficiency (CE), indicating that biodegradation rate was not the only influential factor in the resulting power and current output and that the removal percentage was also critical. Maximum power and current densities of 6533.3 mW m^{-3} and 14933.3 mA m^{-3}, respectively, were achieved at a loading rate of 35.8 mg COD L^{-1} h^{-1} (lowest biodegradation of 26.5 mg COD L^{-1} h^{-1}) when COD removal efficiency was at the highest value of 74.1%.

Chapter 8

Research overview, Conclusions and Recommendations

8.1. Research overview

In this PhD project, microbial fuel cells (MFCs) with suitable structure were utilized for biodegradation of different organics with the overall goal to gain greater understanding of the biological processes occurring in the MFC ecosphere. Biodegradation studies were conducted in H-type configured MFCs under varying conditions. Model organic compounds commonly found in wastewaters particularly fatty acids, lactate and acetate, and an aromatic compound, phenol, individually or in mixtures of different compositions were utilized as substrates. This was then followed by treatment of a process stream wastewater in MFC as the next logical step. Two electrode configurations, one in the form of graphite single rods and the other as graphite granules, were investigated. Single rod electrodes were employed to allow suspension of microbial cells in the anodic chamber creating a CSTR-like bioreactor, while granules were utilized for promotion of cell immobilization and enhancement of electron transfer, turning the anodic chamber into a packed-bed type bioreactor. Furthermore, in all cases two modes of operation namely batch including sequential batch and continuous were employed in all experiments.

With more focus on the biodegradation aspects of MFC technology, especially in an attempt to gain an insight on the interconnecting relationship among microbial growth, substrate degradation

and MFC electrochemical output, the biodegradation kinetics of model organic compounds were investigated with the utilization of *Pseudomonas putida* as biocatalyst. In the process of kinetics evaluation for biodegradation of organics and corresponding energy output, kinetic modeling of microbial growth and biodegradation of model compounds under conditions prevailing in MFCs was performed.

8.1.1 Biodegradation of lactate and acetate

Experiments were started in batch MFCs equipped with single rod electrodes which allowed suspension of microbial cells in the anodic liquid. Lactate and acetate, being the more simple structured organic compounds were individually fed as substrates at concentrations of 1000, 2500 and 5000 mg L^{-1}. Increase in initial concentration improved the biodegradation rate of lactate, while no effect on acetate biodegradation was observed. Sequential batch degradation of lactate also led to improved biodegradation rates but did not impact the acetate. Biodegradation of lactate led to accumulation of biologically produced acetate but at a level lower than that expected from the stoichiometry of incomplete oxidation pathway indicating that both complete and incomplete lactate oxidation pathways occurred simultaneously. Accumulated acetate was immediately utilized but at rates lower than that for biodegradation of acetate as the original substrate.

During the continuous mode of operation, the MFC was fed with 5000 mg L^{-1} of lactate. Complete degradation of lactate was achieved for a wide range of loading rate and biodegradation rate increased with increase in loading rate. Biodegradation rate eventually reached a peak after which decline in MFC performance in terms of lactate biodegradation was seen. Accumulation of biologically produced acetate was coupled to lactate biodegradation but at a rate which was lower

than that expected from stoichiometry of lactate incomplete oxidation, confirming oxidation of lactate occurred through both complete and incomplete pathways resulting in acetate and CO_2 as end products. In a similar MFC operated continuously with acetate as substrate, difficulty in degradation of acetate was encountered and complete removal of acetate was not achieved even at the lowest applied loading rate.

Employment of the relatively simple H-type configuration with single rod electrodes and freely suspended cell decreased the complexity in the investigation of biodegradation kinetics of lactate and acetate in the MFC ecosphere by allowing the continuous and accurate monitoring of biomass along with substrate concentration and circuit potential. Just as in conventional bioreactors, monitoring of biomass growth is critical in understanding the biological processes that transpire in an MFC but has largely been disregarded in most MFC studies. In developing biokinetic models, biomass and substrate concentrations were the critical information required for development of the model and determination of associated parameters. The model developed was able to predict the experimental data with reasonable accuracy and revealed that biokinetic coefficients in an MFC, particularly maximum growth rate (μ_{max}) and yield (Y), to be lower than those calculated from conventional bioreactors. Moreover, based on the sensitivity analysis μ_{max} and Y were found to be the most influential biokinetic coefficients affecting the model predictions and their closeness to the actual data.

Graphite granules were employed as electrodes in the H-type MFC with the aim of immobilizing biomass and to enhance the electron transfer through the extended surface offered by this electrode configuration. Effect of electrode structure on lactate and acetate biodegradations and energy

production was then investigated. Operation of MFC in batch and subsequently in continuous mode revealed improved performance in terms of both biodegradation rate and energy output when compared to MFCs with single rod electrodes. With granular electrodes, biodegradation of lactate in the continuous system was more than 7 times faster than the rates observed in batch operation. A substantial improvement was also attained in the biodegradation of acetate with rates observed during the batch operation being at least 13 fold higher than those in MFCs with rod electrodes. Additionally, continuous degradation of acetate at loading rates as high as 246.3 mg L^{-1} h^{-1} was achieved, while with rod electrodes continuous operation of MFC was not successful. The results described above as well as BET analysis and SEM examination of fresh and used graphite granules revealed successful immobilization of bacterial cells and formation of substantial biofilm that together with the enhanced electron transfer through the extended surface area of granules led to superior performance of the MFC systems with granular electrodes.

Regardless of type of electrodes or mode of operation, biodegradation rates with lactate were substantially higher than those with acetate and the latter proved to be a challenging substrate. The lower biodegradation activity with acetate as substrate could be attributed to its lower anodic potential compared to lactate as indicated from Gibb's free energies of lactate and acetate oxidations.

8.1.2 Biodegradation of phenol

H-type MFCs with both rod and granular electrode structures were utilized to study biodegradation of an aromatic compound, specifically phenol. Similar to lactate and acetate, biokinetics of phenol degradation and microbial growth along with electrochemical outputs were investigated. Given

the more complex structure of phenol and its toxic nature, lower concentrations of 100, 250, 500 and 1000 mg L^{-1} were evaluated. As expected, biodegradation of phenol was more challenging as compared to lactate or acetate. In batch MFCs with single rod electrodes, biodegradation of phenol displayed a lag phase, which was more pronounced at higher initial concentrations and contrary to lactate, biodegradation rate showed no improvement with increase in initial concentration pointing to the potential inhibitory effect of phenol. In MFCs with granular electrodes, no lag phase was seen and inhibition effect was only observed at the highest initial concentration (1000 mg L^{-1}) revealing superior performance of MFCs with granular electrodes.

Phenol biodegradation rates obtained in the MFC with rod electrodes were 7 and 3 folds lower than those of lactate and acetate, respectively. The use of granular electrodes resulted to 4-7 fold increase in phenol biodegradation rates but these rates were still lower compared to those for lactate and acetate in similar granular electrode MFCs (5 and 10 times lower than lactate and acetate, respectively).

Similar findings were observed in continuous flow MFC with rod electrodes whereby the possible applied phenol loading rates that led to removal of phenol was much narrower and resulting biodegradation rates were much lower than lactate (maximum biodegradation rate: 0.83 vs 1668.2 mg L^{-1} h^{-1}). Maximum phenol biodegradation rate improved to 11.52 mg L^{-1} h^{-1} with the use of granular electrodes but this still was markedly lower than those obtained in similar MFC operated with lactate (11925.7 mg L^{-1} h^{-1}) and acetate (93.4 mg L^{-1} h^{-1}). The biodegradation and electrochemical outputs obtained in MFCs systems equipped with either rod or granular electrodes

and run either batchwise or continuously confirmed the challenging nature of phenol biodegradation, as has been observed in conventional bioreactors.

To enhance phenol biodegradation, an electron mediator, specifically neutral red (NR), was utilized in an MFC operated in both batch and continuous modes. The presence of NR in MFCs operated batchwise improved the overall biodegradation of phenol substantially, with rates being up to 4 times faster than in the same MFC without the mediator. Moreover, increase in phenol biodegradation rate was observed as initial concentration was increased with no indication of inhibition effect even at the highest evaluated concentration of 1000 mg L^{-1}. These findings indicate positive impact of NR on batch biodegradation of phenol, with the exception of a phenol concentration of 100 mg L^{-1} where no improvement in biodegradation rate was observed. One could only speculate that given the remarkable improvement in phenol biodegradation when granular electrodes were employed, NR did not have a marked effect on biodegradation of low level of phenol ($\leq$ 100 mg L^{-1}).

A similar pattern was observed in continuously operated MFC with granular electrode, fed with the same amount of phenol (100 mg L^{-1}), where biodegradation rates achieved with or without NR were relatively close. The addition of NR, on the other hand, enhanced energy output considerably with power and current densities in the presence of NR almost twice as high as that in the absence of NR. With the interrelating factors transpiring in an MFC, including biological and electrochemical processes among others, results indicate that electrochemical performance was not only influenced by the biodegradation rate, but removal efficiency was also a contributing factor. To be more specific, despite comparable maximum biodegradation rates with and without

NR, the higher power and current output in the MFC with NR corresponded with higher phenol removal percentage.

In MFCs with suspended cells and rod electrodes, monitoring and collection of biomass and substrate information allowed a proper biokinetic evaluation of microbial growth and phenol degradation in MFCs. Using a first-order rate expression and Monod kinetics in the batch and continuous systems, respectively, relevant biokinetic parameters were determined. In batch MFCs, the rate constant for phenol degradation was considerably lower at higher initial concentrations of 500 and 1000 mg L^{-1}, suggesting inhibition effects of phenol at these concentrations. Using the data generated in continuously operated MFC, biokinetic coefficients including μ_m, Y, K_s and K_e were determined which, as of this writing, appear to be the first report on the intrinsic biokinetic aspects of phenol biodegradation in an MFC.

8.1.3 Co-biodegradation of lactate and phenol

Following a thorough investigation of lactate, acetate and phenol biodegradation as individual substrates, co-biodegradation of lactate and phenol in mixtures of different compositions was investigated. The main goals were to understand whether the presence of lactate, a compound more amenable to biodegradation, could facilitate and promote biodegradation of phenol through creating an environment conducive for improved biomass growth and biodegradation through release of the required enzymes, and to verify if phenol, as a toxic and recalcitrant compound, would inhibit biodegradation of lactate. Finally, the use of a mixture of organic compounds of different structures mimicked the practical conditions and challenges that could exist in treatment of actual wastewaters.

Utilization of 100 to 500 mg L^{-1} phenol with lactate at 500 mg L^{-1} in batch MFCs with rod electrodes revealed that biodegradation of phenol improved with increase in initial phenol concentration - a similar trend observed with phenol as sole substrate in the same range of concentrations. However, phenol biodegradation rates were considerably lower than those with phenol as sole substrate (0.37-0.57 vs 0.50-0.91 mg L^{-1} h^{-1}). Maintaining phenol concentration at 100 mg L^{-1} while increasing lactate concentration substantially decreased phenol biodegradation rates (0.06 mg L^{-1} h^{-1} with 5000 mg L^{-1} lactate). Furthermore, a lag phase in the biodegradation of both phenol and lactate was observed when high lactate concentrations (1000-5000 mg L^{-1}) were combined with 100 mg L^{-1} phenol. These findings indicate that the addition of lactate did not enhance the biodegradation of phenol but rather had a negative impact, especially with higher level of lactate.

In terms of lactate biodegradation, increase in initial lactate concentration with a fixed phenol concentration increased its biodegradation rate, a trend previously observed in similarly operated MFCs with lactate as the sole substrate. With a constant lactate concentration, increase in initial phenol concentration from 100 to 250 mg L^{-1} resulted in close lactate biodegradation rate but a lower rate was observed with 500 mg L^{-1} phenol, indicating phenol inhibition at high concentrations. In all evaluated combinations, lactate biodegradation rates were considerably lower compared to those from similar experiments with lactate as sole substrate.

The utilization of granular electrodes in batch MFCs resulted in simultaneous biodegradation of phenol and lactate with no lag phase but lactate degradation was faster than that of phenol. Overall

trend in phenol biodegradation revealed an increase in biodegradation rate with increase in initial phenol concentration which reached a peak at concentrations between 306-437 mg L^{-1} and eventually diminished with further increase in initial concentration. Similar trend to lactate degradation was observed where biodegradation rate increased with initial phenol concentration which then diminished after reaching a peak with its lowest level reached when combined with the highest phenol concentration. As has been observed in previous experiments, these findings are indications of inhibitory effects of phenol especially at high concentrations.

During the co-biodegradation of lactate and phenol in MFC with granular electrodes, biologically produced acetate was not detected similar to the trend observed with lactate as sole substrate. In the presence of phenol, however, biodegradation rate of both lactate and phenol were considerably lower than that with lactate or phenol as sole substrate.

In the continuous system, phenol biodegradation was also diminished when combined with lactate, both in terms of biodegradation rate and removal efficiency, as compared to similarly operated MFC with phenol as the only substrate. Again, these findings indicate that the presence of lactate negatively affected the biodegradation of phenol whether in batch or continuously operated MFCs with granular electrodes. On the other hand, continuous lactate degradation including accumulation of biologically produced acetate appeared to be unaffected by phenol. Finally, when compared to similar experiments in MFCs with rod electrodes, biodegradation of phenol and lactate were considerably improved (at least 3 folds) when granular electrode was employed.

Addition of NR in the batch operated MFC with granular electrode improved the overall performance of MFC in terms of biodegradation of phenol and lactate substantially. Compared to similar batch MFC without NR, biodegradation rates of phenol and lactate were 5 and 9 folds faster, respectively. In fact, lactate biodegradation rates were comparable to those in similarly operated MFC with lactate as sole substrate at the same concentration, effectively rendering the effect of phenol as an inhibitory substrate negligible. Moreover, phenol biodegradation rates were found to improve with increase in initial phenol concentration.

When the MFC was switched to continuous mode, addition of NR did not improve phenol or lactate biodegradation and instead resulted in deterioration of overall performance – which is a similar finding observed in the continuously operated granular electrode MFC with phenol as sole substrate. Throughout the applied loading rates, biodegradation of phenol was practically ineffective (maximum removal efficiency of only 12.8%), a result which is inferior when compared with the continuous biodegradation of phenol as the sole substrate. No enhancement in terms of biodegradation rate and removal efficiency was observed for lactate when NR was added. Biodegradation of lactate and accumulation of biologically produced acetate, including power and current output, were not affected by the initial phenol concentration and their variations were mainly due to change in lactate loading rate. Deterioration in MFC performance as a result of NR addition could be due to issues with diffusion of the mediator in and out of the bacterial environment brought about by the switch to continuous operation from batch, a phenomenon that requires further study in MFCs.

8.1.4 Electrochemical outputs in context of biodegradation

In all investigated cases, biodegradation of different model organic compounds as substrate in MFCs equipped with either rod or granular electrodes was accompanied by biomass growth and concomitant generation of electrical energy. In MFCs with rod electrodes, enabling simultaneous monitoring of biomass growth, substrate degradation and corresponding OCP and power and current output, substrate utilization led to increase in biomass concentration along with rise in open circuit potential (OCP). As the substrate was depleted, both biomass concentration and OCP started to decline.

With lactate as substrate, increase in initial concentration led to higher OCP levels along with improvement in biodegradation rate. With acetate as substrate, corresponding biodegradation rates were slower than those from lactate and hence, OCP levels were generally lower compared to those measured with lactate. Power and current output also followed this pattern where corresponding power and current densities generated from the degradation of lactate were higher at higher initial concentrations. Similarly, with higher lactate biodegradation rates, power and current densities generated with lactate were also higher than those with acetate as substrate.

During biodegradation of phenol, lower OCP levels were observed when compared to those from lactate and acetate. However, power and current output from biodegradation of phenol were comparable to those from lactate and acetate despite its lower biodegradation rates. The higher power and current densities generated from phenol could be explained through the effectiveness in electrical energy recovery as revealed by the corresponding coulombic efficiencies that correlate with current output. CE values from MFCs degrading phenol (0.38-2.30%) were found

comparable, if not higher, to those MFCs operating with lactate (0.18-1.79%) and acetate (0.51-1.14%).

During the co-biodegradation of phenol and lactate in MFCs with rod electrodes, preferential use of lactate by microbial cells was observed which was also reflected in the resulting energy output. Between the two substrates, biodegradation rates of lactate were considerably higher than phenol and so was the electrochemical output. In other words, the resulting power and current densities appeared to correlate with the biodegradation performance in terms of removal percentage and rate. In all evaluated combinations of lactate and phenol, biodegradation rates and generated power and current densities were considerably lower than those when phenol and lactate were utilized as sole substrates in the same MFC systems.

Similar findings were also observed in batch operated MFCs with granular electrodes. Biodegradation rates of lactate were considerably higher than those of phenol, especially at the higher initial concentrations, but resulting power and current densities as well as corresponding CE values were comparable. With acetate as substrate, biodegradation rates were markedly higher, even when compared to lactate due to improved biomass presence at startup (as discussed in Section 4.3), and thus resulted to substantially higher power (up to 11 folds) and current (up to 3 folds) output. Regardless of the type of substrate used, biodegradation rates attained in MFCs with granular electrodes were considerably higher than those from MFCs with rod electrodes, and so were the power and current output and CE. This finding indicates that the use of granular electrodes enhanced both biodegradation performance and energy generation in batch MFCs.

This trend was further confirmed in continuous flow MFCs whereby biodegradation rates improved compared to that in batch operated MFCs and so did the power and current densities. For example, biodegradation rates of up to 1668.2 mg L^{-1} h^{-1} in rod electrode MFCs fed continuously with 5000 mg L^{-1} lactate were substantially higher than in the same MFC operated batchwise with only 17.3 mg L^{-1} h^{-1}. As a result, power output was also considerably higher with a maximum of 8.13 mW m^{-2} as compared to only 1.76 mW m^{-2} in the batch system. However, there was no improvement in the current output (28.7 vs 29.5 mA m^{-2}) which again was reflected in the corresponding CE wherein its value in the continuous system was not as high as that in the batch system.

In the continuous MFCs, power and current output were not only affected by the biodegradation rate but also by removal efficiency. Continuous lactate biodegradation in the MFC system with rod electrodes revealed that removal percentage and CE was directly correlated. The highest CE was observed when removal percentage was at the highest and decrease in removal efficiency corresponded to lower CEs.

Similar to results from batch MFCs, power and current output and the corresponding CE values attained from continuously operated MFCs were higher when granular electrodes were used instead of rod electrodes. Moreover, addition of NR enhanced electrical energy recovery as indicated by increased values of CE in the biodegradation of phenol either as sole substrate or in combination with lactate. Throughout this project, the highest power output of 9444.4 mW m^{-3} was generated when MFC with granular electrodes was fed continuously with lactate as sole

substrate. Being fed with the most amenable of all substrates tested, the same MFC also achieved the highest biodegradation rate of 5162.5 mg L^{-1} h^{-1}.

8.1.5 Treatment of domestic wastewater

Towards the latter portion of this research, a preliminary investigation on the treatment of a process stream wastewater using the evaluated MFC system was conducted. Sludge and representative wastewater collected from the Saskatoon wastewater treatment plant (SWTP) were utilized as inoculum and influent, respectively, in MFC with granular electrodes without any electron mediator. Following a batchwise start-up, MFC was switched to continuous mode and its performance at varying loading rates in the range 35.8-645.5 mg COD L^{-1} h^{-1} was assessed. Increase in loading rate resulted in increase in COD removal/ biodegradation rate up to 318.2 mg COD L^{-1} h^{-1} which was achieved at the highest applied loading rate.

Full potential of MFC in biodegradation of organics in wastewater was not demonstrated due to operational challenges posed by fluctuations in COD concentration of wastewater samples that made the application of higher loading rates impractical. Given the increasing trend of COD biodegradation/removal for the applied loading rate, one could expect higher removal rates if MFC had been operated at higher loading rates.

A maximum COD removal efficiency of 74.1% was attained during the treatment of wastewater which was lower than those observed with either lactate, acetate or phenol. This lower removal efficiency indicates the complex nature of wastewater as compared to the model organic compounds. On the other hand, a familiar pattern was observed where COD removal percentage

was associated with CE. The highest CE value as well as power and current densities of 16.8%, 6533.3 mW m^{-3} and 14933.3 mA m^{-3}, respectively, were achieved when removal percentage was the highest.

8.2. Conclusions

Successful biodegradations of lactate, acetate and phenol in H-type MFCs were achieved with concomitant generation of electrical energy. The biodegradation of model organic compounds was accompanied by microbial growth and rise in OCP. The biodegradation of lactate led to the accumulation of biologically produced acetate. Preferential use of model compounds and effectiveness of biodegradation was observed with lactate being the favourable substrate followed by acetate and phenol. Utilization of lactate at higher initial concentrations led to higher biodegradation rates, while increase in phenol concentrations did not improve the biodegradation performance and slower rates were observed at high concentrations. Finally, initial concentration did not have any effect on acetate degradation.

Similar findings, in terms of biodegradation performance, were revealed when granular electrodes were utilized. However, biodegradation rates with this type of electrode were significantly higher than those with rod electrodes. In both evaluated MFC systems (MFC with rod or granular graphite electrodes) and regardless of type of substrate, higher substrate biodegradation rates or removal efficiencies led to higher OCP, power and current output indicating a correlation between biodegradation performance and electrochemical output.

The detailed biokinetic evaluation in MFCs with rod electrodes and freely suspended cells that focused on microbial growth and substrate biodegradation allowed development of suitable biokinetic models and determination of associated coefficients that were able to predict the microbial growth and biodegradation kinetics in MFC with high accuracy. The magnitude of biokinetic coefficients determined in MFC environmental conditions were markedly lower than those determined in conventional bioreactors, indicating the slow nature of microbial growth and activity in MFCs and thus raising the need for development of culture suitable for this purpose along with the design of more sophisticated MFC bioreactor configuration.

Continuous biodegradation of model organic compounds in MFCs equipped with either rod or granular electrodes improved biodegradation performance as compared to similar MFCs operated batchwise. Corresponding to the faster biodegradation, associated power and current output were improved as well. Biodegradation rate was not the only influential factor in the resulting power and current output and removal efficiency also played a critical role such that at comparable biodegradation rates, the higher removal efficiency led to higher power and current output. Moreover, a correlation between removal efficiency and coulombic efficiency was evident where higher removal percentage resulted in higher CE and ultimately higher electrochemical output.

Application of neutral red during biodegradation of phenol in batch MFCs resulted in higher biodegradation rates and eliminated the inhibition effects. However, neutral red did not offer any advantage during continuous operation of MFC. During co-biodegradation of phenol and lactate, contrary to expectation, the addition of lactate as a compound more amenable to biodegradation did not enhance phenol biodegradation. Presence of phenol at high concentrations (around 500 mg

L^{-1}) negatively impacted the biodegradation of lactate indicating the inhibitory effect of the recalcitrant substrate. Moreover, biodegradation of lactate was more effective than phenol, especially in the continuous systems were phenol degradation was substantially low, and thus power and current output were correlated to the extent of lactate oxidation.

The use of internal process stream wastewater as influent in a continuously operated MFC revealed a more challenging scenario as opposed to model organic compounds as the highest removal of organics (COD) was close to 75%. The maximum removal rate of COD achieved in this system was 318.2 mg COD L^{-1} h^{-1} and achieved at a loading rate of 645.5 mg COD L^{-1} h^{-1}. This however did not represent the ultimate performance of the MFC as technical difficulties did not allow operation of the MFC at higher loading rates. Similar to what was observed with model compounds, relation between biodegradation of organic contents of wastewater and electrochemical output was evident whereby the highest power and current output were achieved when COD removal efficiency and CE were at maximum.

8.3 Recommendations for future work

The operation and performance of an MFC system constitute both biological and electrochemical processes. The current work appears as one of very few studies focusing on a detailed kinetic study of microbial growth and biodegradation kinetics in an MFC environment, development of suitable kinetic models and determination of associated parameters. Additionally, results of the current study have shown the importance of microbial activity on biodegradation performance and its subsequent effect on resulting electrochemical output. Given the complex nature of municipal and industrial wastewaters, a similar biokinetic study that has been conducted on the model organic

compounds needs to be carried out for typical wastewaters to generate a better understanding of biodegradation kinetics in such wastewaters and their relation to the electrochemical outputs.

In order to achieve a comprehensive understanding and insight of MFC systems and to generate the detailed information required for the design, scale up, operation and control of MFC systems, the next logical step would entail a holistic approach to evaluate biological and electrochemical processes in context of each other and to establish the link between these processes. The generated information could be helpful in mathematical modelling of MFC type bioreactors that at some point should become the focus of attention.

As far as recommendations that specifically arose as part of the current research are concerned, one could refer to the necessity of more frequent monitoring of electrochemical outputs such as power and current using an accurate monitoring tool such as a potentiostat is recommended. Specifically, development of polarization and power curves for all experimental runs under different operating conditions would have yielded a better understanding of interconnection between biodegradation and electrochemical output.

In the same context, development of a method to quantify the biomass hold-up in MFCs with granular electrodes or in any other type of electrode with immobilized cells without disrupting the anodic processes would be a necessity in future studies. This will allow the accurate monitoring of biomass hold-up that is an essential information in understanding of biokinetic performance of MFC systems. Further biokinetic studies should look into utilization of MFCs in a configuration that could provide optimal electrochemical performance in order to understand the intrinsic biokinetics of high energy output systems.

Utilization of neutral red, as an electron shuttle/mediator was found to improve biodegradation of phenol (a recalcitrant model compound) in the batch MFCs but its effectiveness was not realized in the continuous systems. A critical issue with mediated electron transfer in MFCs is the diffusion of the electron shuttle in and out of the bacterial cells. The involved processes transpiring in the transfer of electrons has not been fully understood and thus require further studies especially with substrates that possess inhibitory effects on biodegradation and are recalcitrant in nature.

REFERENCES

Abourached C., Catal T., Liu H., "Efficacy of single-chamber microbial fuel cells for removal of cadmium and zinc with simultaneous electricity production," Water Res. 51, 228-233 (2014).

Aelterman P., Rabaey K., Pahm T.H., Boon N., Verstraete W., "Continuous electricity generation at high voltages and currents using stacked microbial fuel cells," Environ. Sci. Technol. 40, 3388-3394 (2006).

Agarry S.E., Solomon B.O., Layokun S.K., "Kinetics of batch microbial degradation of phenols by indigenous binary mixed culture of *Pseudomonas aeruginosa* and *Pseudomonas fluorescence*," African J. Biotechnol. 7, 2417-2423 (2008).

Agarry S.E., Audu T.O.K., Solomon B.O., "Substrate inhibition kinetics of phenol degradation by *Pseudomonas fluorescence* from steady state and wash-out data," Int. J. Environ. Sci. Technol. 6, 443-450 (2009).

Ahn Y., Logan B.E., "Effectiveness of domestic wastewater treatment using microbial fuel cells at ambient and mesophilic temperatures," Bioresour. Technol. 101, 469-475 (2009).

Aldrovandi A., Marsili E., Stante L., Paganin P., Tabacchioni S., Giordano A., "Sustainable power production in a membrane-less and mediator-less synthetic wastewater microbial fuel cell," Bioresour. Technol. 100, 3252-3260 (2009).

Allen R.M., Bennetto H.P., "Microbial fuel cells: Electricity production from carbohydrates," Appl. Biochem. Biotechnol. 39, 27-40 (1993).

Allsop P.J., Chisti Y., Moo-Young M., Sullivan G.R., "Dynamics of phenol degradation by *Pseudomonas putida*," Biotechnol. Bioeng. 41, 572-580 (1993).

Al-Khalid T., El-Naas M., "Aerobic biodegradation of phenols: A comprehensive review," Critical Rev. Environ. Sci. Technol. 42, 1631-1690 (2012).

Al-Zuhair S., El-Naas M., "Immobilization of *Pseudomonas putida* in PVA gel particles for the biodegradation of phenol at high concentrations," Biochem. Eng. J. 56, 46-50 (2011).

An S., Stone H., Nemati M., "Biological removal of nitrate by an oil reservoir culture capable of autotrophic and heterotrophic activities: Kinetic evaluation and modeling of heterotrophic process," J. Hazard Mater. 190, 686-693 (2011).

An S., Loden B., Nemati M., "Evaluation of heterotrophic nitrite removal by a sulphide and acetate oxidizing mixed culture originated from an oil reservoir," J. Chem. Technol. Biotechnol. 87, 410-417 (2012).

Angenent L.T., Karim K., Al-Dahhan M.H., Wrenn B.A., Dominguez-Espinosa R., "Production of bioenergy and biochemicals from industrial and agricultural wastewater," Trends Biotechnol. 22, 477-485 (2004).

Annadurai G., Juang R.S., Lee D.J., "Biodegradation and adsorption of phenol using activated carbon immobilized with *Pseudomonas putida*," J. Environ. Sci. Health 37, 1133-1146 (2002).

Antony M., Nair I.C., Jayachandran K., "Analysis of the pathway of phenol biodegradation by *Alcaligenes* sp. d2," in: Sabu A., Augustine A. (Eds.), "Prospects in bioscience: Addressing the issues," Springer, India (2013) pp. 209-220.

Babich H., Davis D.L., "Phenol: A review of environmental and health risks," Regulatory Toxicol. Pharmacol. 1, 90-109 (1981).

Behera M., Jana P.S., More T.T., Ghangrekar M.M., "Rice mill wastwater treatment in microbial fuel cells fabricated using proton exchange membrane and earthen pot at different pH," Bioelectrochemistry. 79, 228-233 (2010).

Bennetto H.P., "Electricity generation by microorganisms," Biotechnol. Educ. 1, 163-168 (1990a).

Bennetto H.P., "'Bugpower' - the generation of microbial electricity," In: "Frontiers of Science," ed. Scott A., Chapter 6. Blackwell, Oxford, (1990b) pp 60-82.

Bennetto H.P., Delaney G.M., Mason J.R., Roller S.D., Stirling J.L., Thurston C.F., "The sucrose fuel: efficient biomass conversion using a microbial catalyst," Biotechnol. Lett. 7, 699-704 (1985).

Bond D.R., Lovley D.R., "Electricity production by *Geobacter sulfurreducens* attached to electrodes," Appl. Environ. Microbiol. 69, 1548-1555 (2003).

Boyles, W., "The science of chemical oxygen demand. Technical information series, booklet no. 9," Hach Company, Loveland, Co, USA (1997).

Bretschger O., Cheung A.C.M., Mansfeld F., Nealson K.H., "Comparative microbial fuel cell evaluations of *Shewanella* spp.," Electroanalysis 22, 883-894 (2009).

Buitron G., Moreno-Andrade I., "Performance of a single-chamber microbial fuel cell degrading phenol: effect of phenol concentration and external resistance," Appl. Biochem. Biotechnol. 174, 2471-2481 (2014).

Caccavo F., Clegern W., Miller I., Montoya C., "The biological fuel cell," Am. Biol. Teach. 65, 615-618 (2003).

Call D.F., Logan B.E., "Lactate oxidation coupled to iron or electrode reduction by *Geobacter sulfurreducens* PCA," App. Environ. Microbiol. 77, 8791-8794 (2011).

Carawan, R.E., Waynick, J.B., "Reducing water use and wastewater in food processing plants: How one company cut costs," North Carolina Cooperative Extension Service, Publication number: CD-35. Available from http://www.p2pays.org/ref/01/00039.htm (1996).

Cheng S., Logan B.E., "Increasing power generation for scaling up single-chamber air cathode microbial fuel cells," Bioresour. Technol. 102, 4468-4473 (2011).

Cheng S., Liu H., Logan B.E., "Increased power generation in a continuous flow MFC with advective flow through porous anode and reduced electrode spacing," Environ. Sci. Technol. 40, 2426-2432 (2006).

Christen P., Vega A., Casalot L., Simon G., Auria R., "Kinetics of aerobic phenol biodegradation by the acidophilic and hyperthermophilic archaeon *Sulfolobus solfataricus*," Biochem. Eng. J. 62: 56-61 (2012).

Clauwaert P., van der Ha D., Boon N., Verbeken K., Verhaege M., Rabaey K., Verstraete W., "Open air biocathode enables effective electricity generation with microbial fuel cells," Environ. Sci. Technol. 41, 7564-7569 (2007).

Clauwaert P., Mulenga S., Aeltreman P., Verstraete W., "Litre-scale microbial fuel cells operated in a complete loop," Appl. Microbiol. Biotechnol. 83, 241-247 (2009).

Cookson J.T., "Bioremediation engineering: Design and application," McGraw-Hill Inc., New York (1995) pp 7-9.

Corcoran E., Nellemann C., Baker E., Bos R., Osborn D., Savelli H. (eds), "Sick water? The central role of wastewater management in sustainable development. A rapid response assessment." United nations environment programme, UN-Habitat, Grid-Arendal. http://www.grida.no/publications/218 (2010).

Dapaah S.Y., Hill G.A., "Biodegradation of chlorophenol mixtures by *Pseudomonas putida*," Biotechnol. Bioeng. 40, 1353-1358 (1992).

Daniel D.K., Mankidy B.D., Ambarish K., Manogari R., "Construction and operation of a microbial fuel cell for electricity generation from wastewater.," Int. J. Hydrogen Energy 34, 7555-7560 (2009).

Dekker A., Heijne A.T., Saakes M., Hamelers, H.V.M., Buisman C.J.N., "Analysis and improvement of a scaled-up and stacked microbial fuel cell," Environ. Sci. Technol. 43, 9038-9042 (2009).

Delaney G.M., Bennetto H.P., Mason J.R., Roller S.D., Stirling J.L., Thurston C.F., (1984) "Electron-transfer coupling in microbial fuel-cells. 2. Performance of fuel cells containing selected microorganism-mediator-substrate combinations," J. Chem. Technol. Biotechnol. 34, 13-27 (2009).

Droste R.L., "Theory and practice of water and wastewater treatment," John Wiley and Sons Inc., New York, (1997) pp 549.

dos Santos V.L., Monteiro A., Braga D.T., Santoro M.M., "Phenol degradation by *Aureobasidium pullulans* FE13 isolated industrial effluents," J. Haz. Mat. 161, 1413-1420 (2009).

Du Z., Li H., Gu T., "A start of the art review on microbial fuel cells: A promising technology for wastewater treatment and bioenergy," Biotechnol. Adv. 25, 464-482 (2007).

El-Naas M.E., Al-Muhtaseb S.A., Makhlouf S., "Biodegradation of phenol by *Pseudomonas putida* immobilized in polyvinyl alcohol (PVA) gel," J. Haz. Mat. 164, 720-725 (2009).

Environment and Climate Change Canada, "Second Priority Substances List (PSL2)," [cited 2016 April 16]. Available from: http://www.ec.gc.ca/ese-ees/default.asp?lang=En&n=C04CA116-1/.

Fan Y., Sharbrough E., Liu H., "Quantification of the internal resistance distribution of microbial fuel cells," Environ. Sci. Technol. 42, 8101-8107 (2008).

Fan Y., Han S.K., Liu H., "Improved performance of CEA microbial fuel cells with increased reactor size," Energy Environ. Sci. 5, 8273-8280 (2012).

Feng Y., Lee H., Wang X., Liu Y., He W., "Continuous electricity generation by a graphite granule baffle air-cathode microbial fuel cell," Bioresour. Technol. 101, 632-638 (2010).

Feng C., Huang L., Yu H., Yi X., Wei C., "Simultaneous phenol removal, nitrification and denitrification using microbial fuel cell technology," Water Res. 76, 160-170 (2015).

Flemming, H.C., "Why microorganisms live in biofilms and the problem of biofouling" In: "Marine and industrial biofouling," eds. Flemming H.C., Murthy P.S., Venkatesan R., Cooksey K., Chapter 1. Springer, Berlin Heidelberg, (2009) pp 3-12.

Friman H., Schechter A., Nitzan Y., Cahan R., "Effect of external voltage on *Pseudomonas putida* F1 in a bio electrochemical cell using toluene as sole carbon and energy source," Microbiol. 158, 414-423 (2012a).

Friman H., Schechter A., Ioffe Y., Nitzan Y., Cahan R., "Current production in a microbial fuel cell using a pure culture of *Cupriavidus basilensis* growing in acetate or phenol as a carbon source," Microb. Biotechnol. 6, 425-453 (2012b).

Gonzales G., Herrera M.G., Garcia M.T., Pena M.M., "Biodegradation of phenol in a continuous process: comparative study of stirred tank and fluidized-bed bioreactors," Bioresour Technol. 76, 245-251 (2001).

Gorby Y.A., Yanina S., McLean J.S., Rosso K.M., Moyles D., Dohnalkova A., Beveridge T.J., Chang I.S., Kim B.H., Kim S.K., Culley D.E., Reed S.B., Romine M.F., Saffarini D.A., Hill E.A., Shi L., Elias D.A., Kennedy D.W., Pinchuk G., Watanabe K., Ishii S., Logan B.E., Nealson K.H., Fredrickson J.K., "Electrically conductive bacterial nanowires produced by *Shewanella oneidensis* strain MR-1 and other microorganisms," Proc. of the Nat. Acad. Sci. 103, 11358–11363 (2006).

Goudar C.T., Ganji S.H., Pujar B.G., Strevett K.A., "Substrate inhibition kinetics of phenol biodegradation," Water Environ. Res. 72, 50-55 (2000).

Greenman J., Galvez A., Giusti L., Ieropoulos I., "Electricity from landfill leachate using microbial fuel cells: comparison with a biological aerated filter," Enzyme Microb. Technol. 44, 112–119 (2009).

Gude V.G., "Wastewater treatment in microbial fuel cells – an overview," J. Clean. Prod. 122, 287-307 (2016).

Hamelers H.V.M., Heijne A.T., Stein N., Rozendal R.A., Buisman C.J.N., "Butler-Volmer-Monod model for describing bio-anode polarization curves," Bioresour. Technol. 102, 381-387 (2011).

Hao O.J., "Sulphate-reducing bacteria" In: "Handbook of water and wastewater microbiology," eds. Mara D, Horan N., Academic Press, London (2003) pp. 459-467.

He Z., Minteer S.D., Angenent L.T., "Electricity generation from artificial wastewater using an upflow microbial fuel cell," Environ. Sci. Technol. 39, 5262-5267 (2005).

He Z., Wagner N., Minteer S.D., Angenent L.T., "An upflow microbial fuel cell with an interior cathode: Assessment of the internal resistance by impedance spectroscopy," Environ. Sci. Technol. 40, 5212-5217 (2006).

Hedbavna P., Rolfe S.A., Huang W.E., Thornton S.F., "Biodegradation of phenolic compounds and their metabolites in contaminated groundwater using microbial fuel cells," Bioresour. Technol. 200, 426-434 (2016).

Heijne A.T., Liu F., van Rijnsoever L.S., Saakes M., Hamelers H.V.M., Buisman C.J.N., "Performance of a scaled-up microbial fuel cell with iron reduction as the cathode reaction," J. Power Sources. 196, 7572-7577 (2011).

Hernández-Fernández F.J., de los Rios A.P., Salar-Garcia M.J., Ortiz-Martinez V.M., Lozano-Blanco L.J., Godinez C., Tomas-Alonso F., Quesada-Medina J., "Recent progress and perspectives in microbial fuel cells for bioenergy generation and wastewater treatment," Fuel Process. Technol. 138, 284-297 (2015).

Hill G.A., Robinson C.W., "Substrate inhibition kinetics: Phenol degradation by *Pseudomonas putida*," Biotechnol. Bioeng. 17, 1599-1615 (1975).

Ishii S., Watanabe K., Yabuki S., Logan B.E., Sekiguchi Y., "Comparison of electrode reduction activities of *Geobacter sulfurreducens* and an enriched consortium in an air-cathode microbial fuel cell," Appl. Environ. Microbiol. 74, 7348-7355 (2008).

Jadhav G.S., Ghangrekar M.M., "Performance of microbial fuel cell subjected to variation in pH, temperature, external load and substrate concentration," Bioresour. Technol. 100, 717-723 (2009).

Jang J.K., Pham T.H., Chang I.S., Kang K.H., Moon H., Cho K.S., Kim B.H., "Construction and operation of a novel mediator- and membrane-less microbial fuel cell," Process Biochem. 39, 1007-1012 (2004).

Janicek A., Fan Y., Liu H., "Design of microbial fuel cells for practical application: a review and analysis of scale-up studies," Biofuels. 5, 79-92 (2014).

Jayashree C., Arulazhagan P., Kumar S.A., Kaliappan S., Yeom I.T., Banu R., "Bioelectricity generation from coconut husk retting wastewater in fed batch operating microbial fuel cell by phenol degrading microorganism," Biomass Bioenerg. 69, 249-254 (2014).

Juang D.F., Yang P.C., Lee C.H., Hsueh S.C., Kuo T.H., "Electrogenic capabilites of gram negative and gram positive bacteria in microbial fuel cell combined with biological wastewater treatment," Int. J. Environ. Sci. Tech. 8, 781-792 (2011).

Jung S., Regan J.M., "Comparison of anode bacterial communities and performance in microbial fuel cells with different electron donors," Appl. Microbiol. Biotechnol. 77, 393-402 (2007).

Kafilzadeh F., Farhangdoost M.S., Tahery Y., "Isolation and identification of phenol degrading bacteria from Lake Parishan and their growth kinetic assay," Afr. J. Biotechnol. 9, 6721-6726 (2010).

Kim H.J., Park H.S., Hyun M.S., Chang I.S., Kim M., Kim B.H., "A mediator-less microbial fuel cell using a metal reducing bacterium, *Shewanella putrefaciens*," Enzyme Microb. Technol. 30, 145-152 (2002).

Kim J.R., Cheng S., Oh S.E., Logan B.E., "Power generation using different cation, anion and ultrafiltration membranes in microbial fuel cells," Environ. Sci. Technol. 41, 1004-1009 (2007).

Kumar A., Kumar S., Kumar S., "Biodegradation kinetics of phenol and catechol using *pseudomonas putida* MTCC 1194," Biochem Eng J. 22, 151-159 (2005).

Kumar P., "Remediation of high phenol concentrations using chemical and biological technologies," PhD Dissertation, College of Engineering, University of Saskatchewan, Saskatoon, Canada (2010).

Lee S.K., Chun Y.N., Kim S.I. "Characteristics of phenol degradation by immobilized activated sludge," J. Ind. Eng. Chem. 15, 323-327 (2009).

Liu H., Logan B.E., "Electricity generation using an air-cathode single chamber microbial fuel cell in the presence and absence of a proton exchange membrane," Environ. Sci. Technol. 38, 4040-4046 (2004).

Liu H., Cheng S., Logan B.E., "Production of electricity from acetate or butyrate using a single-chamber microbial fuel cell," Environ. Sci Technol. 39, 658-662 (2005a).

Liu H., Cheng S., Logan B.E., "Power generation in fed-batch microbial fuel cells as a function of ionic strength, temperature, and reactor configuration," Environ Sci Technol. 39, 5488-5493 (2005b).

Logan B.E., "Microbial fuel cells," John Wiley & Sons Inc., New York, (2008).

Logan, B.E., "Exoelectrogenic bacteria that power microbial fuel cells," Nat. Rev. Microbiol. 7, 375-381 (2009).

Logan B.E., "Scaling up microbial fuel cells and other bioelectrochemical systems," Appl. Microbiol. Biotechnol. 85, 1665-1671 (2010).

Logan B.E., Regan J.M., "Microbial fuel cells- challenges and applications," Environ. Sci. Technol. 40, 5172-5180 (2006).

Logan B.E., Cheng S., Watson V., Estadt G., "Graphite fiber brush anodes for increased power production in air-cathode microbial fuel cells," Environ. Sci. Technol. 41, 3341-3346 (2007).

Lovley D.R., "Bug juice: harvesting electricity with microorganisms," Nature Rev. Microbiol. 4, 497-508 (2006a).

Lovley D.R., "Microbial fuel cells: novel microbial physiologies and engineering approaches," Curr. Opin. Biotechnol. 17, 327-332 (2006b).

Lovley D.R., Phillips E.J.P., Lonergan D.J., "Hydrogen and formate oxidation coupled to dissimilatory reduction of iron or manganese by *Alteromonas putrefaciens*," Appl. Environ. Microbiol. 55, 700-706 (1989).

Lu N., Zhou S.G., Zhuang L., Zhang J.T., Ni J.R., "Electricity generation from starch processing wastewater using microbial fuel cell technology," Biochem. Eng. J. 43, 246–251 (2009).

Luo H., Liu G., Zhang R., Jin S., "Phenol degradation in microbial fuel cells," Chem. Eng. J. 147, 259-264 (2009).

Madiraju K., “On the prediction of power outputs in a microbial fuel cell employing *Escherichia coli* K12 as the biocatalyst,” MSc Thesis. Department of Bioresource Engineering, McGill University (2013).

Majumder D., Maity J.P., Tseng M.J., Nimje V.R., Chen H.R., Chen C.C., Chang Y.F., Yang T.C., Chen C.Y., “Electricity generation and wastewater treatment of oil refinery in microbial fuel cells using *Pseudomonas putida*,” Int. J. Mol. Sci. 15, 16772-16786 (2014).

Mancy K.H., Weber W.J., “Analysis of industrial wastewaters,” John Wiley and Sons Inc. (1971) pp 490.

Manohar A.K., Mansfeld, F., “The internal resistance of a microbial fuel cell and its dependence on cell design and operating conditions,” Electrochim. Acta 54, 1664-1670 (2009).

Marcus A.K., Torres C.I., Rittmann B.E., “Conduction-based modeling of the biofilm anode of a microbial fuel cell,” Biotechnol. Bioeng. 98, 1171-1182 (2207).

Mathuriya A.S., Yakhmi J.V., “Microbial fuel cells – Applciations for generation of electrical power and beyond,” Crit. Rev. Microbiol. 42, 127-143 (2016).

Min B., Logan B.E., “Continuous electricity generation from domestic wastewater and organic substrates in a flat plate microbial fuel cell,” Environ. Sci. Technol. 38, 5809-5814 (2004).

Min B., Kim J.R., Oh S., Regan J.M., Logan B.E., “Electricity generation from swine wastewater using microbial fuel cells,” Water Res. 39, 4961–4968 (2005a).

Min B., Cheng S., Logan B.E., “Electricity generation using membrane and salt bridge microbial fuel cells,) Water Res. 39, 1675-1686 (2005b).

Min B., Roman O.B., Angelidaki I., “Importance of temperature and anodic medium composition on microbial fuel cell (MFC) performance,” Biotechnol. Lett. 30, 1213-1218 (2008).

Mohan S.V., Saravanan R., Raghavulu S.V., Mohanakrishna G., Sarma P.N., “Bioelectricity production from wastewater treatment in dual chambered microbial fuel cell (MFC) using selectively enriched mixed flora: Effect of catholyte,” Bioresour. Technol. 99, 596-603 (2008).

Mohan S.V., Mohanakrishna G., Velvizhi G., Babu V.L., Sarma P.N., “Bio-catalyzed electrochemical treatment of real field dairy wastewater with simultaneous power generation,” Biochem. Eng. J. 51, 32-39 (2010).

Molin G., Nilsson I., “Degradation of phenol by *Pseudomonas putida* ATCC 11172 in continuous culture at different ratios of biofilm surface to culture volume,” Appl Environ Microbiol. 50, 946-950 (1985).

Monteiro A.A.M.G., Boaventura R.A.R., Rodrigues A.E., "Phenol biodegradation by *Pseudomonas putida* DSM 548 in a batch reactor," Biochem. Eng. J, 6, 45-49 (2000).

Mordocco A., Kuek C., Jenkins R., "Continuous degradation of phenol at low concentration using immobilized *Pseudomonas putida*," Enzyme Microbial Technol. 25, 530-536 (1999).

Niessen J., Schröder U., Scholz F., "Exploiting complex carbohydrates for microbial electricity generation – a bacterial fuel cell operating on starch," Electrochem. Commun. 6, 955–958 (2004).

Oh S.T., Kim J.R., Premier, G.C., Lee T.H., Kim C., Sloan W.T., (2010) "Sustainable wastewater treatment: How might microbial fuel cells contribute," Biotechnol. Adv. 28, 871-881 (2004).

O'Sullivan M., "The degradation of phenol and mono-chlorophenols by a mixed microbial population," PhD Thesis, School of Biotechnology, Dublin City University (1998).

Pandit S., Patel V., "Wastewater as anolyte for bioelectricity generation in graphite granule anode single chambered microbial fuel cell: effect of current collector," Int. J. Environ. Technol. Manage. 17, 252-267 (2014).

Pant D., Van Bogaert G., Diels L., Vanbroekhoven K., "A review of substrates used in microbial fuel cells (MFCs) for sustainable energy production," Bioresour. Technol. 101, 1533-1543 (2010).

Park D.H., Zeikus J.G., "Electricity generation in microbial fuel cells using neutral red as an electrophore," Appl. Environ. Microbiol. 66, 1292-1297 (2000).

Paslawski J., "The kinetics of biodegradation of trans 4-methyl-1-cyclohexane carboxylic acid," PhD Dissertation, College of Engineering, University of Saskatchewan, Saskatoon, Canada (2008).

Pazarlioglu N.K., Telefoncu A., "Biodegradation of phenol by *Pseudomonas putida* immobilized on activated pumice particles," Process Biochem. 40, 1807-1814 (2005).

Picioreanu C., Head I.M., Katuri K., van Loosdrecht M.C.M., Scott K., "A computational model for biofilm-based microbial fuel cells," Water Res. 41, 2921-2940 (2007).

Polymenakou P.N., Stephanou E.G., "Effect of temperature and additional carbon sources on phenol degradation by an indigenous soil *Pseudomonad*," Biodegradation 16, 403-413 (2005).

Potter M.C., "Electrical effects accompanying the decomposition of organic compounds," Proc. Roy. Soc. London Ser. B, 84, 260-276 (1911).

Pradeep N.V., Anupama S., Navya K., Shalini H.N., Idris M., Hampannavar U.S., "Biological removal of phenol from wastewaters: a mini review," Appl. Water Sci. 5, 105-112 (2014).

Puig S., Serra M., Coma M., Cabre M., Balaguer M.D., Colprim J., "Effect of pH on nutrient dynamics and electricity production using microbial fuel cells," Bioresour. Technol. 101, 9594-9599 (2010).

Rabaey K., Verstraete W., "Microbial fuel cells: novel biotechnology for energy generation," Trends Biotechnol. 23, 291-298 (2005).

Rabaey K., Lissens G., Siciliano S.D., Verstraete W., "A microbial fuel cell capable of converting glucose to electricity at high rate and efficiency," Biotechnol. Lett. 25, 1531-1535 (2003).

Rabaey K., Boon N., Siciliano S.D., Verhaege M., Verstraete W., "Biofuel cells select for microbial consortia that self-mediate electron transfer," App. Environ. Microbiol. 70, 5373-5382 (2004).

Rabaey K., Boon N., Hofte M., Verstraete W., "Microbial phenazine production enhances electron transfer in biofuel cells," Environ. Sci. Technol. 39, 3401-3408 (2005a).

Rabaey K., Clauwaert P., Aelterman P., Verstraete W., "Tubular microbial fuel cells for efficient electricity generation," Environ. Sci. Technol. 39, 8077-8082 (2005b).

Rabaey K., Van de Sompel K., Maignien L., Boon N., Aelterman P., Clauwaert P., De Schamphelaire L., Pham H.T., Vermeulen J., Verhaege M., Lens P., Verstraete W., "Microbial fuel cells for sulfide removal," Environ. Sci. Technol. 40, 5218-5224 (2006).

Rabaey K., Rodriguez J., Blackall L.L., Keller J., Gross P., Batstone D., Verstraete W., Nealson K.H., "Microbial ecology meets electrochemistry: electricity-driven and driving communities," ISME J. 1, 9-18 (2007).

Rabus R., Hansen T.A., Widdel F., "Dissimilatory sulfate- and sulfur reducing prokaryotes," Prokaryotes 2, 659-768 (2006).

Rahimnejad M., Ghoreyshi A.A., Najafpour G., Jafary, T., "Power generation from organic substrate in batch and continuous flow microbial fuel cell operations," Appl. Energy 88, 3999-4004 (2001).

Rahimnejad M., Ghoreyshi A.A., Najafpour G.D., Younesi H., Shakeri M., "A novel microbial fuel cell stack for continuous production of clean energy," Int. J. Hydrogen Energy 37, 5992-6000 (2012).

Read R.R., Costerton J.W., "Purification and characterization of adhesive exopolysaccharides from *Pseudomonas putida* and *Pseudomonas flourescens*," Can. J. Microbiol. 33, 1080-90 (1987).

Reguera G., McCarthy K.D., Mehta T., Nicoll J., Tuominen M.T., Lovley D.R., "Extracellular electron transfer via microbial nanowires," Nature 435, 1098–1101 (2005).

Reguera G., Nevin K.P., Nicoll J.S., Covalla S.F., Woodard T., Lovley D.R., "Biofilm and nanowire production leads to increased current in *Geobacter sulfurreducens* fuel cells," App. Environ. Microbiol. 72, 7345–7348 (2006).

Rezaei F., Xing D., Wagner R., Regan J.M., Richard T.L., Logan B.E., "Simultaneous cellulose degradation and electricity production by Enterobacter cloacae in a microbial fuel cell," Appl. Environ. Microbiol. 75, 3673–3678 (2009).

Ringeisen B.R., Henderson E., Wu P.K., Pietron J., Ray R., Little B., Biffinger J.C., Jones-Meehan, J.M., "High power density from a miniature microbial fuel cell using *Shewanella oneidensis* DSP10," Environ. Sci. Technol. 40, 2629-2634 (2006).

Rodriguez J., Premier G.C., "Towards a mathematical description of bioelectrochemical systems," In: "Bioelectrochemical systems: From extracellular electron transfer to biotechnological application," eds. Rabaey K., Angenent L., Schroeder U., Keller J., IWA Publishing, London, (2010) pp. 442.

Roller S.D., Bennetto H.P., Delaney G.M., Mason J.R., Stirling J.L., Thurston C.F., "Electron-transfer coupling in microbial fuel-cells. 1. Comparison of redox-mediator reduction rates and respiratory rates of bacteria," J. Chem. Technol. Biotechnol. 34, 3-12 (1984).

Rozich A.F., Colvin R.J., "Effects of glucose on phenol biodegradation by heterogenous populations," Biotechnol. Bioeng. 28, 965-971 (1986).

Schroder U., "Anodic electron transfer mechanisms in microbial fuel cells and their energy efficiency," Phys. Chem. Chem. Phys. 9, 2619-2629 (2007).

Seker S., Beyenal H., Salih B., Tanyolac A., "Multi-substrate growth kinetics of *Pseudomonas putida* for phenol removal," Appl. Microbiol. Technol. 47, 610-614 (1997).

Shizas I., Bagley D.M., "Experimental determination of energy content of unknown organics in municipal wastewater streams," J. Energy Eng. 130, 45-53 (2004).

Shuler M.L., Kargi, F. "Bioprocess Engineering Basic Concepts" 2nd Ed., Prentice Hall (2001) pp 211-220.

Song T., Wu X., Zhou C.C., "Effect of different acclimation methods on the performance of microbial fuel cells using phenol as substrate," Bioprocess Biosyst. Eng. 37, 133-138 (2014).

Sorensen A.H., Winther-Nielsen M., Ahring B.K., "Kinetics of lactate acetate and propionate in unadapted and lactate-adapted thermophilic, anaerobic sludge: the influence of sludge adaptation for start-up of thermophilic UASB-reactors," Appl. Microbiol. Technol. 34, 823-827 (1990).

Tchobanoglous G., Burton F.L., Stensel H.D., "Wastewater Engineering, Treatment and Reuse," Metcalf & Eddy, Inc., 4th edition, McGraw-Hill, Boston (2003).

Thurston C.F., Bennetto H.P., Delaney G.M., Mason J.R., Roller S.D., Stirling J.L., "Glucose metabolism in a microbial fuel cell. Stoichiometry of product formation in a thionine-mediated *Proteus vulgaris* fuel cell and its relation to coulombic yields," J. Gen. Microbiol. 131, 1393-1401 (1985).

Torres C.I., "On the importance of identifying, characterizing, and predicting fundamental phenomena towards microbial electrochemistry applications," Curr. Opin. Biotechnol. 27, 107-114 (2014).

Tremouli A., Martinos M., Bebelis S., Lyberatos G., "Performance assessment of a four-air cathode single-chamber microbial fuel cell under conditions of synthetic and municipal wastewater treatments," J. Appl. Electrochem. 46, 515-525 (2006).

Tziotzios G., Teliou M., Kaltsouni V., Lyberatos G., Vayenas D.V., "Biological phenol removal using suspended growth and packed bed reactors," Biochem Eng J. 26, 65-71 (2005).

United States Environmental Protection Agency, "Priority pollutants," [cited 2016 May 6]. Available from: http://water.epa.gov/scitech/methods/cwa/pollutants.cfm/.

Vidali M., "Bioremediation: An overview," Pure Appl. Chem. 73, 1163-1172 (2001).

Wang K.W., Baltzis B.C., Lawandowski, G.A., "Kinetics of phenol biodegradation in the presence of glucose," Biotechnol. Bioeng. 51, 87-94 (1996).

Wang S.J., Loh K.C., "Biotransformation kinetics of *Pseudomonas putida* for cometabolism of phenol and 4-chlorophenol in the presence of sodium glutamate," Biodegradation 12, 189-199 (1999).

Wang Y., Song J., Zhao W., He X., Chen J., Xiao M., "In situ degradation of phenol and promotion of plant growth in contaminated environments by a single *Pseudomonas aeruginosa* strain," J. Haz. Mat. 192, 354-360 (2011).

Wang H., Ren Z.J., "A comprehensive review of microbial electrochemical systems as a platform technology," Biotechnol. Adv. 31, 1796-1807 (2013).

Wang H., Park J.D., Ren Z.J., "Practical energy harvesting for microbial fuel cells: A review," Environ. Sci. Technol. 49, 3267-3277 (2015).

Wen Q., Wu Y., Cao D., Zhao L., Sun Q., "Electricity generation and modeling of microbial fuel cell from continuous beer brewery wastewater," Bioresour. Technol. 100, 4171–4175 (2009).

You S.J., Zhao Q.L., Jiang J.Q., Zhang J.N., Zhao S.Q., "Sustainable approach for leachate treatment: electricity generation in microbial fuel cell," J Environ Sci Heal A. 41, 2721-2734 (2006).

You S., Zhao Q., Zhang J., Jiang J., Wan C., Du M., Zhao S., "A graphite-granule membrane-less tubular air-cathode microbial fuel cell for power generation under continuously operational conditions," J. Power Sources. 173, 172-177 (2007).

Zellner G., Neudorfer F., Diekmann H., "Degradation of lactate by an anaerobic mixed culture in a fluidized-bed reactor," Water Res. 28, 1337-1340 (1993).

Zhang X., He W., Ren L., Stager J., Evans P.J., Logan B.E., "COD removal characteristics in air-cathode microbial fuel cells," Bioresour. Technol. 176, 23-31 (2015).

Zuo Y., Cheng S., Call D., Logan B.E., "Tubular membrane cathodes for scalable power generation in microbial fuel cells," Environ. Sci, Technol. 41, 3347-3353 (2007).

Zuo, Y., Xing, D., Regan, J.M., Logan, B.E., "Isolation of the exoelectrogenic bacterium *Ochrobactrum anthropi* YZ-1 by using a U-tube microbial fuel cell," App. Environ. Microbiol. 74, 3130-3137 (2008).

Appendices

A. Calibration of biomass concentration

A 50 mL culture of *P. putida* was diluted 2, 5 and 10 times and corresponding optical density readings at these dilutions were determined. The entire culture was then processed in a centrifuge to facilitate concentration of cell suspension. This was then placed in an oven for at least 24 h to determine the dry weight of the biomass. From this, the biomass concentration of *P. putida* was determined. Biomass concentration and corresponding OD readings at different dilution rates were used to develop the calibration curve as shown below.

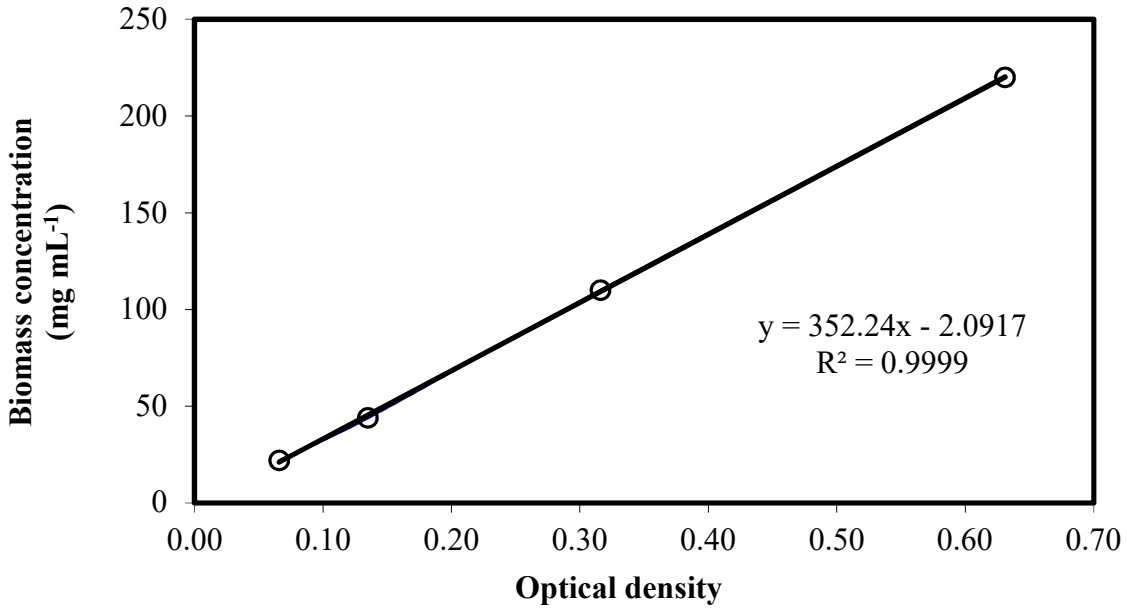

Figure A.1 Calibration of biomass concentration in terms of optical density (OD).

B. Calibration of model organic compounds concentration

Standard solutions of lactate, acetate, pyruvate and phenol were prepared by mixing specified amounts of each of the model organic compounds with modified McKinney's medium. Calibration procedures specific to the type of HPLC detector and column were followed and resulting calibration curve for each model organic compound is shown below. In all cases, concentration of model organic compound is in mg L^{-1}.

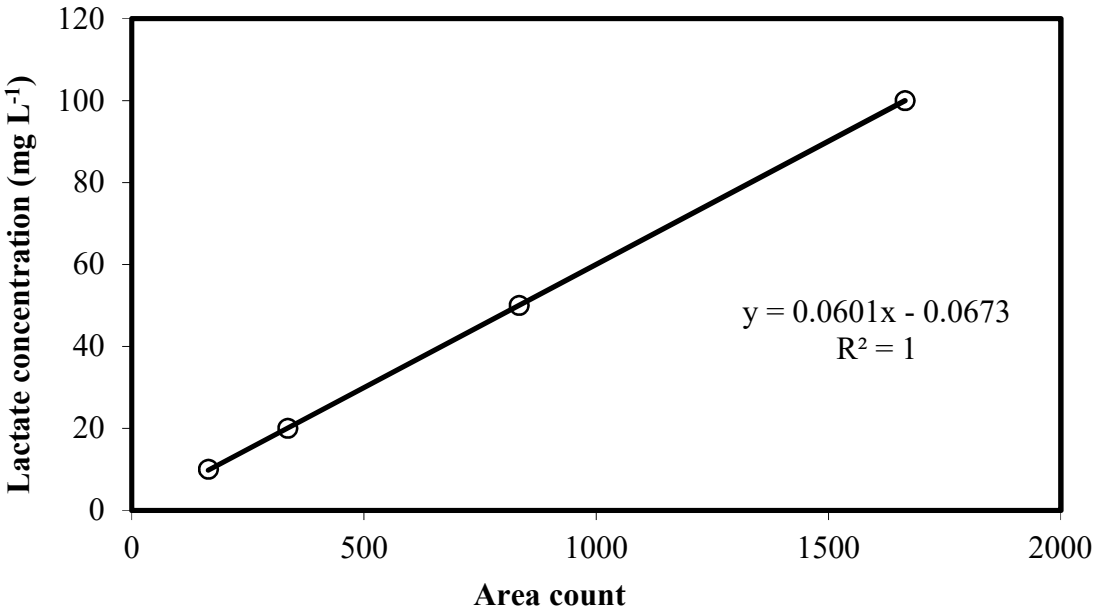

Figure B.1 Calibration of lactate concentration.

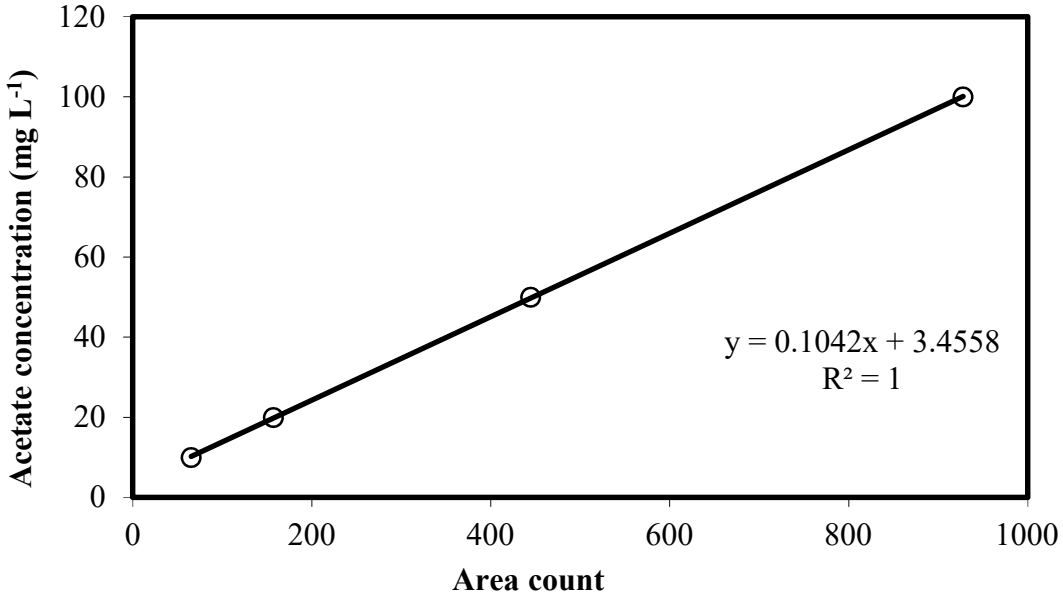

Figure B.2 Calibration of acetate concentration.

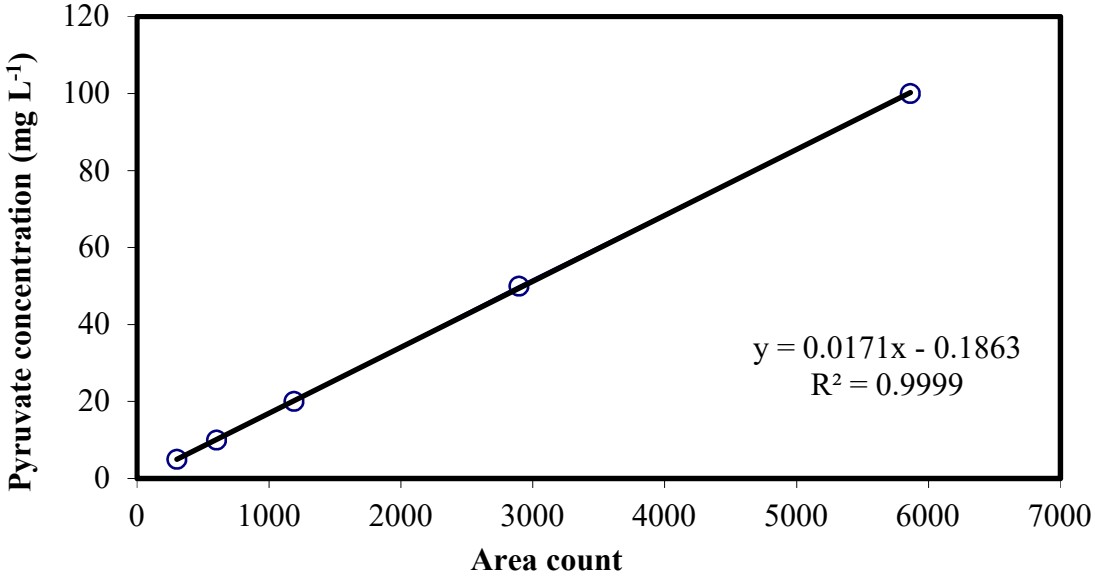

Figure B.3 Calibration of pyruvate concentration.

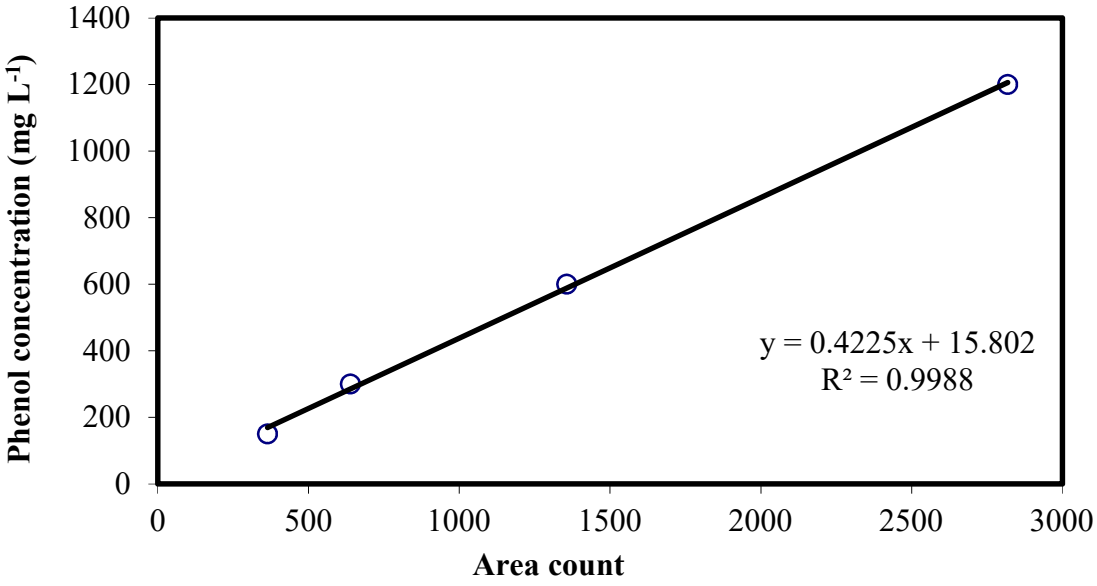

Figure B.4 Calibration of phenol concentration.

C. Sensitivity analysis results of the biokinetic model for the accumulation of biologically produced acetate

Biokinetic coefficients from the accumulation of biologically produced acetate were also tested for sensitivity analysis which showed unnoticeable effects especially when compared to results from the biodegradation of lactate and acetate as original substrate shown in Figure 3.17.

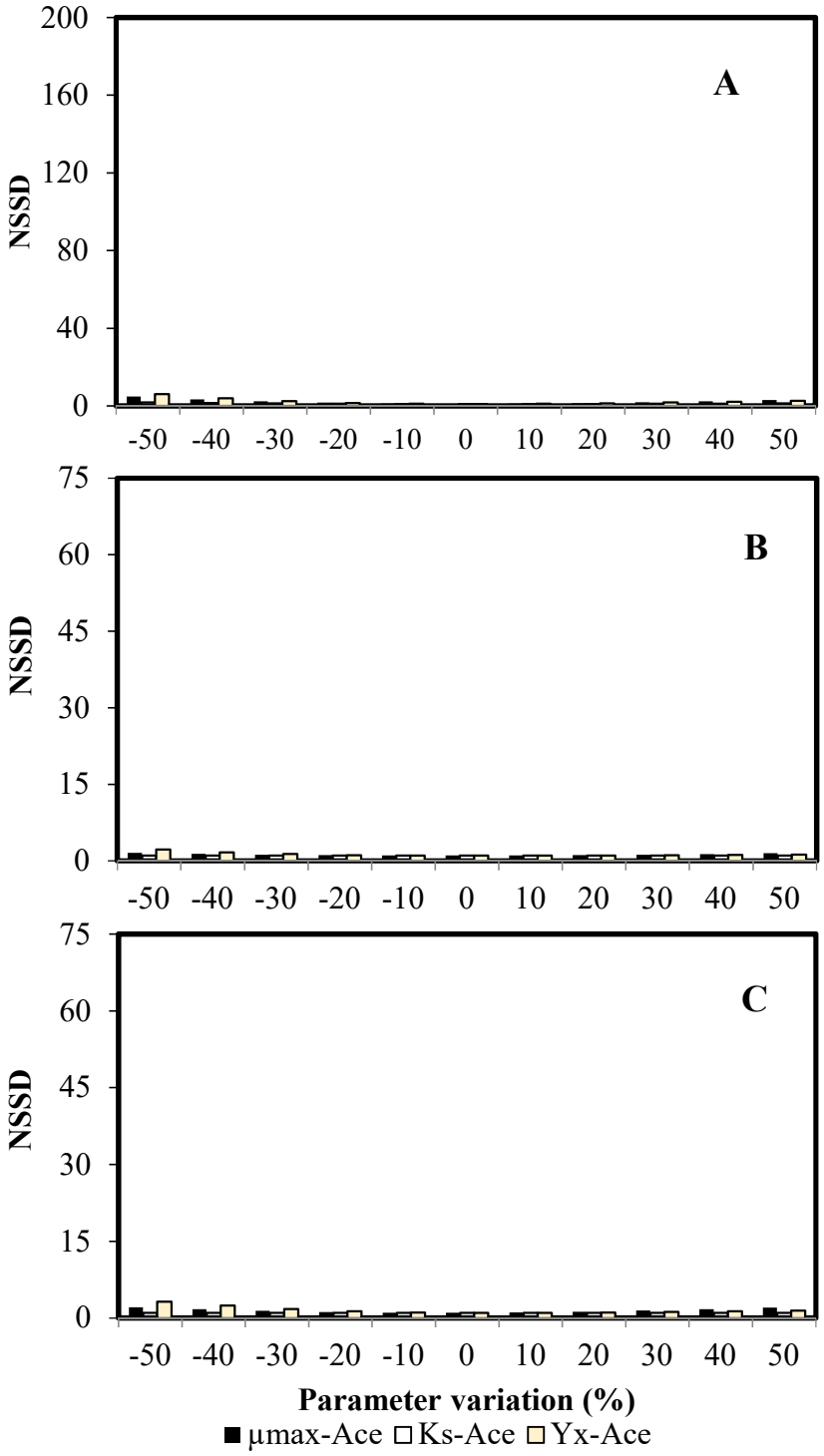

Figure C.1 Analysis of model sensitivity to various biokinetic coefficients calculated from the accumulation of biologically produced acetate resulting from the biodegradation of A) 1,000, B) 2,500 and C) 5,000 mg L^{-1} lactate.

D. Model predictions of phenol biodegradation in MFC with rod electrodes operated batchwise evaluated following Monod kinetics

A similar approach employed in the biokinetic evaluation of lactate and acetate biodegradation in similar MFCs with rod electrodes and suspended cells was also conducted for phenol. It was assumed that microbial growth and phenol utilization followed Monod kinetics. The mass balances for biomass and phenol are given by equations below. Calculation of biokinetic parameters was carried out using 4th order Runge-Kutta method and Excel software. The objective function used for the least square minimization is given by equation D.3.

$$\frac{dX}{dt} = \left(\frac{\mu_{max-P} \quad S_{Phe}}{K_{S-Phe}+S_{Phe}} - K_{d-Phe}\right) X \tag{D.1}$$

$$\frac{dS_{Phe}}{dt} = -\frac{1}{Y_{X-Phe}}\left(\frac{\mu_{max-P} \quad S_{Phe}}{K_{S-Phe}+S_{Phe}} - K_{d-Phe}\right) X \tag{D.2}$$

$$f = \sum_i^n \left(S_{i-Phe-measured} - S_{i-Phe-predict} \quad\right)^2 + \left(S_{i-X-measured} - S_{i-X-predicted}\right)^2 \tag{D.3}$$

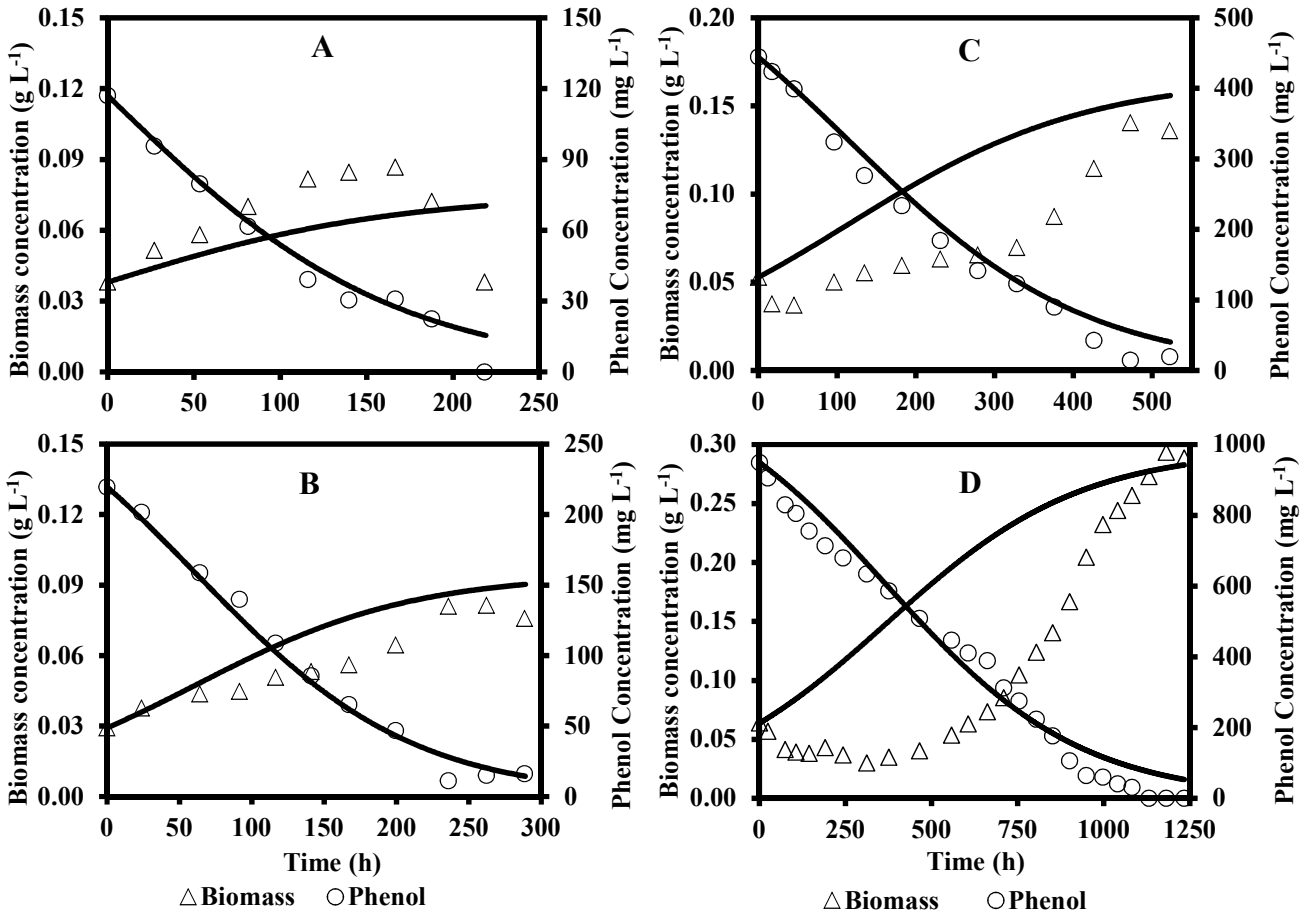

Figure D.1 Goodness of fit of model predictions (solid lines) and experimental data (symbols) for biomass growth and phenol biodegradation in batch MFCs with rod electrodes operated with 100 (A), 250 (B), 500 (C) and 1000 mg L^{-1} (D) phenol.

E. Data used in determination of first order rate constant of phenol biodegradation in MFCs with rod electrodes operated batchwise.

Table E.1. Calculated values for modeling of 100 mg L^{-1} phenol biodegradation in batch operated MFC.

t (h)	C (mg L^{-1})	ln (C/C_0)	X (mg L^{-1})	$\bar{X}$ (mg L^{-1})	$\bar{X}$t (mg L^{-1} h)
21.7	117.1	0.00	38.05	0.00	0.00
48.7	95.6	0.20	51.43	44.74	2178.96
75.0	79.7	0.38	58.13	54.78	4108.52
103.0	61.7	0.64	70.10	64.11	6603.70
137.7	39.1	1.10	81.72	75.91	10453.12
161.3	30.5	1.34	84.54	83.13	13409.26
188.3	30.9	1.33	86.65	85.60	16118.07
209.3	22.5	1.65	72.21	79.43	16625.60

Table E.2. Calculated values for modeling of 250 mg L^{-1} phenol biodegradation in batch operated MFC.

t (h)	C (mg L^{-1})	ln (C/C_0)	X (mg L^{-1})	$\bar{X}$ (mg L^{-1})	$\bar{X}$t (mg L^{-1} h)
25.0	219.62	0.00	29.25	0.00	0.00
48.7	201.56	0.09	37.70	33.47	1630.10
89.0	158.73	0.32	43.69	40.69	3621.61
116.3	139.94	0.45	44.74	44.21	5142.12
141.3	108.88	0.70	50.73	47.74	6745.14
166.0	85.63	0.94	53.20	51.96	8625.81
192.0	65.20	1.21	56.01	54.60	10484.01
224.3	46.88	1.54	64.47	60.24	13511.70
260.7	11.34	2.96	81.02	72.74	18963.97

Table E.3. Calculated values for modeling of 500 mg L^{-1} phenol biodegradation in batch operated MFC.

t (h)	C (mg L^{-1})	ln (C/C_0)	X (mg L^{-1})	$\bar{X}$ (mg L^{-1})	$\bar{X}$t (mg L^{-1} h)
5.7	444.38	0.00	52.84	0.00	0.00
22.7	423.62	0.05	37.70	45.27	1027.65
50.7	399.23	0.11	36.99	37.35	1893.46
101.7	323.80	0.32	50.03	43.51	4424.96
140.3	276.25	0.48	55.31	52.67	7389.19
187.7	233.44	0.64	59.54	57.42	10778.07
236.7	184.17	0.88	63.06	61.30	14508.76
284.0	141.51	1.14	65.52	64.29	18258.27
333.7	122.93	1.29	69.75	67.64	22570.00
381.3	89.73	1.60	87.36	78.55	29952.56
431.7	42.82	2.34	114.48	100.92	43566.52
477.7	14.50	3.42	140.54	127.51	60911.34

Table E.4. Calculated values for modeling of 1000 mg L^{-1} phenol biodegradation in batch operated MFC.

t (h)	C (mg L^{-1})	ln (C/C_0)	X (mg L^{-1})	$\bar{X}$ (mg L^{-1})	$\bar{X}$t (mg L^{-1} h)
5.0	948.98	0.00	63.76	0.00	0.00
29.0	905.73	0.05	56.72	60.24	1746.94
79.3	829.56	0.13	41.22	48.97	3883.24
111.0	804.95	0.16	39.11	40.16	4458.20
148.7	754.85	0.23	38.05	38.58	5736.71
195.7	713.29	0.29	42.98	40.52	7929.02
247.0	679.58	0.33	36.64	39.81	9833.51
316.0	634.08	0.40	29.95	33.30	10521.57
380.3	586.50	0.48	34.88	32.42	12327.65
469.7	507.91	0.63	40.16	37.52	17624.32
562.3	447.08	0.75	53.55	46.86	26347.02
611.3	410.36	0.84	63.06	58.30	35640.20
667.0	389.20	0.89	73.27	68.16	45465.32
714.3	311.97	1.11	85.25	79.26	56614.13
759.0	275.07	1.24	104.62	94.93	72052.70
809.3	223.03	1.45	123.64	114.13	92362.17
856.0	176.72	1.68	140.19	131.91	112916.76

905.3	106.32	2.19	166.60	153.40	138869.67
954.0	64.29	2.69	204.29	185.45	176915.96
1002.0	60.03	2.76	232.11	218.20	218637.50
1045.3	40.32	3.16	244.09	238.10	248886.35
1087.0	30.62	3.43	256.77	250.43	272214.58

F. Data used in determination of rate constant of phenol biodegradation in MFCs with rod electrodes operated continuously and evaluated based on Monod kinetics.

Table F.5. Calculated values for modeling of continuous biodegradation of 100 mg L^{-1} phenol.

D (h^{-1})	C_0 (mg L^{-1})	C (mg L^{-1})	X (mg L^{-1})	$(C_0-C)/X$	$(C_0-C)D/X$	$C/(D+K_e)$
0.005	100.54	5.82	22.83	4.15	0.02	1016.90
0.008	93.88	11.81	20.73	3.96	0.03	1403.87
0.014	97.01	52.75	9.41	4.71	0.07	3575.61
0.021	99.86	60.66	9.87	3.97	0.08	2825.62

G. Polarization and power curves generated from granular electrode MFC with neutral red and fed continuously with phenol and lactate.

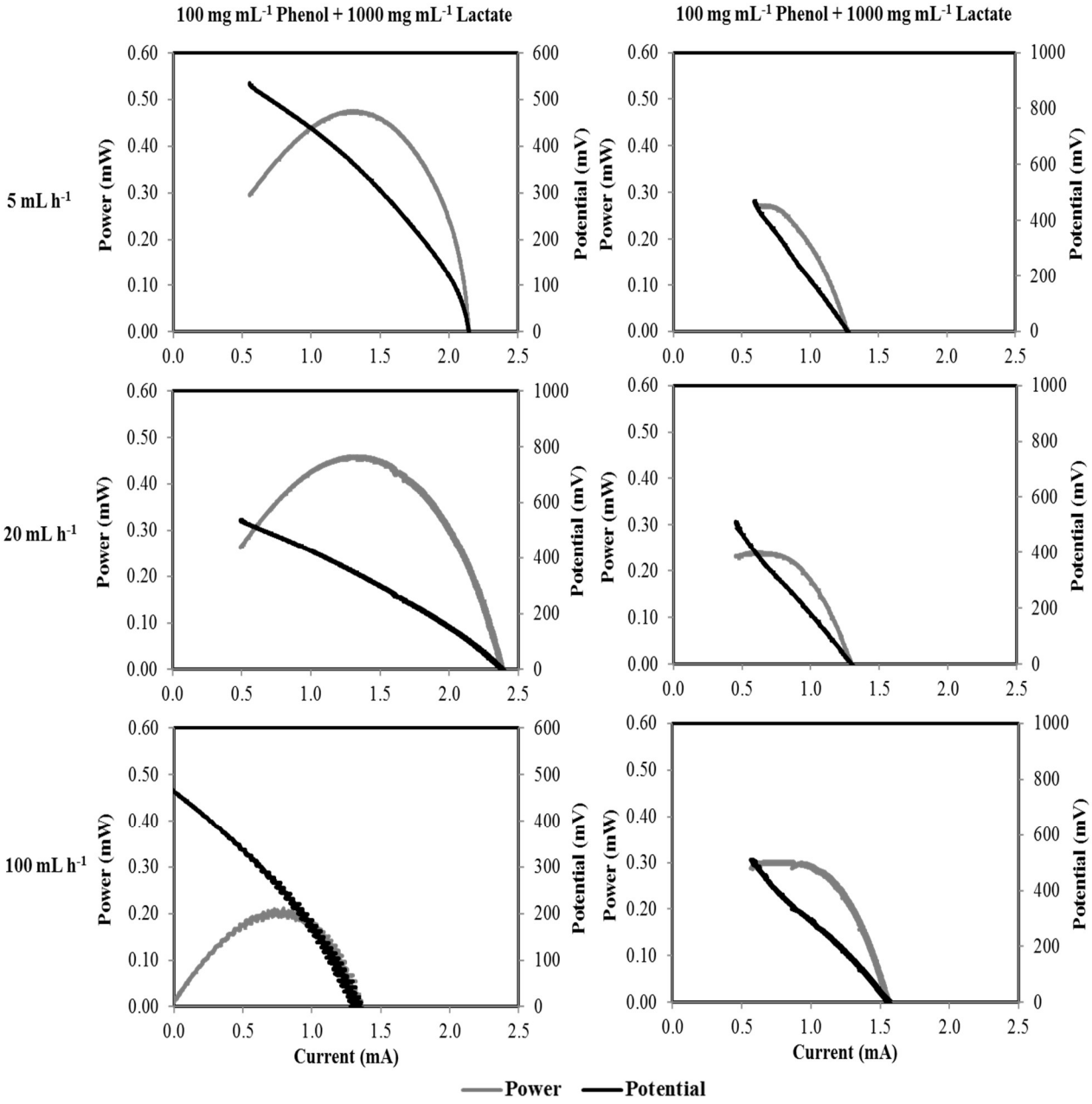

Figure G.1 Polarization and power curves from the biodegradation of 1000 mg L^{-1} lactate in combination with 100 mg L^{-1} phenol at various feed flowrates.

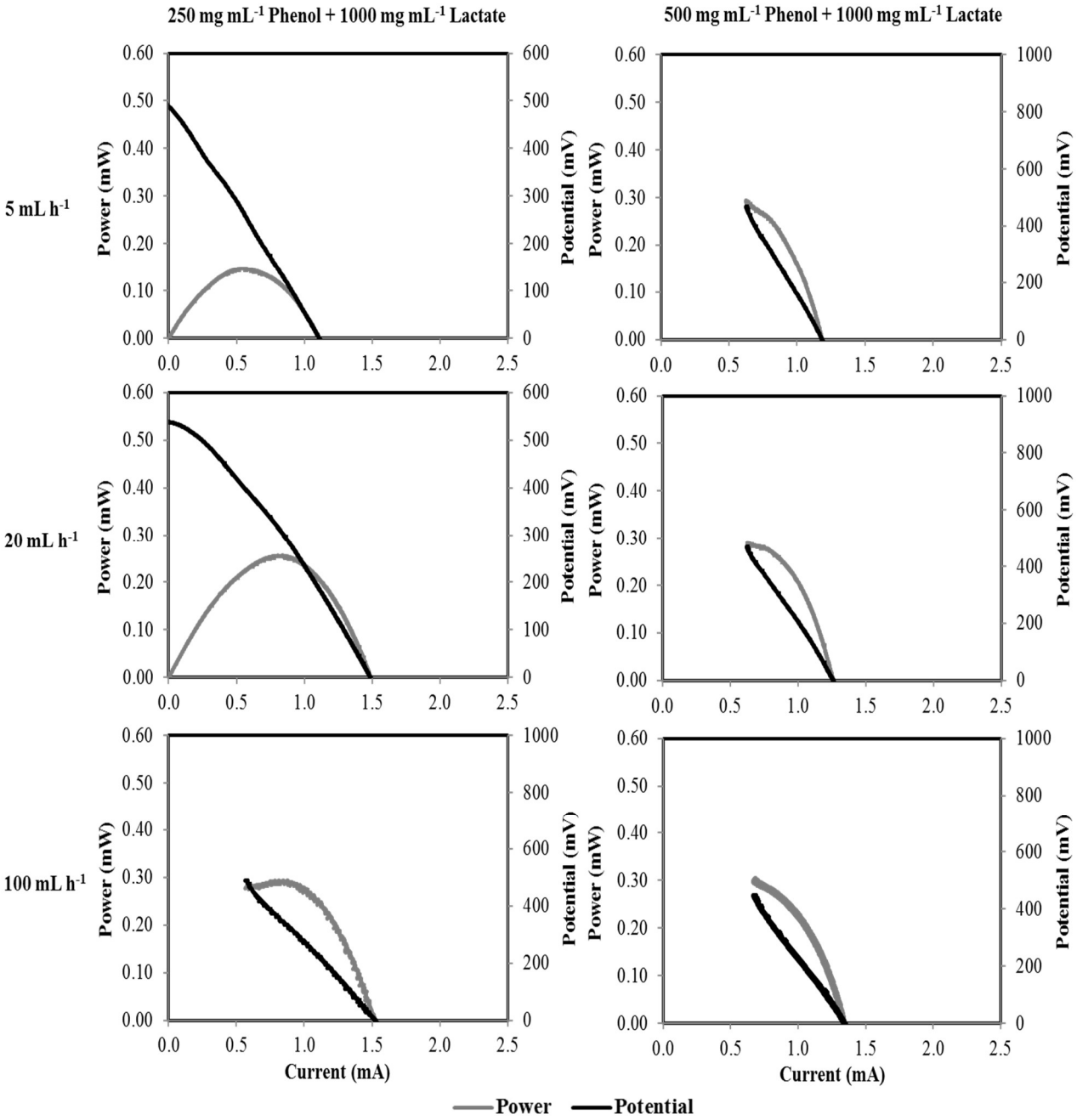

Figure G.2 Polarization and power curves from the biodegradation of 1000 mg L^{-1} lactate in combination with 250 and 500 mg L^{-1} phenol at various feed flowrates.

H. Coulombic efficiency calculation

Coulombic efficiency (CE) is the ratio of actual charge, in Coulombs, produced in the MFC from degradation (oxidation) of one mole of substrate to the theoretical charge that can be generated from the degradation of same amount of substrate as described below in Equation H.1 (Rabaey et al., 2005b; Bretschger et al., 2009).

$$CE = \frac{ItM}{FbV(S - S_0)}\ 100 \qquad (H.1)$$

Where:

I = current generated at time t, A

t = experiment time, s

M = molecular weight of substrate, g mol^{-1}

F = Faraday's constant, 96485 C mol^{-1}

b = number of moles of electrons produced per mole of substrate oxidized

V = volume of liquid in the anodic chamber, L

S = residual concentration of substrate, g L^{-1}

S_0 = initial concentration of substrate (batch system) or concentration of substrate in feed (continuous system), g L^{-1}

The corresponding values of constants M and b for each substrate is summarized in Table H.1.

Table H.1 Values of *M* and *b* utilized in the calculation of CE for each type of substrate.

	Lactate	Acetate	Phenol	Wastewater
M	90.08	60.05	94.11	32.00
b	12	8	28	4

I. COD calibration

Hach COD reagent vials were mixed with 2 mL of lactate, used as an standard organic compounds, at specified concentrations. The vials were then heated to 150 °C for 2 hours in a Hach COD reactor (Digestion reactor 45600, Hatch, Loveland, Co). After cooling the vials to room temperature, absorbance of the mixture was measured in a spectrophotometer (Shimadzu Uvmini 1240) at 620 nm. Resulting optical density (OD) readings were then plotted against the COD concentrations calculated for lactate to generate the calibration curve shown in Figure F.1.

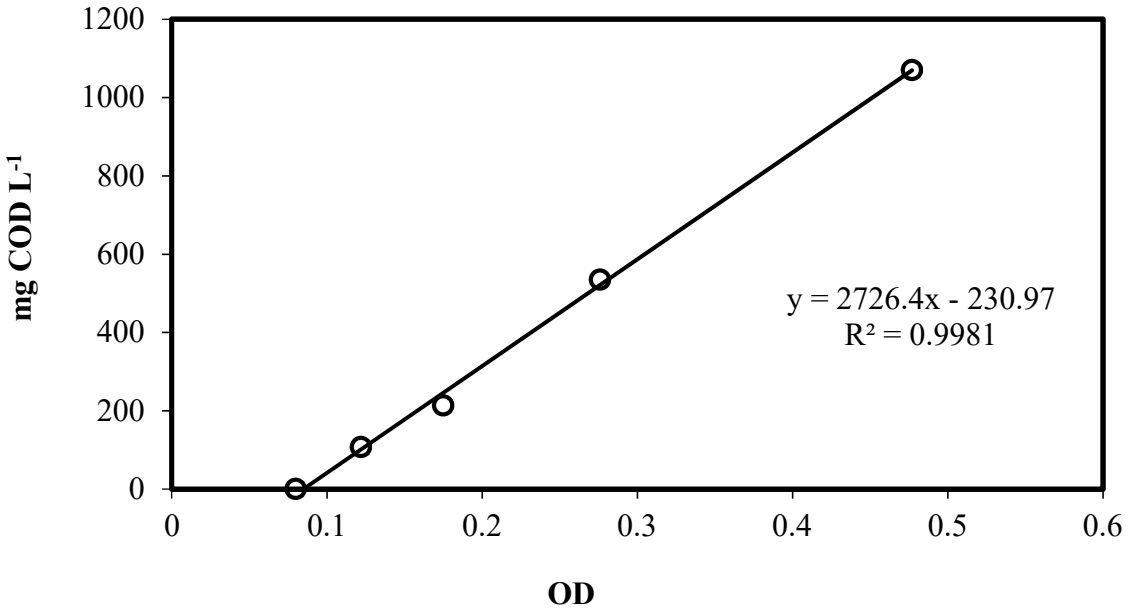

Figure I.1 Calibration of chemical oxygen demand (COD) concentration in terms of optical density (OD).

G. List of contributions

Publications

Moreno, L., Predicala, B. and Nemati (2017). Biodegradation of phenol in batch and continuous flow microbial fuel cells with rod and granular graphite electrodes. Environmental Technology 3:1-13

Moreno, L., Predicala, B. and Nemati (2015). Biokinetic evaluation of fatty acids degradation in microbial fuel cell type bioreactors. Bioprocess and Biosystems Engineering 38:25-38

Moreno, L., Predicala, B. and Nemati (2015). Treatment of phenolic wastewaters in microbial fuel cell using freely suspended and immobilized cells, Canadian Society for Bioengineering AGM, Edmonton, Jul 5-8, Paper No. CSBE15-50

Moreno, L., Nemati, M. and Predicala, B. (2012). Treatment of model organic compounds in microbial fuel cell type bioreactors, ICEPR 12, 2nd International Conference on Environmental Pollution and Remediation, Montreal, Aug 28-30, Paper No. 253

Conferences

"Treatment of organic wastewaters using microbial fuel cell technology." 60th Chemical Engineering Conference, Saskatoon, SK, Oct 24-27, 2010

"Application of microbial fuel cells in treatment of waters contaminated by short chain fatty acids and aromatic compounds." Usask World Water Day Conference, Saskatoon, SK, Mar 22, 2011

"Application of microbial fuel cells in treatment of waters contaminated by short chain fatty acids." Western Canada Water Conference, Saskatoon, SK, Sep 20-23, 2011

"Treatment of organic wastewaters using microbial fuel cell technology." EnerCan West 2012: Energy and the Environment Conference, Regina, SK, Feb 13-14, 2012

"Biodegradation of short chain fatty acids and aromatic compounds in microbial fuel cell bioreactors." 62nd Chemical Engineering Conference, Vancouver, BC, Oct 14-17, 2012

"Treatment of phenolic wastewaters in microbial fuel cell using freely suspended and immobilized cells." CSBE/SCGAB 2015 Annual Conference, Edmonton, AB, Jul 5-8, 2015

"Biodegradation of model pollutants in wastewater using microbial fuel cells." College of Engineering Research Day, University of Saskatchewan, Saskatoon, SK, Nov 10, 2015 (Awarded 2nd Place in Graduate Student Research Competition)